PHD

Improving the Efficiency of Aminolevulinate-Photodynamic Therapy of Skin Cells by Combining UVA Irradiation and Potent Iron Chelating Agents

Radka, Tina

Award date:
2014

Awarding institution:
University of Bath

Improving the efficiency of aminolevulinate-photodynamic therapy of skin cells by combining UVA irradiation and potent iron chelating agents

Tina Radka

A thesis submitted for the degree of Doctor of Philosophy

University of Bath

Department of Pharmacy and Pharmacology

October 2013

TO MY FAMILY...

TABLE OF CONTENT

CHAPTER THREE- RESULTS

ACKNOWLEDGEMENTS

I am greatly indebted to my lead supervisor Dr Charareh Pourzand for giving me the opportunity to complete my PhD degree under her full supervision. I would like to express my sincere gratitude for the continuous support, advice, and guidance.

I am also very appreciative to my co-supervisor Dr Ian Eggleston for his supervision and continuous support and great discussions throughout my PhD.

I am very thankful and appreciative to Professor Rex Tyrrell for his useful advice and for giving me the possibility to use the photobiology equipment of his laboratory.

A special thanks and great appreciation will go to Dr Olivier Reelfs for being a great mentor and sharing his knowledge and his never ending help and support throughout my PhD.

I would like to thank Professor Irene Leigh (University of Dundee) for providing the Met2 cell line and her advice on organo-typic cultures.

I am also very appreciative to Dr Adrian Rodgers from the Bioimaging suite for his help and advice as well as Mr Kevin Smith and Mrs Jo Carter for their practical help.

Many thanks to the previous and present members of our laboratory 5W 2.20 for their continuous help and support and creating a friendly and relaxed environment to work in.

From Dr Eggleston’s group, I would like to thank my dear friend and former colleague Dr Ben Young for providing me with the CICs for my project and the friendly support that he always gave me. Also I am grateful to Dr Ruggero Dondi for helping me with the HPLC data and his help and advice.

Last but not least my greatest appreciation of all has to go to my loved ones including my dear parents, whom have always guided me in the right way and supported and loved me through everything in life unconditionally. So everything I have achieved today, I owe to them. Also my lovely brother, Nezam who is my greatest friend and support, and Shahin who always encouraged me through my PhD and supported me fully, so thank you all!

ABSTRACT

Photodynamic therapy (PDT) is widely used for the treatment of skin cancer. Mechanistically, in delta-aminolevulinic acid (ALA)-mediated PDT, the addition of ALA to cells bypasses the negative feedback control of heme biosynthesis, leading to accumulation of photosensitizing concentrations of protoporphyrin IX (PPIX). Subsequent activation of cellular PPIX with an external light source (usually red light, 550-750 nm) leads to generation of reactive oxygen species (ROS), resulting in cell death. The major side effect of ALA-PDT treatment is the pain experienced by patients. Management of treatment-related pain still remains a considerable challenge in patients. Further optimization of the treatment protocol including light source, dose and duration therefore seems crucial to try and address this issue. To improve the efficiency of ALA-PDT of skin cells in the present study three approaches were used: (i) The conventional light source was changed to UVA (320-400 nm) that is absorbed more efficiently by PPIX and is 40-fold more potent in killing cultured skin cells than red light; (ii) ALA treatment was combined with the potent iron chelators, salicylaldehyde isonicotinoyl hydrazone (SIH), pyridoxal isonicotinoyl hydrazone (PIH) or desferrioxamine (DFO) to further increase the accumulation of PPIX through the depletion of iron available for ferrochelatase-mediated bioconversion of PPIX to heme; (iii) ALA treatment was combined with UVA-activatable caged iron chelators (CICs) that do not chelate iron unless activated by UVA. The CICs used were aminocinnamoyl-based SIH derivatives, ‘BY123’ and ‘BY128’. Upon activation by UVA, these CICs release the active SIH allowing for specific localised release of iron chelator in the cells. Spontaneously immortalised HaCaT cell line and Met2 cancer line (squamous cell carcinoma) were used as cell models. Cells were pre-treated (or not) for 18 h with SIH, PIH or DFO (20-100 μM),

then subjected to ALA (0.5 mM) for 2 h and irradiated with low doses of UVA (5-50 kJ/m^2). The quantification of intracellular PPIX was carried out by both HPLC and spectrofluorimetry after treatments of cells with ALA alone or combined with chelators. Cell death was examined 24 h after UVA exposure of ALA+/-chelators-treated cells by flow cytometry using Annexin V-propidium iodide dual staining assay. Pretreatment of HaCaT cells with ALA caused a substantial increase in the intracellular levels of PPIX which in turn sensitized the cells to very low non-cytotoxic UVA doses. Pre-treatment with DFO, PIH and SIH followed by ALA treatment further enhanced the PPIX level in HaCaT cells and caused an additional level of photosensitization to low UVA doses. Among the chelators used, SIH combined with ALA provided the most efficient increase in PPIX and cell killing following UVA irradiation, even at a lower SIH concentration of 20 µM. Among the CICs used, both UVA-activated BY123 and BY128 were as effective as SIH in increasing the level of PPIX and cell killing in ALA-treated cells following exposure to low doses of UVA. UVA-based ALA-PDT combined with SIH (or its caged-derivatives BY123 and BY128) appears therefore to be a promising modality for topical PDT. The high lipophilicity of SIH (and its caged-derivatives) which facilitates skin penetration and their potent cytotoxicity at low UVA doses should therefore allow the current modality for topical PDT to be improved, through a reduction of the time of irradiation and therefore the duration of pain experienced during the treatment. The use of SIH-based CICs will be a safer alternative to topical ALA-PDT than ‘naked’ SIH, as application of these pro-chelators will substantially decrease the exposure of the surrounding normal skin tissue to strong iron chelators and their toxic side effects.

ABRREVIATIONS

ADL	Argon-dye laser
AFXL	Ablative fractional laser
AFXL-PDT	Ablative fractional laser-Photodynamic therapy
AK	Actinic Keratosis
AlPcS2	Chloroaluminium sulphonated phthalocyanine
ALA	5-aminolevulinic acid
ALA-D	Aminolevulinate dehydratase
ALA-S	Aminolevulinate synthase
AMD	Age related macular degeneration
Apaf-1	Apoptosis protease activator 1
BCC	Basal Cell Carcinoma
BD	Bowen's disease
BPD-MA	Benzoporphyrin derivative monoacid ring A
BY123	4,5-dimethoxyaminocinnamoyl-SIH derivative
BY128	4,5-methylenedioxyaminocinnamoyl-SIH derivative
CA	Calcein
CIC	Caged iron chelator
CM	Condition media
CM-H_2DCFDA	Chloro-methyl 2', 7'-dichlorodihydrofluorescein diacetate
CP94	1,2-diethyl-3-hydroxypyridin-4-one hydrochloride
CR	Clearance rate
CSFs	Colony Stimulating Factors
Cyt C	Cytochrome C
3D	Three dimensional

DED	De-epidermalised
DFO	Desferrioxamine mesylate (Desferal)
DMEM	Dulbeco's Minimum Essential Medium
DMSO	Dimethyl sulphoxide
DNA	Deoxyribonucleic acid
EDTA	Ethylenediaminetetraacetic acid
EMEM	Earl's modified minimum essential medium
FCS	Foetal Calf Serum
Fe	Iron
Fe^{2+}	Ferrous iron
Fe^{3+}	Ferric iron
FITC	Fluorescein isothiocyanate
5-FU	5-Fluorouracil
GABA	gamma-aminobutyric acid
GAG	Glycosaminoglycans
GPx	Glutathione peroxidase
GSH	Glutathione (reduced)
H	Hour/hours
H_2DCFDA	2', 7'-dichlorodihydrofluorescein diacetate
H_2O_2	Hydrogen Peroxide
H_2O	Water
HP	Hematoporphyrin
HPD	Hematoporphyrin Derivative
HPLC	High performance liquid chromatography
HPPH	2-[1-Hexyloxyethyl]-2-devinyl pyropheophorbide-a
ICRF-187	Dexrazoxane
ICT	Iron chelation therapy

IL-6	Interleukin-6
INF-α	Interferon-α
IPL	Intense Pulsed Light
kJ/m^2	Kilojoules per meter square
KC	Keratinocyte
LED	Light Emitting diode
LI	Labile Iron
LIP	Labile Iron Pool
Lu-tex	Lu(III)-complex of a texaphyrin
MAL	Methyl-aminolevulinate
Min	Minutes
mBCC	Morphoeiform Basal Cell Carcinoma
m-THPBC	Meta-tetra-hydroxyphenyl bacteriochlorin
m-THPC	Meta-tetrahydroxyphenyl chlorine
MT	Metalothionein
MTT	3-(4,5-Dimethylthiazol-2-ye)-2,5-diphenyltetrazolium bromide
MW	Molecular weight
nBCC	Nodular Basal Cell Carcinoma
NF-kappaB	Nuclear Factor kappa B
NMSC	Non Melonoma Skin Cancer
NPe$_6$	mono-L-aspartyl chlorin e$_6$
2-NPE-PIH	2-Nitrophenylethyl pyridoxal isonicotinoyl hydrazone
2-NPE-SIH	2-Nitrophenylethyl salicylaldehyde isonicotinoyl hydrazone
$^3O_2$	Triplet Oxygen
O_2	Oxygen molecule
$^{\bullet}O_2^-$	Superoxide radical anion

$^1O_2$	Singlet oxygen
$^{\bullet}OH$	Hydroxyl radical
PBG	Porphobilinogen
PBGD	Porphobilinogen deaminase
PBS	Phosphate buffered saline
PDD	Photodynamic diagnosis
PDL	Pulsed dye laser
PDT	Photodynamic Therapy
PI	Propidium Iodide
PIH	Pyridoxal Isonicotinoyl Hydrazone
PPIX	Protoporphyrin IX
P/S	Penicillin/Streptomycin
PS	Phosphatidylserine
PS	Photosensitiser
PUVA	Psoralen UVA
RMM	Relative Molecular Mass
ROS	Reactive Oxygen Species
RR	Ribonucleotide reductase
sBCC	Superficial Basal Cell Carcinoma
SC	Strateum corneum
SCC	Squamous Cell Carcinoma
SD	Standard deviation
SFM	Serum Free Media
SIH	Salicylaldehyde isonicotinoyl hydrazone
$SnET_2$	Tin etiopurpurin
Tf	Transferrin
TfR	Transferrin receptor

TNF	Tumor Necrosis Factor
TPPS4	Tetra-sodium-meso-tetraphenylporphine-sulfonate
UV	Ultraviolet
VPL	Variable pulse light

CHAPTER ONE

INTRODUCTION

1.1. Human Skin

Human skin is the largest organ in the body. The skin consists of multilayers of ectodermal tissue and also has the role of protecting the underlying muscles, bone and internal organs. In an average person, it weighs around six pounds and comprises approximately 10% of the total body mass (Williams, 2003). Due to skin interactions with the outside environment, it has the very important role of protecting the body against pathogens (Proksch *et al*., 2008) and also excessive water loss (Madison, 2003).

Other important functions of the skin include maintaining the body temperature, insulation, synthesis of vitamin D etc.

Human skin is divided into three distinctive layers: epidermis, dermis, hypodermis (subcutaneous adipose layer).

1.1.1. Epidermis:

The epidermis starts at the outermost surface of the skin and works inwards. It acts as a waterproof base for the skin and consists of stratified squamous epithelia with an underlying basal lamina. The main type of cells that exist in the epidermis include Markel cells, Langerhans cells, keratinocytes and melanocytes, with keratinocytes being the major epidermal cells, making up around 95% of the epidermis (McGrath *et al*, 2004).

The thickness of the epidermis varies depending on the area of the body; it ranges from the thinnest on the eyelid at around 0.05 mm, to the thickest on the palms and soles of around 1.5 mm (Brannon, Heather, 2007).

The epidermis itself can be further subdivided into four to five distinct layers depending on the site of the skin:

- Cornified layer (*stratum corneum*).
- Granular layer (*stratum granulosum*) - where epidermal nuclei disintegrate.
- Spinous layer (*stratum spinosum*) - the bulk of living epidermal keratinocytes.
- Basal layer (*stratum basale*) – the only keratinocytes in normal epidermis which undergo cell division.
- Clear/ translucent layer (*stratum lucidum*) – This layer only exists in palms and soles.

The epidermis is constantly renewed by the cell division which takes place in the *stratum basale*, with cells undergoing several stages of differentiation and moving upwards in the layers as they do so, until new keratinocytes are produced. In this process these keratinocytes lose their nuclei, dehydrate and flatten out to what forms the cornified external layer *stratum corneum* (SC) (McGrath *et al*, 2004).

Keratinocytes in the basal layer divide on average every 4 weeks and the daughter cells undergo modifications as they move to up to the skin surface. At the most external layer i.e. *stratum corneum*, dead cells are constantly shed, while new cells are being produced at the same level in basal layer. However, in the case of hyper-proliferative diseases such as skin cancer or psoriasis as well as pathological conditions such as Actinic keratosis (AK), the rate of this division

is much higher which indicates a risk factor as there may be some alterations to permeability barrier functions (Lippens *et al*, 2009).

Other cells of the epidermis mentioned above, also play important roles in maintaining the epidermis.

Langerhans cells are antigen presenting cells which derive from the bone marrow and have an important role in the immune surveillance system of the skin (Benjamin *et al*, 2008).

Melanocytes secrete melanosomes which contain melanin. They form a UV absorbing barrier, which in turn reduces the amount of radiation that may penetrate the skin (Benjamin *et al*, 2008). The skin colour is determined by the melanogenesis activity of these cells (Biro *et al*, 2009).

Markel cells act as mechanoreceptors, responsible for the sensation of touch and pressure (Biro *et al*, 2009). *Stratum corneum* (SC) is a non-viable epidermal layer with a thickness of around 10 µM. Its nucleated keratinocytes form a barrier to the transdermal delivery of drugs through the skin.

Moving downwards through the layers of epidermis, the *stratum granulosum* is up to 3 cell layers thick and contains enzymes that may degrade vital cell organelles i.e. nuclei and production of corneocytes (Benjamin *et al*, 2008).

Stratum spinosum (otherwise known as spinous layer), is another viable layer consisting of 2-6 columnar keratinocyte layers that rearrange themselves into polygonal shapes. Desmosomes are produced within this layer from keratins (Benjamin *et al*, 2008).

1.1.2. Dermis:

The dermis is the middle layer of skin, which acts as a connective tissue matrix between the upper epidermis and the subcutaneous layer. The dermis is around 3-5 mm thick (Barry, 1983) and consists of two layers: the superficial area called the papillary region, which is adjacent to the epidermis and a deep thicker layer called reticular dermis (James *et al*, 2005). The upper dermis (papillary region), consists of capillaries which nourish the epidermis and the lower thicker layer (reticular layer). The major cells in the dermis are fibroblasts which synthesise elastin, and components of dermis are elastin fibres providing elasticity, collagen providing strength and the extrafibrillar matrix, which is an extracellular gel-like substance composed of glycosaminoglycans (GAG). GAG provides viscosity, hydration and allows the dermis's limited movement. There are also mechanoreceptors in the dermis that maintain the senses of heat and touch, hair follicles, sweat glands, sebaceous glands, lymphatic vessels and blood vessels (James *et al*, 2005).

Other cells embedded in the reticular layer are fat cells, mast cells, macrophages, dermal dendrocytes and lymphocytes.

1.1.3. Subcutaneous Layer (Hypodermis):

This layer is a fibrous fatty layer that spreads all over the body with the exception of eyelids and the male genital region (Barry, 1983). This layer is composed of adipocytes, fibroblasts and macrophages and is supplied by a network of blood vessels and nerve fibres (Biro *et al*, 2009).

The hypodermis is known as a site of synthesis of the preadipocytes and adipocytes, with availability of high energy chemicals (Barry *et al*, 1983; Driskell *et al*, 2013).

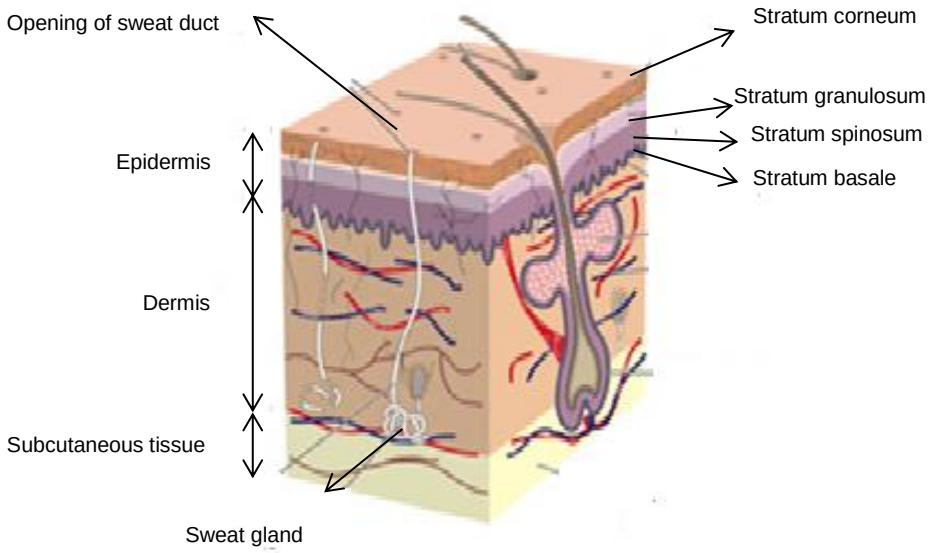

Figure 1.1: Anatomy of the skin. Reproduced from (training.seer.cancer.gov /melanoma/anatomy).

1.2. Skin Cancer

Skin cancers are classified based on the type of cells they initiate from. There are three types of skin cancers:

1.2.1. **Non Melanoma Skin Cancer:**

Non melanoma skin cancer (NMSC) is a collective term used to describe basal cell carcinoma (BCC) and squamous cell carcinoma (SCC).

BCC occurs mostly in white-skinned individuals and it accounts for 80% of NMSC. BCCs are slow growing and often appear in local tissues and the chances of metastases are very rare (Rajpar *et al*, 2008).

The possible signs that should give an indication to non-melanoma skin cancer are as follows (Rajpar *et al*, 2008):

- Raised, smooth, shiny, and look pearly.
- Raised, and red or reddish brown.
- Firm and look like a scar, and may be white, yellow or waxy.
- Scaly, bleeding or crusty.

- **Basal Cell Carcinoma (BCC):** This type of cancer is initiated from the lower layer of the epidermis. It is the most common and yet least dangerous type of skin cancer. BCC is subdivided into three major growth patterns: nodular (nBCC), superficial (sBCC) and morphoeiform (or sclerotic; mBCC). Superimposed on any of these growth patterns may be ulceration or pigmentation. The likelihood of metastasis is extremely small; the related morbidity to BCC is linked to local tissue invasion and destruction, which mostly occurs on the head and neck. Most sBCCs will progressively enlarge over months to even years and with time, may adopt nodular or even sclerotic growth patterns. sBBCs do not penetrate very deeply into the skin but are able to grow outward and up to several centimetres in size (Rajpar *et al*, 2008).

nBCCs lesions that are found on the neck and head of old patients, will progressively grow into nodules which may also ulcerate. Central ulcerations in a nodule will appear as a raised and rolled edge (Rajpar *et al*, 2008). On the other hand, mBCCs have a sclerotic growth pattern and present themselves as pale scars that tend to be deeply invasive, making surgical and non-surgical treatments less effective (Albert and Weinstock, 2003). Their appearance ranges from a translucent to a fleshy colour - very small blood vessels are visible on the surface of the lesions which often appear as a raised smooth bump, and ulceration may sometimes be seen.

The most well-known risk factor causing NMSC is exposure to UV which is directly related to sun-exposure habits. Therefore the majority of such lesions are often observed on sun-exposed sites in patients. There are some factors making the appearance of SCC more probable such as lighter complexion, male gender, increasing age, ionizing radiation, immunosuppression, psoralen phototherapy and also precancerous skin lesions (Albert and Weinstock, 2003).

The areas of the body that are most exposed to UV, are the areas that are most prone to BCC, i.e. the face. The chances of their metastasis are very low and they are usually treatable by surgery or radiotherapy.

- **Actinic Keratosis (AK):** is a pre-malignant condition (Prajapati *et al*, 2008) which appears as thick, scaly or crusty patches of skin (Freeberg *et al*, 2003; Quaedvlieg *et al*, 2006). Its occurrence rate is higher in people with fair skin and also those who are frequently exposed to sun, as the incident of AK is often related to solar damage. AK lesions are known to be potentially pre-cancerous and if not treated there is about 20% chance that they could progress to SCC (Quaedvlieg *et al*, 2006; Weedon, 2010).

  AK sites often range from 2-6 mm in size and may appear in different colours of dark to light brown, tan, pink, or a combination of colours, or indeed they may have the same pigment as the surrounding skin. AK often appear at areas of the skin that are mostly exposed to sun, such as the face, scalp, ears, neck, lips, backs of hands etc.

  AK is subdivided into the following types (Rapini *et al*, 2007):

- Hyperkeratotic Actinic Keratosis
- Pigmented Actinic Keratosis
- Atrophic Actinic Keratosis
- Lichenoid Actinic Keratosis

The prevalence of AK in Australia is estimated to be approximately 40% (Berlin, 2010). Sometimes the lesions may increase in thickness and become thick and horny and also may cause bleeding. Pathological evidence suggests that AK should be regarded as very early SCC (Czarnecki *et al*, 2002). Since 3-4% of SCCs metastasize (Lober and Lober, 2000), it has been recommended that early actions should be taken in treating AK in order to avoid malignancy and the need for more extensive treatment.

- **Squamous Cell Carcinoma (SCC):** This type of cancer arises from the middle layer of the skin. It is less common but there are more chances of metastasis. If SCC is not treated it may cause death. The tumours are very fast-growing with a red, crusted thickened patch on the sun-exposed area. If SCC is not treated it may develop further and have more serious consequences. SCC is the second most common skin cancer as is quite dangerous but not as much as melanoma.

Among NMSC conditions, Bowen's disease (BD) is also a persistent form of intra-epidermal (*in situ*) SCC that normally appears as an enlarging, well-demarcated, erythematous plaque with an irregular border, a crusted or scaling surface and potential for extending along the cutaneous appendages. Nevertheless BD has a small potential for invasive malignancy (Morton, 2005). As the incidence of NMSC increases, so does the number of modalities used to treat this condition.

- **Melanoma**: derives from the pigment producing cells melanocytes. It is less common than the other two types of skin cancer, however it is much more aggressive and spreads very rapidly, and if untreated it may prove fatal (Kasper *et al*., 2005). The predominant cause of malignant melanomas is UVA radiation via indirect DNA damage, which is caused by the production of free radicals and reactive oxygen species (ROS) by UVA leading to cell damage. They often irregular

in shape with colour variation within the lesion and usually have a diameter greater than 6 mm (Kanay and Gerstenblith, 2011).

Most melanomas are brown to black in colour. There are however some melanomas that are red or a fleshy colour. These are the more aggressive lesions. Signs of melanoma could be a change in shape, colour, or size of the lesion, itching or pain and even evolvement of new moles in adulthood (Rajpar *et al*, 2008).

Figure 1.2 illustrates some images of all three types of skin cancer.

Figure 1.2 A: Top: Basal Cell Carcinoma (BCC) (Ref: http://www.skcin.org/Skin-Cancer/Types/Basal-Cell-Carcinoma-(BCC)).

Figure 1.2 B: Right: Squamous Cell Carcinoma (SCC)(Ref: http://www.skincancer.org/skin-cancer-information/squamous-cell-carcinoma). Left: Melanoma (Ref: http://www.missinglink.ucsf.edu/melanoma)

Non melanoma skin cancer (NMSC) is the most widely occurring cancer in UK with official figures reporting around 114000 cases registered in England and Wales (Levell *et al,* 2013). Since non melanoma skin cancers are relatively easy to treat a lot of the referred cases are not reported so the actual number is quite likely to be higher (Cancer Research UK). The vast majority of NMSC are BCC which comprise 75% of all NMSC cases. This makes SCC the second most common type of skin cancer in the UK (i.e. 20% of skin cancers). In the USA, one million new cases of NMSC are diagnosed each year and of these 80% are BCC and 16% are SCC. The overall incidence of SCC is increasing across Europe, the USA and the southern hemisphere (see Neville *et al*, 2007; Schmook and Stockfleth, 2003).

As mentioned above, the main factor involved in many skin cancers, is sun exposure. This could be a long term exposure or short episodes of intense exposure and burning (Kanay and Gerstenblith, 2011).

1.2.2. Diagnosis of Skin Cancer:

To identify if a lesion is cancerous, a nurse or doctor will discuss the patient's medical history to see if there is a family history of skin cancer. Also the number of previous sunburns will be recorded. This will then be followed by a skin examination where the suspected lesion will be tested for shape, colour, size and texture. The lymph glands will also be examined for signs of swelling, which is a potential sign of skin cancer.

The only way to actually diagnose various types of skin cancer is to take a biopsy of the suspected area. A biopsy can reveal very useful information such as the tumour depth. Biopsy methods include (http://www.cancerresearchuk.org/skincancer)

1. Shave biopsy: This is performed using either a scalpel blade or a curved razor blade. If this procedure is performed smoothly, a small fragment of the skin should be removed with minimal blemish. This method is ideal for diagnosis of BCC and SCC and melanoma *in situ*.
2. Punch biopsy: A circular blade is used ranging in size from 1-8 mm. The blade is attached to a long handle, and is rotated down through the epidermis and dermis, and into subcutaneous tissue, producing a cylindrical core of tissue (Zuber, 2002). This is a particularly good biopsy method where a smaller punch i.e. 1-1.5 mm is desirable for areas where cosmetic appearance is important as minimal bleeding occurs and no stitching is required. The only disadvantage of a 1 mm punch is that the tissue obtained is very difficult to observe.
3. Incisional biopsy: A cut is made through the dermis down to the subcutaneous tissue. Incisional biopsies can include the whole lesion (excisional), part of a lesion, or part of the affected skin and also part of the normal skin (this is to show the interface between the normal and abnormal skin). Long and thin deep incisional biopsies are excellent on the lower extremities as they allow a large amount of tissue to be analysed with minimal tension on the surgical wound.
4. Excisional biopsy: This method is very similar to the incisional biopsy, except that the entire lesion or tumour is included. This method is ideal for small melanomas, and is often performed with a narrow surgical margin to assure the deepest thickness of the melanoma is given before prognosis is decided. As many melanomas *in situ* are quite large, on the face, multiple small punch

biopsies are often taken, before committing to a large excision for diagnostic purposes alone (http://www.cancerresearchuk.org/sckincancer).

1.2.3. Treatment of Small Skin Cancers:

There are several existing treatments for diagnosis of small skin cancers. The treatment options vary depending on the site of cancer, its size and depth, as follows (ref: cancerresearchuk.org/skincancer):

- One of the most common options is operation, which is done under local anaesthesia in order to cut the cancer out.
- Cryosurgery, which is also known as the freezing treatment with liquid nitrogen, destroys the cancer cells. This modality is used for low risk tumours that are less than 6 mm in diameter.
- Curettage and cautery- This modality is used for low risk tumours that are less than 6 mm in diameter. The tumour or the lesion is scrapped off (curettage). This may cause some bleeding to the area which is often stopped by application of small electrical burns that are achieved with an electric needle (cautery).
- Chemotherapy creams are another alternative. These creams are applied on the area of skin cancer to diminish the cancer cells. Examples of these are 5-fluorouracil (5-FU) or imiquimod.

  5-Fluorouracil (5-FU) (trademarked as Efudex) is a pyrimidine analogue that is widely used in cancer treatment. It belongs to the antimetabolite drug

family and works via the irreversible inhibition of thymidylate synthase, interrupting this enzyme's action which leads to blocking of the synthesis of the pyrimidine nucleoside thymidine, which is required for DNA replication. 5-FU is a recommended topical application for AK and some carcinomas. Due to some toxicity observed with 5-FU, its precursor 5-Fluoroorotic acid is commonly used in laboratories to screen against organisms capable of synthesising uracil (Longly *et al*, 2003).

Imiquimod (trademark name: Aldara and Zyclara) is known as an immune response modifier. This topical cream is used to treat AK and BCC and SCC. It is known that imiquimod activates immune cells through the toll-like receptor 7 (TLR7), commonly involved in pathogen recognition (Hemmi *et al*, 2000). Cells that are activated via TLR-7 secrete cytokines (primarily interferon- α (INF-α), interleukin-6 (IL-6), and tumour necrosis factor-α (TNF-α) (Bilu *et al*, 2003). It has been shown that upon imiquimod application, Langethans cells are activated which in turn activaes the local lymph nodes that result in activating the adaptive immune system. Other cells activated could be named natural killer cells, macrophages and B-lymphocytes (Miller *et al*, 1999).

- Moh's micrographic surgery: This involves cutting the area of cancer, piece by piece and looking at each piece under the microscope to confirm the cancer cells. It is done bit by bit to assure that healthy tissues are not also cut away. This method was first developed in 1938 by the general surgeon named Frederic E. Mohs. This therapy is recommended for common types of skin cancer. Moh's surgery is amongst many methods which obtain complete margin control during removal of skin cancer using frozen section histology

(Minton, 2008). Treatment modalities already in use are tailored to tumour type, location, size and histological pattern. However with the increasing incidence of NMSC, there is a requirement for designing new non-invasive treatments that target cancer cells more generally throughout all stages of tumorogenesis.

- Photodynamic therapy (PDT) with topical aminolevulinate-based ALA or MAL formulations is considered to be one of the most promising treatments for NMSC (e.g. Cairnduff *et al*, 1994; Fink-Punches *et al*, 1997; Omrod and Jarvis, 2000; Peng *et al*, 1997; Lehmann, 2007; Morton *et al*, 2008; Morton, 2005). It is a light-dependent treatment that kills the cancer cells (Rajpar *et al*, 2008).

In this project we applied PDT in combination with ALA and a range of iron chelators in order to improve the efficiency of PDT for treatment of NMSC.

1.3. Photodynamic Therapy (PDT)

1.3.1. Definition:

The combination of photosensitising agents and light in order to treat skin cancers has been widely used in the field of dermatology for centuries. This goes back to ancient Egypt, Greece and India where psoralen-containing plant extracts were applied in combination with a light source to treat psoriasis, and skin cancer (see Wilson and Mang, 1995). This concept is known as photo-chemotherapy and represents a common basis for various present day treatment procedures such as PUVA (i.e. psoralen UVA), and also PDT.

PDT depends upon the combination of molecular oxygen (O_2), light, and a photosensitiser (PS) (see **Figure 1.3**).

The first component of PDT is the PS that is a photosensitive molecule that localizes to a target cell and/or tissue. This is followed by administration of a light source of a specific wavelength that is absorbed by the particular PS applied, thus activating it. In the mechanism of PDT, the PS transfers energy from light to molecular oxygen, generating reactive singlet oxygen. These reactions occur in the immediate local of the light-absorbing PS, such that the biological responses are induced only in the particular areas that have been exposed to light (Wang *et al*, 2002).

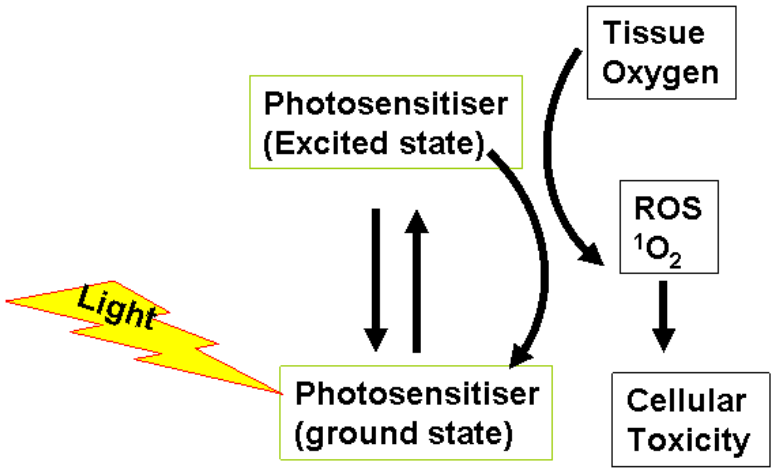

Figure 1.3. Mechanism of action of photodynamic therapy (PDT). PDT requires three elements: light, a photosensitiser and molecular oxygen (O_2). When the photosensitiser is exposed to specific wavelengths of light, it becomes activated from a ground to an excited state. As it returns to the ground state, it releases energy, which is transferred to O_2 to generate singlet oxygen ($^1O_2$) which mediates cellular toxicity.

1.3.2. Mechanism of Action

Photodynamic therapy (PDT) is a selective treatment modality that targets the area to be treated with high efficiency. This selectivity is based on a difference in the PS concentration between normal and targeted tissues and by directing light into the target tissue only. One advantage of PDT is that the PS can be administered either intravenously or by topical application to the skin. However, depending on the route of administration chosen, the bio-distribution of the PS may change over time (Dolmans *et al*, 2003). Managing the timing of light exposure is yet another way to control the effects of PDT. Depending on the PS applied, it takes 3-96 hours (h) to accumulate in the target tissue. After the accumulation period, light directed to the tissue activates the PS and, in the presence of ground-state (triplet) oxygen ($^3O_2$), ROS are formed. Briefly, following the absorption of light (photons), the PS is transformed from its ground state (single state) into a relatively long-lived electronically excited state (triplet state) via a short-lived excited singlet state (Henderson and Dougherty, 1992). The excited triplet can undergo two kinds of reactions (see **Figure 1.4**). Radicals are formed by transferring hydrogen atom (electron) via reacting either directly with a substrate i.e. cell membrane or a molecule i.e. protoporphyrin IX. In type I reactions, these radicals can transfer their excessive energy to $^3O_2$ to form singlet oxygen ($^1O_2$) and other oxygenated reactive species, whereas in type II reactions, the triplet can transfer its energy directly to $^3O_2$, to form $^1O_2$.

In both types of mechanism, the reactions occur simultaneously and the ratio between these processes depends on the type of the PS used, the concentrations of biological substrates and O_2, as well as the binding activity of the PS for the substrate. Due to the high reactivity and the short half-life of ROS, only cells that are

located near the area of the ROS production (i.e. areas of PS localisation) are directly affected by PDT (Moan and Berg, 1991). Among ROS generated, $^1O_2$ is regarded as the main mediator of phototoxicity in PDT as it is a powerful oxidant that can react with many kinds of biomolecules. These include unsaturated triacylglycerols, cholesterol, phospholipids, amino acids such as tryptophan, histidine and methionine, as well as nucleic acid bases such as guanine and guanosine (Milgrom and MacRobert, 1998; Stemberg *et al*, 1998). The generated ROS thus damage vital structures and functions of cells, which results in tissue destruction (see Bonnet, 1999 and Milgrom and MacRoberts, 1998; Nyman and Hynninen, 2004). Eventually, the PS is degraded through absorption of light by a process known as 'photo-bleaching'. The photo-bleaching can result from either type I or type II reactions. Photosensitized, O_2-dependent reactions in biological systems are known collectively as photodynamic action (see Spikes, 1997).

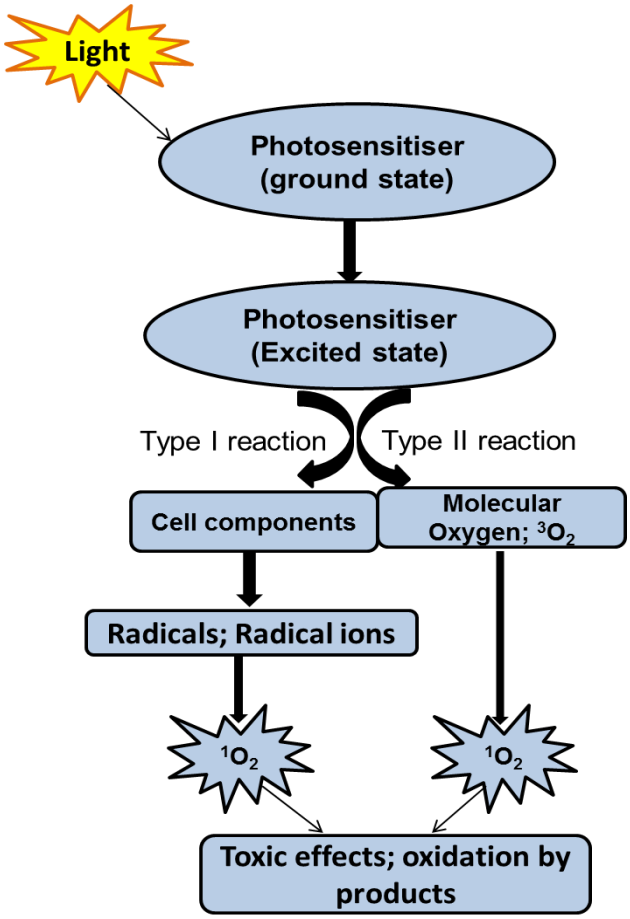

Figure 1.4. Type I and Type II reactions in PDT. There are two types of reactions occurring during PDT. Following the absorption of light, the photosensitiser is transformed from its ground state into an excited state. The activated photosensitiser can undergo two different types of reactions. It can either react directly with a substrate such as the cell membrane or a molecule, transferring a hydrogen atom to form radicals. The radicals interact with oxygen to produce oxygenated products (type I reaction). Alternatively the activated photosensitiser can transfer its energy directly to oxygen to form $^1O_2$ (type II reactions). These species oxidise various substrates and damage vital structures and functions in cells.

The extent of photo-damage and cytotoxicity caused by PDT depends on many factors such as the type of PS used, its extracellular and intracellular localisation, the administered dose, the total light exposure dose, light fluence rate, oxygen availability and the time between the drug administration and the light exposure. All these influence the efficiency of PDT independently (Palumbo, 2007; Dolmans *et al*, 2003; Nowis *et al*, 2005).

The tumour damage resulting by PDT is caused by three independent processes: direct tumour cell killing, damage to the vasculature, and activation of non-specific immune responses (Golab *et al*, 2000; van Duijnhoven *et al*, 2003; Abels, 2004).

The most important effect caused by photo-activation is direct cell killing (Henderson *et al*, 1985). This killing is the result of the local production of ROS. Cell death in PDT may occur by apoptosis or necrosis, depending on the PS, PDT drug-light dose and on the cell genotype (Almeida *et al*, 2004). However the therapeutic responses may not be fully achieved due to some factors such as the non-homogenous distribution of oxygen within the tumor that would result in non-homogenous activation of the PS and also the non- homogenous distribution of the PS within the tumor tissue and the surrounding areas (Korbelik *et al*, 1996). Oxygen shortage can arise as a result of the photochemical consumption of oxygen during the photodynamic process as well as from the immediate effects of PDT on the tissue vasculature. Indeed rapid and substantial reduction in the tissue oxygen tension during and after illumination of photosensitised tissue has been reported (Tromberg *et al*, 1990; Pogue *et al*, 2001). The development of microvascular damage and hypoxia after PDT has been shown to contribute to the long-term tumor response, but the reduction in oxygen that occurs during PDT can limit the response. There are two ways to overcome this problem. One is to lower the light fluence rate to reduce oxygen consumption rate, and the other is to fractionate the PDT light delivery to allow re-oxygenation of the tissue (Messman *et al*, 1995; Pogue and Hasan, 1997).

1.3.2.1. Reactive Oxygen Species (ROS)

Oxygen is the most abundant element in the earth's crust which is required for all animals and plants except those that live under anaerobic conditions. Despite its important role in energy production, it can also lead to the generation of a variety of ROS as part of normal metabolism.

Oxidative stress occurs when cells are in a situation where the equilibrium between pro-oxidant and antioxidant species is broken to favor the pro-oxidant state, due to production of ROS.

Free radicals is a name given to species capable of independent existence which contain one or more unpaired electron and are able to react with other molecules to lead to potentially damaging effects due to their role in the initiation of free radical chain reactions (Riley, 1994; Ryter and Tyrrell, 1998). A biological free radical chain reaction can be initiated at the lipid bilayer of the membrane in a process called lipid peroxidation. This process will generate in the first instance fatty acid radicals and consequently fatty acid peroxyl radicals and aldehydes. The consequence of lipid peroxidation is the loss of cellular membrane integrity and necrotic cell death (see Girotti *et al*, 2001; Reelfs *et al*, 2010). Proteins and carbohydrates may also be oxidized by free radicals (see Halliwell and Gutteridge, 1999).

ROS is a collective term given not only to oxygen-based radicals but also to non-radical derivatives of oxygen which are able to form radicals. Examples of oxygen-based radicals include superoxide radical anion ($^{\bullet}O_2^-$), hydroxyl radical ($^{\bullet}OH$). Non radical derivatives of oxygen include $^1O_2$ and H_2O_2.

Both exogenous and endogenous factors can generate ROS. Examples of endogenous factors include phagocytic oxidative burst, mitochondrial respiration and

microsomal and nuclear membrane electron transfer (Danpure and Tyrrell, 1976; Tyrrell and Pidoux, 1989). Exogenous factors include ozone, ionizing and UV radiations.

ROS including $^1O_2$ may also be formed as a consequence of photochemical reactions between light, O_2 and light-reactive PS (Halliwell and Gutterridge, 1990; Foote, 1982). These include many natural substances such as porphyrins (hematoporphyrin and protoporphyrin IX), chlorophylls (*a, b*), bilirubin IXa, retinal (rhodopsin), quimones and flavins (riboflavin) (see Spikes, 1986).

Uncontrolled production of ROS is harmful to biomolecules causing cell injury and cell death (i.e. apoptosis or necrosis). In addition excessive ROS production has been implicated in initiation and progression of a number of pathologic disorders notably chronic inflammatory disease and cancer [see Halliwell and Gutteridge, 1999; De Groot, 1994; Stohs and Bagchi, 1995; Tenopoulo *et al*, 2005; Trenam *et al*, 1992].

1.3.2.1.1. ROS Production by UVA Radiation

UVA (320-400 nm) radiation, the oxidizing component of sunlight produces $^1O_2$ and other ROS namely hydroxyl radical ($^{\bullet}OH$), superoxide anion ($^{\bullet}O_2^-$) and hydrogen peroxide (H_2O_2) through interaction with endogenous photosensitisers such as porphyrins in exposed tissues (Tyrrell, 1991; Tyrrell, 1994; Black, 1987; Trenam *et al*, 1992, Yasui *et al*, 2000).

Absorption of UVA by biomolecules may have two different outcomes:

1. Formation of reactive species in a metastable excited state.
2. Production of free radicals.

Both of the above are formed extremely fast, since chemical reactions usually occur within microseconds but could last for hours. These fast processes are eventually translated into photobiological responses which could occur in seconds but can take years to become apparent i.e. cancer.

Amongst the intracellular ROS that are generated by UVA, $^1O_2$ and H_2O_2 are thought to be the most important species, promoting biological damage in exposed tissues via iron-catalysed oxidative reactions (Vile and Tyrrell, 1995). It has been demonstrated that physiologically relevant doses of UVA, induce lipid peroxidation in membranes of human primary fibroblasts and keratinocytes via pathways involving iron and $^1O_2$ (Vile and Tyrrell, 1995; Morlier *et al*, 1991; Punnonen *et al*, 1991).

In relation to UVA, current data suggests that $^{\bullet}O_2^-$ is not involved in any of the cellular effects mediated by UVA, including lipid peroxidation and protein oxidation (Vile and Tyrrell, 1995; Giordani *et al*, 1997).

Immediate cellular effects of physiologically relevant doses of UVA include depletion of cellular glutathione (GSH) content, membrane lipid peroxidation and alteration in nuclear transcription factor activity and gene expression (Tyrrell, 1996; Vile & Tyrrell, 1995; Djavaheri *et al*, 1996; Wlaschek *et al*, 1997; Klotz *et al*, 1997).The potential that UVA has in photokilling by GSH depletion provides further evidence for ROS involvement in UVA effects (Tyrrell and Pidoux, 1988). The UVA-induced generation of $^1O_2$ has been shown to play an important role in UVA-induced peroxidation of membrane lipids of cultured human skin fibroblasts as well as activation of nuclear

transcription factors such as nuclear factor kappa-B (NF-kappaB) (Gaboriau *et al*, 1995; Reelfs *et al*, 2004).

A major consequence of UVA irradiation of human skin cells is the immediate release of chelatable 'labile' iron (LI) in the cytosol that appears to exacerbate the oxidative damage exerted by ROS generated by UVA. The UVA-mediated increase in LI in human skin fibroblasts plays a key role in activation of NF-kappa B and UVA-induced necrotic cell death (Pourzand, 1999; Zhong, 2004; Pourzand and Tyrrell, 1999; Reelfs *et al*, 2004; Reelfs *et al*, 2010). Studies with iron chelators have further demonstrated that iron-catalysed ROS are also certainly involved in UVA-induced NF-kappaB activation, membrane damage and cell death (Reelfs *et al*, 2004; Zhong *et al*, 2004; Yiakouvaki *et al*, 2006; Reelfs *et al*, 2010).

1.3.3. Cell Death:

The cells which form a multicellular organism belong to a very highly controlled community. This is controlled not only by maintaining the rate of cell division but also controlling the rate of cell death. Cell death is a normal part of development which continues throughout life and this loss is replaced by cell division. It is now evident that cell death may occur via different pathways. Historically three distinct ways of cell death have been identified in mammalian cells by morphological criteria.

1) Apoptosis: Also named type I cell death, is a programmed cell death that often occurs in multicellular organisms (Douglas, 2011). The morphological changes include chromatin condensation and fragmentation which results in an overall shrinkage of cell, blebbing of the plasma membrane and thus formation of apoptotic bodies that includes nuclear or cytoplasmic material.

Apoptosis is a tightly controlled, energy-consuming process of suicidal cell death involving activation of hydrolytic enzymes such as proteases and nucleases leading to DNA fragmentation and degradation of intracellular structures (see Reed, 2000).

2) Autophagic Cell death: otherwise known as type II cell death, is described by a huge accumulation of double membrane vacuoles otherwise called autophagosomes which would in turn fuse with lysosome vacuoles (Proskuryakov *et al*, 2003).

3) Necrosis: or type III cell death that leads to the premature cell death in living tissues (Proskuryakov *et al*, 2003). Necrosis is considered as an irreversible cell injury and concludes in dense clumping and disruption of genetic material. Typical morphological changes include cytoplasmic swelling and vacuolation, degradation of plasma membrane, dilation of organelles i.e. mitochondria. Upon swelling of cells they burst open and thus elicit a damaging inflammatory response (Festjens *et al*, 2006). Furthermore during necrosis an elevated level of intracellular calcium is observed which generally accumulates within the cytosol which in turn triggers mitochondrial calcium overload, resulting in inner mitochondrial membrane depolarization and prevention of ATP production (Orrenius *et al,* 2003). Increased calcium levels will in turn activate calcium-dependent proteases, (e.g. calpains), and calcium fluxes, ATP depletion and oxidative stress are results of this. These events that occur inside the cell often happen under excessive trauma. Necrosis can also be the result of death receptor activation or chemotherapy. These were conditions that were originally thought to lead to cell death by apoptosis.

Table 1.1 shows some distinctive features of apoptosis versus necrosis.

Table 1.1. Morphological, biochemical and physiological features in apototic and necrotic cells

Apoptosis	Necrosis
Morphological features Membrane blebbing, no loss of integrity	Loss of membrane integrity
Aggregation of chromatin at the nuclear membrane	No chromatin aggregation
Begins with shrinking of cytoplasm and nucleus condensation	Cytoplasm and mitochondrial swelling
Preservation of mitochondria	Swelling of organelles
Formation of apoptotic bodies	Total cell lysis
Biochemical features Tight regulation involving mediators and enzymes	Loss of ion homeostasis
Energy (ATP) dependent (active process)	No energy required (passive process)
Non-random inter-nucleosomal DNA fragmentation.	Random digestion of DNA
Release of some mitochondrial proteins i.e. cytochrome C	Oxidative stress, calcium overload, ATP depletion
Activation of caspase cascade	Activation of calcium depletion proteases
Loss of plasma membrane	

Physiological features Removal of damaged, transformed or infected cells	Back up mechanism of apoptosis failure
Initiates via physiological stimuli	Induced by severe physical or chemical injuries
Phagocytosis by adjacent cells or macrophages	Phagocytosis by macrophages
No inflammatory response	Extreme inflammatory response

Note: Adapted from “Apoptosis, cell toxicity and cell proliferation”, fourth edition, Roche.

1.3.4. PDT and Cell Death

Cell death in PDT may occur by apoptosis or necrosis, depending on the PS, PDT drug-light dose and on the cell genotype (Almeida *et al*, 2004). Necrosis is the pathological process, which occurs when cells are exposed to a serious of physical or chemical insults whereas apoptosis or programmed cell death is the physiological process responsible for the elimination of superfluous, aged or damaged cells.

Apoptosis was initially determined as the main mode of cell death caused as a result of PDT in various experimental settings applying different PS and cell types (Oleinick *et al*, 2002). It was however, the only form of cell death investigated in many of these studies. Recent research studies suggest that depending on the PDT conditions, cells may also die by necrotic cell death. Indeed increasing amounts of experimental data indicate that at optimal PDT conditions such as sufficient PS concentration and light exposure, tumour cells die mainly by necrosis (see Nowis *et al*, 2005). Induction of necrosis post-PDT is in fact desirable. This is not only due to the finding that tumour cells are resistant to apoptosis (Ahn *et al*, 2004), but also due to the fact that

necrosis also triggers a potent inflammatory response which may result in tumour-specific immunity (Krishna *et al,* 2012). Factors influencing necrosis may include extra-mitochondrial localization of PS, high dose of PDT, and glucose starvation (Almeida *et al*, 2004; Dellinger, 1996; Kiesslich *et al*, 2005; Oberdanner *et al*, 2002; Kirveliene *et al*, 2003; Plaetzer *et al*, 2002), although the research in this field is still ongoing.

Apoptotic cell death in PDT is mostly observed with PS that accumulate in mitochondria (Krieg *et al*, 2003; Fabris *et al*, 2001). Increasing the concentration of the PS and the light dose usually changes the mode of death from apoptosis to necrosis. The latter appears to be related to the availability of intracellular ATP following PDT, as the progression of cell death to apoptosis or necrosis is known to be dependent on the effect that the damage to the mitochondrial membrane imposes on the cellular level of ATP (see Reed *et al*, 1998). Damage to the mitochondrial membrane triggers a series of events that include opening of a high conductance permeability transition pore in the inner membrane of the mitochondria and release of cytochrome c from these organelles. These events lead to interruption of electron chain transport resulting in ROS production, loss of electrochemical gradient across the inner membrane leading to ATP depletion followed by necrosis (see Reed, 1999 and Reed *et al*, 1998). As the presence of ATP is essential for the activation of apoptosis protease activating factor-1 (Apaf-1) and subsequent activation of caspases that induce apoptosis (see Pourzand and Tyrrell, 1999 ; Reelfs *et al*, 2010), it appears that the high PDT dose insult (i.e. causing ATP depletion as a result of severe damage to the mitochondrial membrane as well as glucose starvation (i.e. interrupting the main supply of intracellular ATP) may trigger predominantly necrotic cell death in treated cells/tissues. Therefore the extent of

photochemical damage to cellular targets involved in energy supply especially mitochondria may be the crucial determinant for the mode of cell death.

For example, in a study by Plaetzer and coworkers (2002) using a human epidermoid carcinoma cell line, it has been shown that in cells treated with a phthalocyanine-based PS, the intensity of light dose is a major determinant of mode of cell death after PDT, depending on the changes occurring in mitochondrial function and intracellular ATP. With a moderate dose of light, 50% of cells died by either apoptosis or necrosis, but at a higher light dose, cells exclusively died by necrosis. The study of mitochondrial function and intracellular level of ATP in the PS-treated cells revealed that after PDT, necrosis was associated with a rapid decrease in mitochondrial activity and intracellular ATP, while with apoptosis, the decline in mitochondrial activity was delayed and the ATP level was maintained at near control levels. The results of this study indicate that the magnitude of light dose rather than the type of PS plays an important role in the decision of the cell to undergo either apoptotic or necrotic cell death after PDT. Hence, apoptosis and necrosis may not necessarily be two independent pathways and may even share common events, at least in the early phases of the cell death process. This assumption is endorsed by a series of studies demonstrating that the magnitude of initial insult of various oxidants could be the main determinant of apoptotic and/or necrotic cell death processes (e.g. Bonofoco *et al*, 1995; Hampton *et al*, 1997).

Kirveliene and coworkers (2003) demonstrated that in a murine hepatoma cell line, the intracellular ATP concentration correlates with the mode of cell death in cells treated with PS that localise to mitochondria but not to lysosomes. Photosensitisation of cells with $TPPS_4$ (meso-tetra(4-sulfonatophenyl)-porphine) that localises to lysosomes caused necrotic cell death and the mode of cell death was independent of

the energy metabolism. In contrast, photosensitisation of cells with ALA that localises predominantly in mitochondria, under conditions favourable to glycolysis, led to cell death by apoptosis, however under conditions unfavourable to glycolysis (ATP depletion), caused necrotic cell death. These data suggest that in ALA-mediated PDT, intracellular ATP level and caspase activation are the downstream controllers of the mode of cell death, directing the photosensitised cells toward either apoptotic or necrotic cell death depending on intracellular ATP availability.

Nevertheless in general in PDT, during the illumination, the photo-bleaching of the PS as well as vasculature stasis and tumour oedema can decrease the concentration of PS. Under these conditions as well as in deep tumour regions (illuminated with suboptimal light from the very beginning of treatment), the effectiveness of PDT is compromised and tumour cells will either oppose or repair damage induced by the treatment. Upon damage repair, tumour cells will survive the treatment and will contribute to tumour relapse (if not damaged by lethal ischemia or activation of immune response) (Nowis *et al*, 2005). In all other cases tumour cells will undergo apoptosis or necrosis, depending on the severity of the PDT insult and ATP depletion.

1.3.5. Photosensitisers in PDT:

1.3.5.1 First Generation Photosensitisers

The use of porphyrin-based photosensitisers, with which many clinical studies have been conducted in PDT, was first introduced in 1961 by Lipson and coworkers. Through the period of 1961-1983, hematoporphyrin (HP) and its derivatives were the

most common photosensitisers used in PDT research (see Bonnett, 1999). Therefore these tetrapyrroles comprise the first generation of photosensitisers.

In 1960, HP was purified and solubilised by Lipson and Baldes by treatment with 5% sulphuric acid in acetic acid, then basification and neutralization to pH 7.4 with hydrochloric acid. The purified compound was called hematoporphyrin derivative (HPD) which had a better affinity for tumour cells than HP, and it could also be visualised by fluorescence endoscopy when injected into the tumour (Lipson *et al*, 1961). In 1972, Diamond and colleagues suggested that the combination of tumour localizing and tumour phototoxic properties of porphyrins might be exploited to diminish cancer cells (Diamond *et al*, 1972). In 1978, a study was carried out by Dougherty and co-workers which demonstrated that parenterally administered HPD could be activated by light in the red region of the spectrum (630 nm) to cause complete eradication of spontaneous or transplanted mammary tumours in mice and rats (Dougherty *et al*, 1978). Meanwhile, Kelly and co-workers found that light activation of HPD also eliminated bladder carcinoma in mice (Kelly *et al*, 1975). These studies classified HPD as the benchmark PS for the development of forthcoming drugs (see Kalka *et al*, 2000 and Dolmans *et al*, 2003).

HPD is a complex mixture, thus a further chemical purification allows better penetration. The purified compound known as Photofrin has shown enhanced photosensitising properties (see Liu, 1992; Dougherty, 1987). Photofrin was the first approved photosensitising drug for clinical PDT of lung, gastric and cervical cancer (see Evensen, 1995).

1.3.5.2 Second Generation Photosensitisers

The poor selectivity of first generation photosensitisers between tumour and normal tissue, and their long clearance time that led to prolonged skin photosensitivity in subjects, stimulated the design of improved synthetic photosensitisers for PDT. These compounds are referred to as ‘second generation photosensitisers’.

Second generation photosensitisers have been designed to assure these compounds are pure and also able to absorb at higher wavelengths i.e. far red (660-700 nm) or near infrared (700-850 nm) regions of the spectrum. This also allows deeper penetration of activating light (up to 20 mm compared to 5-10 mm in 630 nm) into tissues than the first generation photosensitisers. This would thus provide more efficient therapeutic effects subject to the presence of a sufficient amount of oxygen (Nyman and Hynninen, 2004; Wilson *et al*, 1984).

Furthermore, unlike the photosensitisers that absorb in the visible range, the ability of second generation photosensitisers absorbing within the near-infrared range allows the treatment of highly pigmented tumours such as melanoma metastases. Light with a wavelength longer than 850 nm is not typically used however because it does not yield enough energy to trigger a photochemical reaction (Calzavara-Pinton *et al*, 2007).

The second generation of photosensitisers comprise families of molecules such as modified porphyrins, bacteriochlorins, phthalocyanines, naphthalocyanines, pheophorbides and purpurins. These photosensitisers have been used as PDT agents in clinical trials to treat various cancers including cutaneous malignancies.

A brief description of these photosensitisers is provided below.

- **Phthalocyanines and** naphthalocyanines**:** This group of photosensitisers contain four benzene or naphthalene rings joined to the π-pyrrolic framework of porphyrins, with the methine bridge carbons replaced with nitrogens (see **Figure 1.5**). These compounds are known to absorb light at longer wavelengths than simple porphyrins, and for this reason may be used in much smaller doses than photofrin (i.e. 4-5 folds lower than photofrin). Their absorption at higher wavelengths than 400-600 nm also lowers the risk of generalised photosensitivity with sunlight compared to porphyrins (Moan and Berg, 1992; Jori, 1992).

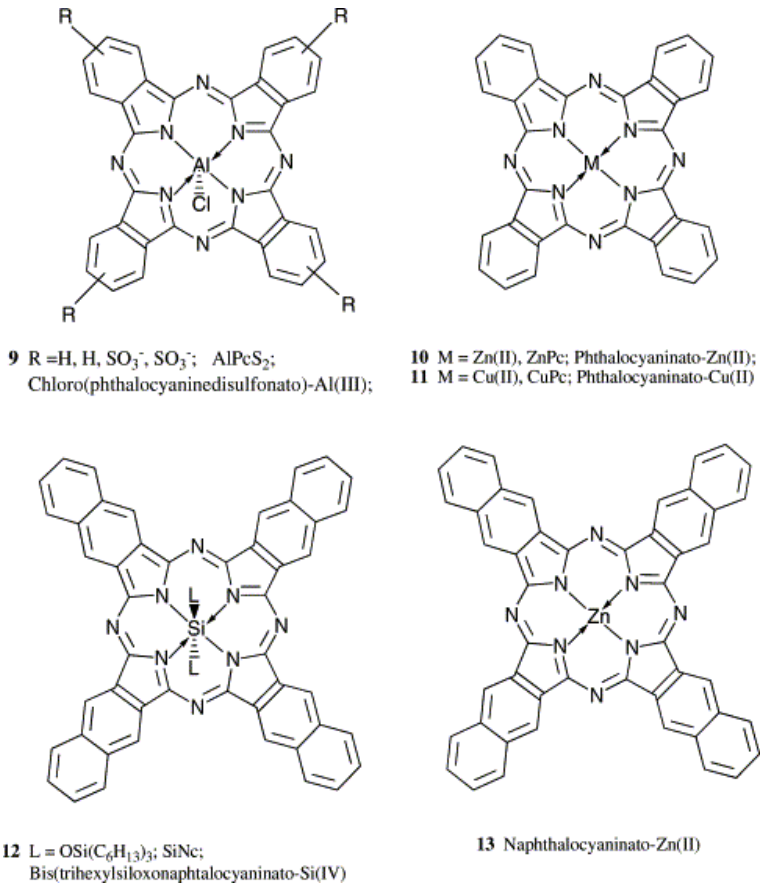

Figure 1.5. Chemical structures of phthalocyanines and naphthalocyanines relevant to PDT. (Source: Nyman and Hynninen, 2004).

There have been some promising effects seen by application of phthalocyanines for PDT of cancer. The incorporation of diamagnetic metals such as Zn or Al into the phthalocyanine macromolecule increases the half-life of the triplet state and in turn increases the yield of $^1O_2$ generation to obtain sufficient photosensitisation and resulting phototoxicity in the target tissue (see Jori, 1992). One such derivative is $AlPcS_2$ (chloroalmunium sulphonated phthalocyanine).The advantages of these compounds may be defined in terms of higher chemical stability, superior direct tumour cell phototoxicity, and a strong absorption peak in the red spectrum (650-700 nm), which assures deeper penetration into the tissue in comparison to porphyrins (Spikes, 1986; Oleinick *et al*, 1993; Rosenthal, 1991). These properties together with negligible dark toxicity and excellent photodynamic activity at increased wavelengths has resulted in clinical evaluation of $AlPcS_2$ for PDT (Ben-Hur E, 1992; Gerber-Leszczyszyn *et al*, 2004). A recent study by Shao and colleagues (2012) has focused on developing a new photosensitiser namely “photocyanine” that has evolved from meta phthalocyanine that is specifically designed for the treatment of cancer and has been tested on hepatocellular carcinoma (HCC) HepG2 cells. The chemical structure of photocyanine is shown in **Figure 1.6**.

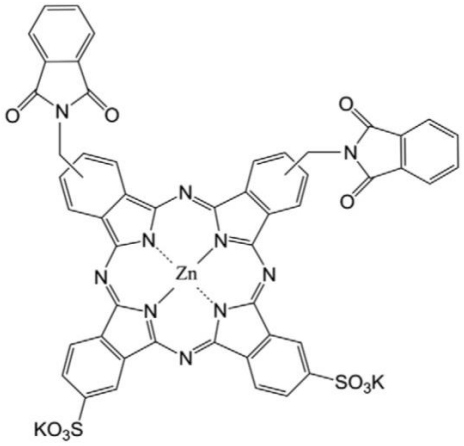

Figure 1.6. Chemical structure of Photocyanine.

Photocyanine has a high photodynamic activity and low dark toxicity. It is only excited at a wavelength of 670 nm, therefore no side effects are produced upon exposure to light in the visible range. Once excited, photocyanine has a high quantum yield and an appropriate half-time. Furthermore it has a very high selectivity for tumour tissue. Photocyanine has currently completed phase I human clinical trials.

- **Chlorin and Bacteriochlorin derivatives:**

Chlorins are dihydroporphyrins that are formed by reduction of a peripheral double

bond in the porphyrin skeleton. This moves the absorption peak to the red (Nyman and Hynninen, 2004). Amongst the chlorin derivatives, the meta-tetrahydroxyphenyl chlorine (m-THPC) is widely used in the treatment of respiratory, and head and neck cancers (see Hopper, 2000 and **Figure 1.7**). m-THPC (Temoprofin, Foscan®; Biolitech Pharma, Edinburgh, Scotland, UK) is a pure compound which is 200-fold more effective than Photofrin (see Sharman *et al*, 1999). It is excited at higher wavelengths than Photofrin (650 nm rather than 630nm) and has a higher molar absorption coefficient (i.e. 15-fold higher). Also with its higher half-life in the excited triplet state and higher hydrophobicity which makes the cellular uptake easier, it has shown much improved features for use in dermatological treatments (e.g. Copper *et al*, 2003; Campbell *et al*, 2004). A water-soluble formulation of m-THPC named Fospeg®, shows much reduced dark toxicity in comparison to Foscan® but a similar phototoxic efficiency. Both these compounds have been shown to induce apoptosis in the epidermoid carcinoma cell line, A431 over a wide range of fluences (Allison *et*

al, 2004; Berlanda *et al*, 2010). Nevertheless the residual photosensitivity of m-THPC is comparable to that of Photofrin (see Palumbo, 2007).

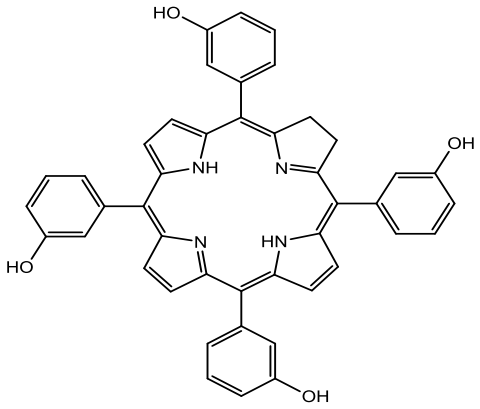

Figure 1.7. Chemical structure of meta-tetrahydroxyphenyl chlorin (m-THPC).

A number of companies have also developed promising bacteriochlorins with improved optical properties absorbing light at more than 740 nm that might be particularly useful for PDT of pigmented tumours (see Jori, 1992 and **Figure 1.8**). Amongst these compounds, SQN400 (trade name for meta-tetra-hyroxyphenyl bacteriochlorin; mTHPBC) has been used in some clinical phase I studies (e.g. van Duijnhoven *et al*, 2005) (see **Figure 1.9**).

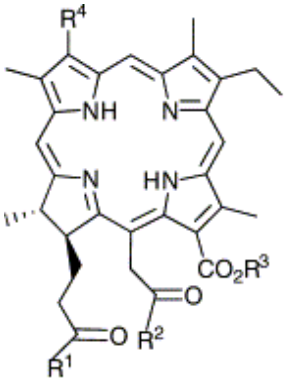

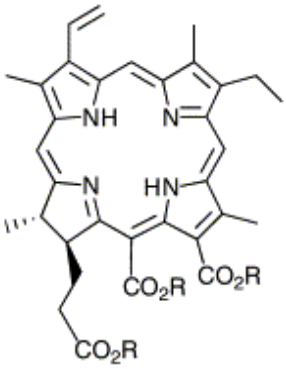

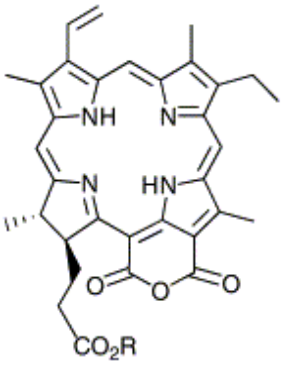

50 $R^1 = R^2 = OH$, $R^3 = H$, $R^4 = CH{=}CH_2$; chlorin e_6;
51 $R^1 = OCH_3$, $R^2 = OH$, $R^3 = H$, $R^4 = CH{=}CH_2$; methyl chlorin e_6;
52 $R^1 = R^2 = OCH_3$, $R^3 = H$, $R^4 = CH{=}CH_2$; dimethyl chlorin e_6;
53 $R^1 = NH(CO_2H)CHCH_2CO_2H$, $R^2 = OH$, $R^3 = H$, $R^4 = CH{=}CH_2$; mono-L-aspartyl chlorin e_6;
54 $R^1 = R^2 = NH(CO_2H)CHCH_2CO_2H$, $R^3 = H$, $R^4 = CH{=}CH_2$; di-L-aspartyl chlorin e_6;
55 $R^1 = R^2 = OH$, $R^3 = H$, $R^4 = CH_2CH_3$; mesochlorin e_6

56 R = H; chlorin p_6;
57 R = CH_3; trimethyl chlorin p_6

58 R = H; purpurin 18;
59 R = CH_3; methyl purpurin 18

Figure 1.8. Completely synthetic chlorin and bacteriochlorin drivatives that have been proposed for PDT. (Source; Nyman and Hynninen, 2004).

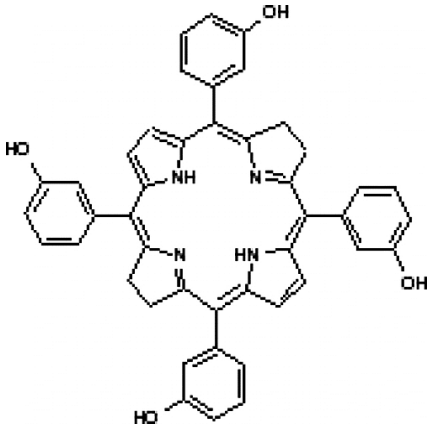

Figure 1.9. Chemical structure of meta-tetra-hydroxyphenyl bacteriochlorin (mTHPBC).

- Other porphyrin- and chlorophyll-derived photosensitisers:

Among synthetic porphyrins, porphines exhibit high photosensitising and anti-mitotic potency in tumours (see Kreimeier-Birnbaun, 1989). $TPPS_4$ (tetra-sodium-meso-

tetraphenylporphine-sulfonate) is a member of this family. Despite its hydrophilic nature, it has been investigated for the treatment of skin tumours (Santoro *et al*, 1990). $TPPS_4$ is activatable at 630 nm and localizes preferentially in the tumour stroma (Kessel *et al*, 1987). Furthermore in comparison to HPD, it is highly effective as a PS (Calzavara-Pinton *et al*, 2007). The major limitation of $TPPS_4$ is its neurotoxicity (Lui and Anderson, 1992).

The benzoporphyrin derivative monoacid ring A (BPD-MA) that is also known as verteporphin (Visudyne®, Novartis AG, basel) is a semi-synthetic porphyrin derived from protoporphyrin (Henderson and Dougherty, 1992) (see **Figure 1.10**). Because of its poor solubility, this PS has been formulated successfully either in liposomes or emulsions (Knobler *et al*, 1999). BPD-MA has an absorbance peak at 650 nm and is used in the treatment of choroidal neovascularisation in age-related macular degeneration (AMD). This PS has also been evaluated for PDT of BCC and SCC (Kalka *et al*, 2000). Phase III clinical trials (see Gerber-Leszczyszyn *et al*, 2004) have shown that injectable BPD-MA provides a significant and rapid accumulation in the tumour and a low residual skin photosensitivity, and the overall cosmetic effect has been found acceptable.

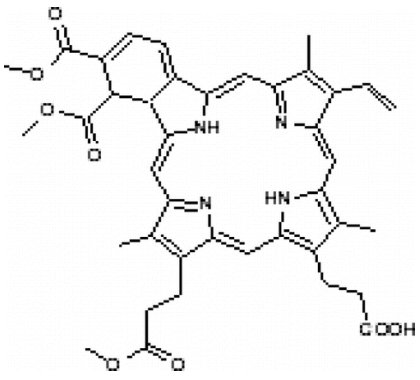

Figure 1.10. Chemical structure of benzoporphyrin derivative monoacid ring A (BPD-MA).

Porphycenes are structural isomers of porphyrins and texaphyrins are modified porphyrins in which a phenyl ring replaces one pyrrole ring. Porphycenes have potential to be used as diagnostic tools (Palumbo, 2007) as they possess high fluorescence yields and show a 10-fold increase in light absorption at 630 nm when compared with HPD (Kreimer-Bimbaum, 1989). The porphycene dye 9-acetoxy-2,7,12,17-tetrakis-methoxyethyl-porhycene has also been evaluated for potential topical PDT of skin lesions (Karrer *et al*, 1997) (see **Figure 1.11**).

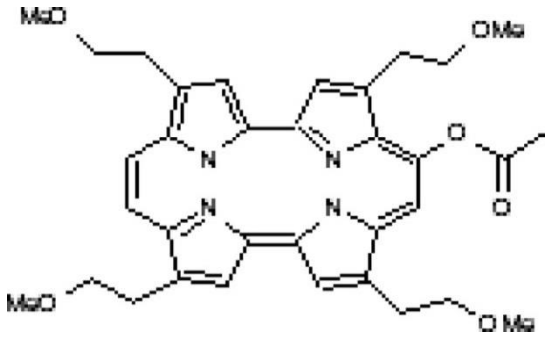

Figure 1.11. Chemical structure of 9-acetoxy-2,7,12,17-tetrakis-methoxyethyl-porphycene.

Texaphyrins can easily be complexed with large metal cations such as Lu (III) to give metal complexes that are photoactive *in vivo* (Nyman and Hynninen, 2004). The Lu(III)-complex of a texaphyrin, also known as Lu-Tex or Lutryn® (Pharmacyclics Inc., CA, USA; see **Figure 1.12**) is a highly fluorescent dye. It absorbs strongly at 732 nm (Woodburn *et al*, 1996), and rapidly accumulates in neoplastic tissue allowing irradiation within 2-4 h after administration (Kalka *et al*, 2000). One of the main advantages of Lu-Tex is its lack of persistent skin phototoxicity (Sessler and Miller, 2000). As a result, Lu-Tex has been evaluated in the therapy of various malignancies, such as recurrent breast cancer, invasive SCC, malignant melanoma, Kaposi's sarcoma and BCC. These evaluations have demonstrated the best

response rates in breast cancer lesions and partial responses in other treated tumours (Renschler *et al*, 1997; Palumbo, G, 2007). Lu-Tex is known to cause severe cutaneous pain during PDT however (Kreimer-Bimbaum, 1989).

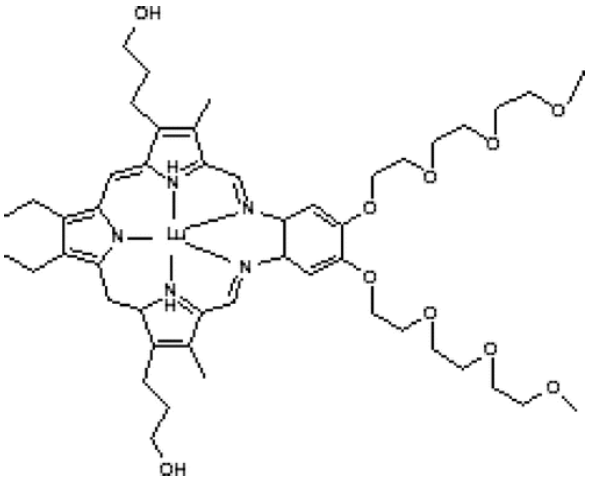

Figure 1.12. Chemical structure of Lu (III) texaphyrin (Lu-Tex).

Pheophorbides are a group of chlorophyll-derived photosensitisers. Within this group of photosensitisers, 2-[1-hexyloxyethyl]-2-devinyl pyropheophorbide-a (HPPH) has been assessed successfully in Phase II clinical trials (NCT00281736) for the treatment of oesophageal cancers with very mild skin photosensitivity declining rapidly within days (Bellinier *et al*, 2005). HPPH-23 is a promising member of this group for the management of skin cancer. This PS has been successfully used in PDT of SCC in animal studies and has the advantage of being rapidly cleared from normal skin (Magne *et al*, 1997).

Hypericin (see **Figure 1.13**) is another PS that is recognised as a potent agent in PDT of cancer. It is a naturally occurring substance found in plants (*Hypericum perforforatum*) that possesses strong photosensitising properties, a high yield of $^1O_2$ and fluorescence emission. These properties of hypericin make it a powerful tool for

photodiagnosis of small tumors (e.g. urothelium) (Kubin *et al*, 2005; Olivo *et al*, 2003; Palumbo, 2007).

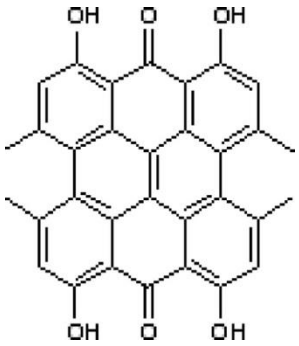

Figure 1.13. Chemical structure of Hypericin

More current studies have been carried out to try and focus on improving the photosensitisers to increase the efficiency of PDT. For example Parihar and colleagues (2013) have used a chlorin p_6-histamine conjugate (Cp_6-his) for improving cellular uptake and phototoxicity of Cp_6 in an oral cancer cell line. This photosensitiser belongs to the chlorin family of photosensitisers and chlorin p_6 itself, has a very basic tetrapyrrole stucture. In the study mentioned above, it was applied intravenously, where the affected tissue was illuminated with red light (660±25 nm, 100 J/cm^2). Its advantages were quick clearance from the body, ~80% 48 h post treatment, and also treating bigger tumours (up to 1000 mm in size). It also had a very high tumour selectivity.

1.3.5.3. Topical Photosensitising Mediators: Aminolevulinic Acid and esters:

An alternative method of photosensitising cells is to stimulate the synthesis of the endogenous photosensitiser protoporphyrin IX (PPIX). PPIX is the immediate precursor of heme. Administration of exogenous δ-aminolevulinic acid (ALA) that is

an intermediate of the heme biosynthetic pathway can bypass the negative feedback control of heme, therefore resulting in intracellular accumulation of photosensitising concentrations of PPIX. The photosensitisation obtained by this treatment regimen, provided a basis for application of ALA-induced PPIX for PDT of cancer (Malik and Lugaci, 1987; Kennedy *et al*, 1990; Wolf and Kerl, 1991; Peng *et al*, 1997).

In ALA-mediated PDT, the porphyrin precursor ALA or its methyl ester derivative, (MAL) is administered topically to the skin. ALA can penetrate the skin cells through the cell membrane with its chemical composition intact. On the other hand its ester derivative MAL once administered goes through a hydrolysis reaction in the cytoplasm of tumour cells to release ALA. ALA then goes through a series of intermediate reactions which are catalysed by various intracellular enzymes to form PPIX. The intracellular accumulation of this PS should then be more concentrated in the target tissue (Matei *et al*, 2013). Supplementation of ALA is followed by application of a light source, often red (630-635 nm laser) or blue (380-420 nm) to the tumour tissue. In the case of a positive treatment response, the photochemically generated ROS formed, will diminish the tumour tissue sparing the surrounding normal structures.

The fluorescence of ALA-induced PPIX can also be used for the purpose of diagnostic detection of tumour cells, i.e. in early stages of skin malignancies. This procedure, termed photodynamic diagnosis (PDD), allocates the poorly defined tumour borders before the use of invasive treatment modalities.

1.3.5.3.1. Heme Metabolism

The heme biosynthetic pathway is initiated by the rate-limiting reaction between glycine and succinyl-coA to produce ALA by a condensation reaction. This enzymatic reaction is catalysed by the enzyme ALA-synthase (Cotter *et al*, 1992), which is regulated via negative feedback mechanism by heme. (See **Figure 1.14**).

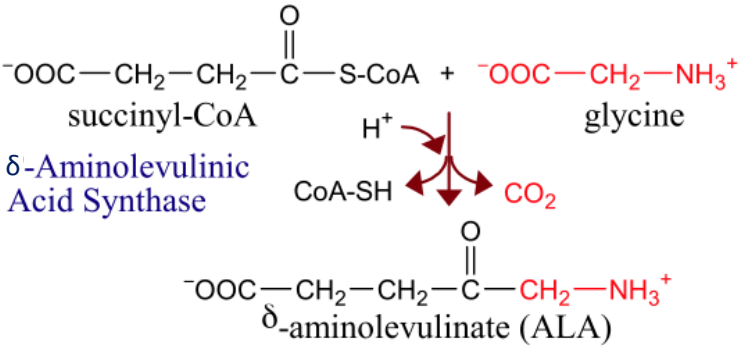

Figure 1.14. Synthesis of delta-aminolevulinic acid (ALA) from glycine and succinyl coA catalysed by ALA-synthase.

Figure 1.15. Illustrates the heme biosynthetic pathway. Following its synthesis, ALA exits the mitochondria and enters the cytosol (see **Figure 1.15)**. The next reaction takes place by joining of two molecules of ALA to form the monopyrrole porphobilinogen (PBG) via another condensation reaction which is catalysed by aminolevulinate-dehydratase enzyme (ALAD) (Erskine *et al*, 1999; Frankenberg *et al*, 1999). A polymer of four molecules of PGB is generated in the cytosol by the combined action of the enzymes PBG-deaminase (PBGD) and uroporphyrinogen III co-synthase, which is followed by cyclisation of the tetrapyrrole chain to form uroporphyrinogen III (Xu *et al*, 1995). The next product named coproporphyrinogen III is formed by removal of four acetic acid carboxyl groups, catalysed by uroporphyrinogen decarboxylase (Moore *et al*, 1987). The subsequent steps in this pathway which take place in the mitochondria lead to the build-up of PPIX. The final

step takes place on the inner surface of the inner mitochondrial membrane where iron is brought into PPIX by the enzyme ferrochelatase to produce heme. If an excess of PPIX is synthesized, it can diffuse from the mitochondrion into the endoplasmic reticulum and also into the plasma membrane, both of which are the other known sites of cellular damage through PDT (Barr *et al*, 2002).

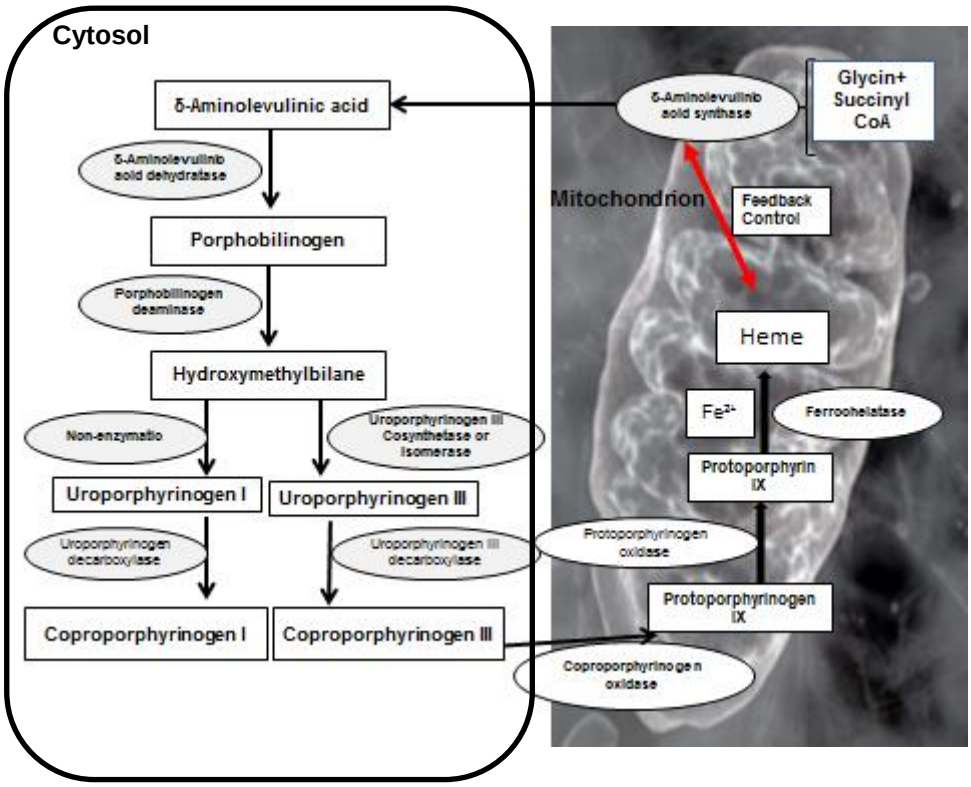

Figure 1.15. Heme biosynthesis pathway.

(modified from:https://www.microbewiki.kenyon.edu/index.php/mitochondria)

1.3.6. Topical ALA-PDT

The most important advantage of application of topical ALA-PDT over the systemic HPD/ Photofrin-PDT is the non-existence of the prolonged cutaneous photosensitivity. With topical ALA-PDT after 24 h there is no sign of photosensitivity

reported by patients, whereas this is clearly seen in the systemic HPD/ Photofrin-PDT up to 4-6 weeks post-treatment. Furthermore, patients treated with systemic HPD/ Photofrin-PDT often have to be kept in hospital for a few days unlike the patients that have undergone topical ALA-PDT who may be discharged immediately.

ALA-PDT is relatively inexpensive since the light source used for this treatment may be ordinary lamps with the appropriate filters, whereas for HPD/ Photofrin-PDT lasers are usually applied as the light source which are much more costly to buy and maintain.

ALA-PDT has been shown to have a very high selectivity for tumour tissues sparing the surrounding normal structures, and the porphyrins generated accumulate predominantly in the target tissue after administration of exogenous ALA. Also with this treatment modality, either a few individual lesions may be targeted and treated at the same time or a repeated treatment may be performed on the same lesion.

The mechanism of ALA penetration through tissues after topical application is not yet fully understood, however the fluorescence of ALA-mediated PDT in both normal and malignant tissue has shown to increase with time after topical ALA application, reaching a plateau within 4-14 h, depending on ALA concentrations used (2-40%) in formulations, the amount to be applied (30-50 mg/ cm^2), and application time (up to 24 h) used (Orenstein *et al*, 1995; Morton *et al*, 1995; Peng *et al*, 1997). When ALA is topically applied and incubated for up to 4 h the PPIX accumulation will be locally at the site of interest. However longer incubation periods with ALA (up to 14 h) or when combined with skin penetration enhancers i.e. DMSO, results in a more generalised photosensitisation of the skin (Orenstein *et al*, 1995; Peng *et al*, 1997).

Generally ALA-induced PPIX fluorescence cannot be detected in the skin 24 h after completion of topical ALA application. There is no proof of ALA's toxicity when concentrations < 50% in water/oil emulsion by weight are topically applied for at least 48 h. Moreover, there is no evidence for toxicity of ALA-mediated PPIX accumulation on tissues before light exposure (Peng *et al*, 1997). Cellular studies have demonstrated that ALA can be administered at very high concentrations without producing cytotoxic effects in the dark. At concentrations lower than 3 mM, no dark cytotoxic effects could be observed (e.g. Pourzand *et al*, 1999b, Berlanda *et al*, 2010 and the present study). The intracellular production of PPIX is almost linear over incubation time (up to 30 h), while the accumulated PPIX from the ALA application degrades quite rapidly, and therefore decreasing the length of light sensitivity after PDT. Another advantage of ALA-induced PPIX is that it is only produced in living cells, which is beneficial for treatment of cells without production of ROS in the surrounding extracellular matrix (Berlanda *et al*, 2010).

While topical ALA-PDT has been shown to have a good cosmetic outcome, it is more suitable for superficial lesions than nodular tumours in comparison to HPD/Photofrin-PDT (Peng *et al*, 1997). The optimal concentration of ALA for topical application and also the incubation period with ALA depends on the characteristic of the targeted cells. For example, abnormal keratin shows increased permeability to ALA, which is partly responsible for the tumour selectivity. Ironically, this phenomenon contributes to a major limitation of ALA-PDT; the poor ALA penetration through intact keratinised surface layers of nodular tumours may be responsible for the therapeutic refractivity of this malignancy with topical ALA-PDT.

ALA's hydrophilic nature limits its penetration into tissues. In mammalian cells ALA is taken up by cells via active transport mechanisms, i.e. Na^+/Cl^--dependent beta-amino acid, including glycine and gamma-aminobutyric acid (GABA) transporters (Rud *et al*, 2000). These systems of uptake seem to be more activated in tumour cells; nevertheless they are saturable and slow processes that need energy in order to function, as well as depending on pH and temperature (Kloek and van Henegouven, 1996; Gaullier *et al*, 1997; Uehlinger *et al*, 2000).

To overcome this problem, the use of ALA-esters i.e. methyl aminolevulinate (MAL) which are lipophilic has improved the penetration of the drug through the skin and moreover known to selectively accumulate in neoplastic tissues similar to that of ALA.

The methyl ester of ALA, MAL, must be hydrolysed at some stage to release the ALA to be absorbed by the targeted tissues, but it is not known at which step this mechanism of hydrolysis takes place (Ericson *et al*, 2008).

An example in WiDr adenocarcinoma cells shows that MAL gets to the targeted tissue via active mechanisms particularly through transporters of non-polar amino acids such as L-alanine, L-methionine, L-tryptophan and glycine (Gederaas *et al*, 2001). An alternative route of MAL uptake by the cells is by passive trans-membrane diffusion which does not require any energy, and is also very efficient in normal cells and even to more extent in neoplastic cells. The plurality and efficiency of these diverse mechanisms determine the enhanced penetration characteristics of MAL in comparison to ALA which could even be seen more significantly in malignant cells (Peng *et al*, 1997). The process of de-esterification of MAL to ALA occurs quickly after absorption of the drug by cells, and from then on the metabolic steps remain

the same as for ALA (Gaullier *et al*, 1997). In addition ALA-ester derivatives achieve maximum intracellular PPIX concentrations with shorter incubation times of around 3 h compared to ALA (i.e. 4-6 h) (Juzeniene *et al*, 2002).

The *stratum corneum* (SC), the outer skin layer, seems to be a major factor in selectivity of uptake since it has an important impact on the penetration of ALA and its methyl esters through the skin (Moan *et al*, 2001). BCC and SCC cause abnormalities to the keratin layer and as a result lead to faster penetration of ALA through the SC. However the adjacent normal SC which is intact seems to allow slower uptake. This has been confirmed *in vivo* (Wennberg *et al*, 2000). There is evidence suggesting that MAL is more selective towards neoplastic tissues than ALA (Angell- Petersen *et al*, 2006), however there are not enough comparative studies to back this up.

There are two examples of studies evaluating the efficiency of MAL-PDT in treating difficult lesions. Horn and colleagues (2003) evaluated 123 recurrent BCCs, in a mid-face location or on severely sun-damaged skin. The response to MAL-PDT was excellent, with a 3-month CR (clearance rate) in sBCCs of 85% (40/47), nBCCs of 75% (38/51). A follow up response to the treatment was carried out at 24 months, which showed a CR of 78% for sBCCs (28/36) and 86% for nBCCs (24/28). The only factor affecting the excellent response was the diameter of the lesions. At 24 months follow up, the lesions larger than 30 mm obtained a 66% CR regardless of the site of occurrence. Also Vinciullo and colleagues (2005) carried out the treatment of 33 patients with BCCs. At 24 month follow up they had obtained 86% CR in all patients with a lower response for the lesions located on the face/ scalp (54%), but a higher response to the ones on the trunk/ neck (88%). They also found the direct relationship between the increase of diameter and decrease of response to the

therapy with 84% of lesions at 3-10 mm, 80% at 11-20 mm and 70% clearance at 20-62 mm.

Because of the significant results obtained from preclinical and clinical studies (e.g. Hongeharu *et al*, 2000), in 2003, ALA-PDT has also been approved for moderate inflammatory *acne vulgaris* in USA.

The efficiency of ALA/MAL-PDT for the treatment of superficial BCC, nBCC, AK and BD has been repeatedly demonstrated in a large number of preclinical and clinical studies that have been carried out in the past 15 years. With the exception of surgery, MAL-PDT has the best outcome for the long term cure of NMSC (Stebbins *et al*, 2011).

A number of other non-malignant conditions such as psoriasis, viral warts and hair removal have also been under clinical investigations worldwide for more than a decade (e.g. Robinson *et al*, 1999; Stender *et al*, 1999; Stender *et al*, 2000; Hongeharu *et al*, 2000; Robinson *et al*, 1999; Huang, 2005). In addition to preventing the development of scars and the dys-pigmentation that occurs with surgery, ALA-PDT has the added benefit of photo-rejuvenation and has been used as a treatment to soften the appearance of acne scars as well as fine lines and wrinkles of photo-damaged skin (e.g. Alster *et al*, 2005; Dover *et al*, 2005).

1.3.6.1. Various Light Sources Used for Topical ALA/MAL-PDT:

The first ever light sources applied in PDT were non-coherent light sources. Ever since, various different studies have been focussed on the effectiveness of long-pulsed dye lasers. Not only do they require much shorter exposure times, but the

laser sources also give the user the option of choosing the optimal wavelength for their purpose. Flash-lamps are also commonly used in PDT of AK, photo-rejuvenation and *acne vulgaris* (Alexiades-Armenakas, 2006). **Table 1.3** provides an overview of light sources used in PDT.

Table 1.3: Common light sources for PDT

Non-coherent lamps	**Laser**	**Other**
- Xenon lamps (400-1200nm) - Halogen lamps (560-800nm)	- Pulsed dye laser (PDL) (585nm) - Long-pulsed dye laser (595nm) - Argon dye laser (ADL) (450-530nm) - Diode laser (800-1000nm)	- Intense pulsed light (IPL) (500-1200nm) - Light emitting diode (LED) (631 ± 2nm) -Fluorescence diagnosis systems

Note: Modified from Klein *et al*, 2008

Photodynamic management of dermatologic conditions is simplified by the accessibility of the skin to light application and offers the option to use any light device with the appropriate spectrum corresponding to the maximum absorption of

the PS. Non-coherent sources of light are taking over from the popular filtered slide projectors especially for their use in PDT. The PDT 1200 lamp (Waldmann) is a metal halogen lamp which emits 600-800 nm radiation at light power density of 200 mW/cm^2; keeping light exposure times within practical limits (see Stables, 1995). An alternative source of light for use in PDT is the short-arc xenon lamp with a band width of 400-1200 nm which is tunable (Whitehurst *et al*, 1993).

Non-coherent light sources are safer, easy to use, and less expensive. They can produce spectra of wavelengths to be absorbed by different photosensitisers. The broad light beam produced by non-coherent lamps is useful for the treatment of large lesions using ALA-PDT. However the lower radiation power at the periphery of the treated lesion as opposed to the centre of the irradiation area may result in insufficient treatment of the tumour borders (Karrer *et al*, 1995). In the case of multiple lesions e.g. multiple AK on the scalp, it is important to deliver light from different directions to ensure the illumination of all the lesions.

Non-coherent light sources can be used in conjunction with optical filters to output selective wavelengths. The disadvantages of conventional lamps include significant thermal effects, low light intensity and difficulty in controlling the light dose. However, nowadays, most of these drawbacks can be overcome by careful engineering design. For example it is known that non-laser light sources emit significant fluences of infrared radiation together with light useful for PDT (Stringer *et al*, 1995). Filtering out the infrared radiations would help in avoiding hyperthermia; however there is evidence that mild hyperthermia (40-42^oC) brings an additional effect or works synergistically with PDT (Waldow and Dougherty, 1984; Kimel *et al*, 1992). The recommended fluence rate in order to avoid hyperthermia has been determined to be lower than 150 mW/cm^2 (Peng *et al*, 1997).

As shown in **Figure 1.16**, PPIX's biggest peak falls in to the blue region of 405-410 nm (soret band), with smaller absorption peaks at 505, 540, 580 and 630 nm. Most light sources for ALA/MAL-PDT aim to utilise the 630 nm in the red region to improve the tissue penetration. However a blue fluorescent lamp called the BLU-Light illuminator (DUSA Pharmaceuticals, Inc), (peak emission 417 nm) is now routinely used in Levulan ALA-PDT of AK in USA. There are now several reports that blue, green and red light can each be effective in topical PDT of AK, but more deeply penetrating red light is superior when treating BD and BCC (Morton *et al*, 2002).

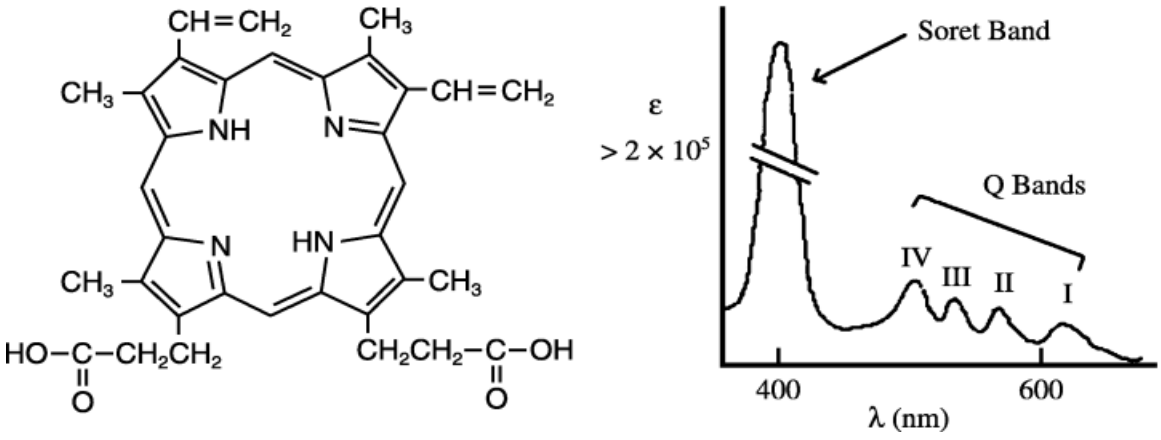

Figure 1.16. The absortion spectrum of porphyrins (right) as exemplified by protoporphyrin IX (the chemical structure; left) (reproduced from Kormeili *et al*, 2004).

Because of the use of ALA-PDT in the treatment of tumours at the surfaces of organs (i.e. the skin, bladder and aero-digestive tract), lamps may be as well suited as lasers. Unlike the traditional luminous lamps, lasers provide the exact selection of wavelengths to match the absorption of the PS of interest and the precise application of light. The tunable argon-dye laser (ADL) is composed of an argon laser that emits a blue-green beam in the 450-530 nm range, pumping a dye laser to obtain light in the range of the desired wavelength (see Kalka *et al*, 2000). Emission of light by ADL

is on a continuous basis and can be tuned to match the absorption properties of the PS of interest within the range of 350-700 nm, making it the most popular light device used in PDT (Fisher *et al*, 1995).

The few advantages that non-laser light sources possess have made them very popular in topical PDT. These include their affordable price, stability, easy application, low maintenance and ability to provide wide area illumination fields.

Retrospective comparison of laser and filtered broadband sources suggests equivalent efficacy in topical PDT (Clark *et al*, 2003). Non-laser light sources have also recently been used in ALA-PDT, as opposed to MAL-PDT which typically applies light emitting diode (LED) sources.

In the last few years, LED sources have shown considerable development, with improvements in design making these relatively inexpensive sources convenient for wide area irradiation and popular for patient use, e.g. the Aktilite 16 and 128 (Galderma, France) and the Omnilux (Phototherapeutics Ltd, Altincham, UK). These LED sources cover the 630/635 nm absorption peak of PPIX while excluding the extraneous wavelengths in broadband sources, therefore allowing shorter and quicker irradiation times. The light source used in PDT should generally present suitable characteristics to show that it does activate the PS of interest i.e. PPIX at the maximum absorption wavelength range in order to produce enough ROS to obtain a cytotoxic effect (Plaetzer *et al*, 2008). In photodynamic laser-mediated therapy usually longer wavelengths of light range are applied to the target tissues to assure increased penetration depth with minimum light scatter and maximum PS activation, which would result in tissue destruction and death (Ochsner, 1996). LED light sources with peak emission of 631± 2 nm may enhance a deeper PDT action in

tissue than a filtered halogen type lamp of 560-740 nm emission, making LEDs a more suitable option for treating deeper parts of tumours

(Juzeniene *et al*, 2004). LEDs can generate high energy light of the desired wavelength and can be assembled in a range of geometries and sizes (Babilas *et al*, 2006).

An *in vitro* study was performed in cultured human epidermal keratinocytes where cells were incubated for 24 h with different concentrations of ALA and then exposed to either incoherent or LED light sources. In terms of cytotoxicity, there were no significant differences between the two light sources. In a subsequent *in vivo* investigation, patients with at least two AK lesions were exposed to these light sources (i.e. half to each light source). There was again no significant difference in remission rates, pain or cosmetic results (see Klein *et al*, 2008). Another study by Babilas *et al* (2007) looked at LED systems and flash lamps (VPL, variable pulsed light; Energist Ultra VPL^{TM}, Energist Ltd, Swansea, UK) for the purpose of MAL-PDT of AK. Both light sources were similarly effective, however the pain experienced during and after the treatment was significantly less using flash lamp illumination than the side of lesion that was exposed to LED. A series of studies have suggested that pulsed light therapy may be useful for treatment /adjunctive treatment in topical PDT of *acne vulgaris*, AK and photo-rejuvenation (see Morton *et al*, 2008). Although in a recent controlled study done in healthy human skin *in vivo* post-microdermabrasion and acetone scrub treatments, it was demonstrated that two pulsed light sources (i.e. the PDL and a broadband flash lamp filtered intense pulsed light (IPL)), showed minimal activation of PS, with significantly smaller photodynamic action than observed with a conventional wave broadband source (Strasswinner and

Grande, 2006). Furthermore IPL and PDL sources deliver intense light in periods (i.e. 20 milliseconds), which might suppress oxygen consumption (Kawauchi *et al*, 2004).

Buchczyk *et al* (2001) also compared the effectiveness of ALA-PDT in human cultured skin fibroblasts with three different light sources of (i) red light source (570-700 nm; PDT1200 illuminator , Waldmann Litchttechnik, Germany) at an intensity of 50 mW/cm^2; (ii) green light source (545 ± 3 nm; PDT Green Light, Saalmann, Herford, Germany) at intensities of 10-20 mW/cm^2; (iii) UVA light (320-400nm; UVA700 illuminator, Waldmann Lichttechnik, Villingen, Germany) at intensities of 44 (without ALA) and 10 mW/cm^2 (with ALA). The results demonstrated that UVA-ALA-PDT i.e. blue light is 40-fold more potent in killing cultured human fibroblasts than the red light source, and 10-fold more potent in killing in comparison with green light.

The high level of cytotoxicity of UVA-ALA-PDT can be explained in terms of effective formation of $^1O_2$ as was demonstrated with modulators of $^1O_2$ -half-life. Therefore ALA-PDT in the region of UVA (320-400 nm) may be preferable to red or green light for the purpose of treatment of readily accessible tissue due to its higher efficiency.

The two major skin cells epidermal keratinocytes and dermal fibroblasts receive different amounts of radiation. The epidermal keratinocytes receive both UVA and UVB radiation while the dermal fibroblasts are significantly protected from UV radiation by the overlying epidermis and only receive UVA radiation (see **Figure 1.17**).

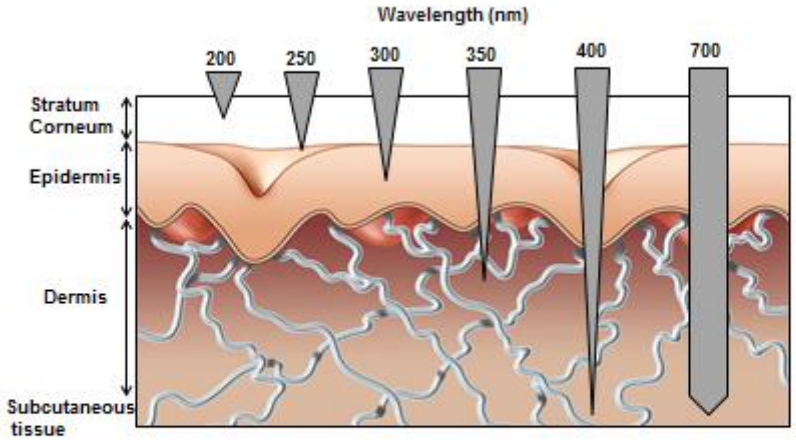

Figure 1.17. The depth of penetration of UV and visible wavelengths into the different layers of skin (modified from http://www.pgbeautygroomingscience.com/the-sun.html)

The latter study further justifies the use of blue light for ALA-PDT of superficial skin lesions such as AK. Despite the more common use of red light in the region of 630 nm for ALA-PDT, light in the Soret band (405-410 nm) is actually a good alternative as it gives the largest cell inactivation down to about 2 mm from the surface in human skin and muscle tissues as well as in superficial BCC. However when treating lesions that exceed 2 mm in depth, application of 630-635 nm light source may be a better alternative than the blue light (see Szeimies *et al*, 1995; Peng *et al*, 1997).

MAL (Metvix®, Photocure ASA, Oslo Norway and Galderma SA. Paris, France) is currently approved for use in Europe with combination with red light for treating AK, superficial and nodular BCC and BD. In the United States, a combination of an alcohol-containing ALA solution in a special applicator (Levulan Kerastick®, DUSA

Pharmaceuticals Inc., USA) with application of blue light (417 nm) has been approved for clinical treatment of AK (see Klein *et al*, 2008).

1.3.6.2. Rate limiting enzymes Influencing the Efficiency of ALA-PDT

The mechanism(s) of ALA-based PDT has been long investigated to evaluate its relative effectiveness in managing and controlling tumour growth *in vivo*. Hua and colleagues (1995) have actually shown that PPIX is the predominant porphyrin species which is formed in tumours after exogenous administration of ALA. This shows the great dependence of ALA-PDT on the rate of PPIX synthesis. However the significant variability in PPIX biosynthesis results in limitations in this therapy.

The different response rates obtained by ALA-PDT are hugely dependent on sub-optimal production and accumulation of PPIX, which in turn limit the overall anticancer photochemical reactions responsible for different clinical responses (Gerritsen *et al*, 2009; Ickowicz *et al*, 2004). It seems from the literature that different expression levels of the rate-limiting enzymes involved in the heme biosynthesis pathway between healthy and malignant cells could play a role in accumulation of PPIX in those cells (Greenbaum *et al*, 2002). These key enzymes include ALAS, ALAD, PBGD, and ferrochelatase. Administration of exogenous ALA circumvents the first enzyme ALAS, therefore the rate of synthesis is hugely dependent upon the other three enzymes notably ALAD, PBD and ferrochelatase, as has been shown in several studies (e.g. Grinblat *et al*, 2006; Ickowicz *et al*, 2004; Miyake *et al*, 2009; Feuerestein *et al*, 2009). It is important to understand that the rate of PPIX accumulation within the cells in not only influenced by the ratio of ALA conversion to PPIX but also related to the ferrochelatase-mediated insertion of ferrous iron into the

porphyrin macrocycle in order to produce the heme molecule. It has been demonstrated that the different patterns of PPIX accumulation *in vivo* may be dependent on the differences in available iron in cells (Licznerski *et al*, 1993). It has been demonstrated that there is some selectivity in the accumulation of PPIX in malignant cells and in some studies this has been linked to their low ferrochelatase activity (Schoenfeld *et al*, 1988; El-Sharabasy *et al*, 1992). A correlation between cell proliferation rates and PPIX synthesis has also been suggested (Rebeiz *et al*, 1992; Malik *et al*, 1989), but these studies lack an explicitly stated proliferation rate. It is difficult to come up with a clear model from all these different studies, as the results which have been obtained came from tumours with different origins and thus the rate of PPIX accumulating in each would be varied according to specific cellular and tissue characteristics. Clinicians could certainly benefit from a standardised PDT protocol; however such protocols must be finely tuned to specific lesions depending on PPIX synthesis capacity in order to improve the clinical outcome. As a result of these findings, there is a need to establish the type of cell and tissue markers that will recognise the tumours that are suitable for ALA-PDT, since the effectiveness of ALA in inducing PPIX within the cells is cell, tissue and organ specific (Kennedy *et al*, 1990; Feuerstein *et al*, 2009). Oseroff and coworkers (Rittenhouse-Diakun *et al*, 1995) used the transferrin receptors (TfRs, also designated CD71) of the cells as a marker for the intracellular level of iron in ALA/PDT. Their findings showed that the expression of CD71 was increased in some activated normal and malignant lymphocytes that demonstrated the high susceptibility of these cells to ALA-PDT and thus could serve as targets for PDT. However there are limitations to this approach such as the fact that in some malignant cell lines, the elevated level of TfR

expression is not directly related to internal iron stores (Neckers, 1991; Reelfs *et al*, 2010).

It is quite difficult to measure the intracellular level of LI in tumour cells. Pourzand and co-workers (1999b) have shown that the sensitive measurement of intracellular levels of LI as monitored by the level of cytosolic IRP-1 activation could have a great potential as a sensitive marker for developing ALA-PDT protocols as it recognises cells and tissue with the tendency to accumulate PPIX and thus is likely to predict the effectiveness of such therapies.

Taketani and colleagues (2011) have carried out a study where they have looked at treating the malignant cells (i.e. Hella cells) with quinolone compounds i.e. enoxacin, norfloxacin etc. in order to enhance the ALA-induced accumulation of PPIX, and therefore provide greater sensitivity of tumour cells to PDT. The use of quinolone compounds as synthetic anti-bacterial agents in treating the respiratory tract infection is well known. The concentrations of these compounds in cells should be within the right range as concentrations above 200 μM proves to be toxic and caused a decrease in accumulation of PPIX in cells (Ohgari *et al*, 2011).

In a study by Tyrrell *et al* (2010) the relationship between the PPIX photo-bleaching during MAL-PDT and resulting clinical outcome has been investigated. Fluorescence imaging was applied to monitor the fluorescent properties of PPIX in order to follow its accumulation and distribution during PDT (Allison *et al*, 2008). They demonstrated that there was an improvement in the outcome of therapy by working out the percentage change in fluorescent during the light irradiation. These observations were made 3 months after the treatment.

1.3.6.3. Improving the Uptake of ALA and MAL for Efficient PDT Response

From various studies carried out on ALA/MAL-PDT, it could be concluded that optimisation of topical formulations for both ALA and MAL should certainly lead to improvement in efficiency using these techniques. For instance, a study in 2007 by Christiansen and co-workers, examined the fluorescence pattern of 20% ALA in a cream vehicle when compared to 0.5% and 1% ALA in a liposomal vehicle using ten young subjects with healthy skin. The results demonstrated that the maximum fluorescence with the liposomal formulation was already achieved after 2 h, but using a cream-based ALA the maximum effect was only obtained after 8 h.

Another advantage in the application of liposomal formulations aside from superior penetration, is that the concentrations may be significantly reduced and yet still give optimal results for PDT.

Nanotechnology has recently been explored as a novel approach in order to improve cancer treatments by designing so called nano-carriers for drugs, i.e. ALA. The aim is to enhance and improve the efficiency of the drug, since the nano-carriers can be engineered in such a way as to modulate drug release, helping improve drug stability, and lengthening the circulation period. These nanoscale carriers can also be tailored to accumulate only in targeted tissues (Cormode *et al*, 2009; Chatterjee *et al*, 2008). So far several types of nanoparticles have been specifically designed for PDT applications. These range from liposomes, oil-based dispersions, polymeric particles and hydrophilic polymer-photosensitiser conjugates (de Leeuw *et al*, 2009; Konan *et al*, 2002; Gomes *et al*, 2007; Jang *et al*, 2005). More recently, silica-based nanoparticles have been developed for efficient drug delivery, based on their small pore size, large surface area and pore volume, as well as their lack of toxicity and

biocompatiblity (Brevet *et al*, 2009; Roy *et al*, 2003). Particularly with attention to ALA penetration, their porous structure makes them ideal carriers for hydrophobic photosensitisers, and allows oxygen permeability which plays a very important role in PDT (Roy *et al*, 2003; Bechet *et al*, 2008).

A study was carried out by Yang and colleagues (2010) to investigate the effect of temperature on the uptake of ALA and therefore improve the efficiency of PDT.

Their conclusions led to the assumption that temperature may have an effect on the outcomes of the *in vitro* anti-tumour PDT effect. A direct relationship was seen between increasing in temperature and an increase in ALA uptake and PPIX accumulation. The rate of ALA uptake was however shown to increase more than PPIX accumulation suggesting that the effect of increased temperature is more significant for ALA than PPIX.

Hyperkeratosis is often the reason for a poor response to topical ALA/MAL-PDT of skin lesions, notably AK and BCC. Limited uptake of topically applied ALA/MAL and suboptimal production of PPIX may account for these differences. A time-consuming aspect of ALA-PDT of skin lesions is the removal of crusts with a curette (keratolysis) to improve penetration and decrease the incubation time of ALA or MAL (e.g. Thissen *et al*, 2000; Morton, 2003; Moore and Allan, 2003). Overnight incubation with an ointment for easy mechanical removal might also be beneficial. Other modalities include the use of keratolytics, tape stripping, microdermabrasion or laser ablation. Penetration enhancers may also be beneficial as they may alter the composition or organisation of the intracellular lipids of the SC.

A recent study carried out by Togsverd-Bo *et al* (2012) used Ablative Fractional Laser Resurfacing (AFXL) to create vertical channels in order to facilitate MAL

uptake that would in turn improve PDT efficacy. This was the first study done to evaluate the efficiency and safety of AFXL-assisted PDT (AFXL-PDT) compared to conventional PDT in treating AK. The light source used was red LED light (630 nm). The results indicated that AFXL-PDT particularly increased the efficiency of AK treatment as opposed to conventional PDT using LED light sources. This improvement was mostly observed on thicker AK lesions (88% vs. 59%) as opposed to thinner AK lesions (100% vs. 80%), suggesting that AFXL-PDT may be more beneficial in the treatment of thick AK lesions.

Several Phase III clinical studies have been performed for the use of liposomal or non-colloidal ALA preparations in the treatment of AK, one of which is the study carried out by Foguet and colleagues (2012) looking at PDT therapy with BF-200 ALA for treatment of AK compared to MAL. BF-200 ALA (Biofrontera Bioscience GmbH, Leverkusen, Germany) is a gel formulation of ALA with a nano-emulsion containing 7.8% ALA (10% ALA hydrochloride) while the registered dug Levulan® (Dusa Pharmaceuticals, Wilmington, MA, U.S.A) (Dusa Pharmaceuticals, 2009) uses 20% ALA hydrochloride, and Metvix® 16% MAL (corresponding to 21% MAL Hydrochloride) (Galderma, 2008). BF-200 ALA has been used for treatment of AK and has proved more successful than ALA alone as it has better solubility and therefore a better skin penetration. Based on these advantages, lower final concentrations of ALA could be applied with a satisfactory outcome. In a recent study, the efficiency and safety of BF-200 ALA was compared with 16% MAL for PDT of AK when both narrow and broad spectrum light sources were applied (Szeimies *et al*, 2010). The results highlighted the higher efficiency of BF-200 ALA than MAL when both light sources were applied. However, better results were

obtained by using the narrow-spectrum light source with BF-200 ALA giving a CR of 84.8% whereas treatment with MAL led to a CR of 67.5%. These figures were somewhat decreased when a broad spectrum light source was applied with BF-200 ALA, but were still superior to MAL with 71.5% and 61.3% CR, respectively. In conclusion the use of BF-200 ALA in PDT of AK has proven to be very effective. The fact that the effect observed with BF-200 ALA is much superior to that obtained with MAL is particularly striking (Dirschka *et al*, 2012).

Several studies have been performed on the use of DMSO, ozone, glycolic acid, oleic acid to increase the penetration of ALA (e.g. Ziolkowski *et al*, 2004; Orenstein *et al*, 1996; Ibboston *et al*, 2006; Lopez *et al*, 2003). One possibility is to administer ALA via a topically applied patch. A marketing authorisation has recently been given to Alacare® (Medac, Hamburg, Germany), which is a 4 cm^2 plaster which contains 8 mg solid ALA hydrochloride which would be in direct contact with the lesions. Despite the good outcome with these plasters, their use is restricted to mild AK lesions (Hauschild *et al*, 2009).

Table 1.4 provides the product name and ingredients of some ALA preparations used in PDT of skin lesions.

Table 1.4: ALA Preparations

Product Name	Ingredients
Metvix®	16% aminolevulinic acid methyl ester hydrochloride
Levulan Kerastick® (not approved in Europe)	20% aminolevulinic acid hydrochloride
Magistral preparation	20% ALA gel/cream/emulsion
Alacare®	4 cm^2 plaster containing 8 mg ALA hydrochloride
BF-200 ALA	5-ALA nano-emulsion containing 7.8% ALA

Note: Reproduced from Klein *et al*, 2008; Foguet *et al*, 2012.

1.3.6.4. Iron Chelators and Topical ALA-PDT:

The important role of iron in determining the efficiency of PPIX accumulation in ALA-MAL PDT has been repeatedly observed in the literature (Curnow *et al*, 2006; Berg *et al*, 1996; Liu *et al*, 2004). Because of this, iron chelator treatment in combination with ALA-PDT has been proposed in order to improve the efficiency of this therapy. Temporary removal of Fe^{2+} by iron chelation prevents its insertion into PPIX, thus preventing formation of heme and therefore helping to accumulate more significant levels of PPIX within the targeted cells/ tissues (Curnow *et al*, 2006). Iron chelators are typically small molecule agents that may enter the cell and bind iron (Richardson,

2011). In general, the use of selective iron chelators could be a therapeutic good strategy in situations wherein a local increase in iron concentration is causing an undesired pathology.

As cancer cells are rapidly dividing, their higher requirement for iron as opposed to normal cells is well known, and this makes the use of chelators very attractive for the therapy of cancer (Richardson, 2005). Pre-clinical studies have already shown that iron chelators such as EDTA, desferrioxamine mesylate (Desferal®, Novartis, Basel, Switzerland), 2-allyl-2-isopropylacetamide and 1,10-phenanthroline have potential for increasing PPIX accumulation upon administration of ALA (e.g. Licznerski *et al*, 1993; Hanania *et al*, 1992; Iinuma *et al*, 1994, He *et al*, 1993; Berg *et al*, 1996; Liu *et al*, 2004).

DFO is a hexadentate siderophore which is isolated from *Streptomyces pilosus,* and has been used clinically for the treatment of iron-overload diseases such as β-thalassemia major. It has been demonstrated that DFO shows anti-proliferative activity against many tumour cells (Buss *et al*, 2003; Kalinowski and Richardson, 2005; Pahl and Horwitz, 2005; Richardson, 2005). The antiproliferative effect that DFO treatment shows towards cells is thought to be due to its ability to inhibit ribonucleotide reductase (RR) activity. RR is the rate-limiting enzyme in the formation of deoxyribonucleotides which are required for DNA synthesis (Oexle *et al*, 1999).

This property of iron chelators such as DFO provided a base for their use in iron chelation therapy of cancer (ICT). ICT may be more advantageous than chemotherapy as the problems of unresponsiveness of cancer cells to

chemotherapeutic drugs may be resolved by using this alternative therapy (Whitnall *et al*, 2006).

However DFO is expensive to produce and its hydrophilic nature makes it unsuitable for topical application. The calculated n-octanol-water partition coefficient, log P_{calc}= -0.14 (Ihnat *et al*, 2000), indicates a very poor plasma membrane permeability. Cellular studies indeed indicate that it takes several hours for DFO to enter the cell via endocytosis. It is then transported into lysosomal compartments where it remains undegraded and decreases the cytosolic labile iron pool (Kurz *et al,* 2006; Kurz *et al*, 2008; Lloyd *et al*, 1991; Glickstein *et al,* 2005). It has also been shown that prolonged exposure to DFO results in iron starvation in tissue due to removal of iron from multiple sites including the healthy tissues which therefore leads to cell cycle arrest and cell death (Doulias *et al*., 2003; Yu *et al*., 2006). These effects also limit the use of DFO for topical ALA-PDT of skin lesions. The chemical structure of DFO is shown in **Figure 1.18**:

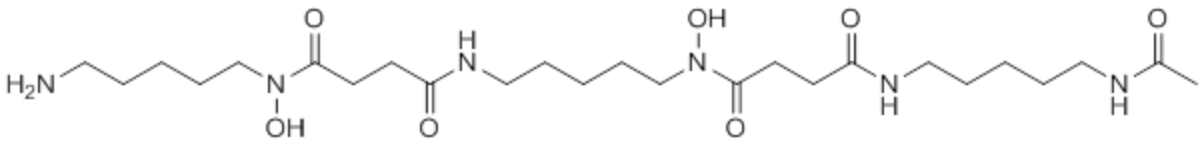

Figure 1.18: Chemical structure of free DFO.

Studies from the MacRobert and Curnow laboratories (2006) have introduced CP94 (1,2-diethyl-3-hydroxypyridin-4-one hydrochloride) which seems to be a better candidate for dermatological ALA-PDT. CP94 is a low molecular weight bidentate chelator that has a high specificity for iron (Hider *et al*, 1994). Unlike DFO and EDTA, CP94 is a lipophilic chelator, which makes it suitable for topical application (Smith *et al*, 1997; Liu and Hider, 2002). CP94 has been shown to be orally active and of very low toxicity. CP94 has also been studied in humans (Hider *et al*, 1994; Porter *et al*, 1994; Hider *et al*, 1992). The effectiveness of this chelator in enhancing PPIX levels following ALA administration has been shown in *in vitro* cell culture studies as well as in *in vivo* animal models and skin explants (Bech *et al*, 1997; Casas *et al*, 1999; Chang *et al*, 1997; Curnow *et al*, 1998 and 2006; Pye and Curnow, 2007; Blake and Curnow, 2010). The use of lipophilic strong iron chelators such as CP94 in combination with ALA/MAL may solve the issues of unresponsiveness of deep dermatological lesions in topical ALA-PDT and should therefore improve the efficiency of ALA-PDT in skin tumours with low response to ALA-PDT alone. In a recent study, Pye *et al* (2008) and Blake *et al* (2010) demonstrated the improved efficiency of ALA/ MAL-PDT of nodular BCC and SCC when combined with CP94. The chemical structure of CP94 is shown in **Figure 1.19**:

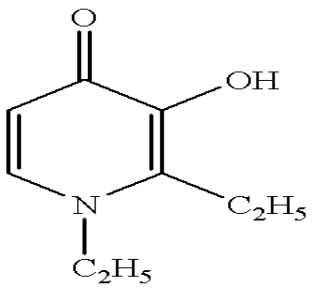

Figure 1.19: Chemical structure of CP94.

Blake *et al* (2011) also proposed Dexrazoxane (ICRF-187) as a potential iron chelating agent for ALA/MAL-PDT in SCC. Dexrazoxane is a hexadentate chelator that binds iron in a 1:1 ratio. This iron chelator is a clinically approved drug which has been successfully used as a cardio-protective agent for the past 20 years (Junjing *et al*, 2010). Blake *et al* (2010) compared the efficiency of the hexadentate Dexrazoxane to the bidentate CP94 which binds iron in a 3:1 ratio. Therefore concentrations of the solutions were determined to provide an equal iron binding potential, which was at 150 µM for CP94 and 50 µM for Dexrazoxane. They also tested equimolar concentrations of both compounds to see if any significant differences were observed. CP94 out-performed both concentrations of 50 and 150 µM of Dexrazoxane, however the clinical use of CP94 still remains experimental and is not yet licenced to be used *in vivo* at the present time.

A quick analysis as to why CP94 and DFO proved to be more efficient in increasing the level of PPIX in tumour cells than EDTA, led to the conclusion that since EDTA is a non-specific chelator and it does also chelate other cation metals, this lowers its affinity for iron compared to DFO and CP94 (Pye *et al*, 2007). EDTA is considered to be a membrane impermeable chelator, although it was amongst the first chelators used in initial ALA-PDT studies. In a study by Berg and colleagues (1996), it was demonstrated that EDTA only moderately increased the levels of intracellular PPIX in epithelial skin tumours in combination with ALA treatment. There are also two studies in which EDTA has been used in ALA-PDT therapy in the form of a cream formulation (2%) in combination with ALA and DMSO (i.e. as penetration enhancer) for topical application of tumour and skin overlying the tumour in mice bearing subcutaneously transplanted C26 colon carcinoma (Heyerdahl *et al*, 1993; Orenstein *et al*, 1995).

The chemical structure of EDTA is shown in **Figure 1.20**.

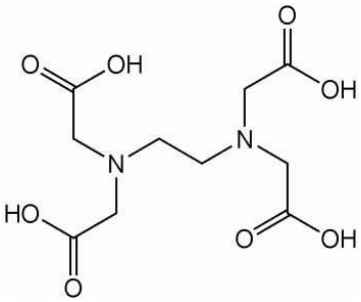

Figure 1.20. Chemical structure of EDTA.

In the present study, the suitability of aroylhydrazone iron chelators pyridoxal isonicotinoyl hydrazone (PIH) and salicylaldehyde isonicotinoyl hydrazone (SIH) was assessed to improve the efficiency of topical ALA-PDT. These iron chelators have presented themselves as effective iron chelators for ICT (Richardson and Ponka, 1994; Richardson *et al*, 1995). Both SIH and PIH are tridentate ligands which bind iron in a 2:1 ratio through the carboxyl oxygen, imine nitrogen and phenolic oxygen. They are able to bind to both ferric and ferrous iron with a stronger affinity for ferric iron similar to that of DFO (Richardson, 1995; Vitolo *et a*l, 1988). At physiological pH PIH and SIH are mostly in the non-ionised form (80% and 86% for PIH and SIH respectively), resulting in efficient permeability of both chelators through cell membranes. The lipophilicity of SIH is sufficient to readily cross the cell membrane and even transport iron to the extracellular media (Yiakouvaki *et al*, 2006). The high lipophilicity of both these compounds (log P= 0.69 for PIH and 2.07 for SIH) (Richardson *et al*, 1995; Ponka *et al*, 1979, 1994; Huang and Ponka, 1983; Epsztejn *et al*, 1997) makes them suitable for topical applications in the treatment of iron-related hyper-proliferative skin disorders, notably skin cancer (see Aroun, 2011, PhD thesis, this laboratory). It has been shown that prolonged treatment of cells with

these chelators may cause iron starvation which leads to cell death (Gao and Richardson, 2001; Buss, Neuzil, *et al*, 2004). There is also considerable literature that shows the great potential of PIH for ICT of mammary tumours and certain leukemias in mice (Sah and Peoples, 1954). In a comparative study, Johnson and colleagues (1982) showed that SIH had a greater chelating activity in tumours than PIH. The antiproliferative activity they show towards cells is related to their ability to chelate the iron pool which is required for RR activity in DNA synthesis, thus leading to apoptotic cell death (Green *et al*, 2001; Chaston and Richardson, 2003).

Figures 1.21 and **1.22** show the chemical structures of free SIH and PIH and their corresponding iron complexes respectively.

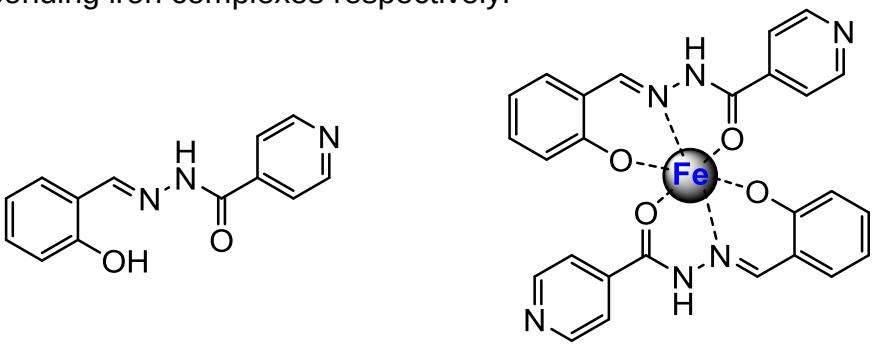

Figure 1.21: Chemical structure of free SIH (on the left) and when complexed with iron (on the right).

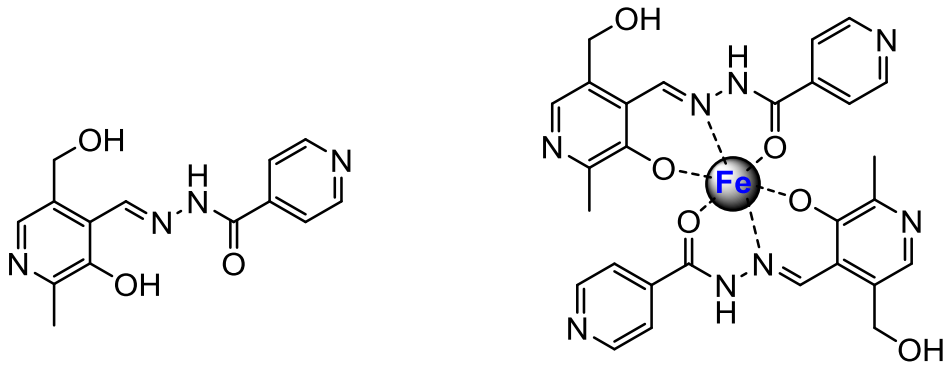

Figure 1.22: Chemical structure of free PIH (on the left) and when complexed with iron (on the right).

1.3.6.5. Caged Iron Chelators

Extensive pre-clinical and clinical studies have demonstrated that prolonged systemic application of iron chelators for therapeutic purposes are accompanied by severe toxicity (Yu *et al*, 2006). This is because iron chelators can inhibit the acitivity of ribonucleotide reductase, the critical enzyme involved in DNA synthesis (Buss *et al*, 2004; Kalinowski and Richardson, 2005) provoking G1 to S arrest in cell cycle that leads to cell death. Unpublished data from this laboratory with both monolayer and 3-dimensional organotypic skin cultures have also demonstrated that prolonged exposure of healthy skin cells to iron chelators such as DFO and SIH leads to cell death due to G1/S arrest in cell cycle (see Aroun, PhD thesis, 2012). So while the potential of iron chelators in improving the efficiency of topical ALA/ MAL PDT has been demonstrated, the topical application of strong iron chelators to skin lesions may affect the normal tissue surrounding the lesion as a result of severe iron starvation. To overcome this problem, there is a clear need to develop smart iron chelating agents that could be administered to the skin lesion as a 'pro-drug' and then activated *w*ithin the lesion. One way of achieving such *in situ* activation is by applying light-activatable caged iron chelators (CICs) that are ordinarily inactive as chelators, but which upon exposure to relevant UVA dose, are converted to free iron chelating agents in a highly selective and dose-controlled manner (Yiakouvaki *et al*, 2006; Reelfs *et al*, 2010). The use of UVA-activatable CICs in conjunction with ALA may provide a powerful and yet a safer alternative for ALA-PDT of skin lesions than the use of 'naked' iron chelators.

In this study, we selected two candidate CICs (i.e. BY123 and BY128) in which a key iron binding function of SIH was blocked by a photolabile aminocinnamoyl-based caging group. Upon activation by UVA, these CICs are uncaged releasing SIH and 3-methylquinolin-2-one co-products. Therefore the effect of these chelators in ALA-treated cells to enhance PPIX production can be triggered on demand allowing controlled and dose- and context-dependent effects within the targeted cells.

The chemical structures of these CICs are shown in **Figure 1.24** (for full details see **Results** and **Materials and Methods** sections).

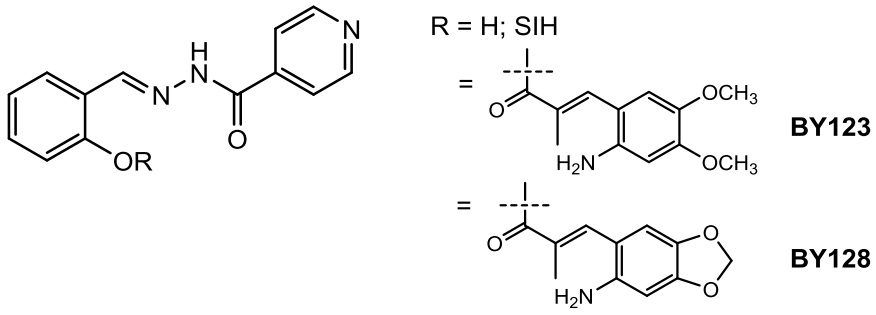

Figure 1.24. SIH and the caged derivatives, BY123 and BY128.

1.3.6.6. Side Effects of ALA- and MAL-PDT

Topical ALA- or MAL-based PDT has considerably advanced the management of NMSC, providing a treatment option for AK, BCC and BD, with good clinical outcomes, low recurrence rates and enhanced cosmetic acceptability. However the key disadvantage of the therapy remains the burning or stinging pain that patients experience during the course of treatment and sometimes even post-exposure in a minority of patients. Pain is restricted to the illuminated area and may reflect nerve stimulation and/or tissue damage by ROS, possibly aggravated by hyperthermia (Morton *et al*, 2002). Treatment of psoriasis and viral warts in particular is frequently limited by pain (Schleyer *et al*, 2006). Pain seems to be more intense in larger area

lesions, in AK, BD and BCC covering an area of > 130 mm^2 being significantly more painful to treat (Grapengisser *et al*, 2002, Sandberg *et al*, 2006).

The pain is most significant when patients are being treated with PDT for AK in the face and scalp (Grapengiesser *et al*, 2002; Sandberg *et al*, 2006). This disadvantage often causes patient incompliance or they will refrain from treatment in the future. It has been demonstrated that if AK lesions are left untreated, there will be a risk of developing SCC in the long run (Anwar *et al*, 2004; Salsche SJ, 2000). As topical ALA/MAL-based PDT has good cure rates in the treatment of extensive AK and gives excellent cosmetic results, it is necessary to find new strategies to reduce the pain experience to an acceptable level.

MAL may offer advantages over ALA in terms of its deeper skin penetration (up to 2 mm in depth) due to potentially enhanced lipophilicity and greater specificity for neoplastic cells (Peng *et al*, 2001). Unlike ALA, the transport pathway of MAL is not by GABA receptors; therefore it is thought that MAL may provoke less nerve fibre stimulations and subsequent pain than ALA (Rud *et al*, 2000). These comparative studies with topical ALA or MAL are still ongoing. While some studies have demonstrated significantly higher amounts of pain in ALA- than MAL-treated sites (both during and after PDT) (Morton *et al*, 2008; Wachowska et al, 2011), there are other studies showing that the difference in pain endured in ALA or MAL-PDT is not significantly different from one another (Haedersdal *et al*, 2008).

A recent study carried out by Ibbotson and colleagues (2012) has weighed up in particular the pain issue of PDT in ALA-treated versus MAL-treated patients using red light (632 nm) with BD and sBCC. Interestingly, there was a slight but not

significant increase in pain scores when patients were treated with ALA as opposed to MAL with very similar clearance rates on a one year follow up.

Literature shows that there is around 20% patient incompliance due to what is described as ‘unbearable pain’ due to application of ALA/MAL using red light for illumination (Wiegell *et al*, 2003, 2006 and 2008; Kasche *et al*, 2006; Kujjpers *et al*, 2006; Moloney *et al*, 2007). More comparative studies are necessary to elucidate the pain associated with either compound, as the high inter-subject variability within small subject group studies potentially obscures any significant relationship.

The degree of pain experienced with ALA/MAL has been linked to age (patients older than 70 experience more pain), lesion size and redness, and Fitzpatrick skin type I or II (Steinbauer *et al*, 2009; Aritz *et al*, 2010; Sandberg *et al*, 2006). The level of pain has also been linked to the intensity of light delivery; fractionated light doses increase tolerance of the procedure and may at the same time increase cure rates (Ericson *et al*, 2004; Babilas *et al*, 2007). Some efforts have been made in the direction of trying to reduce the topical ALA/MAL-PDT related pain and discomfort. These include: local anaesthesia, and cooling the skin with fans or sprayed water. Cold-water spray is used routinely as a pain relief but is not sufficient when larger areas like the scalp or forehead are involved.

The difficulty in finding a pain-relieving strategy has been shown in earlier studies, e.g. three studies have shown the inefficacy of topical anaesthesia such as tetracaine gel, a mixture of lignocaine 2.5% and prilocaine 2.5%, or morphine gel 0.3% (Holmes *et al*, 2004; Langan *et al*, 2006; Skiveren *et al*, 2006). Blowing cold air (-35^{o}C) on the treatment area during PDT also seems to fail to reduce the pain significantly (Pagliaro *et al*, 2004). There is proof from two independent recent

studies that the use of natural daylight instead of red light in ALA-PDT of patients with multiple AK lesions has helped to keep the pain to a lower level (Wiegell *et al*, 2008, 2011). There is more recent evidence of the pain in a few studies in the literature. Drischka and colleages (2012) looked at ALA/MAL PDT with regards to AK and there was a report of local adverse reactions at the application site and discomfort during and after the treatment.

Transcutaneous electrical nerve stimulation has been tried as a pain reducing method but had limited effect. Subcutaneous infiltration anaesthesia has been used during PDT of extensive AK of the cheek. The pain decreased but this type of anaesthesia is not possible to use on the forehead and scalp. Applying local anaesthesia to such areas is also inappropriate due to the large number of painful injections needed. Nerve blocks have also been used to provide effective pain relief during PDT for extensive AK in the face (Paoli *et al*, 2008).

Two studies also combined the benefits of supraorbital and supraocular nerve blocks of the latter study with nerve blocks of the greater and lesser occipital nerves to anesthetize both the forehead and scalp in order to alleviate pain during PDT in these areas (Paoli *et al*, 2008; Halldin *et al*, 2009). However in both studies intervariability was observed between the patients, emphasizing the need for individual considerations to find the most adequate pain-relieving method for each patient.

1.3.6.7. Pre-Clinical and Clinical Studies with ALA- and MAL-PDT

Photodynamic therapy with topical ALA/MAL formulations represents one of the most promising treatments for NMSC, AK and BD. **Table 1.5** summarises the outcome of some of the clinical studies that have been carried out during the last

decade with ALA/MAL-PDT using various light sources for the treatment of BCC, SCC and AK.

Author/Year	**Lesion type**	**ALA/MAL** **[Dose, treatment period]**	**Chelator** **(Dose)**	**Light Source (wavelength) [Dose applied]**	**Results**
Christensen *et al*, 2009	BCC	ALA cream [20% w/v, 3 h]		Broad band halogen lamp (550-700nm, fluence rate: 150-230 mW/cm^2) [dose:120 J/cm^2]	68% CR in two sessions.
Thissen *et al*, 2000	BCC	ALA cream [20% w/v, 6 h]		Versa light, (630-635 nm, fluence rate:100 mW/cm^2) [dose: 120 J/cm^2]	Remission of 22 lesions out of 24.
Souze *et al*, 2009	BCC	ALA cream [20%w/w, 6h]	EDTA [2% w/w, combined with ALA and DMSO]	DLD Red light , (630nm, 100-300J/cm^2) [Exposure time: 30 min]	3 months post treatment, over 90% CR.
Osiecka *et al*, 2012	BCC	ALA cream [20% w/v + 5% imiquimod w/v, 4h]		Broadband halogen lamp, [635±20 nm, fluence rate: 100 mW/cm^2]	75% CR.
Mosterd *et al*, 2008	nBCC	ALA cream [20%, 4 h]		Broadband Halogen light (585-720 nm) [first illumination at 75 J/cm^2 with 1 h interval followed by 150 J/cm^2]	30.3% recurrence rate 3 years post-treatment

Author/Year	**Lesion type**	**ALA/MAL [Dose, treatment period]**	**Chelator (Dose)**	**Light Source (wavelength) [Dose applied]**	**Results**
Itkin *et al*, 2004	BCC	ALA cream [20%, 5 h]		Blue light (417 nm), [dose:10J/cm^2]	Complete remission in 89% of sBCC, and 31% CR in nBCC without any recurrence over 8 months post treatment.
Soler *et al*, 2001	BCC	MAL(Metvix) [160 mg/g, 3 h]		Halogen lamp, (570-670nm, 100-180 mW/cm^2) [50-200 J/cm^2]	89% maintaining remission up to 3 years post treatment.
Li *et al*, 2010	SCC	ALA cream [20%, 6 h]		Red light (632 nm) [340 J/cm^2]	Complete remission.
Foley *et al*, 2009	nBCC	MAL (Metvix) [160 mg/g, 3 h]		Incoherent red light (570-670 nm) [75 J/cm^2]	2 treatment with 3 months interval showed 75% CR.
Togsverd *et al*, 2010	BCC	MAL (Metvix) [160 mg/g, 3 h]		LED (632 nm), [37 J/cm^2]	Complete remission for up to 2 years post treatment.
Eibenschutz *et al*, 2008	BCC	MAL (Metvix) [160 mg/g, 3 h]		Non-coherent red light (630 nm), [dose:75 J/cm^2]	Lesions of 40-49 mm gave 95% CR 6 months post treatment and 66% CR after 3 years.

Author/Year	Lesion type	ALA/MAL [Dose, treatment period]	Chelator (Dose)	Light Source (wavelength) [Dose applied]	Results
Surrenti *et al*, 2007	BCC	MAL (Metvix) [160 mg/g, 3 h]		Non-coherent red light (634 nm), [37 J/cm^2]	85% complete CR
Lehmann, 2007	AK	MAL (Metvix) [160 mg/g, 3 h]MAL (Metvix) [160 mg/g, 3 h]		Red light (570-670 nm), [Dose not stated]	Remission rates of 69-91% up to 3 months post treatment
Morton *et al*, 2006	AK	MAL (Metvix) [160 mg/g, 3 h]		LED red light (630 nm), [37 J/cm^2]	Received 2 sessions with 7 days apart. Gave 89.1%
Moloney *et al*, 2007	AK	ALA [30g/100cm^2, 5 h] MAL [30g/100cm^2, 3 h]		Waldman PDT lamp MSR 1200 (580-740 nm), [50 J/cm^2]	40% CR with ALA and 46% CR with MAL (MAL was preferred, less painful)
Tschen *et al*, 2006	AK	ALA cream [20%, 14-18 h]		Blue light (417 nm), [10 J/cm^2]	Remission rate 12 months post treatment was 78%
Apalla *et al*, 2011	AK	ALA cream [20%, 4 h]		Red light (570-670 nm), [75 J/cm^2	CR of 92% at 3 months post treatment, 88% CR after 12 months

Author/Year	Lesion type	ALA/MAL [Dose, treatment period]	Chelator (Dose)	Light Source (wavelength) [Dose applied]	Results
Van der Geer *et al*, 2009	AK	ALA cream [20%, 4 h] after 3% Diclofenac treatment for 4 weeks, twice daily		Red light (633 nm), [80 J/cm^2]	CR higher that 90% at 12 months post treatment
Tierney *et al*, 2009	AK	ALA cream [20%, 14-18 h]		Blue light (417 nm), [16.4 min of illumination	66% CR 8 weeks after a single treatment, 85% CR 16 weeks after 2 sessions
Redbord *et al*, 2007	AK	MAL (Metvix) [160 mg/g, 3 h]		LED red light (630 nm) [dose: 37 J/cm^2]	88.3% CR after 2 treatments at monthly interval
Calzavara-Pinton *et al*, 2007	AK	MAL (Metvix) [160 mg/g, 3 h]		LED red light [37 J/cm^2]	6 months after treatment no recurrence but 24-36 months after the treatment 10% clinical recurrence
Kim *et al*, 2005	AK	ALA cream [20%, 4 h]		Non-coherent Ellipse Flou (555-950 nm) [12-16 J/cm^2]	72% CR at 2 months follow up. Second treatment given at 2 months. 86% CR at 4 month
Stebbins *et al*, 2011	SCC	MAL (Metvix) [160 mg/g, 3 h]		Red light (570-670 nm), [75 J/cm^2]	93% CR at 3 months, 80% CR at 12 months. At 24 months the relapse rates were 18%.

Author/Year	Lesion type	ALA/MAL [Dose, treatment period]	Chelator (Dose)	Light Source (wavelength) [Dose applied]	Results
Truchuelo *et al*, 2012	SCC	MAL (Metvix) [160 mg/g, 3 h] MAL (Metvix) [160 mg/g, 3 h]		Red light (630 nm), [38 J/cm^2]	76.09% CR after 2 sessions.
Sotiriou *et al*, 2010	SCC	ALA cream [10%, 3 h]		Red light (570-670 nm, 100 mW/cm^2), [dose: 100 J/cm^2]	Complete remission up to 16 months after treatment.
Togsverd-Bo *et al*, 2010	SCC (hairless mice)	MAL [20%, 3 h]		Red light (632nm) [dose: 37 J/ cm^2]	CR of 23-61.5%
Campbell *et al*, 2008	nBCC	ALA [20% w/w, 6 h]	CP94 [5,10,20,40% W/W, 6 h]	Red light (630 nm) [dose: 100 J/cm^2]	The addition of 40% CP94 and 20% ALA made a significant difference to ALA alone and gave the best results.

Pre-clinical studies are still ongoing to try and improve the efficiency of ALA/MAL-PDT. **Table 1.6** provides a summary of some of the more recent studies done in this regard:

Table 1.6

Author/ Year	Cell Type	ALA/MAL [Dose, treatment period]	Iron Chelator [Dose]	Light Source (wavelength)[Dose applied]	Results
Blake *et al*, 2010	U-87 MG(human glioma cells)	ALA [250 µM, 6 h] MAL [1000 µM, 3 h]	CP94 [150 µM]	Red Light (635 nm) [dose: 15 J/cm^2]	6 h incubation with both combinations of ALA+CP94 and MAL+CP94 significantly increased the PPIX as oppose to ALA/MAL alone.
Blake *et al*, 2011	U-87 MG (human glioma cellsA431 (SCC)	ALA [250 µM] MAL [1000 µM ,0-6 h]	Dexrazoxane [50 and 150 µM] CP94 [150 µM, 3 h]	No irradiation (No light therapy)	PPIX levels increased hourly w/wo chelator +ALA/MAL up to 6h in A431. Combination of CP94 +ALA/MAL was superior over the two chelators.
Pye *et al*, 2007	MRC-5 (human fetal lung fibroblast) 84BR(human skin fibroblast) A431(SCC)	ALA [1000 µM, 6 h] 1000 µM MAL (3 h)	CP94 (150 µM) DFO (150 µM)	No irradiation (No light therapy)	CP94 +ALA caused the most significant PPIX increase
Pye *et al*, 2008	MRC-5 (human fetal lung fibroblast) 84BR(human skin fibroblast) A431 (SCC)	MAL [160 mg/g W/W, 3 h]	CP94 [75, 150, 300 µM, 3 h] in conjunction with MAL treatment	LED (635 nm) [dose: 37 J/cm^2]	Incubation of CP94+ALA led to significant increase in PPIX. Skin tumour cells (A431) showed the highest response. Complete remission at 6 weeks check-up.

Author/Year	Lesion type	ALA/MAL [Dose, treatment period]	Iron Chelator (Dose)	Light Source (wavelength) [Dose applied]	Results
Valdes *et al*, 2010	U251 (GFP transfected human glioma cells)	ALA [100 µM , 2 h]	DFO [200 µM, 3 days incubation]	No irradiation (No light therapy)	Chelator and ALA combined treatment, increased PPIX levels to 50% of the untreated control cells.
Yang *et al*, 2010	-Fibroblast (primary skin cell line) - HaCaT (keratinocyte cell line) - Hep-2 (immortalised human epithelial larynx cancer cells)	ALA [2 mM, 3 h]	DFO [0.5 mM, 3 h] combined with ALA treatment	Red light (632 nm), [2.9 J/cm^2 at a fluence rate of 300 mW/cm^2]	DFO+ALA gave a higher accumulation of PPIX than ALA alone. This was the highest in Hep-2 cells. 12 h post UVA, cell death ratios were the lowest in fibroblasts and the highest in Hep-2 cells.
Buchczyk *et al*, 2001	Fibroblast (Primary skin cell line)	ALA [1 mM, 24 h]		- UVA (320-400 nm) [dose: 1 J/ cm^2] - Green light (545±3 nm) [dose: 25 J/ cm^2] - Red light (570-700 nm) [dose: 0.3 J/cm^2]	PPIX increased 8 folds as appose to untreated controls. UVA turned out to be the most efficient.
Xia *et al*, 2009	HaCaT	ALA [2 mM, 3 h]	0.5 mM EDTA 0.5 mM DFO	Red light (632 nm) [dose: 2.9 J/cm^2]	Both apoptosis and necrosis were increased in ALA+DFO> ALA+EDTA> ALA> control.

Tables 1.5 and 1.6: Key pre-clinical and clinical studies performed by ALA-PDT from year 2000 to date.

Because of the significant results obtained from preclinical and clinical studies (e.g. Hongeharu *et al*, 2000), in 2003, ALA-PDT was also approved for moderate inflammatory *acne vulgaris* in USA.

Preclinical and clinical studies have also demonstrated the great potential of ALA/MAL-PDT for treatment of *Mycosis fungoides* (e.g. Stables et al, 1997), human papilloma virus-associated cutaneous pathologies, lymphocytoma cutis, leishmaniasis, alopecia areata, erythroplasia of Queyret and benign familial pemphigusand hidradentis suppurativa (see Tierney *et al*, 2009; Kalka *et al*, 2000; Huang, 2005). Other non-malignant conditions such as psoriasis, viral warts and hair removal are still under clinical investigation worldwide (e.g. Robinson *et al*, 1999; Stender *et al*, 1999; Stender *et al*, 2000; Hongeharu *et al*, 2000; Robinson *et al*, 1999; Stender *et al*, 2000; Huang, 2005). Clinical investigations of ALA-PDT have also extended to basaloid follicular hamartomas, cutaneous T-cell lymphoma and sebaceous gland hyperplasia in recent years (e.g. Leman *et al*, 2002; Hayami *et al*, 2007; Coors *et al*, 2004; Gold *et al*, 2004; Oseroff *et al*, 2005).

1.4. Aims and objectives

While much effort has been invested in the development of protocols to improve the effectiveness and cosmetic outcome of topical ALA-based PDT of skin lesions, notably multiple actinic keratoses (AK), few studies report approaches to reduce the pain associated with the therapy. Most of the time a complete response to ALA-PDT is achieved only following treatment with either high irradiation doses or long irradiation times with high intensity visible light. However, these conditions cause discomfort (stinging and burning pain) and severe complications in 20% of patients treated, despite the number of modalities in use for pain relief. As a consequence, the patient may choose to interrupt the treatment, with the risk that the untreated AK lesions may develop into squamous cell carcinoma (SCC). Therefore, an improvement of the current ALA-PDT protocol, aiming at a reduction of the pain incurred will be clearly beneficial to the patient.

UVA (320-400 nm) is absorbed more efficiently by PPIX and is also 40-fold more potent in killing cultured skin cells than conventional red light (550-750 nm) (Buckczyck *et al*, 2001). In the present project, we hypothesized that the use of UVA as the light source may provide a rapid means to improve the effectiveness of ALA-PDT of skin lesions while reducing considerably the therapy time and the discomfort/pain associated with conventional topical ALA-PDT. Two keratinocyte-based cancer cell models, HaCaT (spontaneously immortalised keratinocyte cell line) and Met 2 (keratinocyte cell line originating from the skin of a patient suffering from SCC) were chosen for the study. The extent of cell damage and cell death in ALA-treated cells was evaluated following UVA irradiation with three independent assays of MTT, Annexin V/propidium iodide and, colony forming.

To further improve the efficiency of ALA-PDT of cells with UVA, ALA treatment was also combined with potent iron chelators salicylaldehyde isonicotinoyl hydrazone (SIH), pyridoxal isonicotinoyl hydrazone (PIH) or desferrioxamine (DFO) to further increase the accumulation of PPIX through the depletion of iron necessary for ferrochelatase-mediated bioconversion of PPIX to heme.

As topical application of ‘naked’ iron chelators to skin lesions may cause toxicity to the surrounding normal tissue due to iron starvation, we also evaluated the potential of UVA-activatable caged- iron chelators (CICs) as a safer alternative to improve the efficiency of topical ALA-PDT of skin lesions. CICs do not chelate iron unless activated by relevant doses of UVA, allowing for specific localised release within the targeted tissue and therefore substantially decreasing the risk of toxicity to the surrounding normal tissue. The caged chelators used in this study were aminocinnamoyl-caged SIH derivatives BY123 and BY128.

The ultimate goal of this project was to demonstrate that UVA irradiation in combination with iron chelators and ALA may be an effective intervention strategy to decrease the time of radiation treatment and therefore reduce the pain associated with prolonged conventional topical ALA-PDT of skin lesions such as AK. The use of caged-chelators may also provide a safer and more targeted strategy for topical ALA-PDT of skin lesions with UVA.

CHAPTER 2

MATERIALS AND METHODS

2.1. Chemicals

All the reagents were from Sigma-Aldrich Chemical Co. (Poole, UK) unless otherwise specified. All the cell culture materials were obtained from Life Sciences Technologies (Paisley, UK), except the foetal calf serum (FCS), which was obtained from PAA (Austria). Dulbeco's Minimum Essential Medium (DMEM) was supplied by Gibco BRL Invitrogen Corporation (Life Technologies, UK).

MilliQ water used to prepare phosphate buffered saline (PBS) and other stock solutions were issued from a Millipore purification system (MilliQ cartridge: Millipore, Bedford, MA) in order to minimize the presence of trace elements such as transition metals.

Annexin V was from Roche (UK), and dimethyl sulphoxide (DMSO) and desferrioxamine mesylate Ph. Eur. (Desferal, DFO) were purchased from Sigma.

5-Aminolevulinic acid hydrochloride (ALA) was supplied from Sigma- Aldrich.

2.2. Cell Culture

All the cell models used in this study were cultured routinely and incubated in a 5% CO_2 cell culture incubator set at 37ºC.

2.2.1. Cell models

HaCaT: Is a spontaneously immortalized human skin keratinocyte cell line that was originally derived from an adult back in Boukamp's laboratory. This cell line

maintains full epidermal differentiation capacity, but remains non-tumorigenic. (Boukamp *et al*, 1988). The medium was 10% FCS DMEM (high glucose Dulbecco's modified Eagles medium) with 0.25% sodium bicarbonate, 2 mM L-glutamine, and 50 IU/ml of each of penicillin / streptomycin (P/S). The FCS stock was heat-inactivated at 56^{o}C for 45 min before use.

Cells were passaged once or twice a week and seeded for experiments as follows:

For MTT, flow cytometry, PPIX measurement and ROS measurement 8x10^{4} cells were seeded per 3 cm plate in 2 ml of media.

For colony forming ability assay, 700 or 1000 cells per condition were seeded in 6 well plates in 2.5 ml of media.

Swiss 3T3: The Swiss 3T3 are spontaneously immortalized mouse embryonic fibroblasts (a kind gift from Prof I. Leigh, Dundee).These cells are used as a feeder layer for the cultivation of keratinocytes (see Proby *et al*, 2000). The 3T3 cells secrete extracellular matrix proteins that help the attachment of keratinocytes and also growth factors that enhance the proliferation rate of the seeded keratinocytes.

3T3 cells were grown in culture in 15% FCS EMEM (Earl's modified minimum essential medium) supplemented with 15 % FCS, 0.25% sodium bicarbonate, 2 mM L-glutamine and 50 IU/ml of each of P/S.

For feeder layer preparation, cells were first grown in flasks till they reached 80% confluency. The cells were then treated with mitomycin C at a final concentration of 4 µg/mL and incubated for 2 h at 37ºC. Mitomycin C is a DNA cross linker that inhibits DNA replication in 3T3 cells in order to stop further growth and any possible interference with keratinocyte growth in culture. After the incubation period, the

medium containing mitomycin C was aspirated and the cells were rinsed with PBS to ensure no mitomycin C remained to inhibit keratinocyte growth. The mitomycin C-treated 3T3 cells were trypsinised and resuspended in RM^+ media (see below). The cell suspension was then used as the feeder layer for the matrix-dependent culture of Met2 keratinocyte cell line.

Met2: Met2 is a squamous cell carcinoma (SCC) keratinocyte cell line, clonally derived from a local recurrence of invasive SCC (a kind gift from Prof Irene Leigh, Univ. Dundee, see Proby *et al*, 2000 and Popp *et al*, 2000).

Met 2 cell lines were cultured routinely in flasks in the presence of the feeder layer and RM^+ medium. The rich medium (RM^+) was prepared by mixing DMEM and Ham's F12 media at a ratio of 3:1 and supplemented with hydrocortisone (0.4 μg/ml), cholera toxin (10^{-10} M), epidermal growth factor (10 ng/ml), insulin (5 μg/ml), transferrin (5 μg/ml), liothyronine (2x 10^{-11} M), 0.25% sodium bicarbonate, 2 mM L-glutamine and 50 IU/ml of P/S.

For the experiments performed with these cells, $5x10^4$ cells were seeded per 3 cm dish containing 2-3 ml of RM^+ media.

2.2.2. Trypsinisation

Stock cells were passaged by trypsinisation once or twice a week. As a general rule, stock cell flasks were maintained in culture until they reached a confluency of 80%, after which they were trypsinised as detailed below:

The medium was removed from the flask and retained in a separate tube. Cells were then washed with PBS and treated with 2ml of 0.25% trypsin. Trypsin is a protease which detaches cells from the surface of the flask. Cells were incubated at 37^{o}C until detached. Retained media was added back to the flask in order to inactivate the trypsin. The cells were then centrifuged for 5 min at 1200 rpm (Jouan B3.11 centrifuge). The supernatant was then removed and the cell pellet was resuspended in fresh media. A small aliquot of the cell suspension was mixed with trypan blue dye and then counted under a microscope using a Neubauer-improved haemocytometer purchased from Marienfeld (Germany). Cell were then diluted with fresh medium at the required density and incubated at 37^{o}C.

2.3. Treatments

2.3.1. Chemical Treatments

2.3.1.1. Stock Solutions

SIH (RMM of 241): The SIH powder was synthesized in Dr Eggleston's laboratory (B.Young, PhD thesis, University of Bath, 2013). The stock solution was prepared at a concentration of 100 mM in DMSO and aliquoted and stored at -20°C.

PIH (RMM of 286): The PIH powder was synthesized in Dr Eggleston's laboratory B.Young, PhD thesis, University of Bath, 2013). PIH powder was first dissolved in 1M HCl at a final concentration of 250 mM and then further diluted in PBS to reach a

final concentration of 25 mM. Since PIH had a tendency to precipitate over time, this stock solution was usually prepared freshly just before adding to the cells.

DFO (RMM of 657): The DFO powder was purchased from Sigma (Cat. No. D9533). The stock solution was prepared at a concentration of 100 mM in H_2O and aliquoted and stored at -20°C.

BY123 (RMM of 460.48): BY123 powder was synthesized in Dr Eggleston's laboratory (B.Young, PhD thesis, University of Bath, 2013). The powder was weighed and accordingly dissolved in DMSO at a final concentration of 100 mM. It was then aliquoted in dark eppendorf tubes to be protected from light and stored at -20ºC.

BY128 (RMM of 444.44): BY128 powder was synthesized in Dr Eggleston's laboratory (B.Young, PhD thesis, University of Bath, 2013). The powder was weighed and dissolved accordingly in DMSO at the final concentration of 100 mM. It was then aliquoted in dark eppendorf tubes to be protected from light and stored at -20°C.

ALA (RMM of 167.59): ALA powder was purchased from Sigma (Cat. No. A3785). The powder was weighed and dissolved in PBS at the final concentration of 100 mM. Solutions of ALA in PBS buffered at physiological pH were found to be unstable over time, hence the ALA solution was prepared fresh every time prior to treatment.

2.3.1.2. ALA and Iron Chelator Treatments

For iron chelator/CICs treatments that were performed for 18h, cells were seeded at the required density and grown for 48 h prior to addition of compounds.

For ALA treatment and iron-chelator treatments that were carried out on the day of UVA irradiation, cells were seeded at the required density for 72 h prior to addition of compounds and UVA irradiation.

2.3.1.3. Iron Chelator Treatment

Iron chelators/CICs treatments were carried in conditioned medium (CM, i.e. the medium in which cells were grown for 48-72 h) for 2 or 18 h at 37ºC in the dark. For HaCaT cells the chelators' concentrations were at a range of 20 -100 μM. For Met2 cells, iron chelators were used at a concentration of 50 μM for SIH and 200 μM for DFO and PIH.

2.3.1.4. ALA Treatment

ALA treatment was carried out in 1% FCS DMEM. Cells were incubated with ALA or not at a final concentration of 0.5 mM in 1% FCS DMEM media and incubated for 2 h at 37^{o}C in the dark prior to irradiation.

2.3.2. UVA irradiation

2.3.2.1.1. UVA Lamp

The broad spectrum 4kW lamp (Sellas, Germany) emits primarily UVA irradiation (significant emission in the range of 350-400 nm) and some near visible radiation longer than 400nm. **Figure 2.1** illustrates the spectrum of the lamp. This lamp is

suitable for ALA-PDT studies, as the absorption spectrum of PPIX is known to have a maximum at 405nm. Excitation at this wavelength produces an intense red emission with its maximum at 635nm (Ericson *et al*, 2004).

Furthermore blue light has been shown to be more potent than red light at activating PPIX (Peng *et al*, 1997).

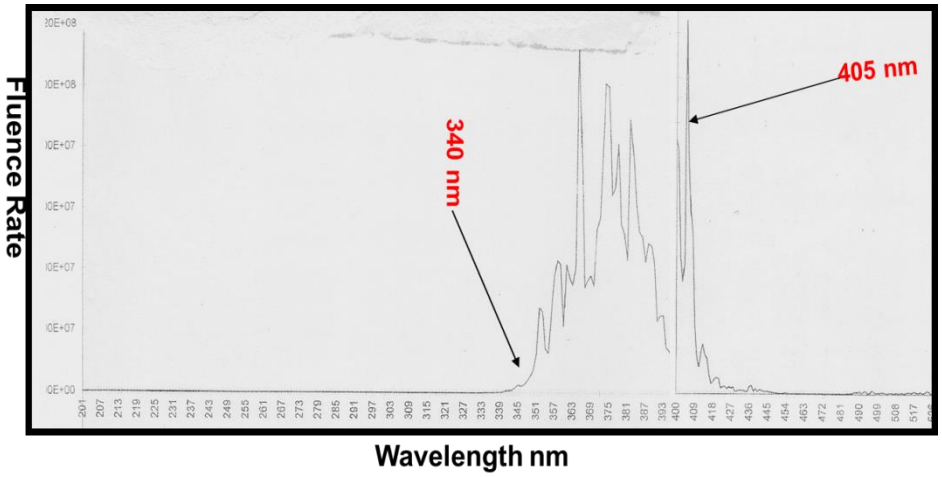

Figure 2.1: The spectrum of the Sellas 4kW UVA lamp as measured in Prof. Rex Tyrrell's laboratory by spectroradiometer (Ref: Radka, T, MPhil thesis, University of Bath, 2010).

2.3.2.2. UVA Doses

The UVA dosimeter was from International Light Technologies Inc. (Peabody, MA, USA) calibrated against spectroradiometric measurements of the source made by a DM150 double monochromator Bentham spectroradiometer (Bentham Instruments, Ltd., Reading, UK) calibrated against national UK standards. The UVA doses were 5, 10, 20 and 50 kJ/m^2. Typically with a fluence rate of 150 W/cm^2, and the distance of 30 cm, the irradiation time was between 15 sec to 2.5 min for all the doses used. At natural sunlight exposure level, these doses will correspond to radiation times of between 2 to 20 min at sea level (see Pourzand *et*

al, 1999). The higher doses of 20 and 50 kJ/m^2 will be more relevant for skin therapeutic purposes. This is because of the attenuation of the applied UVA dose by passage through the outer skin layers. The UVA doses were measured using an IL1700 radiometer (International light, Newbury, MA).

2.3.2.3 Irradiation Procedure

Irradiation was carried out in an air conditioned room at 18ºC in order to maintain the temperature of the cells to approximately 25ºC throughout the radiation procedure. Prior to irradiation, cells were washed with PBS, and covered with PBS containing 5 ppm Ca^{2+} and Mg^{2+}. Cells were then irradiated with UVA doses of 5, 10, 20 or 50 kJ/m^2. After irradiation, cells were incubated in conditioned medium (the retained medium in which the cells had been grown). The control samples were treated in the same manner except that they were not irradiated (i.e. kept in dark).

2.3.2.4. Chemical and Cell Culture-based Uncaging of BY123 and BY128 by UVA Irradiation

The BY123 and BY128 were uncaged by UVA either in a simple chemical system or in a cell culture system.

For simple chemical uncaging, BY123 and BY128 stock solutions were prepared in DMSO at a final concentration of 100 mM and then UVA irradiated in quartz cuvettes.

For experiments involving the addition of uncaged CIC as a control, the compounds were usually uncaged with a UVA dose of 250 kJ/m^2 and then added to the cells at a final concentration of 20 μM in CM.

For experiments involving the determination of the uncaging profile of CICs by reverse HPLC, BY 123 and BY128 stock solutions were prepared in DMSO at a final concentration of 1 mg/ml and then irradiated in quartz cuvettes with increasing UVA doses of 10-500 kJ/m^2.

Uncaging process in a cell culture system was based on the addition of CICs (i.e. BY123 or BY128) to the growth medium of cells over 18 h at 37 ˚C followed by irradiation with UVA doses of 20 or 50 kJ/m^2 which uncaged the compounds inside the cells.

2.4. MTT Assay

2.4.1. Principle of the Assay

Cellular and mitochondrial dehydrogenase enzymes converts MTT [3-(4, 5-dimethylthiazol-2-yl)-2, 5-diphenyl tetrazolium bromide] that is a yellow water soluble substrate into a dark blue formazan product that is insoluble in water. The amount of formazan produced is directly proportional to the number of viable cells. So the MTT colorimetric assay may be used as a cell viability assay (Mosmann, 1983; Doyle and Griffiths, 1998).

2.4.2. MTT Stock Solution: The MTT stock solution was prepared at a final concentration of 5 mg/ml in PBS. The solution was then filtered through a 0.22 μm filter for sterilization and stored in small aliquots at -20ºC.

2.4.3. Procedure

On the day of the experiment, MTT stock solution was diluted in Serum Free DMEM Medium (SFM) to a final concentration of 0.5 mg/ml (i.e. MTT/SFM solution). From this solution, 0.5 ml was added into each 3 cm plate. The cells were then incubated for 3 h at 37ºC. The MTT/ SFM solution was then aspirated and 0.5 ml of DMSO

was added to each well. The plates were then swirled for 3 min on a 3D rocking platform (Stuart Scientific, UK). A small aliquot (i.e. usually 100 μl) was transferred from each plate to a 96 well plate in triplicate for each condition and the optical density was measured by Dynatech plate reader MR-5000 (Dynatech, Guernsey Channel Islands) at 570 nm using DMSO as a blank control.

The mean values calculated from the raw data (optical density) for each condition was then expressed as the percentage enzymatic activity (i.e. dehydrogenases) of the untreated control that was set as 100.

Figure 2.2 provides the summary of various treatments used prior to MTT assay.

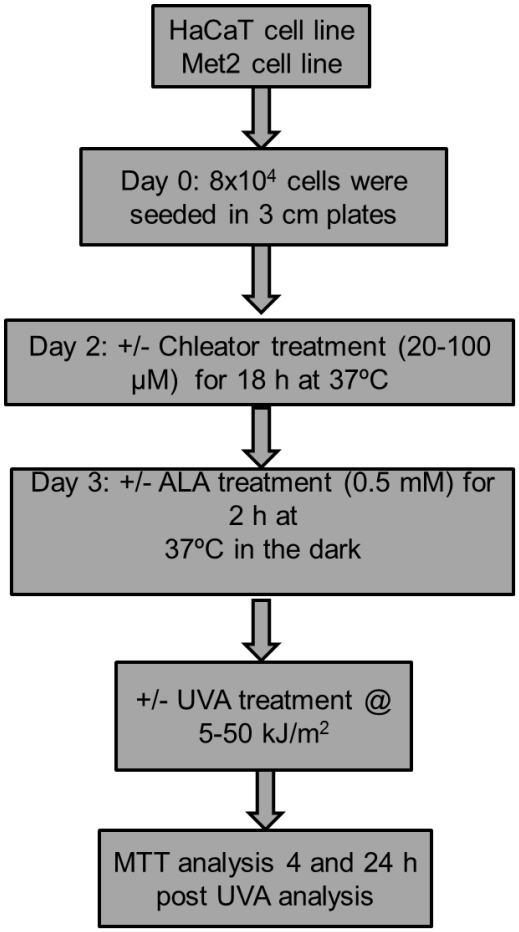

Figure 2.2: Summary of the treatments carried out in cells prior to MTT analysis.

2.5. Colonogenic Assay (Colony Forming Assay)

2.5.1. Principle of the Assay

This assay is considered to be the most reliable technique in cell culture synthesis to assess viable cell numbers. It is based on the ability of a single cell to form a colony and to undergo unlimited division. A colony is considered to consist of at least 50 cells or more (Doyle and Griffiths, 1998).

2.5.2. Methodology

After treatments, cells were trypsinised and seeded back in 6 well plates in triplicate at a density of 700 or 1000 cells/ well for HaCaT cells and 800 cells/ well for Met2 cells in their respective fresh media (i.e. 10% FCS-DMEM for HaCaT and 10% FCS-RM^+ for Met2 cells). Cells were then left to divide for 12 days.

On the day 12, media was removed and cells were fixed and stained with 0.2% w/v crystal violet solution (in 20% v/v methanol, 2% w/v paraformaldehyde) for 15 min. After the 15 min period, the crystal violet was removed and cells were rinsed with water or PBS and left to dry before colonies were counted by hand after the initial confirmation of colony forming was established by microscope. The data were expressed as percentage of survival relative to untreated control.

2.6. Annexin V/Propidium Iodide Dual Staining Assay by Flow Cytometry

2.6.1. Principle of the Assay

Quantification of apoptotic and necrotic cells was scored by flow cytometry after dual staining of cells with Annexin V-Fluoroscein isothiocynate (FITC) and propidium iodide (PI). In the early stages of apoptosis phosphatidylserine (PS) translocates from the inner part of plasma membrane to the outer layer. Annexin-V is a phospholipid-binding protein with a high affinity for PS. Identification of cell surface PS with Annexin-V-FITC serves as a marker for apoptotic cells. On the other hand, necrotic cells that lose cell membrane integrity are stained with both PI and Annexin-V. Thus, Annexin-V-FITC and PI double staining can differentiate between necrotic and apoptotic cells (see Zhong *et al*, 2004).

2.6.2. Procedure: Following various treatments, cells were incubated with incubation buffer (10mM Hepes/NaOH, pH 7.4, 5M NaCl, 100 mM $CaCl_2$) containing Annexin-V-FITC (20 µl/ml) and PI (20 µg/ml) for 15-20 min. Double stained cells were counted as necrotic, whereas Annexin-V-FITC positive, PI negative cells were scored as apoptotic. A minimum of 10000 cells were analysed per sample on a BD FACS Canto™ flow cytometer (Becton Dickinson, Erembodegem, Belgium). These experiments always include a positive control (i.e. ALA-10 kJ/m^2) and a negative control (Control-no UVA). A coefficient variation of 20% was obtained for the positive control.

The following settings were used for the analyzed cell line (HaCaT): FL1 (530+/-15nm) in log data collection and FL3 in log data collection.

Two dimensional dot plots were used to analyse the data of FL3 versus FL1 fluorescent profiles. Cell Quest software (Becton-Dickinson, Eremdodegem, Belgium) was used to analyse the data with a dual parameter of FL1 (Annexin-V-FITC) and FL3 (PI).

2.7. Measurement of Protoporphyrin IX by Spectrofluorimetry

2.7.1. Preparation of Standard Curve

A standard curve for PPIX was obtained by preparing standard solutions containing increasing concentrations of commercial PPIX dissolved in 1.5 M HCl and by measuring the fluorescence with a Perkin-Elmer LS5 luminescence spectrometer (excitation: 404 nm, emission: 604 nm)(see **Figure 2.3**).

Final Conc(uM)	Mean PpIX Fluorescence (n=5)	SD
0	0.17	0.05
0.01	11.05	2.34
0.02	19.57	2.24
0.05	46.67	2.47
0.1	90.01	0.91

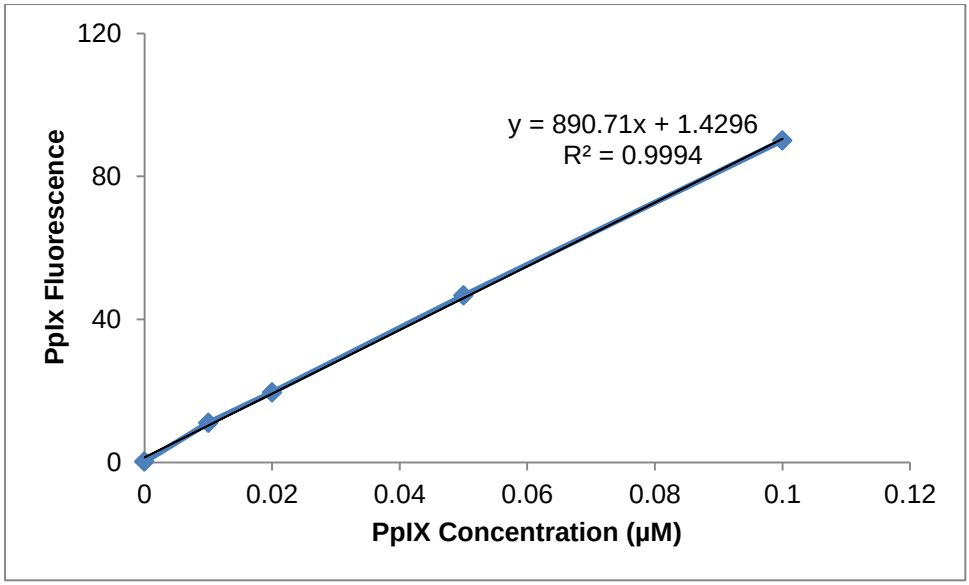

Figure 2.3. Standard curve of PPIX obtained by spectrofluorimetry of a series of PPIX standard solutions.

2.7.2. Procedure

After various treatments, cells were trypsinised with 0.25% trypsin and spun down at 1000 rpm (120 x g) for 10 min in a Falcon 6/300 MSE centrifuge. Cells were then resuspended in PBS and counted for normalisation. Cells were this time re-suspended in acetic acid (750 µl) and kept on ice while sonicated (Branson B-12 sonicater, Branson Sonic Power, Danbury, CT) at 13000 rpm for 7 sec twice with 10 sec interval, before addition of 2.25 ml of ethyl acetate to each sample. The samples were then vortexed and centrifuged at 2500 rpm (120 x g) for 5 min in a Falcon 6/300 MSE centrifuge. The supernatant (organic phase) was collected from each sample and transferred to a new falcon tube and 1 ml of 1.5 M HCl was added to each sample. The samples were vortexed and centrifuged at 2500 rpm (120 x g) for 4 min in a Falcon 6/300 MSE centrifuge.

The porphyrins were isolated in the acetic acid phase and quantified using a Perkin-Elmer LS5 luminescence spectrometer (404 nm excitation and 604 nm emission).

Results were calculated by normalising with cell number ($1x10^6$ cells/ condition) and were then expressed as fold difference compared to the untreated control (i.e. 1).

A stock sample of PPIX was prepared and aliquoted, where every time before measuring the samples, a sample of PPIX was defrosted from the batch and measured. The coefficient variation was shown to be around 5%.

2.8. Reactive Oxygen Species (ROS) Measurement

2.8.1. Principle of the Assay

In this project, a general ROS detector dye named CM-H_2DCFDA was used. This dye is a chloro-methyl derivative of H_2DCFDA (2', 7'-dichlorodihydrofluorescein diacetate). CM-H_2DCFDA exhibits an improved retention in live cells compared to H_2DCFDA. Upon addition of the compound, CM-H_2DCFDA is diffused into cells, where its acetate groups are cleaved by intracellular esterases and its thiol reactive chloro-methyl group reacts with intracellular glutathione and other thiols. Subsequent oxidation gives a fluorescent adduct that is trapped inside the cells. The excitation wavelength for this dye is 492-495 nm and the emission wavelength is 517-527 nm. This dye will be oxidized by air therefore it should be stored under argon or nitrogen.

2.8.2. Procedure

Cells were irradiated with UVA doses of 5 and 10 kJ/m^2 and then were incubated with CM-H_2DCFDA at a final concentration of 5 µM in PBS for 30 min at 37ºC. The dye was then rinsed off the cells with PBS. This was followed by trypsinisation and re-suspension of cells for each condition in 0.1% BSA-PBS and PI (2 µM) before being measured by flow cytometry (Ex 492-495, Em 517-527).

2.9 Reverse Phase HPLC Analysis

2.9.1. Reverse Phase HPLC Analysis for PPIX Detection

To detect and evaluate the level of PPIX in various samples, i.e. ALA or chelator+ALA, porphyrins extracted from each sample were subjected to HPLC analysis.

HPLC was performed on a Dionex Ultimate 3000 system (Sunnyvale, California, USA), equipped with a Phenomenex Gemini, 5 µm C-18 (150x4.6 mm) column, with a flow rate of 1 ml/min, and detection at 404 nm. Mobile phase A was 0.1% TFA in water, and mobile phase B was 0.1% TFA in acetonitrile. Gradient was T = 0 min, B= 20%, T= 3 min, B= 20%, T= 13 min, B= 100%, T= 17 min, B= 100%. The retension time was 11.8-11.9 min for all samples. The detection and quantification limits (LOD and LOQ) were calculated as described by ICH guidelines (ICH-Q2(R1) 2005@ http://www.ich.org/), using equation LOD=3.3xσ and LOQ=10xσ, where σ is the standard deviation of the blank noise. Solutions of PPIX were prepared at the LOD and LOQ, corresponding to 0.01 and 0.1 µM, respectively.

2.9.2. Reverse Phase HPLC Analysis of Uncaged CICs

HPLC chromatograms of BY123 and BY128 along with SIH were obtained after the uncaging of these CICs with a UVA dose of 250 kJ/m^2 in a simple chemical system

.

HPLC was performed on the Dionex system as above with detection at 214 nm. Mobile phase A was 0.1% TFA or HCOOH in water, mobile phase B was 0.1% TFA or HCOOH in acetonitrile. Gradient was *T* = 0 min, B = 5%; *T* = 10 min, B = 95%; *T* = 15 min, B = 95%; *T* = 15.1 min, B = 5%; *T* = 18.1 min, B = 5%.

2.10. Statistical Analysis

Results were expressed as mean +/- standard deviation (SD). Data were analysed using paired and unpaired t-tests (Excell 2010). The *p* value of < 0.05 was considered as a significant difference between groups of data. The ranges given to the number of experiments for each graph presented in the result's section (i.e.n=3-8), indicates the number of independent experiments carried out with different compounds/treatments (e.g. 3) while including the overall number of independent experiments carried out with control conditions (e.g. 8).

CHAPTER THREE

RESULTS

3.1. Background

The use of UVA radiation for selective ALA-PDT of superficial skin lesions such as AK may be advantageous as UVA is potentially more damaging than visible light. Indeed UVA radiation is a strong oxidizing agent that generates ROS in exposed cells. The present study, first investigated the suitability of UVA radiation as a light source to improve the efficiency of cell killing following ALA administration using two different skin cancer cell models of HaCaT and Met 2. As iron chelation has been shown to boost the level of accumulation of PPIX in ALA-treated cells (Curnow *et al*, 2007), three iron chelators SIH, PIH and DFO were tested to assess the potential to further improve the efficiency of ALA-PDT of cultured skin cells using UVA radiation as the light source. Finally since prolonged exposure of skin cells to 'naked' iron chelators may result in toxicity as a result of iron starvation, the potential of UVA-activatable caged-iron chelators (CICs) BY123 and BY128, derived from parental chelator SIH, was investigated as a safer intervention strategy to improve the efficiency of ALA-PDT in skin cells using UVA radiation.

The proof of concept studies were first performed with the spontaneously immortalised keratinocyte HaCaT cell line that is hyper-proliferative and has significantly higher proliferation rate than normal human skin keratinocytes and fibroblasts (A. Aroun, PhD thesis, 2011; this laboratory). In numerous ALA-PDT studies, this cell line has been used as a reliable *in vitro* model for human skin cell carcinoma. In this project, the key data obtained with HaCaT cells was then further confirmed in a skin cancer keratinocyte cell line (i.e. Met 2) clonally derived from a

local recurrence of invasive SCC (originally isolated from the back of the hand of the same patient (see Proby *et al*, 2000 and Popp *et al*, 2000). Unlike HaCaT cells, the growth of Met2 cells's growth is dependent upon a feeder layer composed of mitogen-inactivated 3T3 fibroblasts that complicates its long-term maintenance in culture. As a result, the experiments with Met2 cell line were only carried out to confirm some of the key data obtained with HaCaT cell line.

To evaluate the extent of ALA-induced cell damage and death upon UVA radiation of HaCaT cells, the level of cell damage was first monitored by MTT assay 4 and 24 h following UVA irradiation. The level of cell death was then also scored by flow cytometric Annexin V/PI dual staining 4 and 24 h after UVA radiation. The long-term effect of ALA+/-chelator treatments were also monitored with colony forming assay 10-14 days following UVA irradiation of the cells. The level of cell damage and cell death following various treatments involving ALA + UVA treatment alone or combined with chelator pre-treatment was also correlated with the level of PPIX accumulation obtained with the same treatments. The level of PPIX accumulation in cells treated with chelator +/- ALA-treated cells was also corroborated with the extent of ROS generation under the same conditions following UVA radiation. These evaluations are summarised in **scheme 3.1** and discussed in detail in this section.

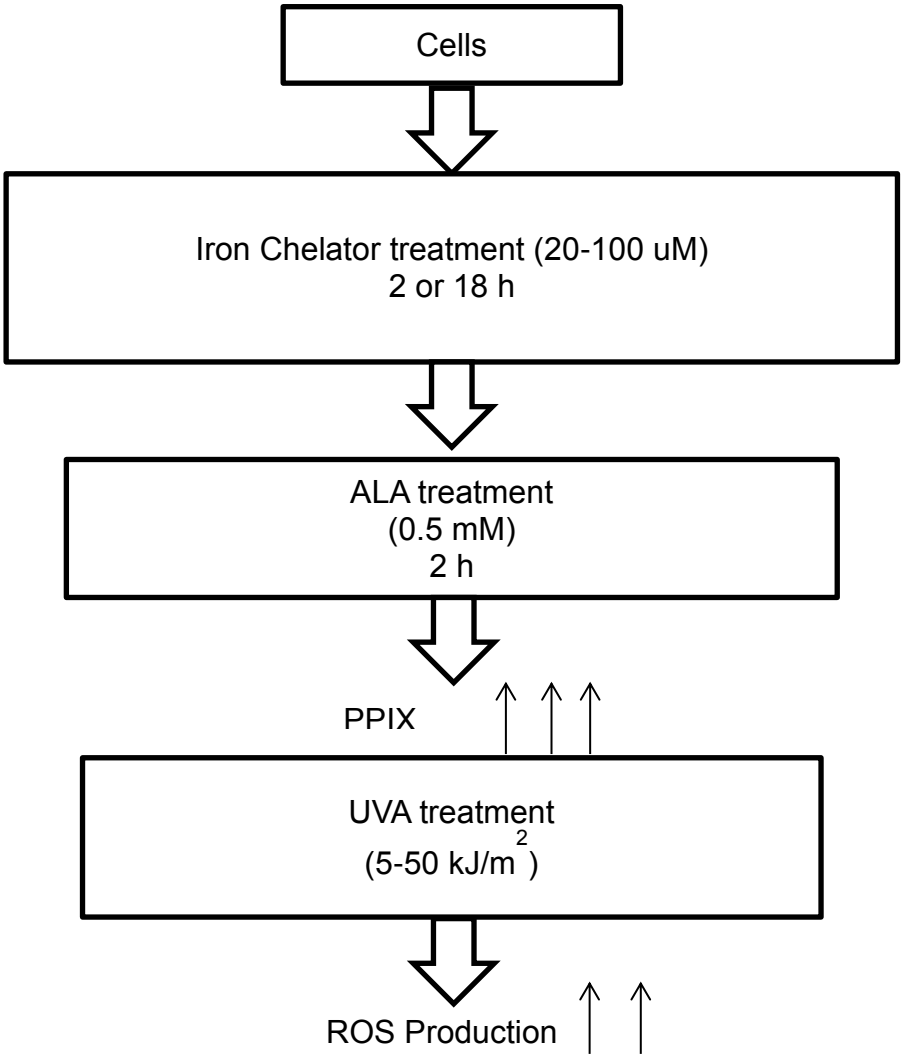

Scheme 3.1. The effect of chelator and ALA treatment on PPIX and ROS production. HaCaT cells were first treated with iron chelators (20-100 μM) and incubated for 2 or 18 h, before treating the cells with 0.5 mM ALA or not and incubated for 2 h in the dark. This increased the PPIX levels significantly. Upon UVA exposure (5-50 kJ/m^2), significant amount of ROS was produced which in effect caused toxicity and cell death.

3.2. The Effect of ALA on HaCaT Cell Survival Following Irradiation with Low Doses of UVA

Data from this laboratory have previously indicated that a 2 h treatment with 0.5 mM ALA could significantly sensitise HaCaT keratinocytes to the damaging effects of UVA (T. Radka, MPhil thesis, 2010). To confirm these data and to establish a range of doses of UVA that may be suitable for the present project, the HaCaT cells were

treated with 0.5 mM ALA for 2 h and then exposed to an increasing doses of UVA (i.e. 10, 20 and 50 kJ/m^2). MTT analysis was performed 4 and 24 h after irradiation. The MTT assay evaluates to what extent cellular dehydrogenases convert the yellow soluble MTT (3-(4,5-dimethylthiazol-2-yl)-2,5-diphenyltetrazolium bromide) into an insoluble purple formazan product. The level of formazan production is directly proportional to the level of cellular dehydrogenases activity and is therefore used as a measure of cell viability. Therefore MTT is often used as a rapid and sensitive first line of evaluation for screening of novel compounds in cytotoxicity studies. The data obtained with MTT analysis in the present study was expressed as a percentage of the enzymatic (i.e. dehydrogenase) activity of the untreated control cells (set as 100%).

The results (**Figures 3.1 A- B**) revealed that in the absence of ALA, low doses of UVA (i.e. 10 kJ/m^2) had no significant effect on the enzymatic activity of cells when compared to the corresponding untreated control cells either 4 or 24 h after irradiation. However 0.5 mM ALA treatment substantially increased the susceptibility of HaCaT cells to UVA-induced damage in a dose-dependent manner 4 h following UVA exposure, as reflected by a significant and dose-dependent decrease in the percentage enzymatic activity of ALA-treated cells, following UVA irradiation. The decrease in the percentage enzymatic activity in ALA-treated cells was even more pronounced 24 h following UVA radiation of cells, especially with UVA doses of 10 and 20 kJ/m^2.

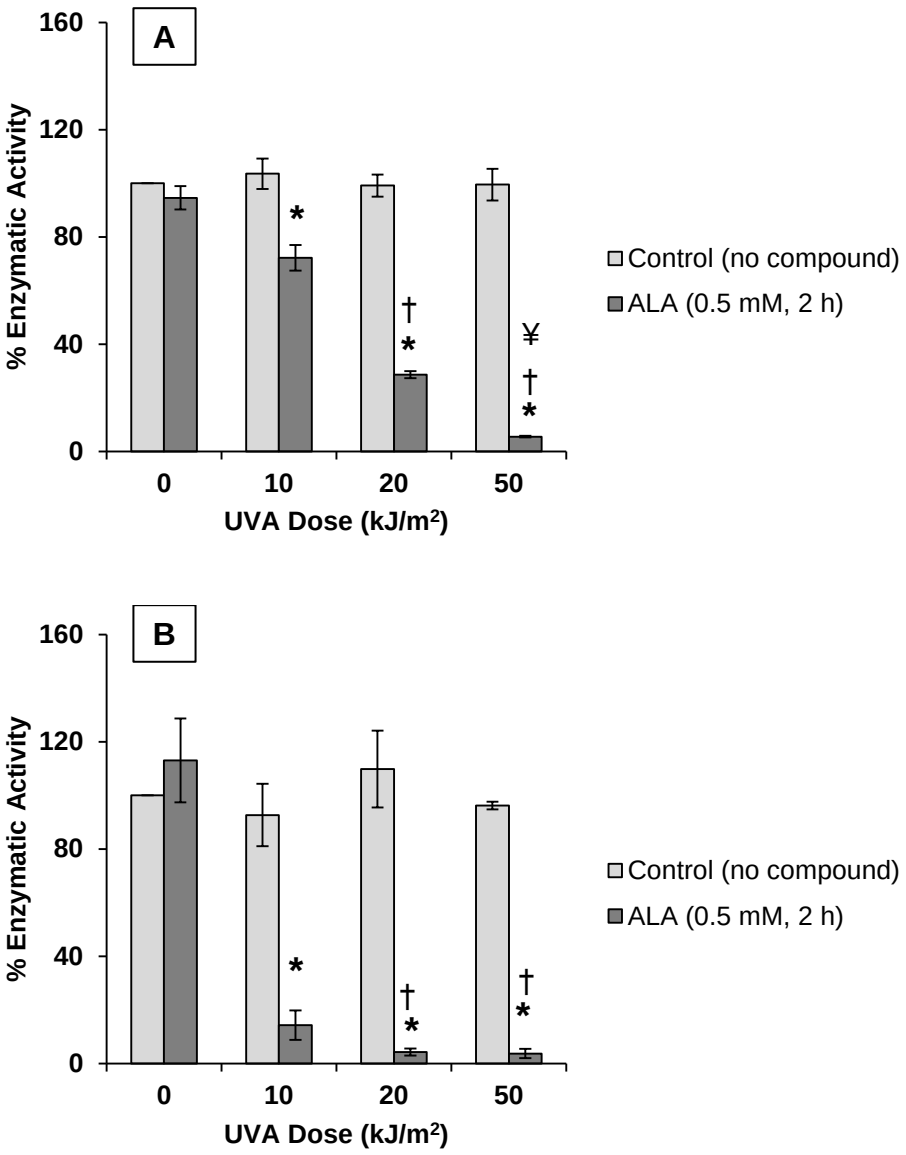

Figures 3.1 A-B: The effect of ALA on cell viability 4 h (A) and 24 h (B) after irradiation of cells with low doses of UVA by MTT assay.

HaCaT cells were treated with 0.5 mM ALA for 2 h at 37ºC in the dark prior to irradiation with UVA doses of 10, 20 or 50 kJ/m^2. Control cells were treated identically except that they were either not irradiated (i.e. 0) and (or) not treated with ALA (i.e. dark grey columns). MTT analysis was performed 4 h (**A**) and 24 h (**B**) after irradiation. The results were expressed as mean ± standard deviation (n=3-4).

*: $p<0.05$, significantly different from the unirradiated ALA-treated cells.

†: $p<0.05$, significantly different from the ALA-treated cells irradiated with UVA dose of 10 kJ/m^2.

¥: $p<0.05$, significantly different from the ALA-treated cells irradiated with UVA dose of 20 kJ/m^2.

To confirm the results obtained with the MTT assay, the level of apoptotic and necrotic cell death was scored by flow cytometry using the dual Annexin V/PI staining method. For this purpose, the ALA-treated cells were exposed to UVA doses of 5-50 kJ/m^2 and then incubated for either 4 or 24 h at 37^{o}C prior to flow cytometry analysis. The results (**Figures 3.2 D-G**) revealed that while UVA irradiation *per se* had no significant effect on cell death in HaCaT cells, in ALA-treated cells, UVA triggered a significant and dose-dependent increase in the percentage of cell death, 4 and 24 h following radiation treatment. Furthermore, with higher UVA doses of 10 and 20 kJ/m^2, the level of necrotic cell death was much higher than apoptotic cell death in ALA treated cells at both 4 and 24 h time points. Since necrotic cell death is known to occur following severe physical or chemical insult in cells, it appears that ALA treatment substantially sensitises the cells to higher doses of UVA, resulting in necrotic cell death. The observed dose-dependent increase in the percentage of cell death in ALA+UVA-treated cells in flow cytometry analysis (**Figures 3.2 D-G**) correlated well with a reciprocal decrease in the percentage of cell viability of the same conditions observed in MTT analysis (**Figures 3.1 A-D**).

Taken together, the flow cytometry analysis was in agreement with the MTT analyses, as both assays confirmed that ALA-treatment strongly sensitises the HaCaT cells to UVA-induced cell damage and death. Furthermore it was apparent that necrosis was the primary mode of cell death induced by higher UVA doses of 20 and 50 kJ/m^2 in ALA-treated cells.

Figure 3.2 (A-C) shows some examples of the raw data obtained by the flow cytometry analysis measured by FACS CANTO machine 24 h post UVA.

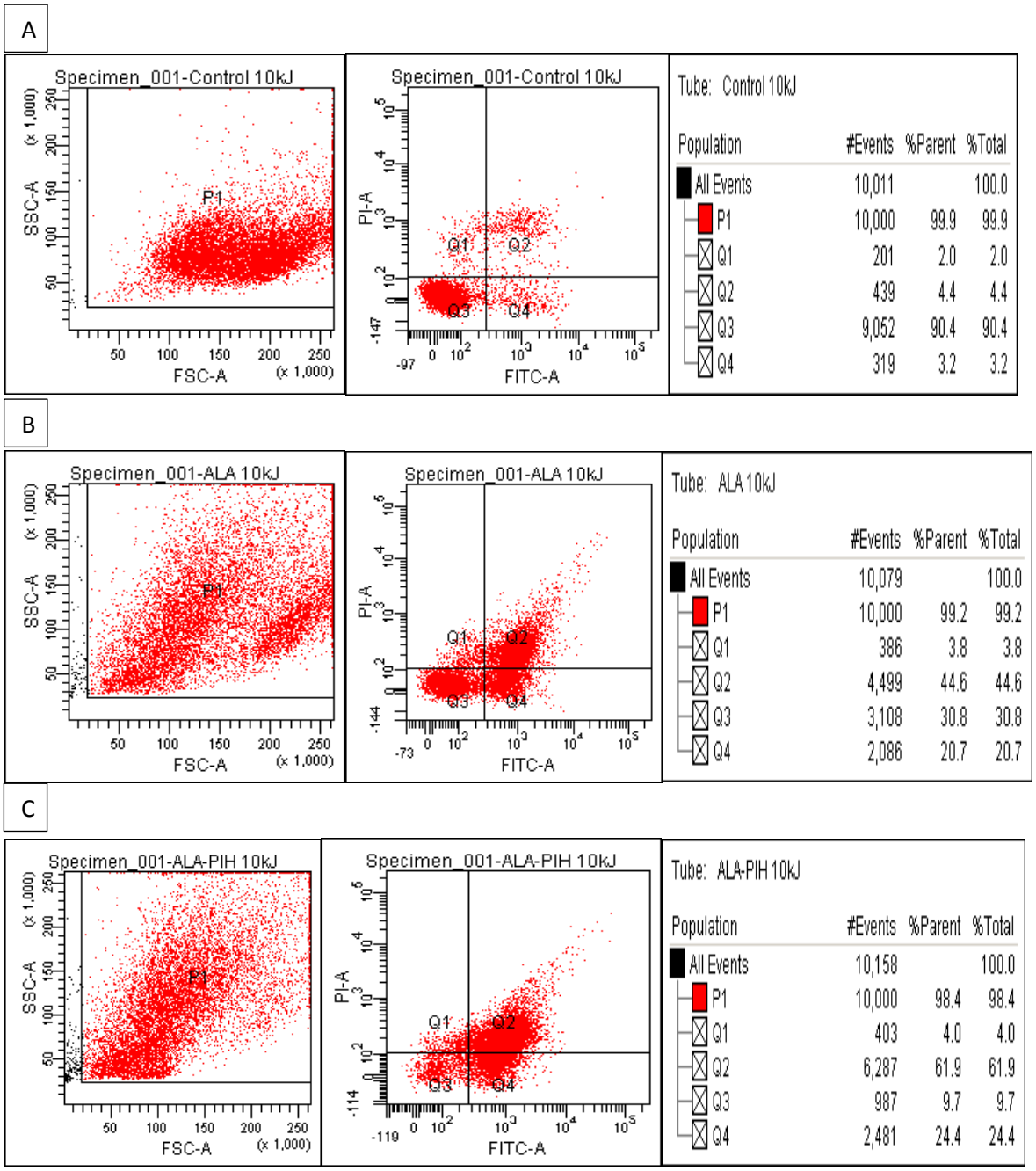

Figure 3.2 (A-C): A representative example of flow cytometry analysis of HaCaT cells with ALA treatment alone or in combination with chelators (e.g. PIH) 24 h following UVA irradiation. HaCaT cells treated with UVA dose of 10 kJ/m^2 alone (**A**) or treated with 0.5 mM ALA for 2 h at 37ºC in dark followed by UVA irradiation with a dose of 10 kJ/m^2 (**B**) or pre-treated with 100 µM PIH for 18 h at 37ºC followed by ALA (2h at 37^{o}C) and UVA (10 kJ/m^2) treatments. Flow cytometry analysis was performed 24 h after UVA irradiation following Annexin V-PI dual staining. The diagrams on the left (P1) represent the gated cell population (i.e. excluding cell debris), while the middle and the right diagram represent the quadrants (Qs) and therespective percentages of live (Q3), apoptotic (Q4) and of necrotic (Q1+2) scored during the analysis.

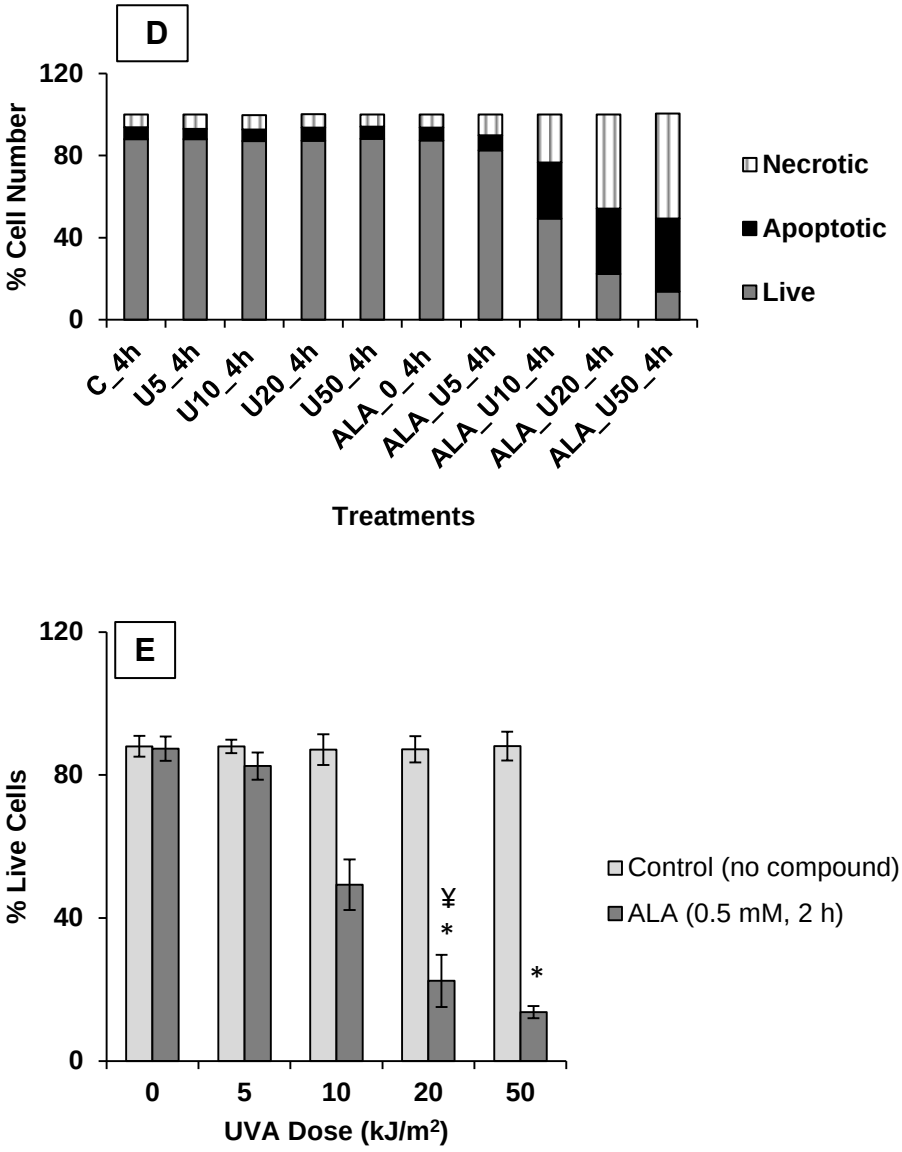

Figures 3.2 D-E: The effect of ALA treatment on the percentage of necrosis and apoptosis in HaCaT cells 4 h following varying UVA doses.

HaCaT cells were treated with 0.5 mM ALA for 2 h at 37ºC in the dark prior to irradiation with UVA doses of 0, 10, 20 or 50 kJ/m^2. Control cells were treated identically except that they were either not irradiated and (or) not treated with ALA. Flow cytometry analysis was performed 4 h after UVA irradiation following Annexin V-PI dual staining (n=7-12). **Figure 3.2 A** represents the percentage of live, apoptotic and necrotic cells 4 h following UVA irradiation of ALA-treated or untreated cells at varying UVA doses; e.g. “U5-4h”. **Figure 3.2 B** compares the percentage of “Live” cell population in ALA-treated and untreated cells 4 h following UVA irradiation. ”U” in the graph refers to the UVA dose applied.

*: $p<0.05$, significantly different from the unirradiated ALA-treated cells.

¥: $p<0.05$, significantly different from the ALA-treated cells irradiated with UVA dose of 10 kJ/m^2.

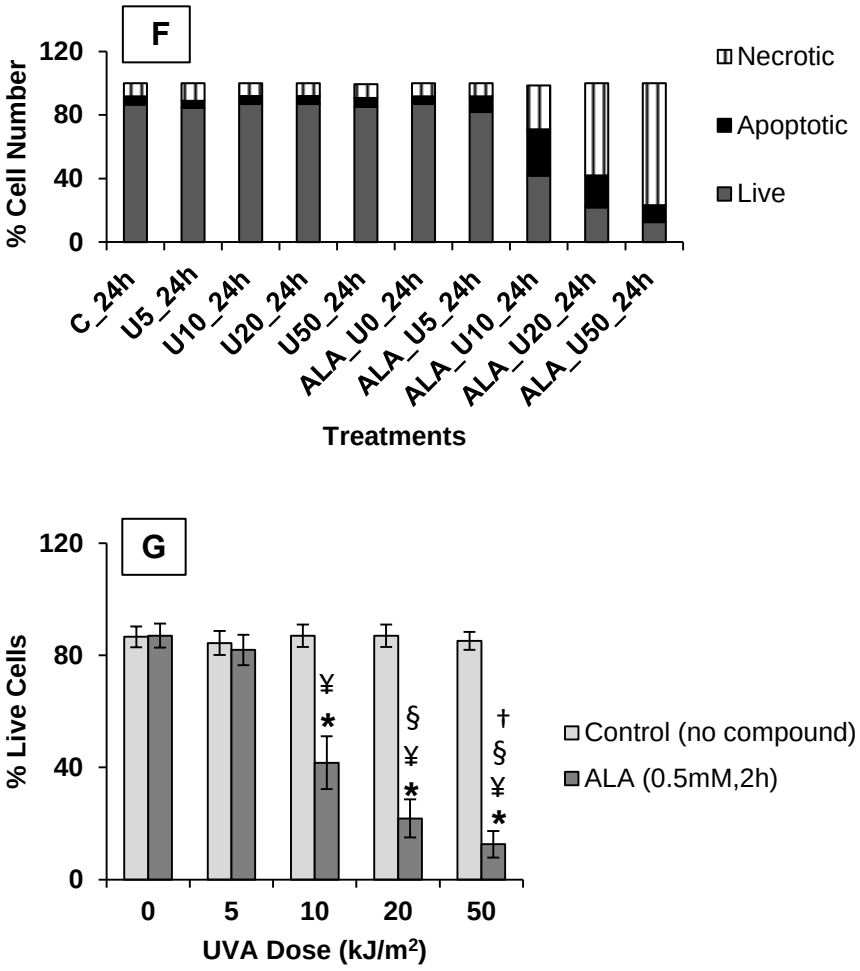

Figures 3.2 F-G: The effect of ALA treatment on the percentage of necrosis and apoptosis in HaCaT cells 24 h following UVA irradiation.

HaCaT cells were treated with 0.5 mM ALA for 2 h at 37ºC in the dark prior to irradiation UVA doses of 5, 10, 20 or 50 kJ/m^2 (i.e. Conditions ALA_U5_24 h, ALA_U10_24 h, ALA_U20_24 h, and ALA_U50_24 h, respectively) . Control cells were treated identically except that they were either not irradiated (i.e. C_24 h and ALA_U0_24 h), and (or) not treated with ALA (i.e. U5_24 h, U10_24 h, U20_24 h and U50_24 h respectively).

Flow cytometry analysis was performed 24 h after UVA irradiation following Annexin V-PI staining (n=7-12). **Figure 3.2 C** represents the percentage of "Live", "Apoptotic" and "Necrotic" cells as scored by flow cytometry, 24 h following UVA irradiation of ALA-treated or untreated cells. **Figure 3.2 D** compares the percentage of "Live" cell population in ALA-treated and untreated cells 24 h following UVA irradiation. "U" in the graph refers to the UVA dose applied.

*: $p<0.05$, significantly different from the unirradiated ALA-treated cells.

¥: $p<0.05$, significantly different from the ALA-treated cells irradiated with UVA dose of 5 kJ/m^2.

§: $p<0.05$, significantly different from the ALA-treated cells irradiated with UVA dose of 10 kJ/m^2.

†: $p<0.05$, significantly different from the ALA-treated cells irradiated with UVA dose of 20 kJ/m^2.

3.3. The Cytotoxic Effect of Iron Chelators on HaCaT Cells

3.3.1. Comparison of the Cytotoxic Effect of Equimolar Concentrations of DFO, PIH and SIH in HaCaT Cells

Prolonged exposure of cells to strong iron chelators has been linked to severe toxicity and cell death due to iron starvation (Richardson *et al*, 2007). Previous studies from this laboratory have shown that short exposure (i.e. 4-18 h) of cultured human skin cell lines FEK4 and HaCaT to iron chelators DFO, PIH and SIH up to a final concentration of 100 μM deplete the basal and UVA-induced levels of labile iron in cells without causing significant toxicity (Yiakouvaki *et al*, 2006; Pourzand *et al*, 1999; Zhong *et al*, 2004; Reelfs *et al*, 2004; Aroun, 2012).

In the present project we re-evaluated the potential toxicity of the above chelators in HaCaT cells under the growing conditions set in **Materials and Methods**. HaCaT cells were exposed to DFO, PIH and SIH at final concentrations of 20, 50 and 100 μM for 24 and 72 h at 37^{o}C, the level of cytotoxicity of the compounds was then evaluated with the MTT assay.

The results (**Figure 3.3**) showed that at 72 h, there was a significant reduction in enzymatic activity in cells treated with DFO and SIH at a final concentration of 100 μM. For example, the comparison of the values obtained from MTT assay in cells treated with 100 μM DFO for 24 or 72 h revealed a significant drop in percentage enzymatic activity from 93.1% at 24 h to 18.5% at 72 h. Similarly in cells treated with 100 μM SIH, the percentage enzymatic value dropped from 60.2% at 24 h to 22.9% at 72 h. However when HaCaT cells were treated with 20 μM SIH, there was no toxicity observed up to 72 h. On the other hand PIH treatment appeared to have no significant toxicity to cells at all concentrations used, either at 24 h or 72 h.

In the light of these data in the present study, the incubation periods with the iron chelators were set up to a maximum of 18 h to avoid toxicity via iron depletion. In terms of concentration, DFO and PIH were used at a final concentration of 100 μM, as these chelators did not exhibit any toxicity when incubated with cells for 24 h. SIH however was used at a lower concentration of 20 μM, as the higher concentrations 50 and 100 μM were toxic to the cells even when incubated for 24 h.

The calcein fluorescence assay was used to confirm that these concentrations of chelators were effective in depleting the intracellular labile iron after a period of 18 h incubation with cells (data not shown).

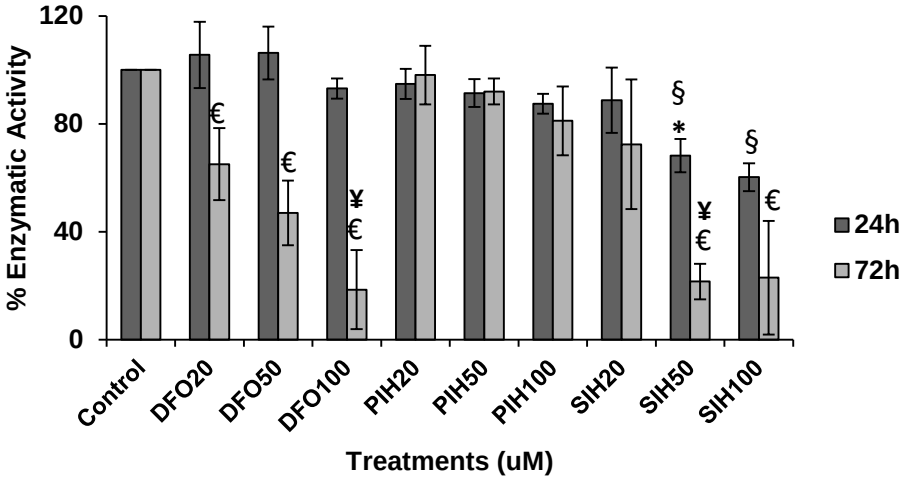

Figure 3.3: Evaluation of the toxicity of DFO, PIH and SIH on HaCaT cells by MTT assay.

HaCaT cells were treated with DFO, SIH and PIH at final concentrations of 20 μM, 50 μM and 100 μM. MTT analysis was performed 24 h and 72 h following addition of the compounds (n=3-4).

*: $p<0.05$, significantly different from cells treated with the corresponding compound at a final concentration of 20 μM at 24 h time point.

¥: $p<0.05$, significantly different from cells treated with the corresponding compound at final concentration of 20 μM at 72 h time point.

§: $p<0.05$, significantly different from the untreated cells at 24 h time point.

€: $p<0.05$, significantly different from the untreated cells at 72 h time point.

3.3.2. The Effect of ALA and Chelator Treatment on the Percentage of Apoptosis and Necrosis in HaCaT Cells 4 and 24 h Following UVA Irradiation

To evaluate the effect of iron chelation in further improving the efficiency of ALA-PDT with UVA, the percentage of cell death was quantified using the sensitive flow cytometry-based Annexin V/ PI dual staining assay. For this purpose the exponentially growing HaCaT cells were treated with DFO (100 μM), PIH (100 μM) and SIH (20 μM) for 18 h at 37ºC prior to ALA administration (0.5 mM, 2 h). Cells were then irradiated with UVA doses of 10, 20 or 50 kJ/m^2 and analysed with flow cytometry 4 or 24 h following irradiation. **Figures 3.4**, **3.5** and **3.6** show the flow cytometry analysis of HaCaT cells that were treated with DFO (100 μM), PIH (100 μM) and SIH (20 μM) prior to ALA and UVA treatments. In general the treatment of cells with all iron chelators alone, UVA alone or iron chelators + UVA combinations did not show any significant toxicity to the cells when compared to the corresponding untreated controls. However ALA-treatment of cells that were pre-treated with iron chelators, substantially sensitised the cells to UVA irradiation as monitored 4 or 24 h following radiation by flow cytometry. In terms of mode of cell death, the chelator + ALA-treated cells died predominantly by necrotic cell death at 24 h time points after UVA irradiation with both UVA doses of 10 and 20 kJ/m^2.

The comparison of the percentage of cell death between UVA-irradiated cells treated with ALA alone or combined with iron chelator pre-treatment clearly showed the higher efficiency of the chelator + ALA treatments in inducing cell death following UVA radiation. While this effect was observed both at 4 and 24 h time points with all UVA doses used, the higher efficiency of the chelators + ALA combination treatments was evident from the higher cell killing observed at the lowest UVA dose of 10 kJ/m^2 when compared to the corresponding ALA-treated cells alone. Indeed

while the percentage of cell death in ALA-treated cells was 50.7% and 56.8% respectively, 4 and 24 h after UVA dose of 10 kJ/m^2, in chelator + ALA-treated cells, the percentage of cell killing increased up to 86.6% and 90.4% respectively, 4 and 24 h after the same UVA dose.

Among the chelators used, SIH (20 μM) appeared to be the most potent chelator when combined with ALA providing a substantial increase in the percentage of cell death following UVA irradiation. For example at 4 h time point with UVA dose of 10 kJ/m^2, the comparison of the percentage of cell death in chelator + ALA-treated cells revealed 71.1% cell death in DFO + ALA-treated cells, 68.1% cell death in PIH+ ALA-treated cells and 86.6% cell death in SIH+ALA-treated cells, when compared to untreated control cells. At 24 h with a UVA dose of 10 kJ/m^2, the percentage of cell death increased up to 87.8% in cells treated with 20 μM SIH and ALA and up to 90.4% and 82.5% in cells treated with 100 μM DFO and ALA and 100 μM PIH and ALA-treated cells, respectively when compared to untreated control cells.

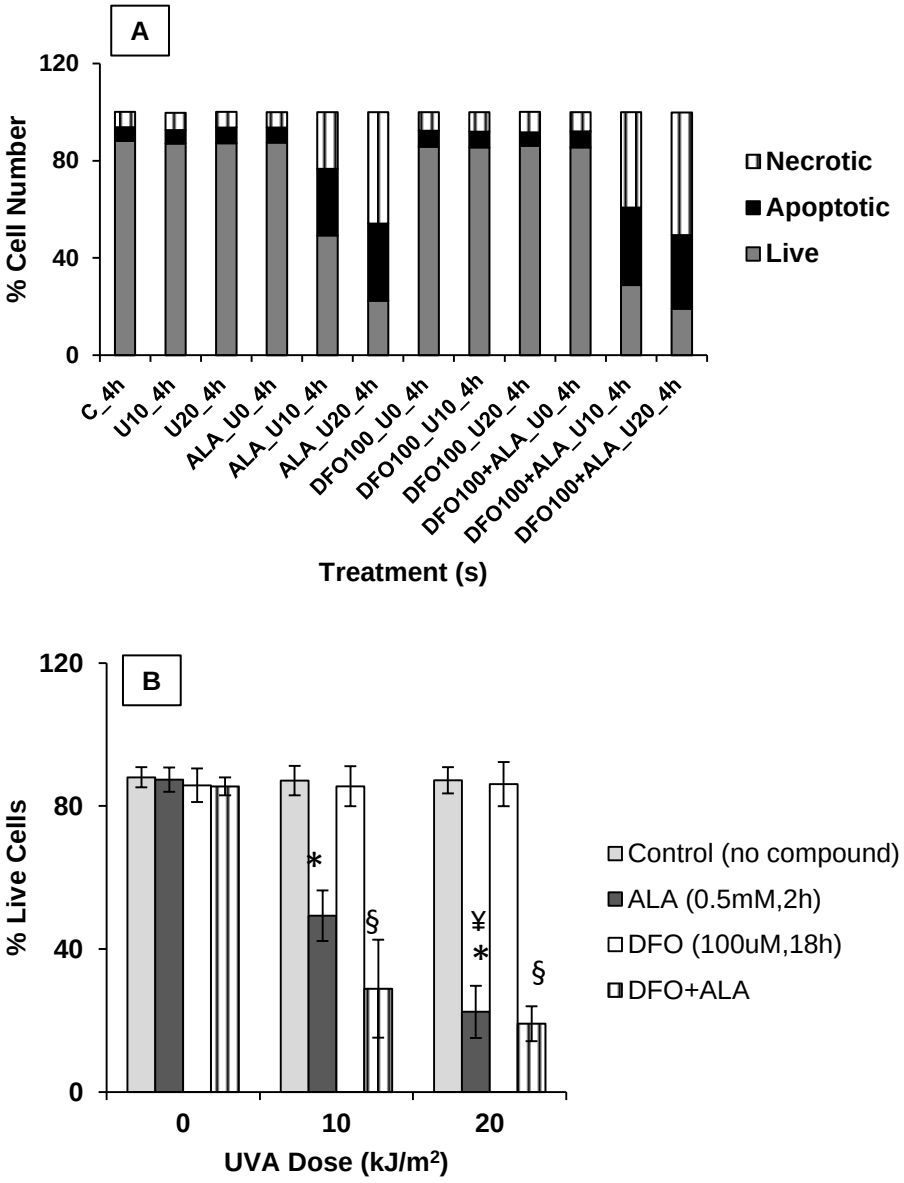

Figures 3.4 A-B: The effect of ALA and DFO (100 µM) on the percentage of necrosis and apoptosis in HaCaT cells 4 h following UVA irradiation.

In **DFO + ALA** condition, HaCaT cells were first treated with 100 µM DFO for 18 h and then with ALA 0.5 mM for 2 h at 37 ^{o}C in the dark followed by UVA irradiation with UVA doses of 10 or 20 kJ/m^2.(i.e. DFO+ ALA_U10_4h and DFO+ ALA_U20_4h). In **ALA** condition, cells were treated with 0.5 mM ALA alone (**ALA**) for 2 h at 37ºC under dark condition, followed by UVA irradiation with UVA doses of 10 or 20 kJ/m^2 (i.e. ALA_U10_4h and ALA_U20_4h). Control cells were treated identically except that they were either not irradiated (i.e. C_4h, ALA_U0_4h, DFO100_U0_4h and DFO100+ALA_U0_4h) and (or) not treated with DFO or ALA (i.e. U10_4h and U20_4h). Flow cytometry analysis was performed 4 h after the UVA irradiation following Annexin V-PI staining (n=3-11). Figure 3.4 A represents the percentage of "Live", "Apoptotic" and "Necrotic" cells as scored by flow cytometry, 4 h following UVA irradiation of ALA-treated only or ALA treated in combination with DFO (100 µM). Figure 3.4B compares the percentage of "Live" cell population in ALA-treated, chelator+ALA treated and untreated cells 4 h following UVA irradiation. "U" in the graph refers to the UVA dose implied.

*: $p<0.05$, significantly different from the unirradiated ALA-treated cells.

¥: $p<0.05$, significantly different from the ALA-treated cells irradiated with UVA dose of 10 kJ/m^2.

§: $p<0.05$, significant difference between UVA-irradiated DFO+ALA and UVA-irradiated ALA conditions at 10 kJ/m^2.

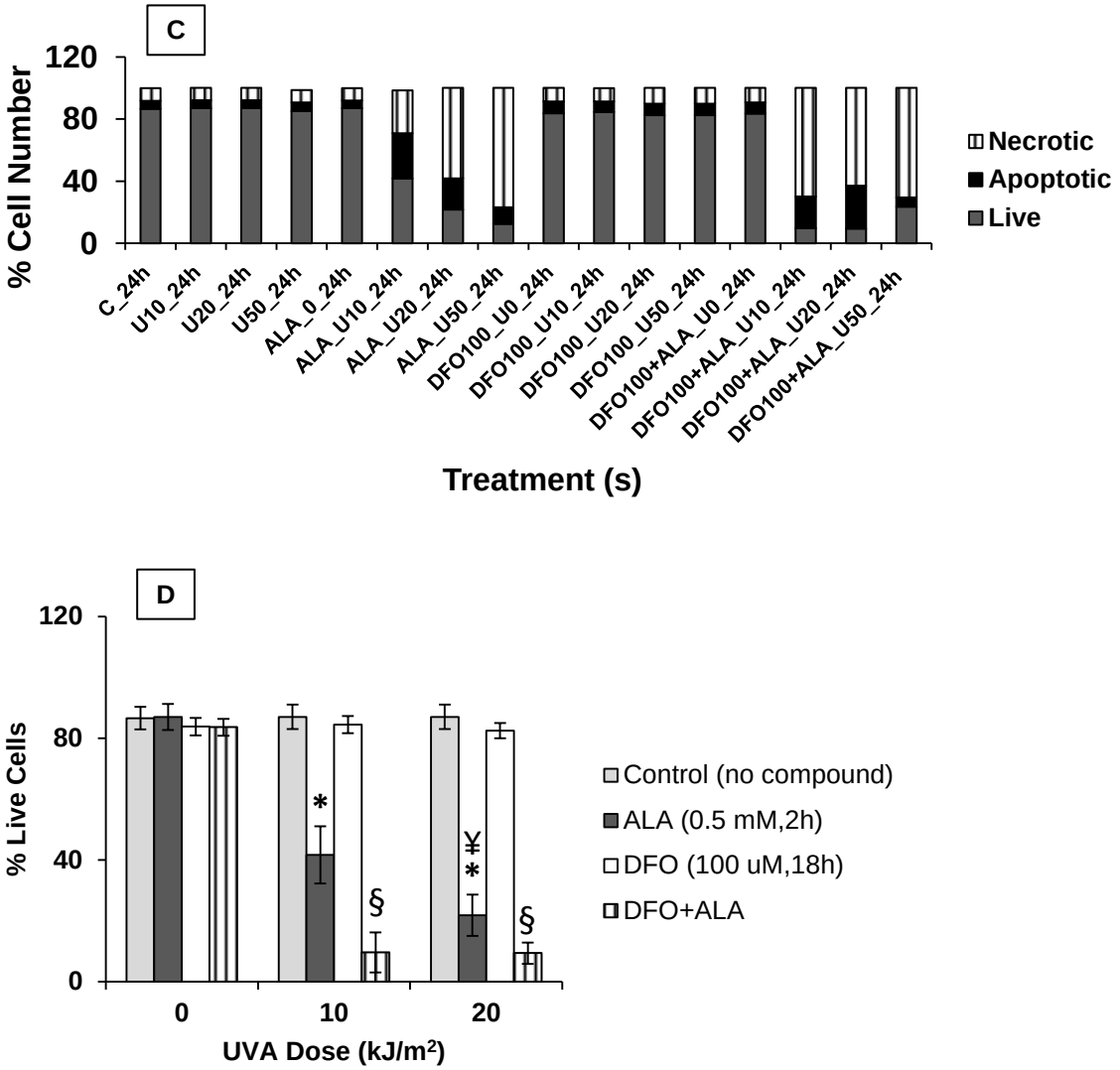

Figures 3.4 C-D: The effect of ALA and DFO (100 µM) on the percentage of necrosis and apoptosis in HaCaT cells 24 h following UVA irradiation.

In **DFO + ALA** condition, HaCaT cells were first treated with 100 µM DFO for 18 h and then with ALA 0.5 mM for 2 h at 37 ^{o}C in the dark followed by UVA irradiation with UVA doses of 10 or 20 kJ/m^{2} (i.e. DFO+ ALA_U10_24h and DFO+ ALA_U20_24h). In **ALA** condition, cells were treated with 0.5 mM ALA alone for 2 h at 37ºC in the dark, followed or not by UVA irradiation with UVA doses of 10 or 20 kJ/m^{2} (i.e.ALA_U10_24h and ALA_U20_24h). Control cells were treated identically except that they were either not irradiated (i.e. C_24h, ALA_U0, DFO100_U0_24h and DFO100+ALA_U0_24h) and (or) not treated with DFO or ALA (i.e. U10_4h and U20_4h). Flow cytometry analysis was performed 24 h after the UVA irradiation following Annexin V-PI dual staining (n=3-11). **Figure 3.4 C** (top) represents the percentage of "Live", "Apoptotic" and "Necrotic" cells as scored by flow cytometry, 24 h following UVA irradiation of ALA-treated only or ALA treated in combination with DFO (100 µM). **Figure 3.4 D** (bottom) compares the percentage of "Live" cell population in ALA-treated, ALA+chelator treated and untreated cells 24 h following UVA irradiation. "U" in the graph refers to the UVA dose implied.

*: p<0.05, significantly different from the unirradiated ALA-treated cells.

¥: p<0.05, significantly different from the ALA-treated cells irradiated with UVA dose of 10 kJ/m^{2}.

§: p<0.05, significant difference between UVA-irradiated DFO+ALA and UVA-irradiated ALA conditions at 10 and 20kJ/m^{2}.

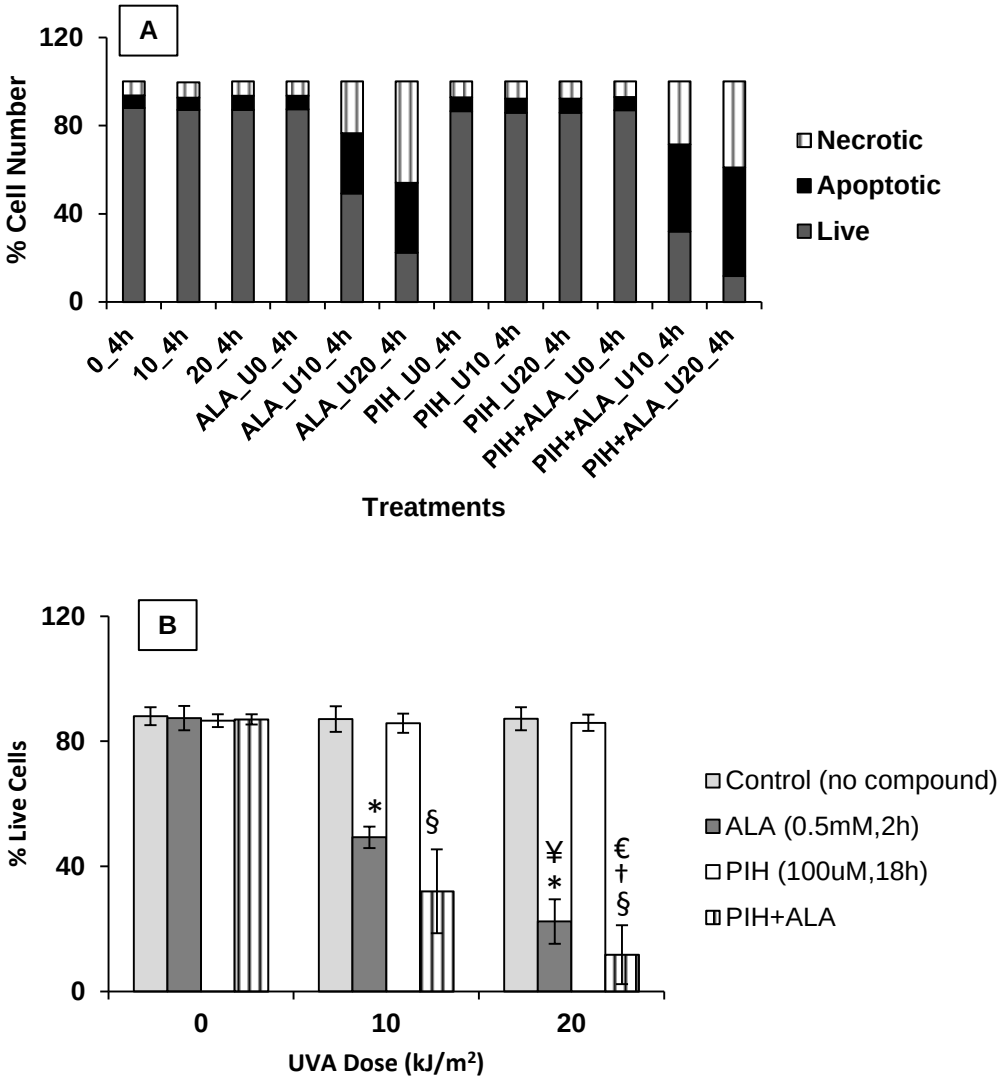

Figures 3.5 A-B: The effect of ALA and PIH (100 µM) on the percentage of necrosis and apoptosis in HaCaT cells 4 h following UVA irradiation.

In **PIH + ALA** condition, HaCaT cells were first treated with 100 µM PIH for 18 h and then with ALA 0.5 mM for 2 h at 37 ^{o}C in the dark followed by UVA irradiation with UVA doses of 10 or 20 kJ/m^2(i.e. PIH+ ALA_U10_4h and PIH+ ALA_U20_4h) . In **ALA** condition, cells were treated with 0.5 mM ALA alone for 2 h at 37ºC in the dark, followed by UVA irradiation with UVA doses of 10 or 20 kJ/m^2 (i.e. ALA_U10_4h and ALA_U20_4h). Control cells were treated the same except that they were either not irradiated (i.e. C_4h, ALA_U0_4h, PIH100_U0_4h and PIH100+ALA_U0_4h) and (or) not treated with PIH or ALA (i.e. U10_4h and U20_4h). Flow cytometry analysis was performed 4 h after the UVA irradiation following Annexin V-PI dual staining (n=3-12). **Figure 3.5 A** (top) represents the percentage of "Live", "Apoptotic" and "Necrotic" cells as scored by flow cytometry, 4 h following UVA irradiation of ALA-treated only or ALA treated in combination with PIH (100 µM). **Figure 3.5 B** (bottom graph) compares the percentage of "Live" cell population in ALA-treated, ALA+chelator treated and untreated cells 4 h following UVA irradiation. "U" in the graph refers to the UVA dose implied.

*: $p<0.05$, significantly different from the unirradiated ALA-treated cells.

¥: $p<0.05$, significantly different from the ALA-treated cells irradiated with UVA dose of 10 kJ/m^2.

§: $p<0.05$, significant difference between UVA-irradiated PIH+ALA and UVA-irradiated ALA conditions at 10 kJ/m^2.

†: $p<0.05$, significant difference between UVA-irradiated PIH+ALA and UVA-irradiated ALA conditions at 20 kJ/m^2

€: $p<0.05$, significant difference between PIH+ALA conditions irradiated with UVA dose of 10 kJ/m^2 and 20 kJ/m^2.

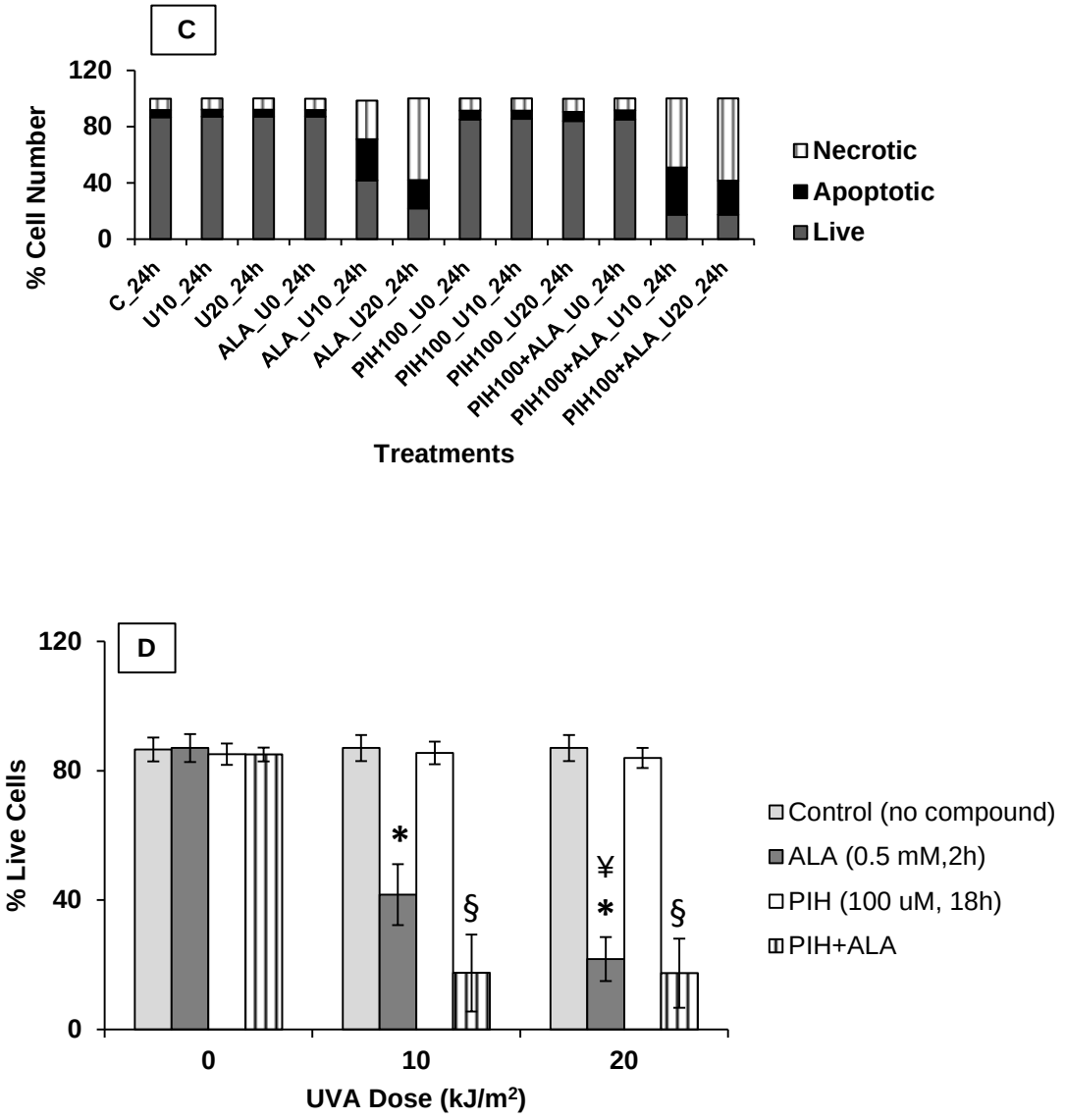

Figures 3.5 C-D: The effect of ALA and PIH (100 µM) on the percentage of necrosis and apoptosis in HaCaT cells 24 h following UVA irradiation.

In **PIH + ALA** conditions, HaCaT cells were first treated with 100 µM PIH for 18 h and then with ALA 0.5 mM for 2 h at 37 ^{o}C in the dark followed by UVA irradiation with UVA doses of 10 or 20 kJ/m^2 (i.e. PIH+ALA_U10_24h and PIH+ALA_U20_24h) In **ALA** condition, cells were treated with 0.5 mM ALA alone for 2 h at 37ºC in the dark, followed or not by UVA irradiation with UVA doses of 10 or 20 kJ/m^2 (i.e. ALA_U10_24h and ALA_U20_24h) . Control cells were treated identically except that they were either not irradiated (i.e. C_24h, ALA_U0_24h, PIH100_U0_24h and PIH100+ALA_U0_24h) and (or) not treated with PIH or ALA (i.e. U10_24h and U20_24h). Flow cytometry analysis was performed 24 h after the UVA irradiation following Annexin V-PI dual staining (n=3-12). **Figure 3.5 C (top)** represents the percentage of "Live", "Apoptotic" and "Necrotic" cells as scored by flow cytometry, 24 h following UVA irradiation of ALA-treated only or ALA treated in combination with PIH (100 µM). **Figure 3.5 D (bottom)** compares the percentage of "Live" cell population in ALA-treated, chelator+ALA treated and untreated cells 24 h following UVA irradiation. "U" in the graph refers to the UVA dose implied.

*: p<0.05, significantly different from the unirradiated ALA-treated cells.

¥: p<0.05, significantly different from the ALA -treated cells irradiated with UVA dose of 10 kJ/m^2.

§: p<0.05, significant difference between UVA-irradiated PIH+ALA and UVA-irradiated ALA conditions at 10 kJ/m^2.

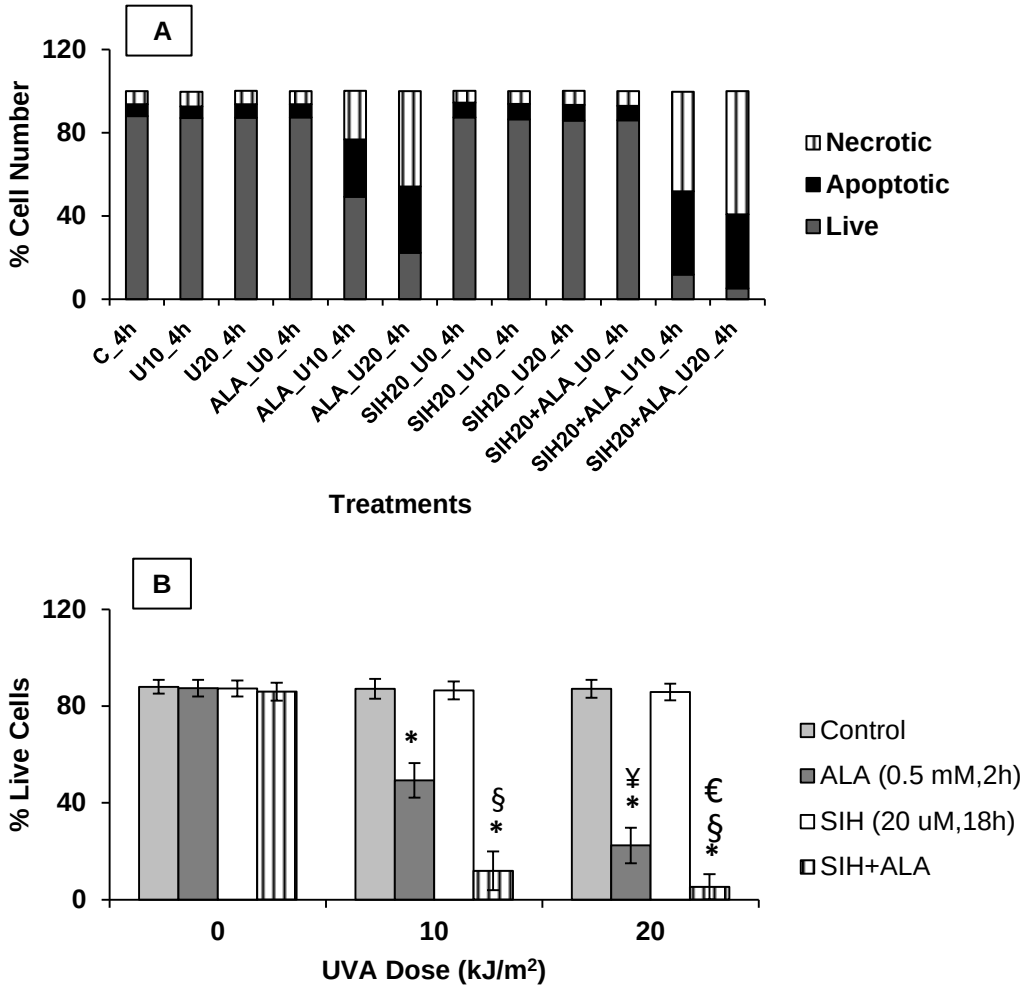

Figure 3.6 A-B: The effect of ALA and SIH (20 µM) on the percentage of necrosis and apoptosis in HaCaT cells 4 h following UVA irradiation.

In **SIH + ALA** conditions, HaCaT cells were first treated with 20 µM SIH for 18 h and then with ALA 0.5 mM for 2 h at 37 ^{o}C in the dark followed by UVA irradiation with UVA doses of 10 or 20 kJ/m^{2} (i.e. SIH+ALA_U10_4h and SIH+ALA_U20_4h). In **ALA** condition, cells were treated with 0.5 mM ALA alone for 2 h at 37ºC in the dark, followed by UVA irradiation with UVA doses of 10 or 20 kJ/m^{2} (i.e. ALA_U10_4h and ALA_U20_4h). Control cells were treated identically except that they were either not irradiated (i.e. C_4h, ALA_U0_4h, SIH20_U0_4h and SIH+ALA_U0_4h) and (or) not treated with SIH or ALA (i.e. U10_4h and U20_4h). Flow cytometry analysis was performed 4h after the UVA irradiation following Annexin V-PI dual staining (n=3-12). **Figure3. 6 A (top)** represents the percentage of "Live", "Apoptotic" and "Necrotic" cells as scored by flow cytometry, 4 h following UVA irradiation of ALA-treated only or ALA treated in combination with SIH (20 µM). Figure **3.6 B (bottom)** compares the percentage of "Live" cell population in ALA-treated, chelator + ALA treated and untreated cells 4 h following UVA irradiation. "U" in the graph refers to the UVA dose implied.

*: $p<0.05$, significantly different from the unirradiated ALA-treated cells.

¥: $p<0.05$, significantly different from the ALA treated cells irradiated with UVA dose of 10 kJ/m^{2}.

§: $p<0.05$, significant difference between UVA-irradiated SIH+ALA and UVA-irradiated ALA conditions at 10 kJ/m^{2}.

€: $p<0.05$, significant difference between UVA-irradiated SIH+ALA and UVA-irradiated ALA conditions at 20 kJ/m^{2}.

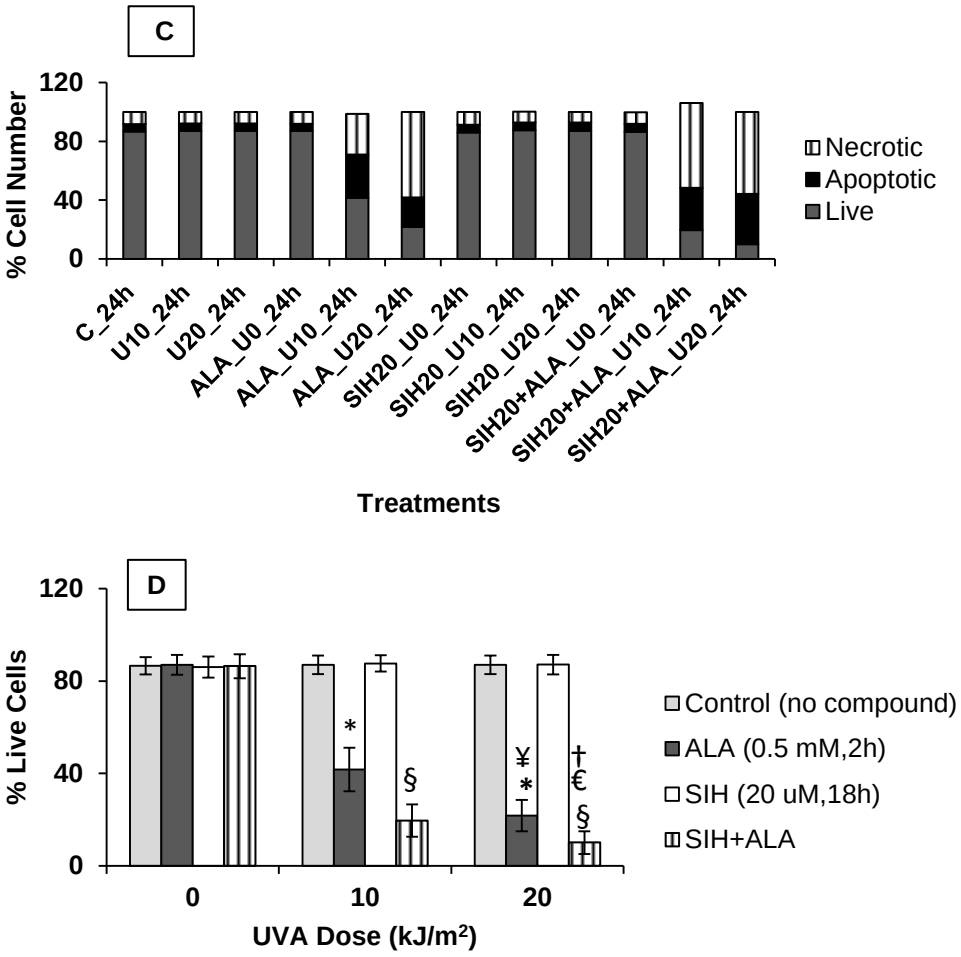

Figures 3.6 C-D: The effect of ALA and SIH (20 μM) on the percentage of necrosis and apoptosis in HaCaT cells 24 h following UVA irradiation.

In **SIH + ALA** conditions, HaCaT cells were first treated with 20 μM SIH for 18 h and then with ALA 0.5 mM for 2 h at 37 ^{o}C in the dark followed by UVA irradiation with UVA doses of 10 or 20 kJ/m^{2} (i.e. SIH+ALA_U10_24h and SIH+ALA_U20_24h). In **ALA** condition, cells were treated with 0.5 mM ALA alone for 2 h at 37ºC in the dark, followed by UVA irradiation with UVA doses of 10 or 20 kJ/m^{2} (i.e. ALA_U10_24h and ALA_U20_24h). Control cells were treated identically except that they were either not irradiated (i.e. C_24h, ALA_U0_24h, SIH20_U0_24h and SIH+ALA_U0_24h) and (or) not treated with SIH or ALA (i.e. U10_24h and U20_24h). Flow cytometry analysis was performed 24 h after the UVA irradiation following Annexin V-PI dual staining (n=3-11). **Figure 3.6 C (top)** represents the percentage of "Live", "Apoptotic" and "Necrotic" cells as scored by flow cytometry, 24 h following UVA irradiation of ALA-treated only or ALA treated in combination with SIH (20 μM). **Figure 3.6 D (bottom)** compares the percentage of "Live" cell population in ALA-treated, chelator + ALA treated and untreated cells 24 h following UVA irradiation. "U" in the graph refers to the UVA dose implied.

*: $p<0.05$, significantly different from the unirradiated ALA-treated cells.

¥: $p<0.05$, significantly different from the ALA -treated cells irradiated with UVA dose of 10 kJ/m^{2}.

§: $p<0.05$, significant difference between UVA-irradiated SIH+ALA and UVA-irradiated ALA conditions at 10 kJ/m^{2}.

€: $p<0.05$, significant difference between UVA-irradiated SIH+ALA and UVA-irradiated ALA conditions at 20 kJ/m^{2}.

†: $p<0.05$, significant difference between SIH+ALA irradiated with UVA doses of 10 kJ/m^{2} and 20 kJ/m^{2}.

3.4. Protoporphyrin IX (PPIX) Measurement in HaCaT Cells

3.4.1. PPIX Detection by HPLC in Chelator +/- ALA-treated HaCaT Cells

To evaluate the level of PPIX produced in ALA-treated HaCaT cells pretreated or not with 20 μM SIH, porphyrins were first extracted from cells as outlined in the **Materials and Methods (section 2.7.2)** section and then subjected to HPLC analysis. To identify the PPIX peak in the HPLC analysis, a pure PPIX standard was obtained from Frontier Scientific (Logan, UT, USA), and injected as a 1 μM solution in 0.1% TFA/ acetonitrile. As depicted in Figure **3.7A**, this standard provided a peak at a retention time of 11.88 min. This was followed by injecting a similar standard PPIX sample prepared at final concentration of 0.1 μM in DMSO from PPIX powder purchased from Sigma (Cat No: P8293-1G). As depicted in **Figure 3.7B**, this sample although less pure than previous standard sample, also showed a major peak at the same retention time. **Figure 3.7C** shows the HPLC profile of the porphyrins extracted from untreated control HaCaT cells. As can be seen, the HPLC profile shows a single peak for PPIX at the expected retention time. **Figures 3.7D**, **E** and **F** illustrate the HPLC profiles obtained for porphyrins (material) extracted from HaCaT cells treated with 0.5 mM ALA alone, SIH+ALA and SIH+ALA, spiked with authentic pure PPIX from the Frontier Scientific kit, respectively. Overlapping these profiles (**Figure 3.7G)** confirms that upon ALA or SIH+ALA treatment of HaCaT cells, PPIX is the predominant porphyrin formed. The only difference is the amount of PPIX formed which as expected increased between ALA treated samples versus untreated controls and SIH+ALA treated samples versus samples treated with ALA alone.

The treated samples were run by HPLC which was carried out by Dr R.Dondi from Dr Eggleston's laboratory.

A. 1 µM PPIX (standard kit)

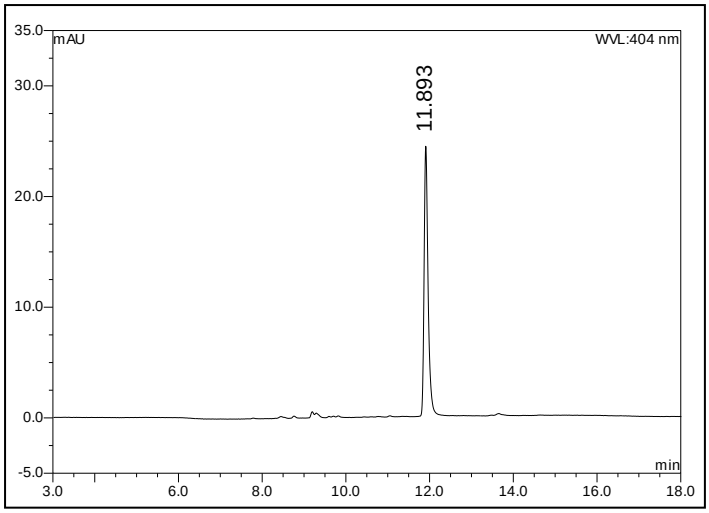

B. 0.1 µM PPIX

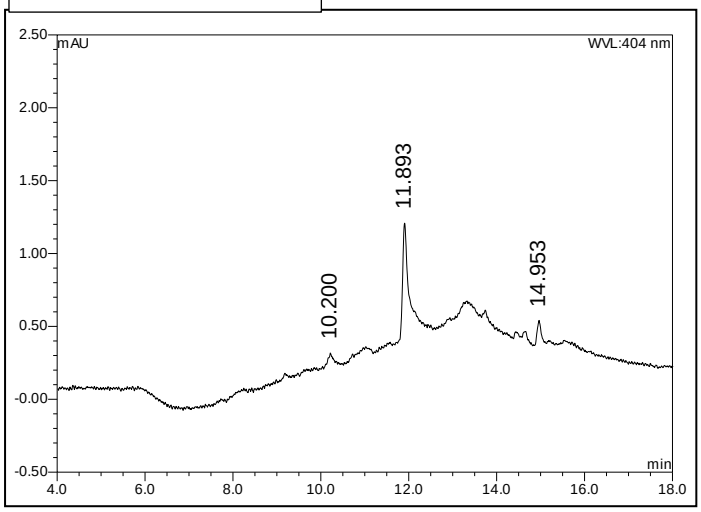

C. Control (untreated)

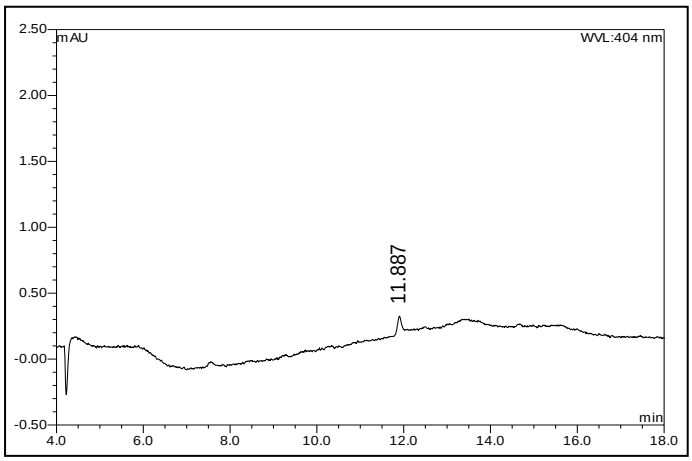

D. ALA (0.5 mM)

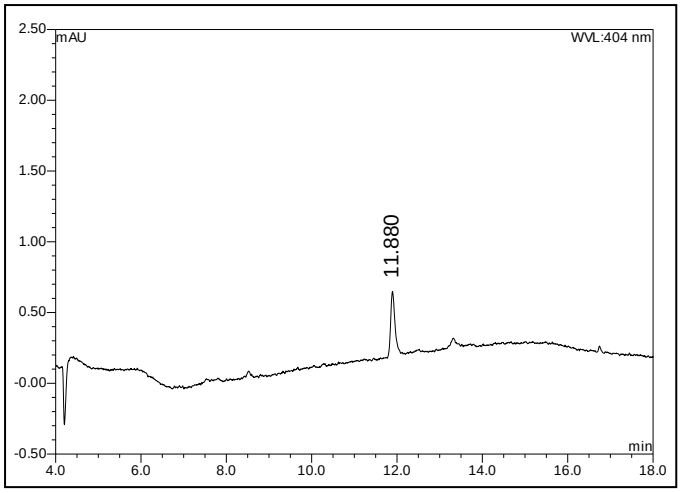

E. SIH+ALA

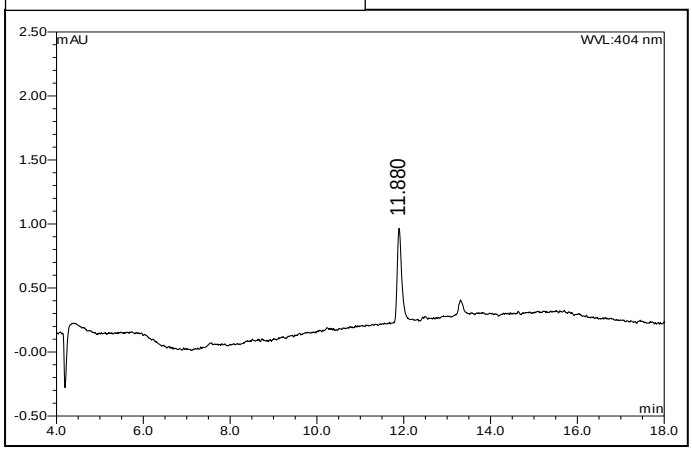

F. SIH+ALA+PPIX

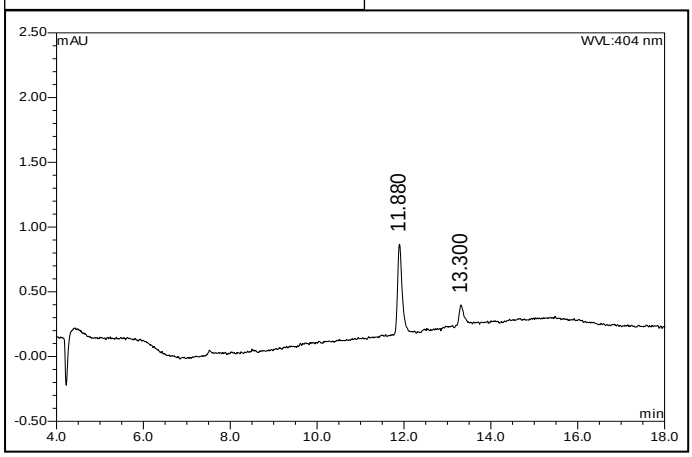

G. ALA, SIH+ALA, SIH+ALA+PPIX

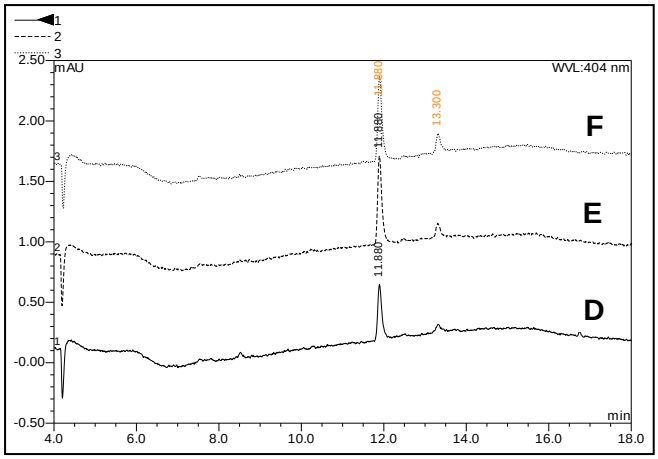

Figures 3.7 A-G: HPLC analysis of porphyrin extracts from HaCaT cells treated with ALA or SIH+ALA. HPLC was performed on a Dionex Ultimate 3000 (Sunnyvale, California, USA), equipped with a Phenomenex Gemini, 5 µm C-18 (150 x 4.6 mm) column, with a flow rate of 1 ml/min, and detecting at 404 nm. Mobile phase A was 0.1% TFA in water, and mobile phase B was 0.1% TFA in acetonitrile. Gradient was T = 0 min, B= 20%, T= 3 min, B= 20%, T= 13 min, B= 100%, T= 17 min, B= 100%. **A** and **B** show the elution profiles obtained for PPIX standards from respectively Frontier Scientific (1 µM in 0.1% TFA in acetonitrile), and Sigma (0.1 µM in DMSO). Porphyrins were also extracted from HaCaT cells treated with 0.5 mM ALA alone or with 20µM SIH+ALA as described in **section 2.9.1**. An equivalent amount of porphyrin extracts from the untreated control- (i.e. **C**), ALA- (i.e. **D**) and SIH+ALA- (i.e. **E**) were injected and the PPIX peak was observed at 11.88 min. **F** shows the HPLC profile of the SIH+ALA sample spiked with pure PPIX standard as in **A**. **G** shows an overlay of the profiles from D-F. Methodology described in section 2.9.1. The LOD value was calculated to be 91 µ AU and the LOQ value was calculated to be 304 µ AU.These results are obtained by Dr R. Dondi.

3.4.2. PPIX Measurement in HaCaT Cells Treated with ALA Alone

As HPLC analysis confirmed that, PPIX was the predominant porphyrin formed in the cells after ALA or SIH+ALA treatments, the quantification of the PPIX induced following various treatments was now performed. This was carried out by fluorometer using the Sigma PPIX as the standard as detailed **in Materials and Method section**.

. **Figure 3.8A** shows that ALA treatment significantly increases the intracellular level of PPIX (i.e.18-fold increase over the untreated control).

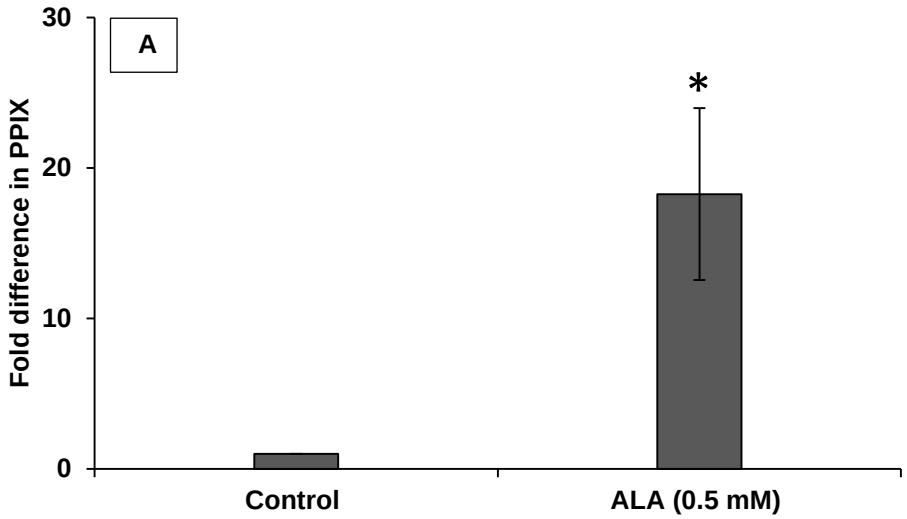

Figure 3.8 A: The effect of ALA treatment on the accumulation of intracellular protoporphyrin IX (PPIX) in HaCaT cells.

HaCaT cells were treated with 0.5 mM ALA and incubated for 2 h at 37ºC in the dark. PPIX was extracted with 1.5 M HCl. The increase in fluorescence was measured 4 h following ALA treatment by spectrofluorometer (excitation 404 nm, emission 604 nm). Data was expressed as mean ± SD (n= 5-13) and plotted as fold increase in PPIX levels when compared to untreated control set as 1.

*: $p<0.05$, significantly different from untreated control cells.

3.4.3. PPIX Measurement in Chelator + ALA-treated HaCaT Cells

The PPIX accumulation in HaCaT cells was also measured in cells that were treated with DFO, PIH and SIH at final concentrations of 20 and 100 μM prior to ALA administration (0.5 mM, 2h). As can be seen in **Figures 3.8B-D**, the chelator treatment *per se* did not significantly increase the PPIX level in cells when compared to the corresponding untreated controls. However when the chelator treatment was followed by ALA administration, the PPIX levels in cells substantially increased when compared to cells treated with ALA alone. While PPIX accumulation in PIH + ALA- and DFO + ALA-treated cells was higher in cells treated with chelator concentrations of 100 μM than 20 μM, in ALA+SIH-treated cells both concentrations of 20 and 100 μM yielded the same increase in PPIX level. In terms of fold-difference in PPIX level, the comparison between ALA-treated and chelator + ALA- treated cells revealed that 20 μM SIH + ALA- and 100 μM DFO + ALA-treated cells accumulated 2.4- and 2.3-fold higher levels of PPIX than ALA-treated cells alone (**Figures 3.8D** and **3.8B**, respectively). On the other hand, PIH+ALA-treated cells accumulated 1.5-fold higher PPIX levels than the corresponding ALA-treated cells alone (**Figure 3.8C**).

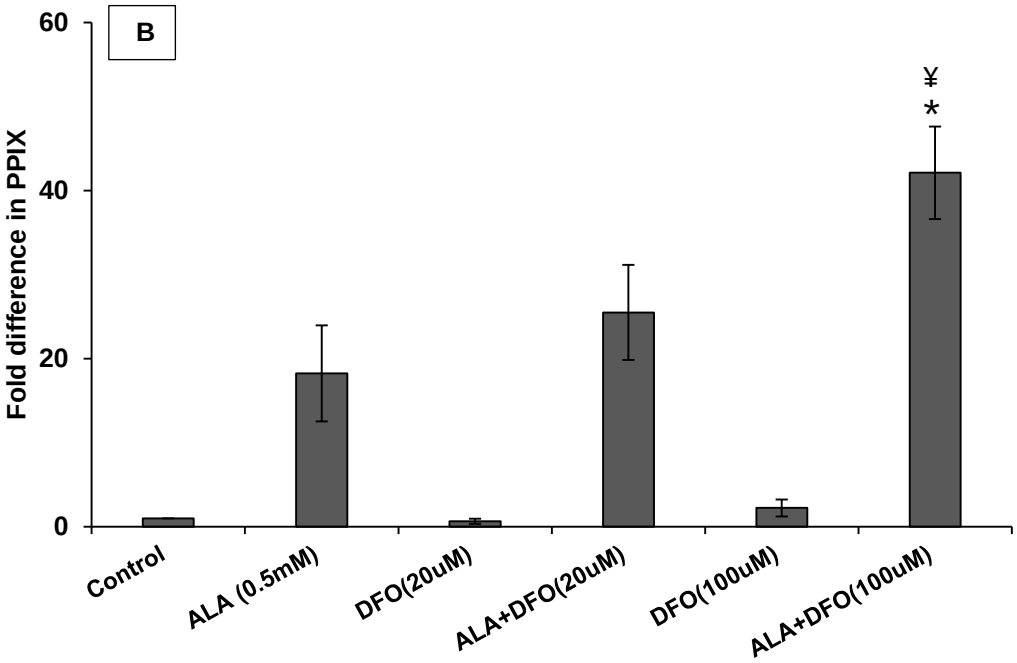

3.8 B: The effect of ALA treatment alone and/or combined with DFO on the accumulation of intracellular protoporphyrin IX (PPIX) in HaCaT cells.

HaCaT cells were treated with DFO at final concentration of 20 or 100 µM for 18 h at 37ºC. Cells were then treated with 0.5 mM ALA and incubated for 2 h at 37ºC in the dark. PPIX was extracted with 1.5 M HCl. The increase in fluorescence was measured 4 h following ALA treatment by spectrofluorometer (excitation 404 nm, emission 604 nm). Data was expressed as mean ± SD (n= 5-13) and plotted as fold increase in PPIX levels when compared to untreated control set as 1.

*: $p < 0.05$, significant difference between ALA(0.5 mM)+DFO(100 µM) and ALA(0.5 mM).

¥: $p<0.05$, significant difference between ALA(0.5 mM)+DFO(20 µM) and ALA(0.5 mM)+DFO(20 µM).

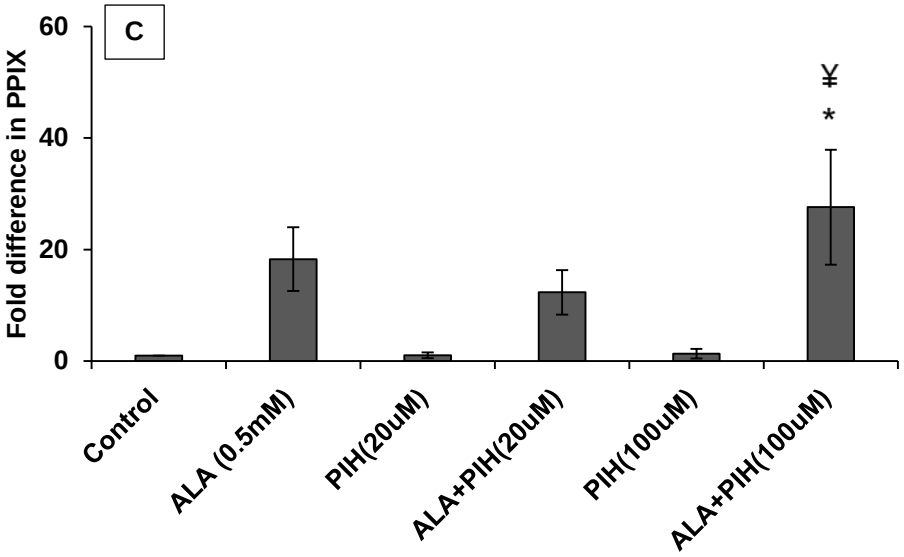

Figure 3.8 C: The effect of ALA treatment alone and/or combined with PIH on the accumulation of intracellular protoporphyrin IX (PPIX) in HaCaT cells.

HaCaT cells were treated with PIH at final concentration of 20 or 100 µM for 18 h at 37ºC. Cells were then treated with 0.5 mM ALA and incubated for 2 h at 37ºC in the dark. PPIX was extracted with 1.5 M HCl. The increase in fluorescence was measured 4 h following ALA treatment by spectrofluorometer (excitation 404 nm, emission 604 nm). Data was expressed as mean ± SD (n=5-13) and plotted as fold increase in PPIX levels when compared to untreated control set as 1.

*: $p < 0.05$, significant difference between ALA (0.5 mM)+PIH(100 µM) and ALA(0.5 mM).

¥: $p<0.05$, significant difference between ALA (0.5 mM)+PIH(20 µM) and ALA(0.5 mM)+PIH(20 µM).

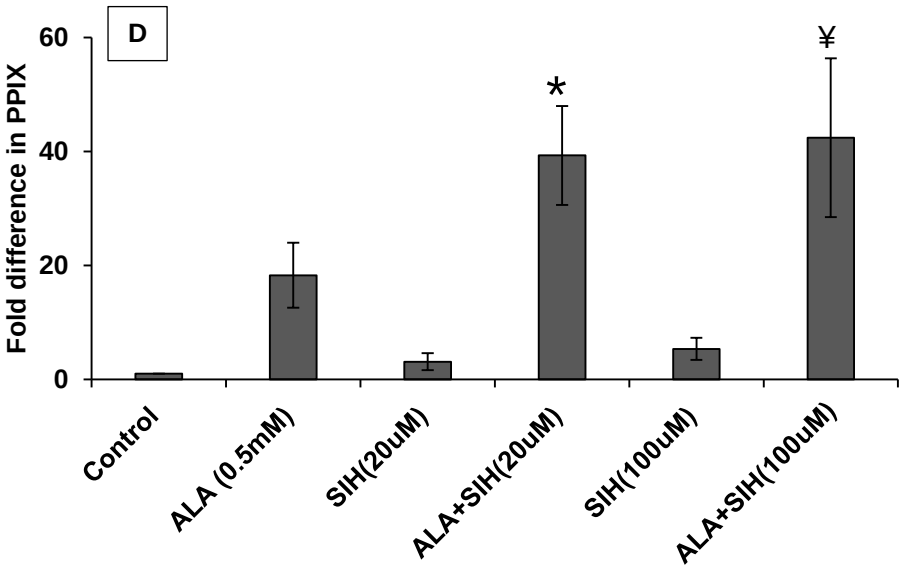

Figure 3.8 D: The effect of ALA treatment alone and/or combined with SIH on the accumulation of intracellular protoporphyrin IX (PPIX) in HaCaT cells.

HaCaT cells were treated with SIH at final concentration of 20 or 100 µM for 18 h at 37ºC. Cells were then treated with 0.5 mM ALA and incubated for 2 h at 37ºC in the dark. PPIX was extracted with 1.5 M HCl. The increase in fluorescence was measured 4 h following ALA treatment by spectrofluorometer (excitation 404 nm, emission 604 nm). Data was expressed as mean ± SD (n=5-13) and plotted as fold increase in PPIX levels when compared to untreated control (i.e. 1).

*: $p < 0.05$, significant difference between ALA(0.5 mM)+SIH(20 µM) and ALA(0.5 mM).

¥: $p<0.05$, significant difference between ALA(0.5 mM)+SIH(100 µM) and ALA(0.5 mM).

3.5. Reactive Oxygen Species (ROS) Measurement in HaCaT Cells

3.5.1. ROS Measurement in HaCaT cells Treated with ALA Alone

To evaluate the level of ROS generation by UVA in ALA-treated HaCaT cells, cells were first treated with ALA (0.5 mM) for 2 h and then exposed to UVA doses of 5 and 10 kJ/m^2. Next, cells were loaded with the dye indicator H_2DCF-DA for 30 min and then the level of fluorescence generated by oxidised H_2DCF-DA was measured by flow cytometry.

In this study we omitted the higher UVA doses of 20 and 50 kJ/m^2, as these doses were highly damaging to ALA-treated cells and therefore it was anticipated that under these conditions, the dye would leak from the cells and as a result the accuracy of the measurement will be compromised. Furthermore the H_2DCF-DA loading was done after UVA irradiation, as the dye is known to be oxidised by UVA radiation (unpublished data, this laboratory).

Figure 3.9 illustrates a representative analysis of the ROS assay by flow cytometry. The displayed samples are the control (no compound) **(3.9A)**, ALA (0.5 mM) **(3.9B)** and ALA+SIH (20μM) **(3.9C)** treated cells irradiated with a UVA dose of 5 kJ/m^2 to show the increase in ROS production after UVA.

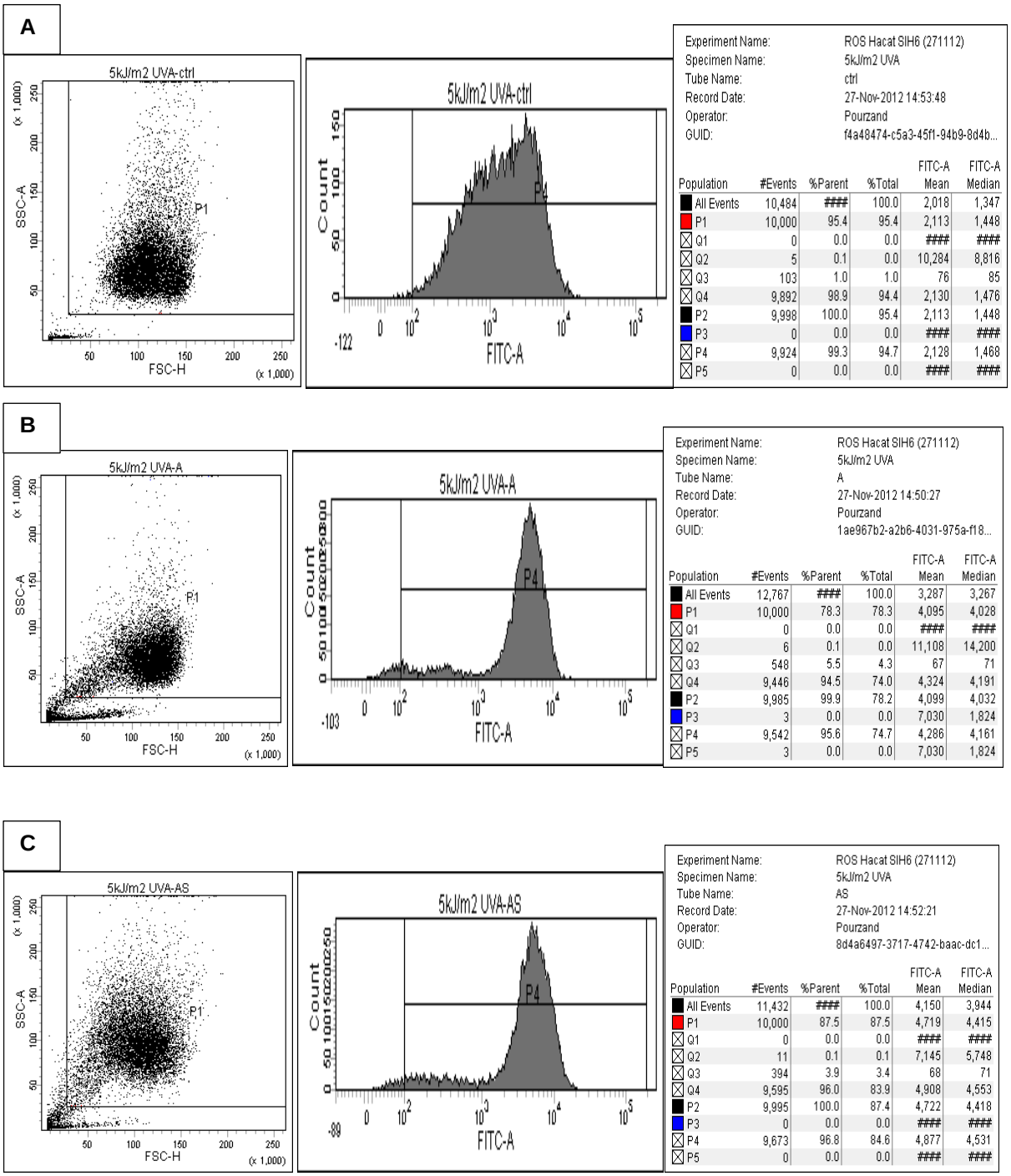

Figure 3.9A-C: Representative example of ROS measurement in ALA/ALA+chelator ± UVA treated HaCaT cells (include the graphs with the shift)

The scatter graphs are obtained from the FACS Canto machine and samples were analysed by flow cytometry. The first graphs on the left represent the gated cell population to be analysed. The graphs in the middle represent the shift to the right depending on extent of damage which expresses the increase level of cell death. The amount of ROS produced are represented in the table as the P4 value of FITC-A mean.

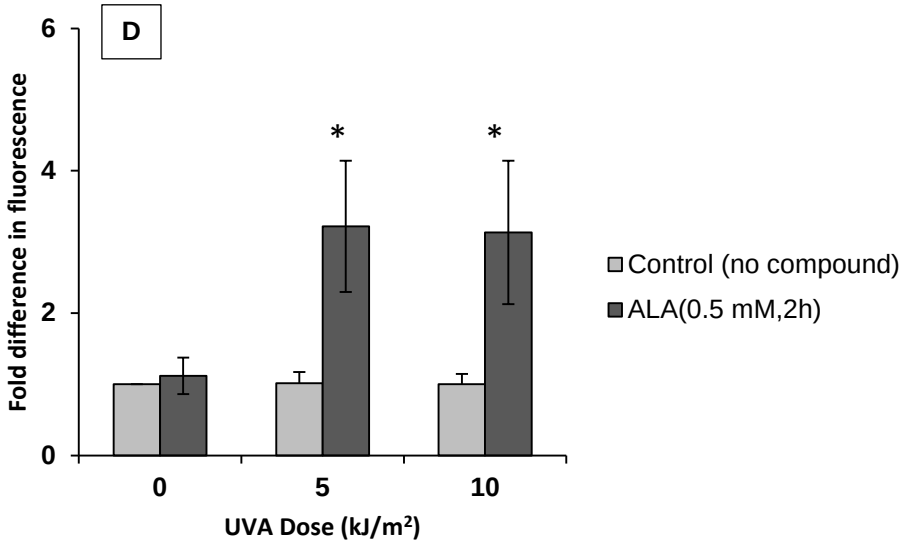

Figure 3.9 D: Measurement of intracellular reactive oxygen species (ROS) in ALA ± UVA treated HaCaT cells

HaCaT cells were first treated with 0.5 mM ALA for 2 h at 37ºC in the dark and then irradiated with UVA doses of 5 and 10 kJ/m^2. Control cells were either not treated with ALA and /or not irradiated.

Cells were then incubated with the fluorophore compound H_2DCF-DA (5 µM final concentration) for 30 min in dark conditions at 37ºC.

Cells were then rinsed and re-suspended in 0.1% BSA-PBS prior to analysis by flow cytometry.

Data was expressed as mean ± SD (n=7) and plotted as fold increase in ROS when compared to untreated control (i.e. 1).

*: $p < 0.05$, significantly different from the corresponding UVA treated cells alone.

3.5.2. ROS Measurement in HaCaT Cells Treated with Chelators +/- ALA

The level of ROS production was also evaluated in UVA-irradiated HaCaTcells that were treated with iron chelators DFO (100 μM), PIH (100 μM) and SIH (20 μM) prior to ALA administration. The results (**Figures 3.9 E-G**) revealed that there was no significant ROS production in cells either irradiated with UVA doses of 5 or 10 kJ/m^2 alone or pre-treated with iron chelators and then irradiated with UVA doses of 5 or 10 kJ/m^2. However irradiation of cells treated with chelators + ALA with UVA dose of 5 kJ/m^2 caused a substantial increase in the production of ROS, although the level was comparable to that observed under identical conditions without chelator. Given the higher accumulation of PPIX observed in chelator + ALA-treated cells when compared to ALA-treated cells alone (see **Figures 3.7A-D**), the latter result suggested that the dye might have leaked out of the cells due to the higher extent of UVA-mediated damage in UVA-irradiated chelator + ALA-treated cells. This assumption was further strengthened by the observation that at a higher UVA dose of 10 kJ/m^2, the level of ROS recorded by flow cytometry in chelators + ALA-treated cells was even lower than that measured with chelators + ALA-treated cells irradiated with the lower UVA dose of 5 kJ/m^2.

These results clearly showed the limitation of the H_2DCF-DA assay in our study, and suggested that although the ROS production in UVA-irradiated chelator + ALA-treated cells must have been higher than the corresponding UVA-irradiated ALA-treated cells alone, the leakage of the dye from damaged cells had compromised the accuracy of these measurements.

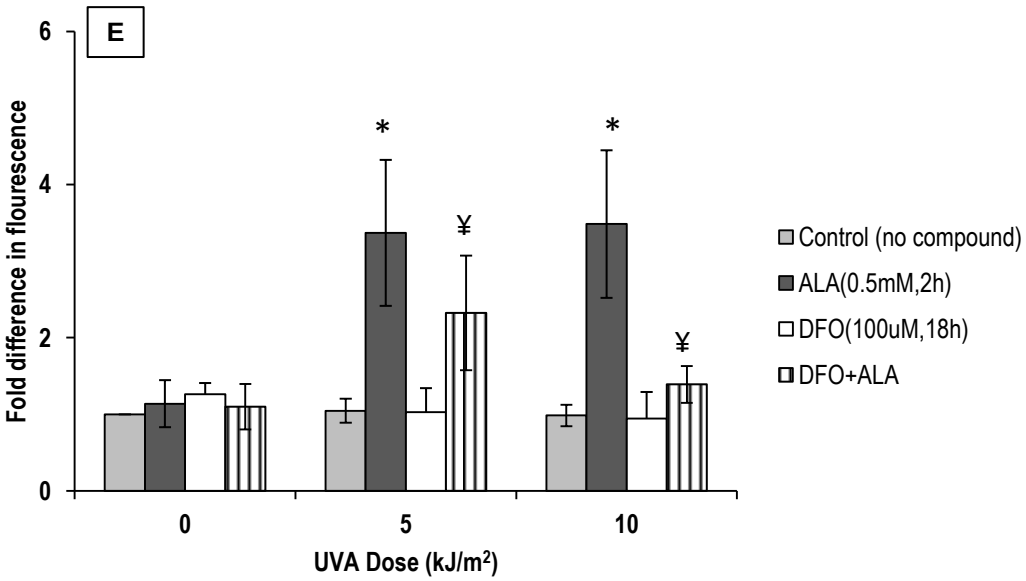
E
6
4
2
0
Fold difference in flourescence
*
*
¥
¥
0
5
10
UVA Dose (kJ/m2)
Control (no compound)
ALA(0.5mM,2h)
DFO(100uM,18h)
DFO+ALA

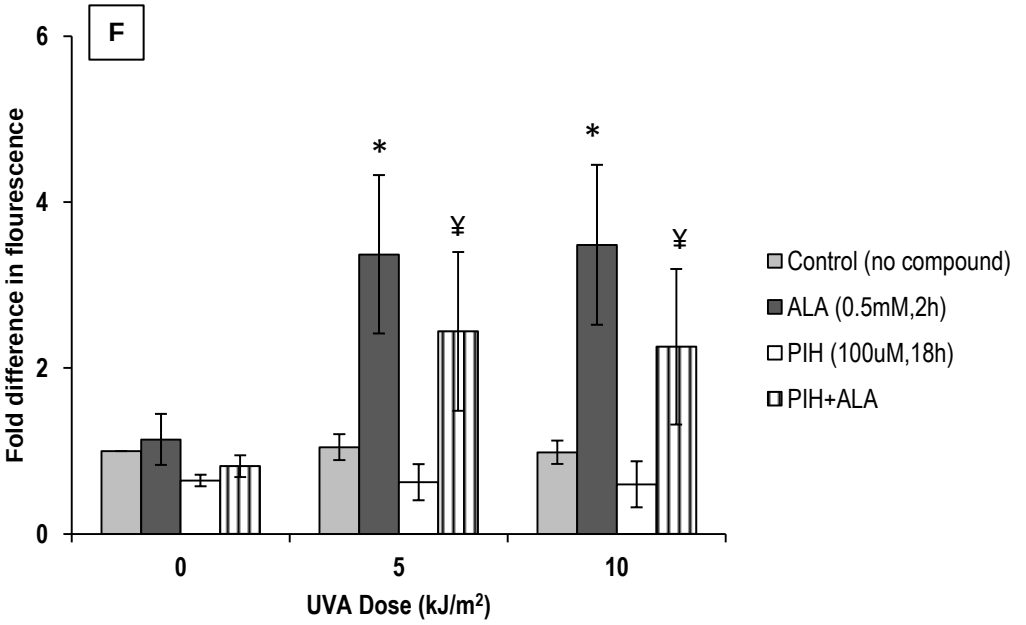
F
6
4
2
0
Fold difference in flourescence
*
*
¥
¥
0
5
10
UVA Dose (kJ/m2)
Control (no compound)
ALA (0.5mM,2h)
PIH (100uM,18h)
PIH+ALA

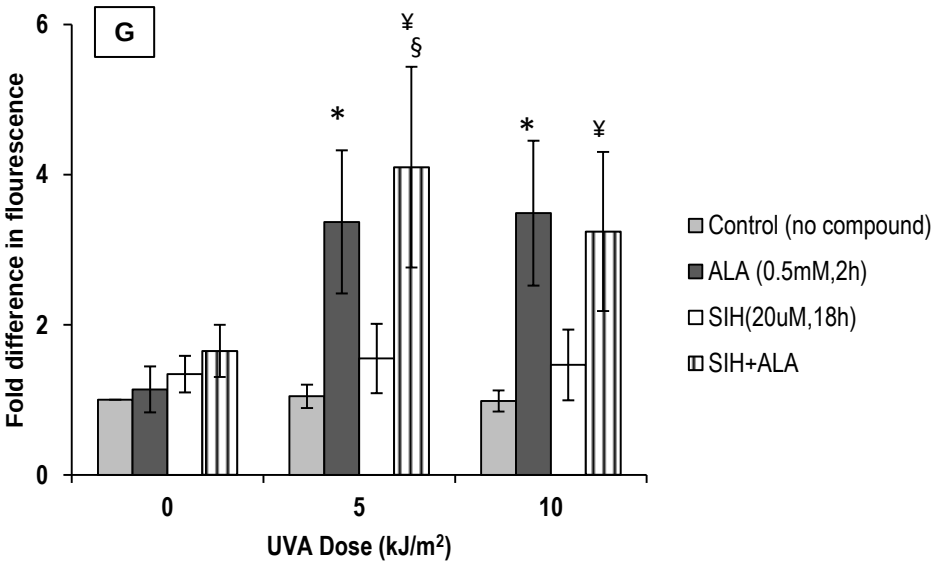

Figure 3.9 E-G: Measurement of intracellular reactive oxygen species (ROS) in ALA- and/ or chelator treated HaCaT cells following UVA irradiation

HaCaT cells were first treated with DFO (E) PIH (F) and SIH (G) at final concentrations of 20 or 100 μM for 18 h followed by treatment with 0.5 mM ALA for 2 h at 37ºC in the dark. Cells were then irradiated with UVA doses of 5 or 10 kJ/m^2. Control cells were either not treated with ALA or chelators or not irradiated with UVA.

Cells were then incubated with the fluorophore compound H_2DCF-DA (5 μM final concentration) for 30 min in dark conditions at 37ºC.

The ROS measurement was performed by flow cytometry after UVA irradiation.

Data was expressed as mean ± SD (n=7) and plotted as fold increase when compared to un-treated control (i.e. 1).

*: $p < 0.05$, significant difference between ALA-treated and the corresponding UVA treated cells alone.

¥: $p<0.05$, significant difference between ALA-+chelator-treated and the corresponding UVA treated cells alone.

§: $p<0.05$, significant difference between SIH+ALA treated and ALA treatment alone in cells UVA-irradiated with the dose of 5 kJ/m^2.

3.6. Effect of Chelators +/- ALA Treatments on HaCaT Cell Survival Using Colony Forming Ability Assay

Colony forming assay (CFA) examines the ability of a single cell to adhere, divide and form colonies 12-14 days following a given treatment. Hence this method shows the long-term effect of a particular treatment in terms of 'true' cell death as reflected by the inability of a cell to divide and form a colony. CFA has been found to be a valuable method for evaluating the effectiveness of iron chelators in improving the efficiency of ALA-PDT in treatment of various cancer i.e. skin cancer (Aroun, 2011, PhD thesis).

In the present study, CFA was used to complement the data obtained by MTT and Annexin/PI flow cytometry assays that had only provided cytotoxicity information in chelator +/- ALA-treated cells up to 24 h after UVA irradiation (i.e. short-term effect).

For the CFA assays, the exponentially growing HaCaT cells were first treated (or not) with SIH (20 µM), DFO (100 µM) and PIH (100 µM) for 18 h at 37ºC and then incubated (or not) with 0.5 mM ALA for 2 h at 37ºC in dark conditions. Cells were then irradiated with UVA doses of 5, 10 or 20 kJ/m^2, and detached by trypsinization and seeded at a density of 1000 cells per plate. Cells were then left to grow and form colonies for 12-14 days at 37^{o}C. After this period, cells were fixed and stained with crystal violet solution. The colonies were then counted and the values were expressed as a percentage of colony forming ability of the untreated control. The results **(Figs 3.10 A-C)** demonstrated that treatment of cells with ALA alone had no effect on cell survival. However UVA irradiation of ALA-treated cells caused a dose-dependent decrease in percentage colony formation when compared to the untreated control cells. The UVA dose of 5 kJ/m^2 already caused a 50% decrease in percentage colony formation of ALA-treated cells when compared to untreated

control cells. At a higher UVA dose of 20 kJ/m^2, few colonies were observed in ALA+UVA-treated cells.

The pre-treatment with chelators caused a substantial decrease in the percentage colony formation of ALA-treated cells with all UVA doses used. **Fig. 3.10A** shows the CFA data obtained with HaCaT cells treated with SIH alone, SIH + ALA followed or not by UVA irradiation. As can be seen, SIH treatment of cells *per se* at a final concentration of 20 μM had no significant effect on percentage colony formation of unirradiated or UVA-irradiated cells when compared to untreated (and unirradiated) control cells. Similarly in unirradiated but SIH+ALA-treated cells, there was no significant decrease in the percentage colony formation when compared to untreated (and unirradiated) control cells. However in UVA-irradiated SIH + ALA-treated cells there was a significant decrease in the percentage colony formation when compared to untreated control cells. The comparison of CFA data between UVA-irradiated ALA -treated cells and UVA-irradiated SIH + ALA-treated cells further illustrated that SIH treatment prior to ALA-treatment of cells had caused a substantial decrease in the percentage colony formation with all UVA doses used. At UVA doses of 10 and 20 kJ/m^2 almost no colony was observed in SIH + ALA-treated plates, in agreement with the notion that increasing the PPIX levels by chelator pre-treatment significantly improves the percentage cell killing of ALA-treated cells following exposure to low doses of UVA.

Figs 3.10B and **3.10C** illustrate the CFA data obtained with cells treated with PIH +/- ALA +/- UVA- and DFO +/- ALA +/- UVA, respectively. As can be seen, in contrast to cells treated with SIH alone at a final concentration of 20 μM, PIH and DFO treatments of HaCaT cells alone at final concentration of 100 μM caused a significant decrease in percentage colony formation when compared to untreated control cells.

These results indicated that overnight treatment of cells with PIH and DFO at a final concentration of 100 μM causes toxicity to cells presumably as a result of severe iron starvation. These results that are in contrast with data obtained with MTT and Annexin V/PI assays (i.e. **Figs 3.3** and **3.4**) and suggest that the CFA approach may provide information about the long-term effect of the chelator treatments which should be a crucial checkpoint for evaluating the cytotoxicity of the chelator treatments. Nevertheless with both PIH and DFO, the CFA data showed that PIH + ALA- and DFO+ALA-treated cells were more efficient in cell killing by UVA than ALA +UVA-treated cells alone, as illustrated with substantial decrease in the percentage colony formation of PIH/DFO + ALA + UVA-treated cells when compared to the corresponding ALA + UVA-treated cells alone.

Overall these data illustrate that a combination of 20 μM SIH with 0.5 mM ALA and UVA radiation is the most effective approach studied for improving the efficiency of the ALA-PDT approach in cultured HaCaT cells. At 20 μM, SIH exhibits no cytotoxicity per se by CFA method, but causes a substantial decrease in cell survival when combined with ALA and UVA radiation.

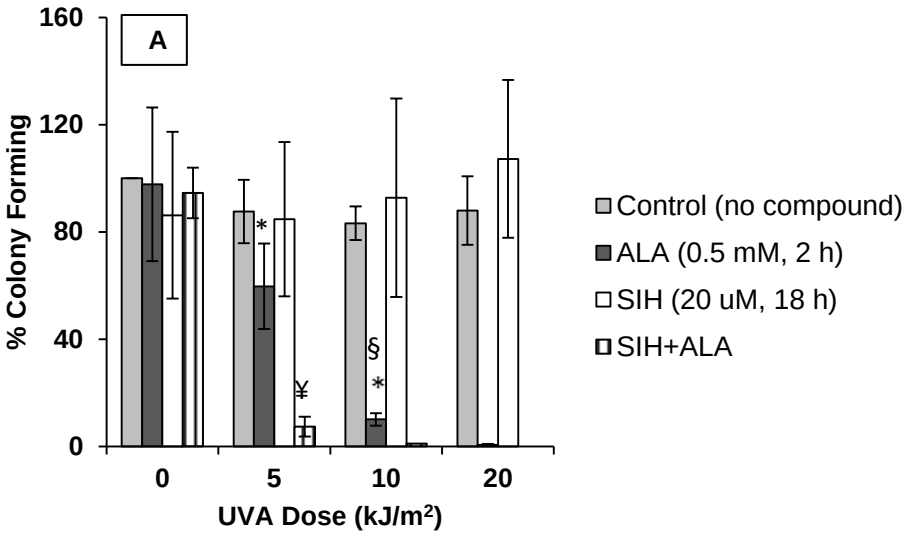
A
160
120
80
40
0
% Colony Forming
0
5
10
20
UVA Dose (kJ/m2)
*
§
*
¥
Control (no compound)
ALA (0.5 mM, 2 h)
SIH (20 uM, 18 h)
SIH+ALA

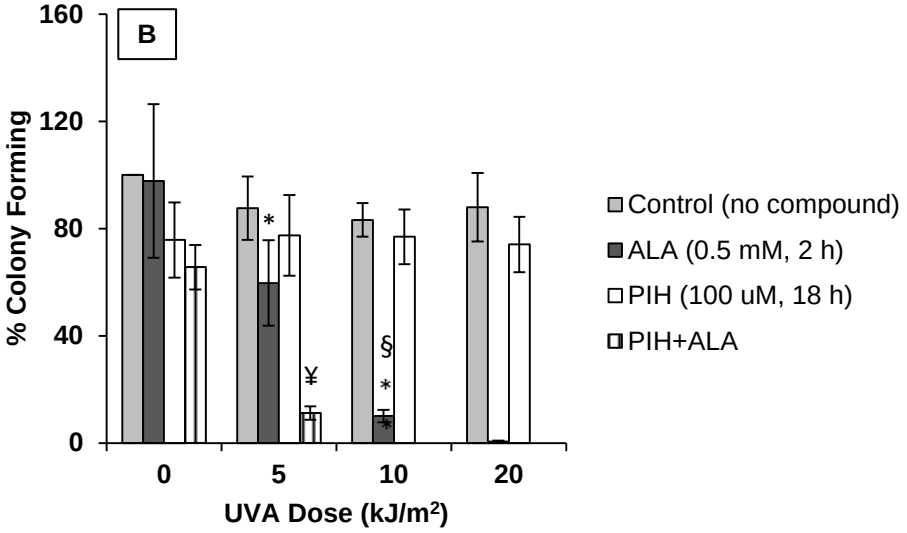
B
160
120
80
40
0
% Colony Forming
0
5
10
20
UVA Dose (kJ/m2)
*
§
*
¥
Control (no compound)
ALA (0.5 mM, 2 h)
PIH (100 uM, 18 h)
PIH+ALA

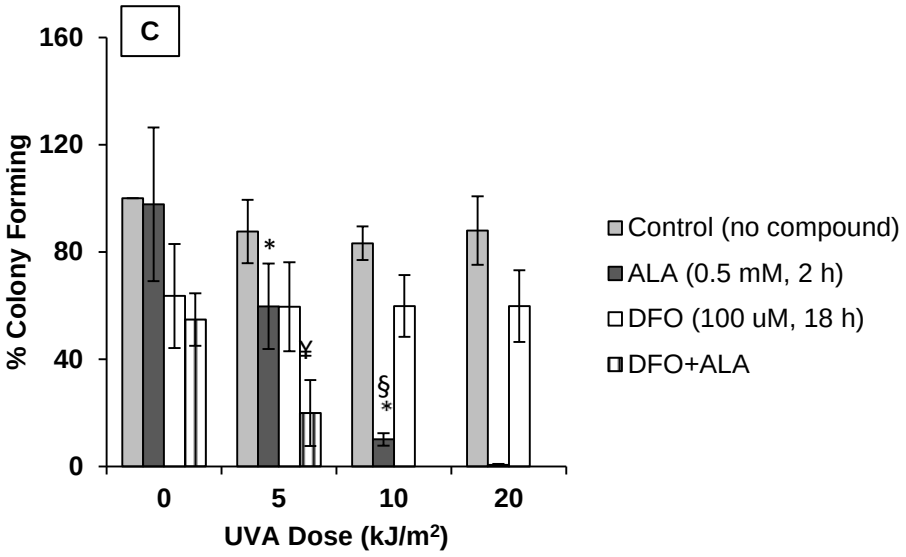

Figure 3.10 A-C: The evaluation of the effect of SIH, DFO and PIH on HaCaT cells treated or not with ALA and/or UVA radiation with colony forming ability assay.

Cells were first treated with A: SIH (20 μM), B: PIH (100 μM) and C: DFO (100 μM) for 18 h at 37ºC and then treated or not with 0.5 mM ALA for 2 h at 37ºC in the dark. Cells were then irradiated (or not) with UVA doses of 5, 10 and 20 kJ/m^2. After treatments, cells were trypsinised and seeded at cell densities of 700 or 1000 cells/plate and allowed to grow for 12-14 days at 37^{o}C. After this period cells were stained with crystal violet dye. The colonies were then counted and expressed as mean percentage colony formation of the untreated control (i.e. set as 100%) ± SD (n=4-7).

*: $p < 0.05$, significant difference between ALA-treated and the corresponding UVA-treated cells alone.

§: $p<0.05$, significant difference between ALA-treated at UVA dose of 5 kJ/m^2 and ALA-treated at UVA dose of 10 kJ/m^2.

¥: $p<0.05$, significant difference between SIH+ALA-treated and ALA treatment alone in cells irradiated with the UVA dose of 5 kJ/m^2.

3.7. A Pilot Study with Met2 SCC Cell Line

3.7.1. The Evaluation of the Cytotoxicity of Chelators SIH, PIH and DFO in Met2 cell line by MTT Assay

Based on the proof of concept data obtained with the HaCaT cell line, a small pilot study was carried out with a genuine skin cancer cell line (i.e. Met2). Met 2 cell line was derived from the skin of a patient suffering from SCC. Previous data from this laboratory using the calcein-based fluorescent assay had revealed that compared to HaCaT cells, Met2 cells have a 2-fold higher basal level concentration of labile iron and require higher concentrations of iron chelator treatment than HaCaT cells for complete labile iron depletion (A. Aroun, 2011, PhD thesis). As a result, in the present study it was speculated that Met2 cells may also require higher concentrations of iron chelator, than HaCaT cells to produce the same damaging effect following ALA and UVA treatments.

For the pilot study, a dose-response study was performed by MTT assay where the Met2 cells were treated with increasing concentrations of the iron chelators DFO, PIH and SIH for 24 or 72 h. The rationale behind this study was to choose the maximum non-toxic concentration of each chelator at 24 h. Based on the IC50 values obtained by A. Aroun (PhD thesis, 2011, this laboratory) for these chelators at 72 h, i.e. 200 μM PIH, 50 μM SIH and 10 μM DFO, the dose-response concentrations for the pilot study in Met 2 cells were chosen as follows: DFO 10-200 μM, SIH 10-200 μM and PIH 50-200 μM. From the MTT data **(Figure 3.11)**, the maximum non- toxic concentrations of chelators at 24 h were 50 μM for SIH, 200 μM for PIH and 100 μM for DFO. These concentrations were chosen for the 18 h chelator treatments of Met 2 cells followed or not by ALA treatment and (or) UVA irradiation.

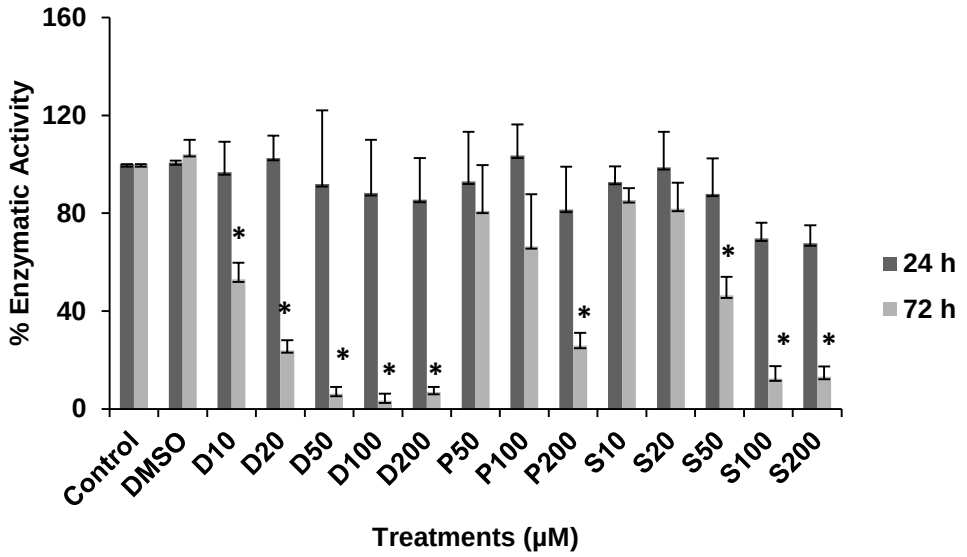

Figure 3.11. The Evaluation of the cytotoxicity of DFO, PIH and SIH in Met2 cells by MTT assay.

Met2 cells were treated with SIH (20, 50, 100 and 200 µM) represented as "S" in the graph, DFO (10, 20, 50 and 100 µM) represented as "D" in the graph and and PIH (50, 100 and 200 µM) represented as "P" in the graph. MTT analysis was performed 24 and 72 h following addition of compounds

(n=3-4).

*: $p < 0.05$, significantly different from chelator-treated cells at 24 h time point.

3.7.2. The Evaluation of the Level of Cell Damage in Chelator + ALA-treated Met2 Cells following UVA Irradiation with MTT Assay

After the optimum concentration of chelators were determined, Met2 cells were treated with chelators for 18 h at 37^{o}C prior to ALA administration (0.5 mM, 2 h) and then irradiated with UVA doses of 5, 10 and 20 kJ/m^{2}. MTT assay was performed 24 h after UVA irradiation. Control cells were treated identically except that they were either not treated with chelators and (or) ALA, or not irradiated. The results (**Fig 3.12 A-C**) showed a dose-dependent increase in cell damage in ALA + UVA-treated cells when compared to untreated, or unirradiated but ALA-treated cells. However compared to HaCaT cells, ALA-treated Met2 cells appeared to be more resistant to the UVA doses used. The chelator treatment of Met 2 cells prior to ALA administration did substantially sensitise the Met2 cells to UVA-induced cell damage, however the latter data was similar to that obtained with HaCaT cells. For example DFO+ALA treated Met2 cells irradiated with a UVA dose 10 kJ/m^{2} exhibited an enzymatic activity of 1.9±0.5% when compared to UVA-irradiated Met 2 cells treated with ALA alone (i.e. 59.4±14.5%). In PIH + ALA- and SIH +ALA-treated Met 2 cells irradiated with a UVA dose of 10 kJ/m^{2}, the percentage enzymatic activity also decreased to 2.2±1.1% and 1.9±0.7% respectively, when compared to untreated control cells (set at 100%).These results illustrated that chelator treatment prior to ALA-administration abolished the observed resistance of ALA-treated Met2 cells to UVA radiation. The latter result demonstrated the effectiveness of the chelator treatment in improving the efficiency ALA-PDT with UVA in a genuine skin cancer cell line.

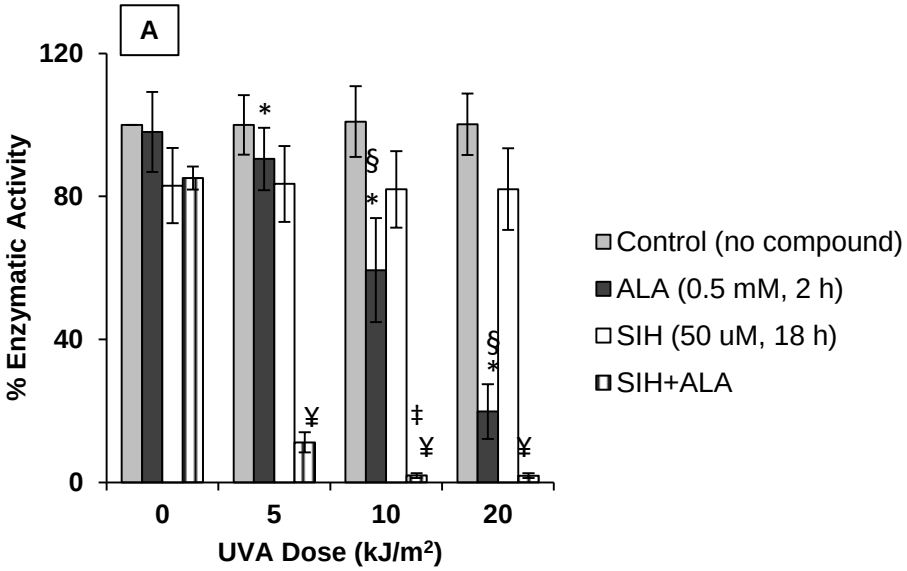
A
120
80
40
0
% Enzymatic Activity
0
5
10
20
UVA Dose (kJ/m²)
Control (no compound)
ALA (0.5 mM, 2 h)
SIH (50 uM, 18 h)
SIH+ALA

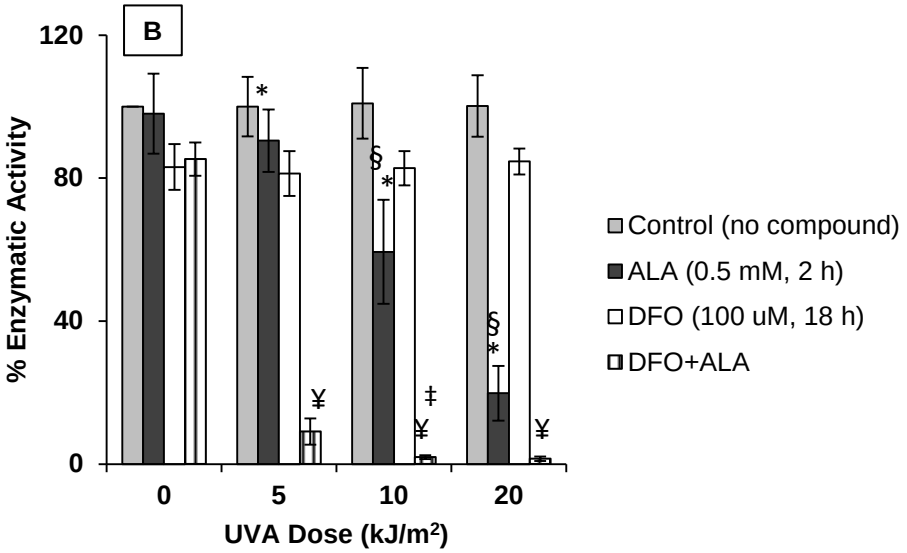
B
120
80
40
0
% Enzymatic Activity
0
5
10
20
UVA Dose (kJ/m²)
Control (no compound)
ALA (0.5 mM, 2 h)
DFO (100 uM, 18 h)
DFO+ALA

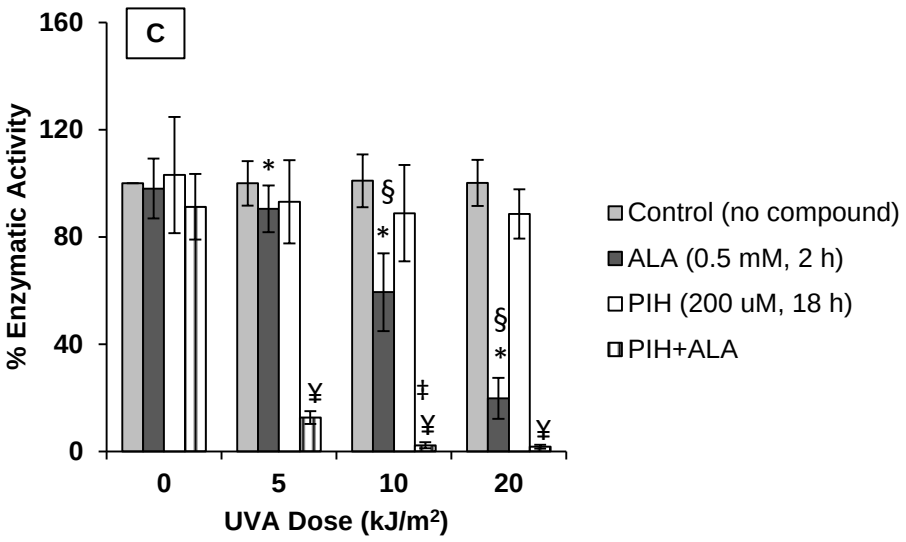

3.12 A-C: The effect of ALA and chelators on cell viability 24 h after irradiation of cells with low doses of UVA by MTT assay.

Met2 cells were first treated with A: 50 µM SIH, B: 100 µM DFO and C: 200 µM PIH for 18 h at 37ºC. Cells were then treated with 0.5 mM ALA alone, for 2 h at 37ºC in the dark, prior to irradiation with UVA doses of 5, 10 or 20 kJ/m. Control cells were treated identically except that they were either not irradiated and (or) not treated with chelator or ALA. MTT analysis was performed 24 h after irradiation. The results were expressed as mean ± SD (n=3-12).

*: $p<0.05$, significantly different from the untreated control cells at corresponding UVA doses.

§ : $p<0.05$, significantly different from the ALA-treated cells.

¥: $p<0.05$, significantly different from the ALA-treated cells irradiated with corresponding UVA doses.

‡: $p<0.05$, significantly different from chelator and ALA treated cells.

3.7.3. The Evaluation of the Level of Cell Survival with CFA in Chelator + ALA-treated Met2 Cells following UVA Irradiation

To study the long-term effect of chelators with or without ALA- and (or) UVA treatments, exponentially growing Met2 cells were first treated with 50 µM SIH, 100 µM DFO or 200 µM PIH for 18 h at 37ºC. This was followed by treatment of cells with 0.5 mM ALA for 2 h at 37ºC in dark condition. Cells were then irradiated with at UVA doses of 5, 10 or 20 kJ/m^2, after which they were detached by trypsinisation, and seeded at a cell density of 400 cells per dish and left to grow and form colonies for 8-10 days at 37^{o}C. After this period, cells were stained with crystal violet dye and the colonies were counted and the values expressed as percentage of colony forming ability of the untreated control. The results (**Figs 3.13 A-C**) demonstrated that in Met2 cells, ALA treatment had substantially decreased the cell survival of UVA-irradiated cells, even with a low dose of 5 kJ/m^2. Indeed, the results revealed that the low dose of 5 kJ/m^2 already decreased the percentage colony forming of ALA-treated Met2 cells to 13±7% of the untreated control. At a higher UVA dose of 10 kJ/m^2, the percentage colony forming of the ALA-treated cells was further decreased to 5.5±2% of the untreated control. At the highest UVA dose of 20 kJ/m^2, no colony was observed in the ALA-treated plates. These data indicated that while the study of the short-term effect by MTT assay suggested that ALA-treated Met2 cells are more resistant to UVA than HaCaT cells, in the long-term, ALA-treated Met2 cells appear to be as sensitive as ALA-treated HaCaT cells to UVA-induced cell killing. The effect of chelator and ALA treatment on Met 2 cells was more drastic than that observed with HaCaT cells, as no colony was observed in chelator + ALA-treated cells with all UVA doses used. Taken together these data suggest that both in HaCaT and Met2 cells, the chelator combination with ALA improves the efficiency of cell killing

following UVA irradiation when compared to ALA-treated cells alone. Furthermore the CFA data demonstrate that unlike HaCaT cells, in Met2 cells, the chelator treatment *per se* does not appear to be toxic to the cells, as the percentage colony forming of the chelator-treated cells is comparable to that of untreated control.

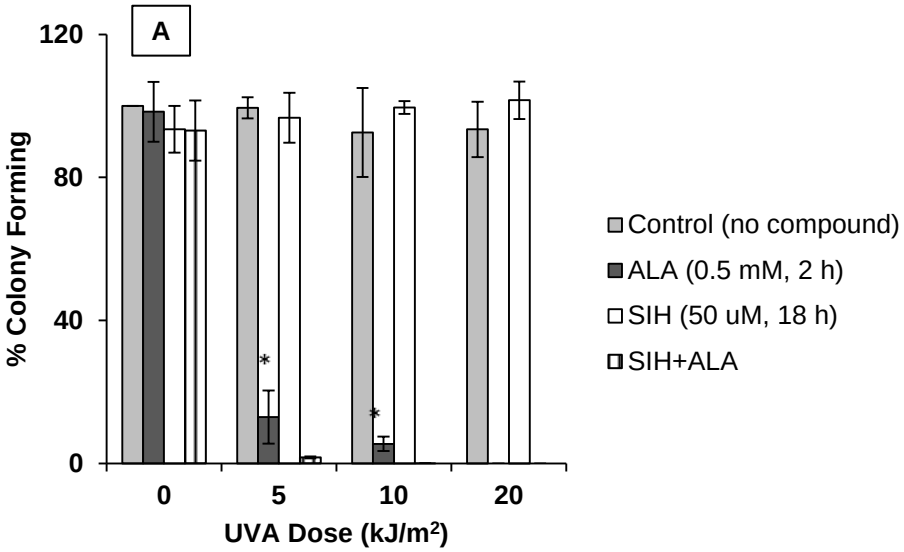
A
120
80
40
0
% Colony Forming
0
5
10
20
UVA Dose (kJ/m2)
Control (no compound)
ALA (0.5 mM, 2 h)
SIH (50 uM, 18 h)
SIH+ALA

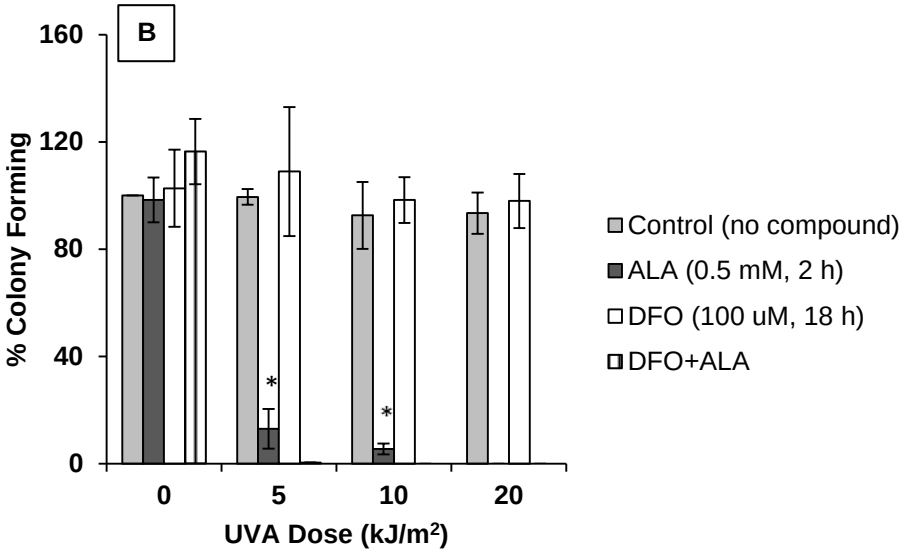
B
160
120
80
40
0
% Colony Forming
0
5
10
20
UVA Dose (kJ/m2)
Control (no compound)
ALA (0.5 mM, 2 h)
DFO (100 uM, 18 h)
DFO+ALA

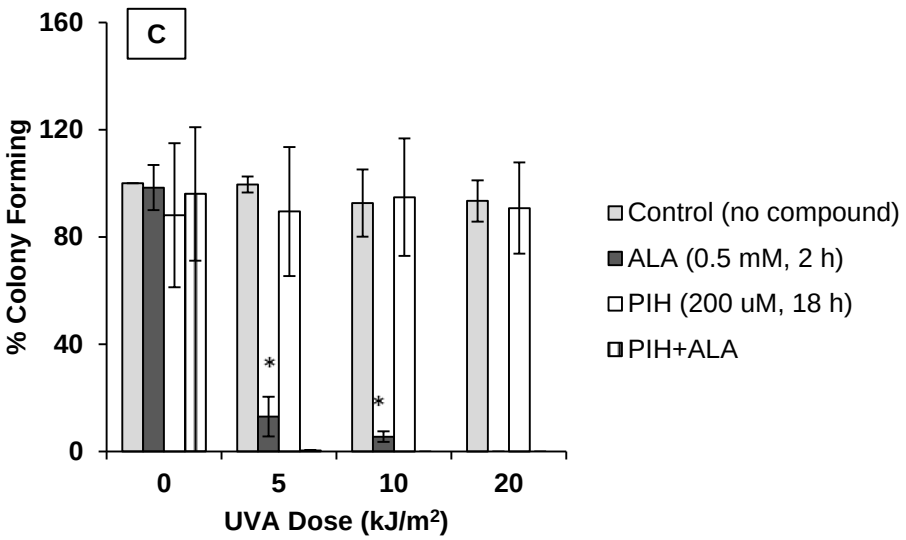

Figure 3.13 A-C: The evaluation of the Met 2 cell survival treated with SIH, DFO and PIH and (or) ALA and (or) UVA radiation with colony forming ability assay.

Cells were first treated with A: SIH (50 µM), B: DFO (100 µM) and C: PIH (200 µM) for 18 h at 37ºC and then treated or not with 0.5 mM ALA for 2 h at 37ºC in the dark. The cells were then irradiated (or not) with UVA doses of 5, 10 and 20 kJ/m^2. After treatments, cells were trypsinised and seeded at 400-800 cells density and allowed to grow for 8-10 days.

After this period cells were stained with crystal violet dye. The colonies were then counted and expressed as mean percentage colony formation of the untreated control (set as 100%) ± SD (n=3-9).

*: $p < 0.05$, significant difference between ALA+UVA-treated and the corresponding UVA treated cells alone.

3.8. Photo-Damaging Effects of Caged Iron Chelators:

Out of all the chelators used in this project, SIH proved to be the optimum chelator for ALA-PDT with UVA despite the much lower concentration used. The lipophilic nature of SIH also makes it suitable for topical ALA-PDT of some skin conditions e.g. SCC. However prolonged topical application with such a chelator will have its own disadvantages as it could cause toxicity due iron starvation affecting the normal tissue surrounding the skin lesion. To overcome this problem, in collaboration with the group of Dr I. M. Eggleston (Pharmacy & Pharmacology department, Bath), we have designed a series of novel caged iron chelators (CICs) for topical application that only become activated upon exposure to UVA light. The caging groups render these compounds temporarily inactive as chelating agents, so 'CICs' do not chelate iron unless activated by external light sources (e.g.UVA), allowing for specific localised release within the targeted tissue (i.e. skin lesion) and therefore substantially decreasing the exposure of the surrounding normal skin tissue to strong iron chelators and their toxic side effects (Yiakouvaki *et al*, 2006). In practice these compounds could be applied topically to the affected area prior to ALA administration and selectively activated within the targeted area with low doses of UVA, sparing the normal tissue surrounding the skin lesion.

In this study we selected two candidate CICs (i.e. BY123 and BY128) in which a key iron binding function of SIH is blocked by a photolabile aminocinnamoyl-based caging group. Upon activation by UVA, these CICs are uncaged releasing SIH and 3-methyl-quinolin-2-one co-product. Therefore the photodamaging effect of these chelators in ALA-treated cells can be triggered on demand allowing controlled and dose- and context-dependent effect within the targeted cells.

Chemical structures of these chelators along with their photo-products are shown in schemes 3.2 (A) and (B) respectively.

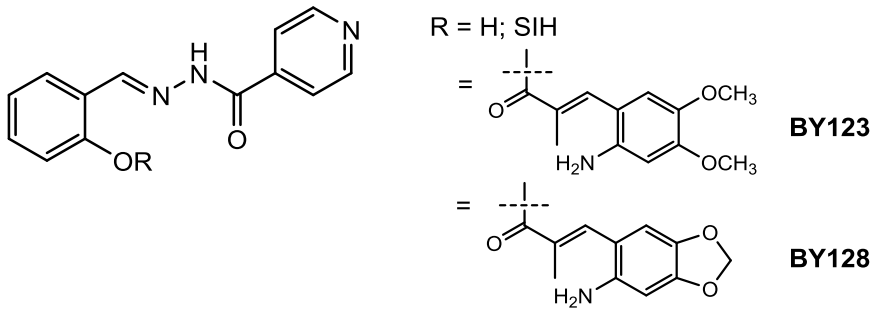

Scheme 3.2 (A): The figure on the left is the chemical structure of SIH (naked chelators, R=H). The two caging groups for BY123 (upper) and BY128 (lower) have been shown.

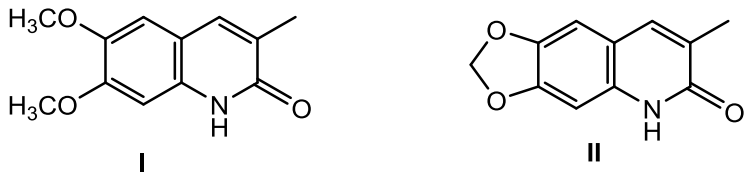

Scheme 3.2 (B): 3-methylquinolin-2-ones, derived from BY123 (I) and BY128 (II).

3.8.1. Chemical Analysis of BY123 and BY128

For the purpose of this thesis, it was necessary to generate data to compare the effect of uncaged CICs generated in a simple chemical system (i.e. when SIH released by UVA) with that of parental chelator SIH in inducing damage in ALA-treated cells following UVA radiation.

BY123 and BY128 have been synthesised in the laboratory of Dr Eggleston (B.L.Young, PhD thesis, University of Bath, 2013), and was fully characterised by ^{1}H

and ^{13}C NMR and mass spectrometry. Purity was assessed to be > 95% by analytical HPLC.

The uncaging of BY123 and BY128 with UVA has been studied in detail in the Eggleston laboratory. For BY123, exposure to a UVA dose of 250 kJ/m^2 leads to clean and efficient uncaging.

Fig 3.13A shows the HPLC chromatogram of the caged BY123, which upon UVA irradiation is transformed to two photoproducts namely SIH and the corresponding 3-methyl-quinolin-2-one shown in **Figure 3.13 B(i).** A magnified profile as shown in **Fig 3.13 B(ii)** confirms the formation of two products.

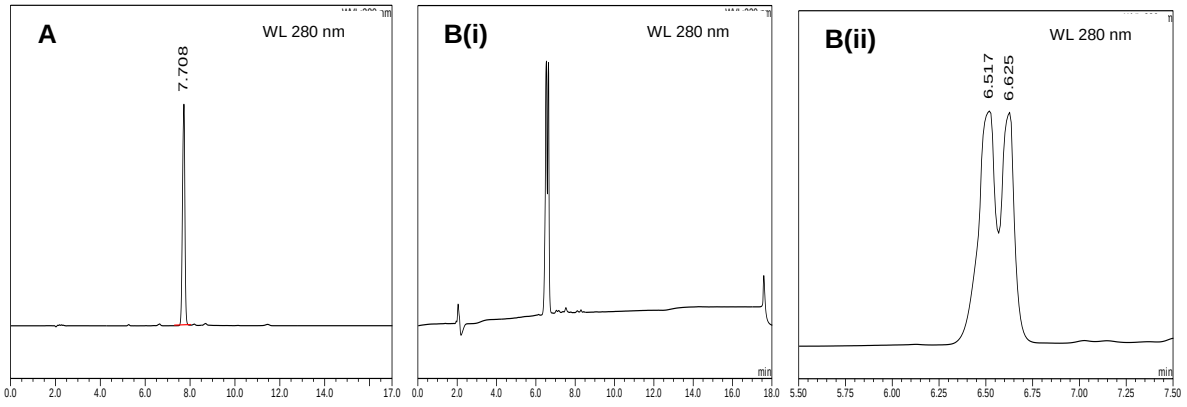

Figure 3.13 A-B (i-ii): HPLC was performed on a Dionex Ultimate 3000 system (Sunnyvale, California, USA),

equipped with a Phenomenex Gemini 5 µm C-18 (150 x 4.6 mm) column, with a flow rate of 1 ml/min, and detecting at 214 nm. Mobile phase A was 0.1% HCOOH in water, mobile phase B was 0.1% HCOOH in acetonitrile. Gradient was *T* = 0 min, B = 5%; *T* = 10 min, B = 95%; *T* = 15 min, B = 95%; *T* = 15.1 min, B = 5%; *T* = 18.1 min, B = 5%. Chromatograms are of 4,5-dimethoxyaminocinnamoyl-SIH derivative **BY123**, showing the intact CIC (**A**) and the UVA (250 kJ/m^2)-irradiated compound (**B (i)**), which is magnified in **B (ii)** for ease of visibility with retention times of 7.708 min (A) and 6.517 and 6.625 (Bi) min.

Taken from Benjamin. L. Young, PhD thesis, University of Bath, 2013 (with permission).

For BY128, HPLC also confirms that exposure to a UVA dose of 250 kJ/m^2 leads to efficient uncaging. Unlike its corresponding 4,5-dimethoxy analogue (i.e. BY123), the uncaging of the methylenedioxy compound BY128 also generated a small amount of an unidentified photoproduct in addition to SIH and the quinolin-2-one **(Fig 3.14 B(i))**. Once again the uncaging profile of BY128 also demonstrated that the retention times for the two photoproducts, namely SIH and the corresponding 3-methyl-quinolin-2-one were very similar as shown in **Figs 3.14 B(i)** and **B(ii)**.

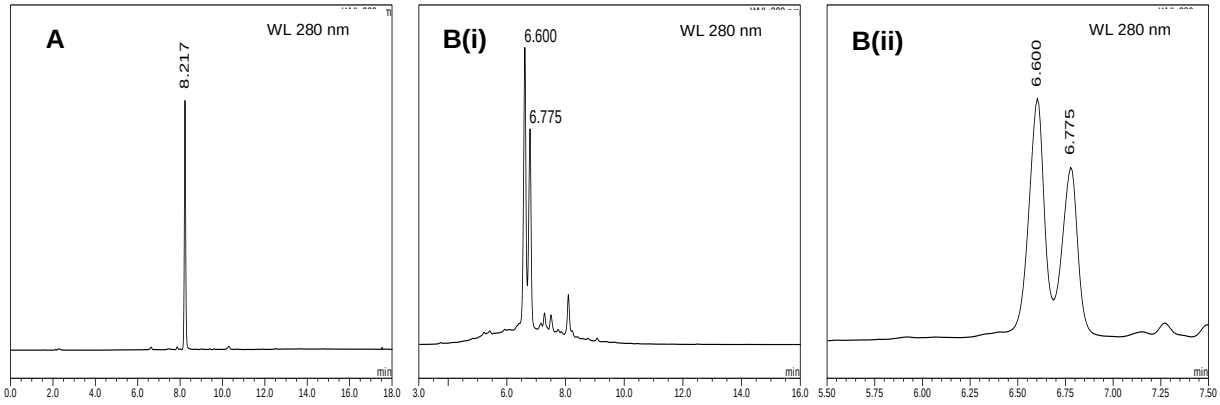

Figure 3.14 A-B(i-ii): HPLC was performed on a Dionex Ultimate 3000 system (Sunnyvale, California, USA), equipped with a Phenomenex Gemini 5 µm C-18 (150 x 4.6 mm) column, with a flow rate of 1 ml/min, and detecting at 214 nm. Mobile phase A was 0.1% HCOOH in water, mobile phase B was 0.1% HCOOH in acetonitrile. Gradient was *T* = 0 min, B = 5%; *T* = 10 min, B = 95%; *T* = 15 min, B = 95%; *T* = 15.1 min, B = 5%; *T* = 18.1 min, B = 5%. Chromatograms are of 4,5-methylenedioxyaminocinnamoyl-SIH derivative **BY128**, showing the intact CIC (**A**) and the UVA (250 kJ/m^2)-irradiated compound (**B (i)**), which is magnified in **B (ii)** for ease of visibility. Retention times were 8.217 min (A) and 6.6 and 6.775 min in B(i).

Taken from Benjamin. L. Young, PhD thesis, University of Bath, 2013 (with permission).

Recent unpublished studies from the laboratories of Pourzand and Eggleston have revealed that aminocinnamoyl-based CICs can be effectively uncaged in a simple chemical systemwith a range of UVA doses between 50-500 kJ/m^2 (see **Figure 3.15**). This is illustrated for BY123 in Figure 3.15. HPLC analysis of uncaging with a range of UVA doses shows that parted uncaging of BY123 may be achieved at as low as 5 kJ/m^2. However the lowest UVA dose that showed an effective uncaging effect was 20 kJ/m^2 which yielded 76.9% of the uncaged compound. Any UVA doses above 20 kJ/m^2 gave a 100% uncaging.

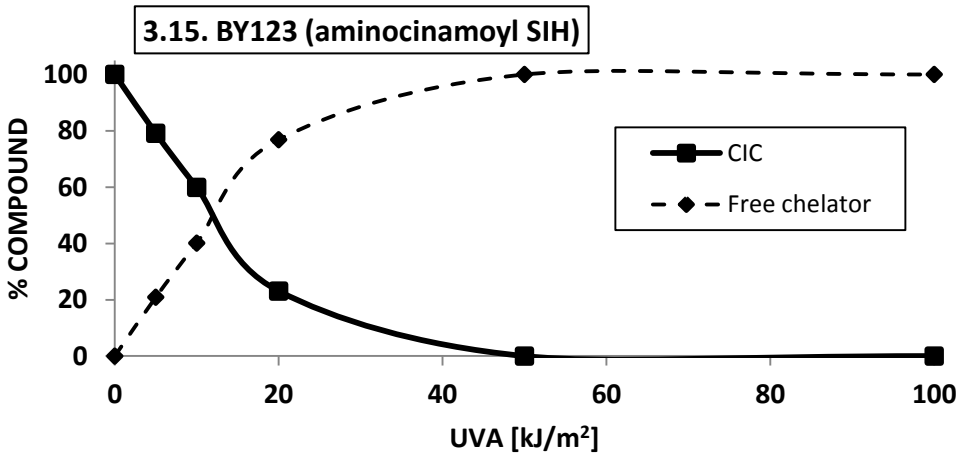

Figure 3.15. The quantification of BY123 uncaging by UVA using HPLC. BY123 was irradiated in a quartz cuvette at exponential UVA doses of 5, 10, 20, 50, 100, 250 and 500 kJ/m^2. The HPLC analysis was performed immediately after UVA irradiation. HPLC was performed on a Dionex Ultimate 3000 system (Sunnyvale, California, USA), equipped with a Phenomenex Gemini 5 µm C-18 (150 x 4.6 mm) column, with a flow rate of 1 ml/min, and detecting at 214 nm. Mobile phase A was 0.1% HCOOH in water, mobile phase B was 0.1% HCOOH in acetonitrile. Gradient was *T* = 0 min, B = 5%; *T* = 10 min, B = 95%; *T* = 15 min, B = 95%; *T* = 15.1 min, B = 5%; *T* = 18.1 min, B = 5%.

Taken from Benjamin Young PhD thesis, University of Bath, 2013 (with permission).

3.8.2. Biological Evaluation of BY123 and BY128

3.8.2.1. The Evaluation of the Cytotoxicity Effect of Uncaged CICs prior to application to cells in ALA-treated HaCaT Cells following UVA Irradiation

The biological evaluations with CICs were first performed with uncaging of BY123 and BY128 ina simple chemical system. The purpose of these experiments was to ensure that in ALA + UVA-treated cells, pre-treatment with uncaged CICs would provide the same superior photodamagaing activity that was observed with the parental chelator SIH when compared to the ALA + UVA-treated cells alone. For this purpose, the compounds were irradiated in quartz cuvettes with a UVA dose of 250 kJ/m^2 and their uncaging profiles were checked by HPLC (see **Figures 3.13** and **3.14**) . HaCaT cells were treated with uncaged CICs (20 μM) or parental iron chelator SIH (20 μM) for 18 h prior to ALA treatment (i.e. 0.5 mM for 2h). Cells were then irradiated with a UVA dose of 10 kJ/m^2. MTT analysis was then performed 24 h following UVA irradiation. The results (**Figs 3.16 A-B**) demonstrated that uncaged CICs *per se* did not cause any damage to the cells. However in CICs + ALA-treated cells, there was a substantial decrease in percentage enzymatic activity following UVA irradiation when compared to ALA + UVA-treated cells. The results also demonstrated that the extent of photodamage in CICs + ALA-treated cells following UVA irradiation is comparable to the effect observed in cells treated with SIH + ALA and UVA-irradiated. The latter data suggested that uncaging the CICs in a cell culture system, exhibits similar iron chelation properties to their parental iron chelator counterpart SIH. In other words the active SIH released by efficient uncaging of CICs by UVA appears to chelate intracellular labile iron to a comparable extent to that of the parental chelator SIH.

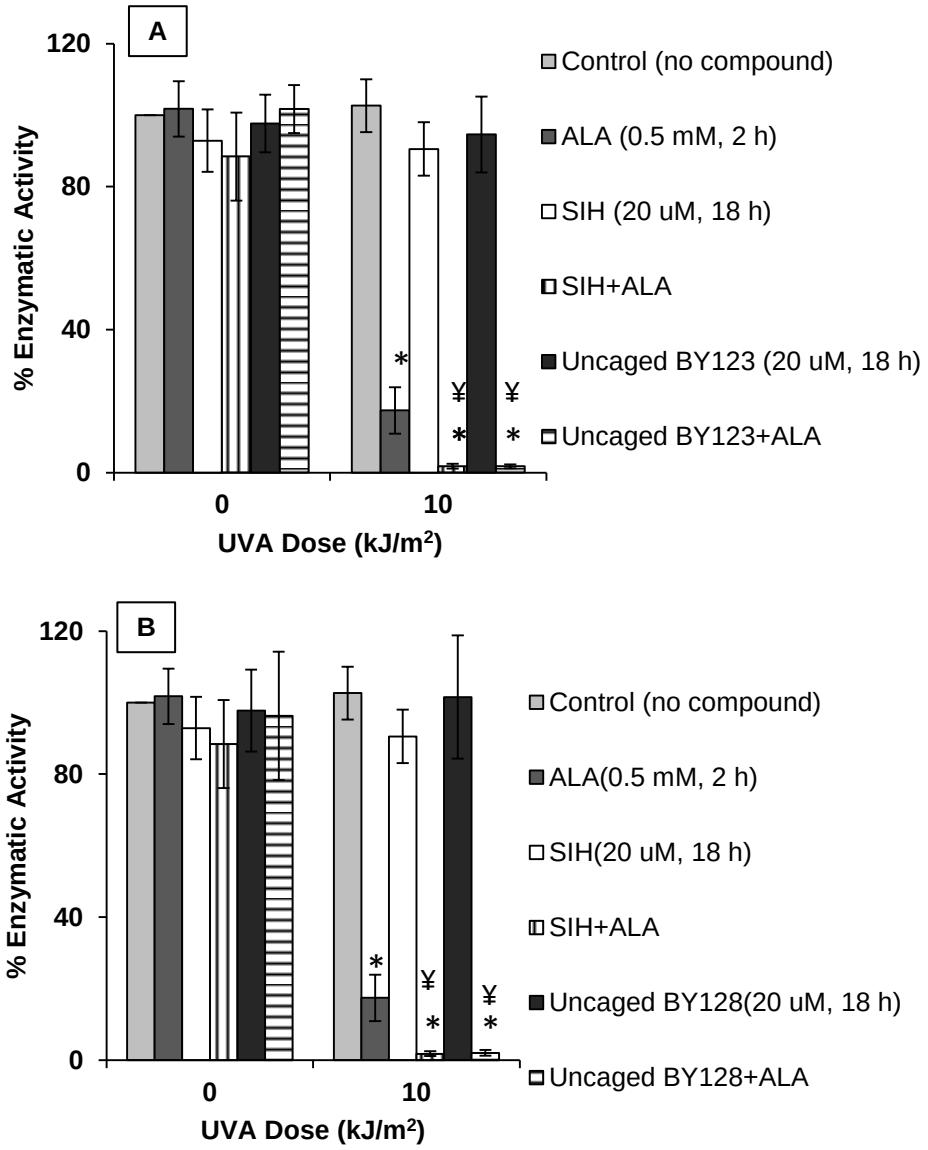

Figure 3.16 A-B: The effect of uncaged BY123 (20 μM) (A) and BY128 (20 μM) (B) on HaCaT cell viability 24 h after UVA irradiation:

HaCaT cells were treated either with SIH (20 μM) or CICs BY123 (20 μM) **(A)** and BY128 (20 μM) **(B)** that were uncaged in a simple chemical system with a UVA dose of 250 kJ/m^2 for 18 h at 37ºC. Cells were then treated/not with 0.5 mM ALA for 2 h at 37ºC in the dark prior to irradiation with a UVA dose of 10 kJ/m^2. Control cells were treated identically except that they were either not irradiated and (or) not treated with ALA or chelator.

MTT analysis was performed 24 h after irradiation. The results were expressed as mean ± SD (n=6-12) and plotted as percentage enzymatic activity of the untreated control.

*: $p<0.05$, significantly different from the UVA irradiated cells alone.

¥: $p<0.05$, significantly different from the ALA-treated cells alone.

3.8.2.2. The Evaluation of the Cytotoxicity Effect of the CICs Uncaged in ALA-treated HaCaT Cells following UVA Irradiation

It was also important to evaluate the photo-damaging effect of BY123 and BY128 uncaged in a cell culture system . For this purpose, exponentially growing HaCaT cells were initially treated with BY123 or BY128 for 18 h at a final concentration of 20 μM, followed by irradiation with UVA doses of 20 or 50 kJ/m^2 in order to uncage these CICs inside the cells. This was then followed by treatment of cells with ALA 0.5 mM for 2 h in dark conditions at 37 ºC and UVA irradiation with a dose of 10 kJ/m^2.

In these experiments, it was anticipated that in CIC-treated plates, UVA irradiation will uncage the compounds, releasing the active SIH inside the cells which then during the 2 h incubation following addition of ALA, will boost the level of PPIX accumulation to a higher extent than ALA-treated cells alone. To mimic the uncaging of CICs in cells by UVA and to ascertain the efficient release of SIH in irradiated cells, SIH was used as a control in some tissue culture plates where treatment was carried out for 2 h in conjunction with ALA treatment. It was anticipated that the response of cells to UVA would be similar in cells pre-treated either with CICs and ALA or SIH and ALA , pending the efficient uncaging of the compounds in cells. Furthermore, to ascertain that the pre-irradiation of cells with UVA doses of 20 or 50 kJ/m^2 does not affect the result obtained, all plates destined to be treated with SIH (20 μM) or ALA (0.5 mM) alone or their combination (i.e. for 2h at 37^{o}C), were also pre-irradiated with UVA doses of 20 or 50 kJ/m^2 (i.e. 20/0 and 50/0 conditions in **Figures 3.17** and **3.18**). The pre-irradiated cells were also subjected to a UVA dose of 10 kJ/m^2 following ALA treatment (i.e. 20/10 and 50/10 condition in **Figures 3.17** and **3.18).** MTT assays were then performed 24 h after UVA irradiation.

The results **(Figures 3.17** and **3.18)** showed that in the absence of pre-irradiation with UVA doses of 20 or 50 kJ/m^2, BY123 or BY128 had no effect on percentage enzymatic activity of unirradiated (0/0 conditions) cells treated or not with ALA 0.5 mM for 2 h. However the pre-irradiation of CIC-treated cells with either UVA doses of 20 or 50 kJ/m^2, significantly decreased the percentage enzymatic activity of ALA-treated cells following UVA irradiation with a dose of 10 kJ/m^2. Interestingly the effect obtained with pre-irradiated CICs + ALA was similar to that obtained with SIH + ALA following UVA irradiation with a dose of 10 kJ/m^2. The latter data implied that both CICs had been efficiently uncaged inside the cells with both UVA doses of 20 or 50 kJ/m^2, as the effects observed was similar to those observed with SIH-treated cells. Finally the data provided in **Figures 3.17** and **3.18** also clearly demonstrated that the pre-irradiation of CICs in cells substantially improves the efficiency of UVA-induced damage in ALA-treated cells when compared to ALA-treated cells alone.

While the effect observed with SIH and pre-irradiated CICs appears to be similar in the treated cells, the CIC approach should have a clear advantage for topical ALA-PDT of skin lesions, as the compounds will be applied as an inactive chelator and then specifically activated by UVA within the targeted lesion, providing a safer modality than the application of naked chelators to improve the efficiency of topical ALA-PDT. Furthermore the dual use of low doses of UVA for activation of CICs in cells and for inducing photodamage after ALA treatment justifies its use as an efficient and practical light source for ALA-PDT of skin lesions with CICs.

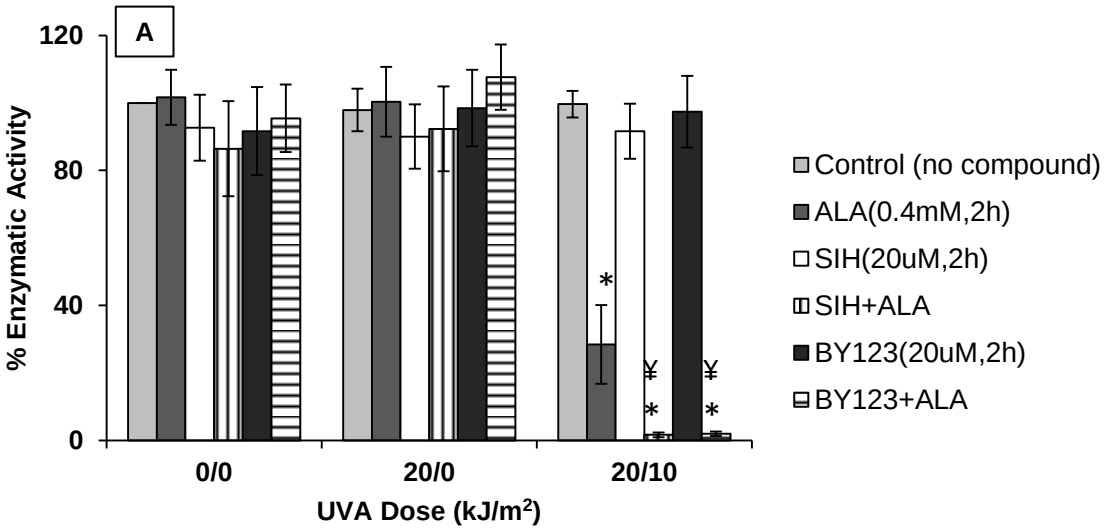

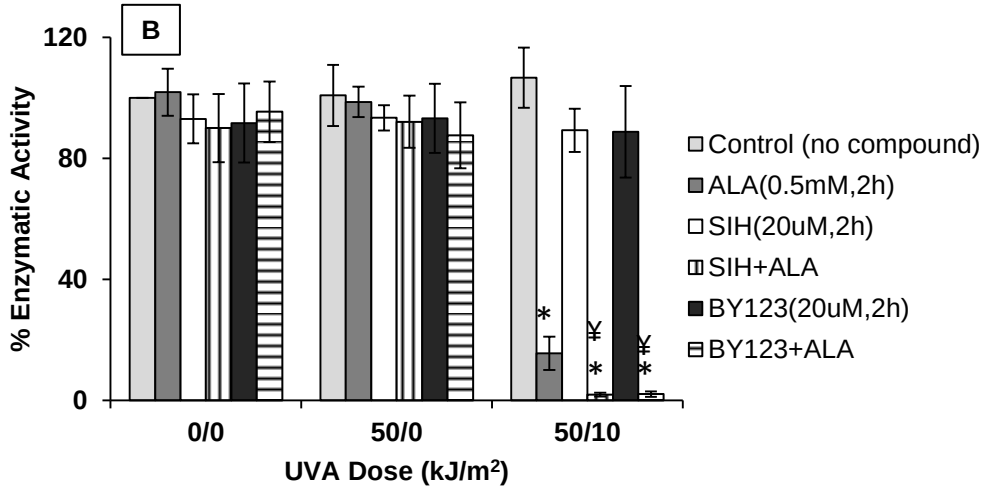

Figure 3.17 A-B: The evaluation of cytotoxicity of HaCaT cells treated with BY123 and ALA 24 h after irradiation of cells with UVA:

HaCaT cells were treated with BY123 (20 µM) for 18 h at 37ºC, followed by irradiation with UVA doses of 20 **(A)** or 50 **(B)** kJ/m^2. Cells were then treated/not with 0.5 mM ALA for 2 h at 37ºC in the dark and then irradiated with a UVA dose of 10 kJ/m^2 (i.e. 20/10 or 50/10). Control cells were treated identically except that they were either not irradiated (i.e.0/0) or only pre-irradiated at UVA doses of 20 **(A)** or 50 **(B)** kJ/m^2 (i.e. 20/0 or 50/0). MTT analysis was performed 24 h after the second irradiation. The results were expressed as mean ± standard deviation (n=3-10).

*: $p<0.05$, significantly different from the UVA irradiated cells at 10 kJ/m^2.

¥: $p<0.05$, significantly different from the corresponding ALA-treated cells irradiated with UVA dose of 10 kJ/m^2.

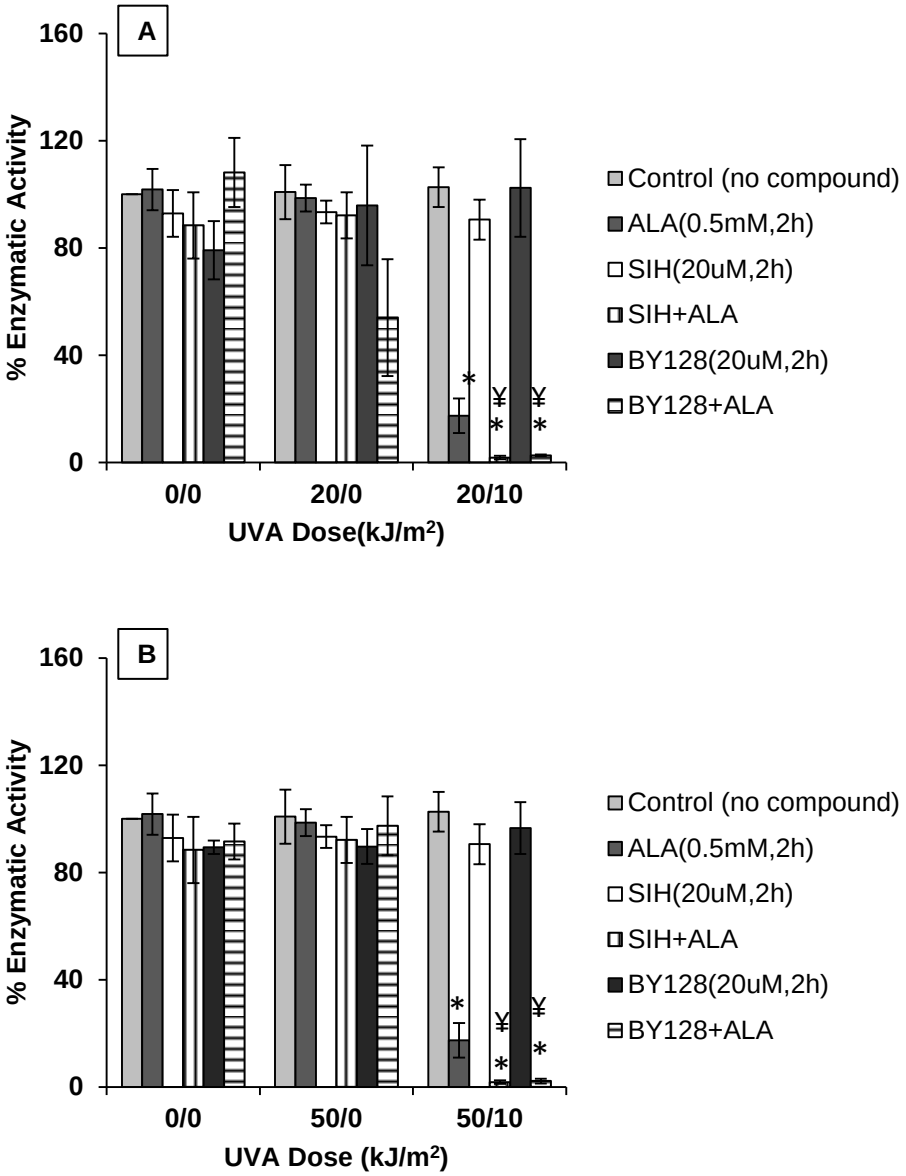

Figure 3.18 A-B: The evaluation of cytotoxicity of HaCaT cells treated with BY128 and ALA 24 h after irradiation of cells with UVA

HaCaT cells were treated with BY128 (20 µM) for 18 h at 37ºC, followed by irradiation with UVA doses of 20 **(A)** or 50 **(B)** kJ/m^2.Cells were then treated or not with 0.5 mM ALA for 2 h at 37ºC in the dark and then irradiated with a UVA dose of 10 kJ/m^2 (i.e. 20/10 or 50/10). Control cells were treated identically except that they were either not irradiated (i.e.0/0) or only pre-irradiated at UVA doses of 20 **(A)** or 50 **(B)** kJ/m^2 (i.e. 20/0 or 50/0). MTT analysis was performed 24 h after the second irradiation. The results were expressed as mean ± standard deviation (n=3-10).

*: $p<0.05$, significantly different from the UVA irradiated cells alone.

¥: $p<0.05$, significantly different from the corresponding ALA-treated cells irradiated with UVA dose of 10 kJ/m^2.

3.8.3. Measurement of the Effect of BY123 and BY128 on Cell Death in HaCaT Cells by Annexin V/ PI Dual Staining Assay

The percentage of cell death was also quantified in cells treated with CICs and ALA following UVA irradiation by flow cytometry using AnnexinV/PI-dual staining assay.

For this purpose, the exponentially growing HaCaT cells were treated overnight with either BY123 (20 μM) or BY128 (20 μM) after being uncaged in a simple chemical systemwith a UVA dose of 250 kJ/m^2. The cells were then treated or not with 0.5 mM ALA and incubated for 2 h at 37ºC in dark condition, before being exposed to UVA doses of 10 and 20 kJ/m^2. The percentage of cell death was measured after staining the cells with Annexin V/ PI fluorescent dyes. The results **(Figure 3.19A)** demonstrated that pre-treatment of cells with the uncaged BY123 significantly sensitised the ALA-treated cells to UVA doses of 10 and 20 kJ/m^2 in comparison to the corresponding ALA-treated cells alone. The comparison of the percentage of cell death obtained with ALA-treated cells that were pre-treated with either SIH or uncaged BY123, revealed that in uncaged BY123 + ALA-treated cells, UVA dose of 10 kJ/m^2 caused slightly less cell death than in SIH + ALA-treated cells (i.e. 74.7±1.4% versus 86.6±7.1%, respectively). Also with higher UVA dose of 20 kJ/m^2, the percentage of live cells in uncaged BY123 + ALA-treated cells was very similar to SIH + ALA-treated cells (i.e. 9.1±1.9% versus 10.1±4.9%, respectively).

A similar experimental set up was also designed for BY128. The uncaging of BY128 was also performed in a simple chemical systemwith a UVA dose of 250 kJ/m^2 and cells were pre-treated or not with uncaged BY128 for 18 h at 37^{o}C prior to ALA treatment and UVA irradiation with UVA doses of 10 or 20 kJ/m^2. The results **(Figure 3.19B)** demonstrated that the percentages of live cells in cells treated with uncaged BY128 and ALA were not significantly different at both UVA doses of 10 and 20

kJ/m^2. On the other hand, the percentage of live cells following UVA dose of 10 kJ/m^2 was 32±10.9% for cells treated with uncaged BY128 and ALA and 19.6±7.0% for ALA+ SIH-treated cells. Following UVA dose of 20 kJ/m^2, the percentages of live cells decreased to 18.4±6.7% and 10.1±4.9% in cells treated with uncaged BY128 + ALA and SIH + ALA, respectively.

Taken together these results demonstrated that the photodamaging effect of uncaged CICs and ALA combination was more effective than the effect observed with ALA treatment alone. Furthermore it appeared that uncaged CICs and ALA combination induced slightly higher photokilling than in cells treated with SIH and ALA.

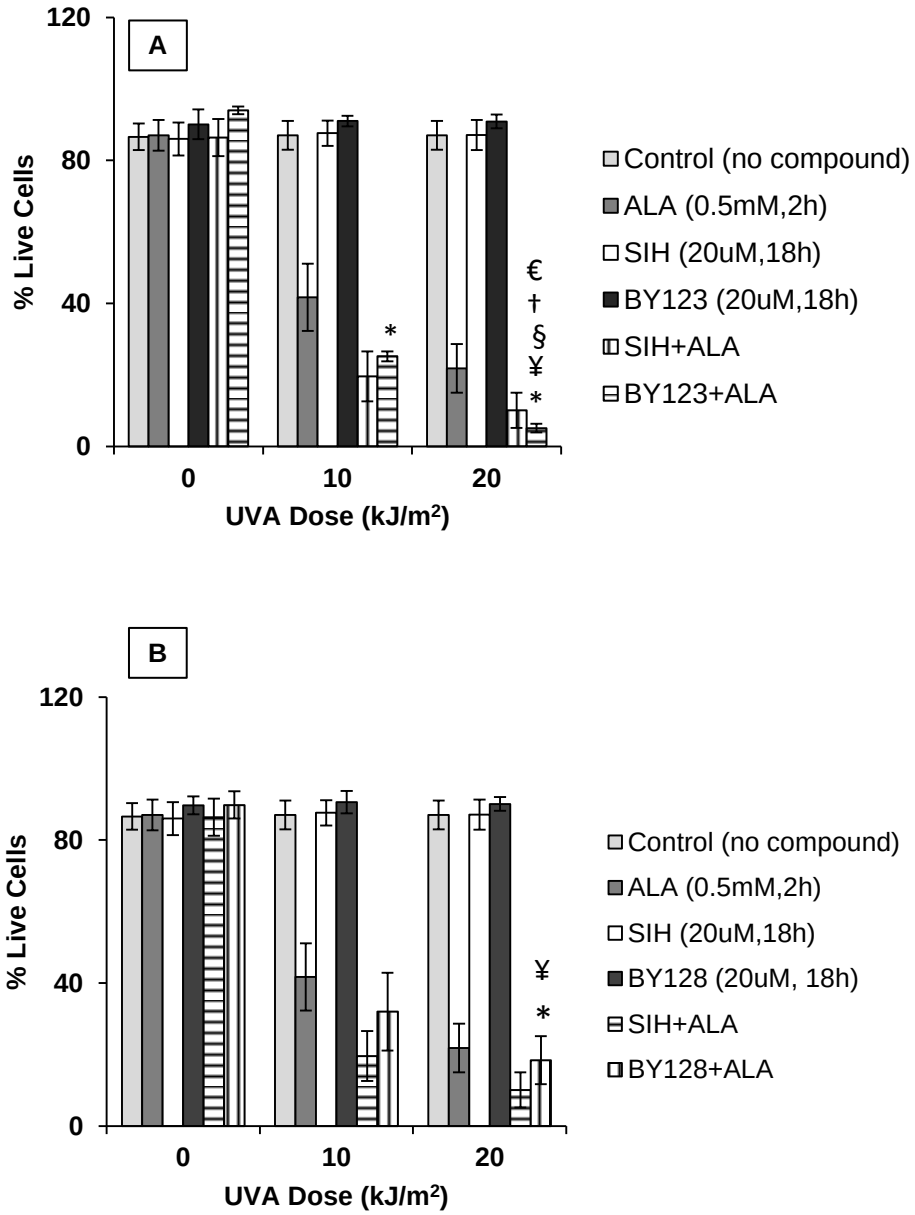

Figure 3.19 A-B: The effect of uncaged BY123 and BY128 (in a simple chemical system) on the percentage of necrosis and apoptosis in HaCaT cells 24 h following UVA irradiation.

HaCaT cells were first treated with uncaged BY123 (20 μM) (A), uncaged BY128 (20 μM) (B) or SIH (20 μM) for 18 h at 37ºC. Cells were then treated (or not) with 0.5 mM ALA for 2 h at 37ºC in the dark prior to irradiation with UVA doses of 10 or 20 kJ/m^2. Control cells were treated identically except that they were either not irradiated and (or) not treated with chelators. Flow cytometry analysis was performed 24 h after the UVA irradiation following Annexin V-PI dual staining (n=3-13).

For A: *: $p<0.05$, significantly different from the ALA-treated cells irradiated with UVA dose of 10kJ/m^2.
¥: $p<0.05$, significantly different from the ALA-treated cells irradiated with UVA dose of 20 kJ/m^2.
§: $p<0.05$, significantly different from the ALA+SIH treated cells irradiated with UVA dose of 10 kJ/m^2.
†: $p<0.05$, signficantly different from the ALA+SIH treated cells irradiated with the UVA dose of 20kJ/m^2.
€: $p<0.05$, significantly different from the ALA+BY123 treated cells irradiated with UVA dose of 10 kJ/m^2.

For B: *: $p<0.05$, significantly different from the ALA-treated cells irradiated with UVA dose of 10 kJ/m^2.
¥: $p<0.05$, significantly different from the ALA-treated cells irradiated with UVA dose of 20 kJ/m^2.

3.8.4. PPIX Measurement in HaCaT Cells Treated with BY123 and BY128:

In order to compare the extent of UVA-induced damage and cell death with the level of PPIX accumulation in cells treated with uncaged CICs and ALA, the exponentially growing HaCaT cells were treated with caged BY123 and caged BY128 at final concentration of 20 µM and incubated for 18 h. For uncaging purposes, the BY123- and BY128-treated cells were irradiated with UVA doses of 20 or 50 kJ/m^2 prior to ALA treatment (0.5 mM). As a control, parental SIH was also added in conjunction with ALA to some plates and cells were then incubated for 2h at 37ºC in dark condition. The latter was to mimic the effect of uncaging of CICs in a cell culture system that would yield SIH as the photoproduct.. Porphyrins were then extracted from the cells and quantified by fluorescence.

The results **(Figures 3.20 A-B)** showed that in the absence of UVA irradiation (i.e. 0/0), the level of PPIX in cells treated with either caged BY123 or BY128 alone had no significant effect on PPIX level when compared to untreated control cells. However when CICs-treated cells were uncaged in the cell culture system with UVA doses of 20 or 50 kJ/m^2 and then treated with ALA for 2h, the intracellular level of PPIX increased significantly when compared to untreated cells. The comparison of the results obtained with uncaged BY123 + ALA- and uncaged BY128 + ALA-treated cells (i.e. both uncaged in cell culture systems) revealed that uncaged BY128 + ALA combination treatment is more effective in increasing the level of PPIX in cells thanuncaged BY123 + ALA combined treatment. Similarly the comparison of uncaged CICs +ALA-treated cells in a cell culture system with cells treated with SIH and ALA revealed that the uncaged BY128 (in a cell sulture system) + ALA combination treatment is as effective as the SIH +ALA combined treatment in

increasing the level of PPIX in cells. However the level of PPIX accumulation for the uncaged BY123 (in a cell sulture system) + ALA combination treatment was much lower than the SIH + ALA combined treatment. One reason for this might have been that BY123 was not effectively uncaged inside the cells prior to ALA addition. This assumption was further strengthened by the observation that treatment of cells with ALA and BY123 that was uncaged in a simple chemical system prior to addition to cells yielded the same increase in PPIX as the SIH + ALA combined treatment.

Overall these data demonstrated that treatment of cells with either uncaging of CICs in a simple chemical system or in a cell culture system, are capable of increasing the level of intracellular PPIX in ALA-treated cells.

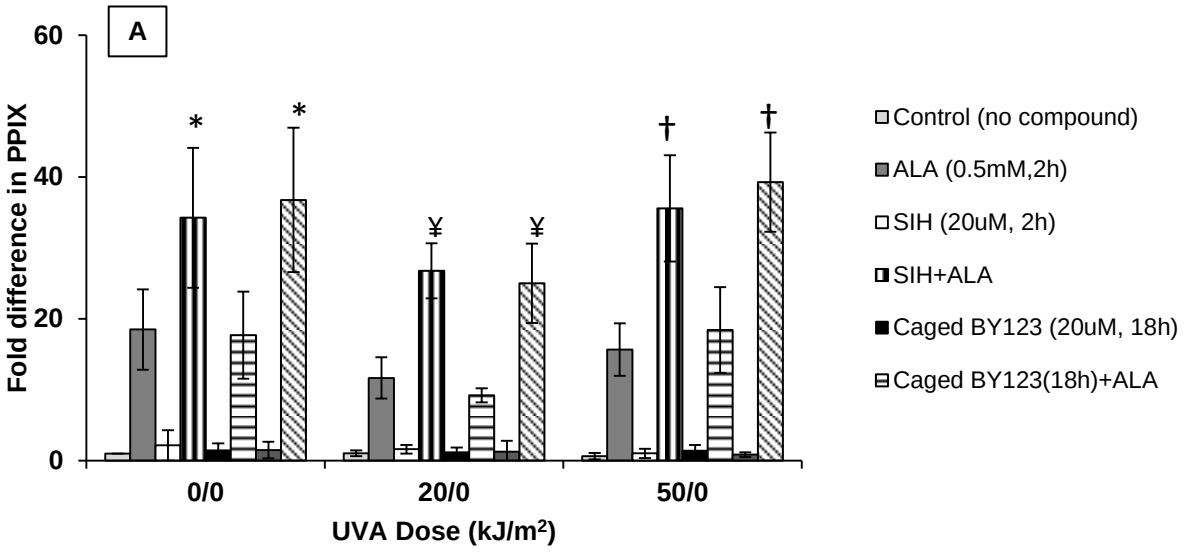

Figure 3.20 A: The effect of ALA treatment alone and/or ALA treatment combined with SIH at 20 µM or BY123 at 20 µM on the accumulation of intracellular protoporphyrin IX (PPIX) in HaCaT cells.

HaCaT cells were treated with 20 µM of caged BY123 (A) for 18 h at 37ºC and then irradiated with UVA doses of 20 or 50 kJ/m^2.SIH was then added at 20 µM either alone or in combination with 0.5 mM ALA and incubated for 2 h at 37ºC in the dark before being trypsinised with 0.25% trypsin. The caged/un-caged BY123 were also treated with the same dose of ALA or not. PPIX was extracted in a final solution of 1.5 N HCl. The increase in fluorescence was measured around 4 h post exogenous addition of ALA at excitation level of 404 nm and emission level of 604 nm by spectrofluorometer and expressed as fold difference in PPIX of untreated control (n=6-15).

*: $p < 0.05$, significantly different from ALA-treated cells pre-irradiated with the UVA dose of 0 kJ/m^2.

¥: $p < 0.05$, significantly different from ALA-treated cells pre-irradiated with the UVA dose of 20 kJ/m^2.

†: $p < 0.05$, significantly different from ALA-treated cells pre-irradiated at the UVA dose of 50 kJ/m^2.

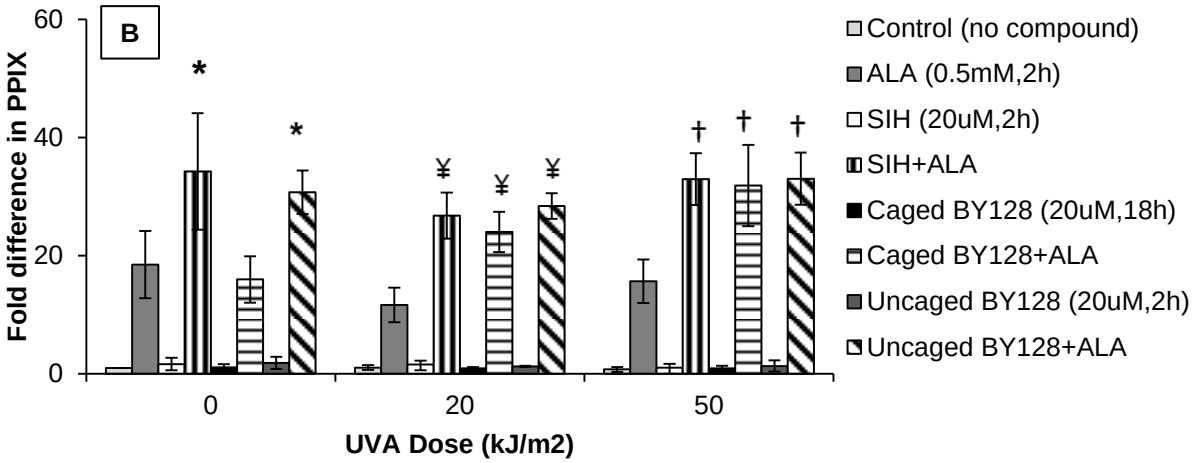

3.20 B: The effect of ALA treatment alone and/or ALA treatment combined with SIH (20 µM) or BY128 (20 µM) on the accumulation of intracellular protoporphyrin IX (PPIX) in HaCaT cells.

HaCaT cells were treated with 20 µM of caged BY128 **(B)** for 18 h at 37ºC and then irradiated with UVA doses of 20 or 50 kJ/m^2.SIH was then added at 20 µM either alone or in combination with 0.5 mM ALA and incubated for 2 h at 37ºC in the dark before being trypsinised with 0.25% trypsin. The caged/uncaged BY128 were also treated with the same dose of ALA or not. PPIX was extracted in a final solution of 1.5 N HCl. The increase in fluorescence was measured around 4 h post exogenous addition of ALA at excitation level of 404 nm and emission level of 604 nm by spectrofluorometer and expressed in terms of fold increase (n=6-15).

*: $p < 0.05$, significantly different from ALA-treated cells pre-irradiated with the UVA dose of 0 kJ/m^2.

¥: $p<0.05$, significantly different from ALA-treated cells pre-irradiated with the UVA dose of 20 kJ/m^2.

†: $p<0.05$, significantly different from ALA-treated cells pre-irradiated at the UVA dose of 50 kJ/m^2.

3.8.5. ROS Measurement in HaCaT Cells Treated with BY123 and BY128:

For ROS measurements, exponentially growing HaCaT cells were treated with SIH or uncagedBY123 and -BY128 (in a simple chemical system)at a final concentration of 20 µM for 18 h at 37ºC prior to ALA treatment (i.e. 0.5 mM, 2h at 37ºC in dark condition). Cells were then irradiated with UVA doses of 5 and 10 kJ/m^2. Next, cells were incubated with H_2DCF-DA for 30 min before being stained with PI and analysed by flow cytometry.

The results **(Figure 3.21 A-B)** demonstrated that treatment with BY123 and BY128 in combination with ALA and UVA dose of 5 or 10 kJ/m^2 showed a lower fold increase in ROS than cells treated with ALA alone or combined with SIH. One explanation for the latter result may be related to leakage of the dye from the damaged cells as previously discussed in **section 3.6**. Nevertheless the ROS values obtained for CICs and ALA are not significantly different from SIH and ALA treatment with UVA doses, consistent with the notion that the combination of CICs with ALA is almost certainly an effective alternative to improve the efficiency of ALA-PDT for treatment of skin cancer and other skin disorders. Furthermore CIC-based ALA-PDT will be a safer modality for topical ALA-PDT of skin cells than the iron-chelator-based ALA-PDT.

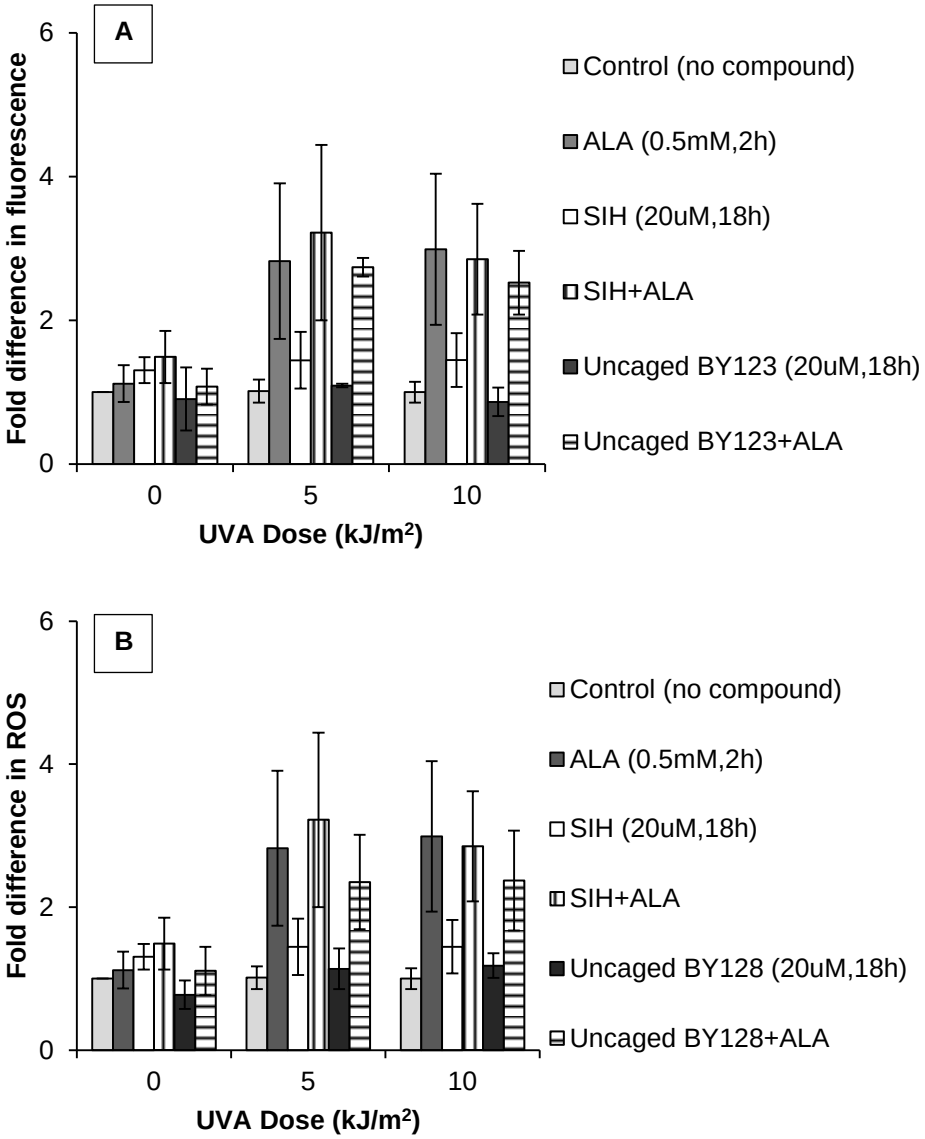

Figure 3.21 A-B: Measurement of intracellular reactive oxygen species (ROS) produced by UVA in HaCaT cells pre-treated with ALA and/or uncaged BY123 (20 μM) and BY128 (20 μM)(in a simple chemical system) tion in HaCaT cells.

HaCaT cells were first treated with uncaged BY123 (A) or BY128 (B) (i.e. uncaged in a simple chemical system at UVA dose of 250 kJ/m^2) for 18 h at 37ºC followed by treatment or not with 0.5 mM ALA for 2 h at 37ºC in the dark. Cells were then irradiated with UVA doses of 5 and 10 kJ/m^2. Cells were then incubated with the fluorophore compound H_2DCF-DA for 30 min in dark conditions at 37ºC and then analysed by flow cytometry. The ROS measurement is performed around 1-1.5h post UVA (n=3-16). There were no significant differences observed.

CHAPTER FOUR
DISCUSSION

Topical ALA- or its methyl ester (MAL)-based PDT has considerably advanced the management of NMSC, providing a treatment option for AK, SCC, and BCC, with good clinical outcomes, low recurrence rates and enhanced cosmetic acceptability. However the most common and troublesome acute adverse effect of topical PDT remains the burning or stinging pain that occurs during light exposure, and may continue post-exposure in a minority of cases. Management of treatment-related pain still remains a considerable challenge in patients. Further optimization of the light source, dose and period of treatment therefore seems crucial to try and alleviate pain.

The study carried out in this PhD project provides strong evidence that applying low doses of UVA radiation to ALA-treated skin cells is a fast and effective approach to promote cell death. Further improvement in the extent of cell killing with lower UVA doses was achieved by the use of iron chelators that were administered to cells either prior to or in conjunction with ALA treatment. Therefore applying low doses of UVA radiation in combination with iron chelators and ALA may be used as an effective intervention strategy to decrease considerably the time of radiation treatment and therefore reduce the pain associated with prolonged conventional topical ALA-PDT of skin lesions with other light sources.

4.1. UVA as a Light Source for Topical ALA-PDT

Application of UVA as a light source in topical ALA-PDT is thought to be more advantageous than the red light currently used in clinics for this therapy. Porphyrins are important UVA chromophores and the porphyrin of interest in this project, PPIX has an absorption peak around 405-410 nm that tails with the UVA range (320-410 nm). The Sellas broad spectrum UVA lamp used in this study that has a distinct peak in 405 nm, making it very suitable for ALA-PDT studies in skin cells. UVA also has the potential of generating ROS notably $^1O_2$ and H_2O_2 which leads to biological damage and cell death in exposed cells/ tissues through iron-catalysed oxidative reactions (Vile and Tyrrell, 1995).

It has previously been demonstrated that accumulating intracellular concentrations of PPIX by application of exogenous ALA, strongly sensitised human skin fibroblasts to low doses of UVA (Pourzand *et al*, 1999b). A study by Buchczyk *et al* (2001) comparing red, green and UVA light sources in ALA-PDT of human skin cells further demonstrated that compared to red light sources, UVA-based ALA-PDT was 40-fold more potent in killing cultured human skin fibroblasts and still 10-fold more potent than ALA-PDT with green light. The high cytotoxicity of UVA-based ALA-PDT relied on the efficient formation of $^1O_2$ as was demonstrated with modulators of $^1O_2$ half-life. In the present project, we also provide further evidence that treatment of skin keratinocytes with ALA strongly sensitises the cells to low UVA doses. Keratinocytes are known to be highly resistant to UVA-induced cell damage and cell death (see Reelfs *et al*, 2010). The higher antioxidant defence mechanism and lower basal level of labile iron in epidermal keratinocytes appear to contribute to their higher resistance to UVA-induced oxidative damage, when compared to dermal fibroblasts (Pourzand and Tyrrell, 1999; Zhong *et al*, 2004; Reelfs *et al*, 2010).

Studies from this laboratory have demonstrated that primary skin keratinocytes as well as the spontaneously immortalised keratinocyte cell line HaCaT are resistant to UVA-induced cell killing up to a high dose of 750 kJ/m^2 (see Reelfs *et al*, 2010). At natural exposure levels this UVA dose translates to over 4.5 h of sun exposure at sea level. The results of this thesis demonstrated that ALA-treatment sensitised HaCaT cells to low doses of UVA within 5-20 kJ/m^2. At natural exposure levels, these UVA doses are achieved within 2-8 min of sunlight exposure to the skin, respectively. The data obtained with colony forming assay (**Figure 3.10**) demonstrated that already with a UVA dose of 5 kJ/m^2, 50% of HaCaT cells are killed. At a higher dose of 20 kJ/m^2, no colonies survived in ALA-treated HaCaT plates. The pre-treatment of cells with iron chelators DFO, PIH and SIH further sensitised the ALA-treated cells to UVA-mediated cell killing with no cell survival at a UVA dose of 10 kJ/m^2. In a clinical setting, typically with a fluence rate of 150 W/cm^2, and a distance of 30 cm, the irradiation time with a UVA dose of 10 kJ/m^2 will be around 30 seconds. The efficient rate of cell killing with such short pulses of UVA is thought to make the pain associated with topical ALA-PDT more tolerable. In comparison, for example in Bath Royal United Hospital, the MAL-PDT of AK is carried out with an LED (631 nm) light source for 9 min to achieve a dose of 37 J/cm^2 with a distance of 5-8 cm. The more effective and specifically the fast damaging consequence of the UVA protocol when compared to prolonged high intensity light radiation treatment, highlights that the proposed strategy here is a rapid and simple means to improve the effectiveness of conventional ALA-PDT of skin lesions while decreasing considerably the time of irradiation that is directly related to the extent of pain endured by patients.

Blue light (417 nm) that tails closely with the Soret band of PPIX (410 nm) has been shown to be very effective in ALA-PDT of superficial skin lesions such as AK and superficial BCC. Compared to red light, blue light provokes a very effective cell inactivation down to about 2 mm from the surface of human skin and muscle tissue (Szeimies *et al*, 1995; Peng *et al*, 1997). In the United States, a combination of an alcohol-containing ALA solution (i.e. Levulan Kerastick) with blue light has been approved for clinical treatment of AK (see Klein *et al*, 2008). The work outlined here addresses further the suitability of UVA-based ALA-PDT as a possible therapy for epidermal diseases, including NMSC. Based on the data presented in this report, the effectiveness of UVA-based ALA-PDT could be further tuned in future studies using a series of cultured AK and SCC cell lines in both monolayer and 3-dimensional organotypic raft cultures. The best protocol could then be evaluated in an open pilot study in collaboration with dermatologists looking at a few patients for instance with symmetrical AK lesions where the effectiveness of UVA-based ALA-PDT could be compared with ALA-PDT with conventional light sources.

The UVA-based ALA-PDT may also have a future in the treatment of psoriasis, as at present the topical ALA-PDT clinical studies with psoriatic patients are often interrupted because of the severe pain experienced by the patients. So decreasing the time of ALA-PDT with the use of UVA as the light source, may provide a powerful alternative to present modalities. Psoralen with UVA has already been used for treatment of psoriasis, but this treatment is accompanied with severe side effects. Furthermore while in general the PUVA therapy doses are between 5-10 kJ/m^2, because of the necessity of repeated therapies, the cumulative UVA doses in PUVA could reach values up to 250-500 kJ/m^2 that are detrimental to patients given the DNA damaging nature of psoralen. In comparison the UVA-based ALA-PDT strategy

is likely to be much more effective with the very low and non-toxic doses used and especially with no cumulative effect.

The limitation of UVA-based ALA-PDT when compared to red light-based therapy may be related to the lower depth of the penetration of UVA. Indeed compared to red light, the proportion of UVA reaching deeper sections of epidermis will be much lower. This will limit the use of the UVA protocol for the treatment of superficial skin lesions only. Therefore the use of UVA-based ALA-PDT may be more suitable for the treatment of AK as well as superficial cases of SCC and BCC but not for thick nodular BCC or advanced SCC cases.

4.2. The Use of Iron Chelators in ALA-PDT

The use of iron chelators has been shown to improve the level of accumulation of PPIX in ALA-treated skin cells. Several cellular studies have evaluated this approach using iron chelators EDTA (Berg *et al*, 1996; Hanania and Malik, 1992), DFO (Berg *et al*, 1996; Ortel *et al*, 1993) and CP94 (Bech *et al*, 1997; Pye and Curnow, 2007). Some cellular studies have also compared directly the ability of the iron chelators EDTA and DFO or alternately CP94 and DFO to enhance PPIX levels in ALA-treated cells (Berg *et al*, 1996; Pye and Curnow 2007). In these studies the order of efficacy of iron chelators in improving the efficiency of ALA-PDT has been proposed as CP94>DFO>EDTA. The efficacy of CP94 compared to other two chelators has been linked to its lower molecular weight and higher lipophilicity (Smith *et al*, 1997). CP94 has been extensively studied in animal models, and has proven to be effective in inducing greater tumour necrosis after light treatment than ALA-treated tumours alone. Nevertheless CP94 is a bidentate chelator and its ability to bind iron is lower

than tridentate chelators such as SIH and PIH or hexadentate chelators such as DFO. Furthermore bidentate chelators are not powerful iron scavengers at low iron concentrations (Ma *et al*, 2004). In the present study we evaluated the ability of tridentate chelators SIH and PIH to improve the efficiency of ALA-PDT in ALA-treated HaCaT and Met2 cell lines. DFO was used as a control here so that the results obtained from this study could be compared to other cellular studies performed with DFO and ALA-PDT. Because of the highly hydrophilic nature of DFO, cellular studies with this chelator are performed after 6-18 h incubation time, allowing DFO to enter the cells and to efficiently mop up the intracellular labile iron. Because of this limitation of DFO, it was decided to incubate all chelators for 18 h, so that iron chelating effects of the compounds could be compared effectively. The results clearly demonstrated that all of the three chelators used were effective in enhancing the level of PPIX after ALA administration which then resulted in efficient photokilling following UVA irradiation with low UVA doses of 5-20 kJ/m^2. Nevertheless the iron chelator SIH appeared to be the most efficient iron chelator as at a lower concentration (20 μM) it provided equal efficiency in photokilling in ALA-treated cells after 2 or 18 h incubation. Furthermore in colony forming assay, in contrast to PIH and DFO, SIH treatment *per se* did not exhibit any toxicity in cells. Moreover SIH is more lipophilic than PIH and therefore it is more suitable for topical application in ALA-PDT protocols. Nevertheless topical application of 'naked' SIH to a skin lesion will affect the normal tissue surrounding the lesion, causing toxicity due to iron starvation. To overcome this problem, SIH-based CICs (BY123 and BY128) are introduced in this report as a safer alternative to topical ALA-PDT with 'naked' SIH. CICs do not chelate iron unless activated by external light sources (e.g.UVA), allowing for specific localised release within the targeted tissue (i.e. skin lesion) and

therefore substantially decreasing the exposure of the surrounding normal skin tissue to strong iron chelators and their toxic side effects. In practice these compounds could be applied topically to the affected area the night before. On the day of ALA-PDT, the isolated skin lesion would be irradiated with a low dose of UVA (20-50 kJ/m^2) to provoke uncaging of the CIC and the release of the active SIH within the targeted area, sparing the normal tissue surrounding the skin lesion. ALA cream would then be applied to the area and isolated from light for 2 h. The skin lesion could then be irradiated with a low dose of UVA (10 or 20 kJ/m^2) consistent with a clinical setting (i.e. UVA fluence rate of 150 W/cm^2, and a distance of 30 cm) for a tolerable time of irradiation of 1 or 2 min.

4.3. Future work

Diagram 4.1 provides the summary of the approaches used in the present study to improve the efficiency of ALA-PDT in skin cells using UVA light. While approaches A and B were studied in depth in both HaCaT and Met 2 cells, due to lack of time the CIC approach illustrated in C was only performed as a pilot study using the HaCaT cell line. Therefore an immediate follow up to the present project will be to check the approach C in Met2 cells that are derived from a SCC patient.

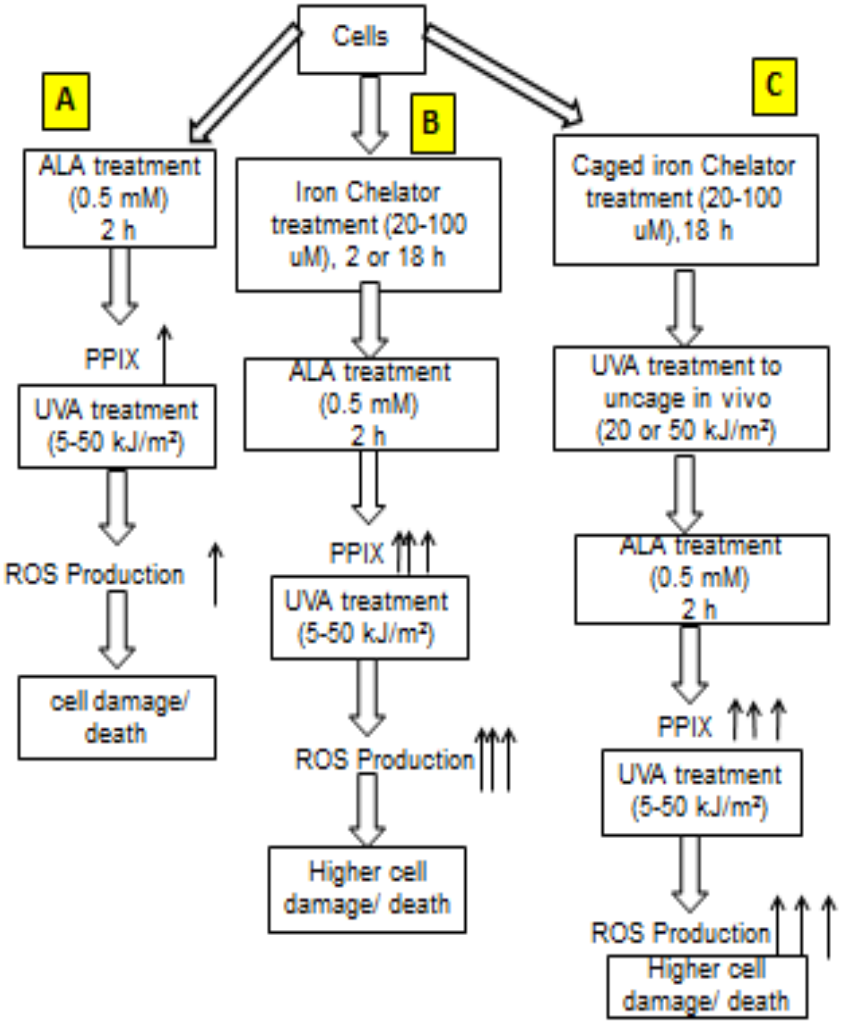

Diagram 4.1. Summary of the different strategies used in the present study to improve the efficiency of ALA-PDT in cultured skin cells.

The CIC approach will then need to be validated in cell lines derived from the skin biopsies of patients suffering from AK and superficial SCC and BCC conditions. The laboratory of Dr Pourzand has expertise in setting up three dimensional (3D) organotypic de-epidermalised (DED) skin raft cultures that closely mimic the structure of the skin. Therefore as a future investigation, it will be possible to evaluate the efficiency of the CIC protocol for ALA-PDT with UVA in a series of 3D-DED raft cultures set up with keratinocytes isolated from AK and superficial SCC and BCC biopsies. The 3D-DED raft culture system will also allow the determination of the exact *in situ* UVA dose necessary for uncaging of the CICs, which might be slightly higher than those set in monolayer culture studies. Dr Reelfs from this laboratory has already established an enzymatic protocol that would permit the separation of the epidermal layer from the raft culture. Following further enzymatic digestions, the obtained keratinocyte cell suspension can be subjected to flow cytometry-based CA-assay to measure the extent of labile iron depletion by uncaged CICs. The level of photodamage and photokilling in CIC + ALA-treated raft cultures pre-irradiated or not with UVA could then be investigated either morphologically following haematoxylin/eosin staining of raft sections or by using more appropriate analytical markers of cell damage and cell death (e.g. TUNEL assay, caspase 3 immuno-histochemistry). Furthermore Dr Eggleston's laboratory is presently designing fluorescent CICs allowing the visualisation of the depth of penetration of the compounds in 3D-DED skin raft cultures. These investigations are crucial to further validate the studies performed in this thesis.

These validation experiments may be followed by further investigations using skin xenografts of cancerous skin cell lines in animal models. Formulation studies may

also be performed in parallel in the animal models used to identify the best topical formulation for effective delivery of the CICs to skin.

Future work may also include the design and study of novel CICs for the purpose of ALA-PDT using chelators such as CP94 for comparison purposes or other clinically useful iron chelators such as Deferasirox (Novartis), an oral lipophilic iron chelator currently in use for iron-overload diseases. Furthermore new caging groups may be designed to allow uncaging at even lower UVA doses than aminocinnamoyl-based caging moieties used in this study. Furthermore the CIC approach offers considerable scope for optimisation/fine tuning, with respect to wavelength of release allowing the design of CICs that will be activatable within the red light range for the CIC-based topical ALA-PDT of advanced NMSC cases such as nBCC. The CIC approach could therefore offer an even wider range of applications than those demonstrated in the present study.

Finally while the pilot studies presented here provide strong evidence for the effectiveness of CIC-based ALA-PDT with UVA, in the future studies it is necessary to repeat these data with MAL, as ALA is not yet approved in Europe for PDT of skin superficial lesions such as AK. The further tuning of the CIC-based protocol involving topical MAL or ALA and UVA in animal studies, could then be tested in pilot clinical studies involving patients with superficial AK lesions. These comparative studies may provide further insights into the effectiveness of either treatments for AK as well as the suitability of ALA- or MAL-based PDT in decreasing the pain experienced by the patients during the therapy.

REFERENCES

- Abels, C. Targeting of thevascular system of solid tumors by photodynamic therapy (PDT). *Photochem Photobiol Sci.* 3 (8): 756-71, **2004**.
- Ahn, W. S., Bae, S. M., Huh, S. W. Necrosis-like death with plasma membrane damage against cervical cancer cells by photodynamic therapy. *Int J Gynecol Cancer*. 14: 475-82, **2004**.
- Albert, M. R., Weinstock, M. A. Kertanicyte carcinoma. *CA Cancer J Clin* 53: 292-302, **2003**.
- Alexiades-Armenakas, M. Laser-mediated photodynamic therapy. *Clin Dermatol* 24: 16-25, **2006**.
- Allison, R. R., Downie, G. H., Cuenca, R., Hu, X. H., Child, C. J. H., Sibata, C. H. Photosensitisers in clinical PDT. *Photodiagn. Photodyn. Ther*.1: 27-42, **2004**.
- Allison, R. R., Mota, H. C., Bagnato, V. S., Sibata, C. H. Bio-nanotechnology and photodynamic therapy-state of art review. *Photodiagnosis Photodyn Ther.* 5 (1): 19-28, **2008**.
- Almeida, R. D., Manadas, B. J., Carvalho, A. P., Duarte, C. B. Intracellular signalling mechanisms in photodynamic therapy. *Biochem Biophys Acta*. 1704: 59-86, **2004**.
- Alster, T. S., Tanzi, E. L., Welsh, E. C. Photorejuvenation of facial skin with topical 20% 5-ALAand intense pulse light treatment: a split-face comparison study. *J. Drugs Dermatol.* 4: 35-38, **2005**.

- Angell, Petersen, E., Sorensen, R., Warloe, T., Soler, A. M., Moan, J., Peng, Q., Giercksky, K. E. Porphyrin formation in actinic keratosis and basal cell carcinoma after topical application of methyl 5-aminolevulinate. *J Invest Dermatol*. 126: 265-71, **2006**.

- Anwar, J., Wrone, D. A., Kimyai-Asadi, A., Alam, M. The development of actinic keratosis into invasive squamous cell carcinoma: evidence and evolving classification schemes. *Clin Dermatol.*22: 189-196, **2004**.

- Apalla, Z., Sotiriou, E., Panagiotidou, D., Lefaki, I., Goussi, C., Ioannides, D. The impact of different fluence rates on pain and clinical outcome in patients with actinic keratosis treated with photodynamic therapy. *Photodermatol Photoimmunol Photomed*. 27 (4): 181-5, **2011**.

- Arits, A. H. M. M., van der Weert, M. M., Nelemans, P. J., Kelleners-Smeets, N. W. J. Pain during photodynamic therapy: uncomfortable and unpredictable. *J Eur Acad Dermatol Venereol.* 24: 1452-57, **2010**.

- Aroun, A. A comparative study of the antiproliferative activity of iron chelators PIH, SIH and their light activated caged derivatives in skin cells. PhD thesis, University of Bath, Department of Pharmacy and Pharmacology, **2011**.

- Aroun, A., Zhong, J. L., Tyrrell, R. M., Pourzand, C. Iron, oxidative stress and example of solar ultraviolet A radiation. *Photochemical Photobiological Sciences*.1-17, **2011**.

- Babilas, P., Knobler, R., Hummel, S., Gottschaller, C., Maisch, T., Koller, M., Landthaler, M., Szeimies, R. M. Variable pulse light is less painful than light-emitting diodes for topical photodynamic therapy of actinic keratoses: a prospective randomized controlled trial. *Br. J. Dermatol.* 157: 111-117, **2007**.

- Babilas, P., Kohl, E., Maisch, T., Backer, H., Gross, B., Brazan, A. L., Baunder, W., Landthaler, M., Karrer, S., Szeimies, R. M. *In vitro* and *in vivo* comparison of two different light sources for topical PDT. *Br J Dermatol.* 154: 712-718, **2006**.
- Barr, H., Kendall, C., Reyes, G. J., Stone, n. Clinical aspects of photodynamic therapy. *Sci Prog*. 85: 131-150, **2002**.
- Barry, B. W. Dermatological formulations: percutaneous absorption. Mercell Dekker, New York, **1983**.
- Bataille, V., Lens, M., Rajpar, S. ABC of skin cancer. Blackwell Publishing. Chapter 2, page 5, **2008**.
- Bech, O., Phillips, D., Moan, J., MacRobert, A. J. A hydroxypyridnone (CP94) enhances PPIX formation in 5-ALA treated cells. *J. Photochem Photobiol.* 41: 136-144, **1997**.
- Bechet, D., Couleaud, P., Frochot, C., Viriot, M. L., Guillemin, F., Barberi-Heyob, M. Nanoparticles as vehicles for delivery of photodynamic therapy agents. *Trends Biotechnol.* 26(11): 612-621, **2008**.
- Bellinier, D. A., Greco, W. R., Nava, H., Loewen, G. M., Oserof, A. R., Dougherty, T. J. Mild skin photosensitivity in cancer patients following injection of HPPH for photodynamic therapy. *Cancer Chemother. Pharmacol*. 57: 40-45, **2005**.
- Ben-Hur, E. Basic photobiology and mechanism of action of phtalocyanines. In: Photodynamic therapy: Basic principles and clinical applications. *Marcel Decker Publisher, NewYork, USA*. 63-77, **1992**.

- Benjamin, C. L., Ullrich, S. E., et al. p53 tumor suppressor gene: a critical molecular target for UV induction and prevention of skin cancer. *Photochem Phorobiol.* 84 (1): 55-62, **2008**.
- Berg, K., Anholt, H., Bech, Ø., Moan, J. Influence of iron chelators on the accumulation of protoporphyrin IX in 5-amino levulinic acid treated cells. *Br J Cancer*. 74:688-697, **1996**.
- Berlanda, J., Kiesslick, T., Engelhardt, V., Krammer, B., Plaetzer, K. Comparative *in vitro* study on the characteristics of different photosensitisers employed in PDT. *J. Photochem Photobiol B.* 100: 173-180, **2010**.
- Berlin, J. M. Current and emerging treatment strategies for the treatment of actinic keratosis. *Clinical, cosmetic and Investigational Dermatology.* 3: 119-126, **2010**.
- Bilu, D., Sauder, D. N. Imiquimod: modes of action. *Br. J. Dermatol*. 66:5-8, **2003.**
- Biro, T., Toth, B. I., Hasko, G., Paus, R., Pacher, P. The endocannabinoid system of the skin in health and disease: novel prospectives and therapeutic opportunities. *Trends Pharmacol Sci.*30 (8): 411-420, **2009**.
- Black, H. S. Potential involvement of free radical reaction in ultraviolet light mediated cutaneous damage. *Photochem. Photobiol*. 46, 213-221, **1987**.
- Blake, E., Allen, J., Curnow, A. An *in vitro* comparison of the effects of the iron chelating agents, CP94 and Dexrazoxane, on protoporphyrin IX accumulation for photodynamic therapy and/or Fluorescence guided resection. *Photochemistry and Photobiology.* 87: 1419-26, **2011**.

- Blake, E., and Curnow, A. The hydroxypyridinone iron chelator CP94 can enhance PPIX-induced PDT of cultured human Glioma cells. *Photochemistry and Photobiology*. 86: 1154-60, **2010**.
- Bonnett, R. Photodynamic therapy in historical perspectives. *Rev. Contemp. Pharmacother.* 10, 1-17, **1999**.
- Bonofoco, E., Kraine, D., Ancarcroma, M., Nicotera, P., Lipton, S. A. Apoptosis and necrosis: two distinct events induced, respectively by mild and intense insults with N-methyl-D-aspartate or nitric oxide/superoxide in cortical cell cultures. *Proc. NAtl. Acad. SCi.* 92, 7162-7166, **1995**.
- Boukamp, P., Petrussevska, R. T., Breitkreutz, D., Hornung, J., Markham, A., Fusenig, N. E. Normal keratinization in a spontaneously immortalised aneuploid human keratinocyte cell line. *J Cells Biol.* 106 (3): 761-771, **1988**.
- Brannon, Heather. Dermatology of Epidermis. About.com. **2007**.
- Brevet, D., Gary-Bobo, M., Raehm, L.,Richeter, S., Hocine, O., Amro, O., Amro, K., Loock, B., Couleaud, P., Frochot, C., Morère, A., Maillard, P., Garcia, M., Durand, J. O. Mannose-targeted mesoporous silica nanoparticles for photodynamic therapy. *Chem Commun.* 12: 1475-77, **2009**.
- Bruls, W. A. G., Slaper, H., van der Leun, J. C., and Berrens, L. Transmission of human epidermis and stratum corneum as a function of thickness in the ultraviolet and visible wavelengths. Photochem Photobiol. 40: 486-494, **1984**.
- Buchczyk, D. P., Klotz, L. O., Lang, K., Fritsch, C., and Sies, H. High efficiency of 5-aminlevulinate photodynamic treatment using UVA irradiation. *Cancinogenesis.* 22: 879-883, **2001**.

- Buss, J, L., Neuzil, J., Ponka, P. Oxidative stress mediates toxicity of pyridoxal isonicotinoyl hydrazine analogs. *Arch Biochem Biophys*. 421 (1): 1-9, **2004**.
- Buss, J. L., Torti, F. M., Torti, S. V. The role of iron chelation in cancer therapy. *Curr Med Chem.* 10(12): 1021-34, **2003**.
- Cairnduff, F., Stringer, M. R., Hudson, E. J., Ash, D. V., Brown, S. B. Superficial PDT with topical 5-ALA for superficial primary and secondary skin cancer. *Br J Cancer.* 69: 605-608, **1994**.
- Calzavara-Pinton, P., Venturini, M. And Sala, R. Photodynamic therapy. Part 1 and 2. Photochemistry and Photobiology. *J. Eur. Acad. Dermatol. Venereol*. 21(3): 293-302, **2007**.
- Campbell, S. M., Gould, D. J., Salter, L., Clifford, T., Curnow, A. Photodynamic therapy using Foscan® for the treatment of vulval intraepithelial neoplasia. *Br J Dermatol* 151: 1076-1080, **2004**.
- Campbell, S. M., Morton, C. A., Alyahya, R., Horton, S., Pye, A., Curnow, A. Clinical investigation of the novel iron-chelating agent, CP94, to enhance topical photodynamic therapy of nodular basal cell carcinoma. *British Journal of Dermatology*. 159: 387-393, **2008**.
- Casas, A., Batlie, A. M., Butler, A. R., Robertson, D., Brown, E. H., MacRobert, A., Riley, P. A. Comparative effect of ALA derivatives on PPIX production in human and rat skin organ cultures. *Br J Cancer.* 80: 1525-1532, **1999**.
- Chang, S. C., MacRobert, A. J., Porter, J. B., Bown, S. G. The efficacy of an iron chelator (CP94) in increasing cellular Protoporphyrin IX following intravesical 5-

aminolevulinic acid administration: An *in vivo* study. *J. Photochem Photobiol. B* 38: 114-122, **1997**.

- Chaston, T. B., Richardson, D. R. Interactions of the pyridine-2-carboxaldehyde isonicotinoyl hadrazone class of chelators with iron and DNA: implications for toxicity in the treatment of iron overload disease. *J Biol Inorg Chem*. 8 (4): 427-438, **2003**.

- Chatterjee, D. K., Fong, L. S., Zhang, Y. Nona particles in photodynamic therapy: an emerging paradigm. *Adv Drug Deliv Rev.* 60(15): 1627-37, **2008**.

- Christiansen, K., Bjerring, P., Troilius, A. 5-ALA for photodynamic rejuvenation-optimization of treatment regimen based on normal-skin fluorescence measurements. *Lasers Surg Med*. 39: 302-310, **2007**.

- Clark, C., Bryden, A., Dawe, R., Moseley, H., Ferguson, J., Ibbotson, S. H. Topical 5-ALA-PDT for cutaneous lesions : outcome and comparison of light sources. *Photodermatol Photoimmunol Photomed* 19: 134-141, **2003**.

- Coors, E. A., von den Driesch, P. Topical photodynamic therapy for patients with therapy resistant lesions of cutaneous T-cell lymphoma. *J Am Acad Dermatol.* 50(3): 363-7, **2004**.

- Copper, M. C., Tan, I. B., Oppelar, H., Oppelaar, H., Ruevekamp, M. C., Stewart, F. A. Meta-tetra (hydroxyphenyl) chlorine photodynamic therapy in early stage squameous cell carcinoma of the head and neck. *Arch Otolaryngol Head Neck Surg* 129: 709-711, **2003**.

- Cormode, D. P., Skajaa, T., Fayad, Z. A., Mulder, W. J. Nanotechnology in medical imaging: probe design and applications. *Arterioscler Thromb Vasc Biol.* 29(7): 992-1000, **2009**.

- Cotter, P. D., Willard, H. F., Gorski, J.L., Bishop, D.F. Assinment of human erythroid delta-aminolevulinate synthase (ALAS2) to a distal subregion of band Xp11.21 by PCR analysis of somatic cell hybrids containing X; autosome translocations, *Genomics*. 13 (1): 211-212, **1992**.
- Curnow, A., Mac Robert, A. J, Bown, S. G. Comparing and combining light dose fractionation and iron chelation to enhance experimental photodynamic therapy with ALA. *Lasers Surg. Med.* 38: 325-331, **2006**.
- Curnow, A., Mcllroy, W., Postle-Hacon, M. J., Porter, J. B., Mac Robert, A. J., Bown, S. G. Enhancement of 5-ALA-induced PDT in normal rat colon using hydroxypyridinone iron-chelating agents. *Br J Cancer.* 78: 1278-1282, **1998**.
- Czarnecki, D., Meehan, C. J., Bruce, F., Culjak, G. The majority of cutaneous squamous cell carcinoma arises in actinic keratosis. *J Cutan Med Surg* 6: 207-209, **2002**.
- Danpure, H. J., and Tyrrell, R. M. Oxygen dependence of near-UV (365 nm) lethality and the interaction of near-UV and X-rays in two mammalian cell lines. *Photochem Photobiol*. 23: 171-177, **1976**.
- De Groot, H. Reactive oxygen species in tissue injury. *Hepato-Gastroenterology.* 41: 328-332; **1994.**
- De Leeuw, J., de Vijlder, H. C., Bjerring, P., Neumann, H, A. Liposomes in dermatology today. *J Eur Acad Dermatol Venereol*. 23(5): 505-516, **2009**.
- Dellinger, M. Apoptosis or necrosis following Photofrin photosensitisation: influence of the incubation protocol. *Photochem Photobiol.* 64: 182-187, **1996**.

- Diamond, I., Granelli, S. G., McDonagh, A. F., Nielsen, S., Wilson, G. B., Jaenicke, R. Photodynamic therapy of malignant tumours. Lancet. 2(7788): 1175-1177, **1972**.

- Dirschka, T., Randy, P., Dominicus, R., Mensing, H., Brüning, H., Jenne, L., Karl, L., Sebastian, M., Oster-Schmidt, C., Klövekorn, W., Rienhold, U., Tanner, M., Gröne, D., Deichman, M., Simon, M., Hübinger, F., Hofbauer, G., Krähn-Senftleben, G., Borrosch, F., Reich, K., Wernicke-Panten, K., Berking, C., Wolf, P., Lehmann, P., Moers-Carpi, M., Hönigsmann, H., Helwig, C., Foguet, M., Schmitz, B., Lübbert, H., and Szeimies, R. M. Photodynamic therapy with BF-200 ALA for the treatment of actinic keratosis: results of a multicentre, randomized, observer-blind phase III study in comparison with a registered methl-5-aminolevulinate cream and placebo. *British Association of Dermatologists*. 166: 137-146, **2012**.

- Djavaheri-Mergny, M., Mergny, J. L., Bertrand, F., Santus, R., Maziere, C., Dubertret, L., J. Maziere, J. C. Ultraviolet-A induces activation of AP-1 in cultered human keratinocytes. *FEBS Lett.* 92-96,384, **1996**.

- Dolmans, D. E., Fukumura, D., Jain, R.K. Photodynmic therapy for cancer. *Nature reviews.* 3, 383-387, **2003.**

- Dougherty, T. J. Studies on the structure of porphyrins contained in photofrin II. *Photochem photobiol*. 46, 569-573, **1987**.

- Dougherty, T. J., Kautman, J. E., Goldfarb, A., Weishaupt, K. R., Boyle, D., Mittleman, A. Photoradiation therapy for the treatment of malignant tumors. *Cancer Res.* 228-235,398, **1978**.

- Douglas, G. Means to an end: Apoptosis and other cell death mechanisms. *Cold Spring Harbor, NT*, **2011**.
- Doulias, P. T., Christoforidis, S., Brunk, U. T., Galaris, D. Endosomal and lysosomal effects of desferrioxamine: protection of Hela cells from hydrpgen peroxide- induced DNA damage and induction of cell cycle arrest. *Free Radic Bio Med*. 35 (7): 719-28, **2003**.
- Dover, J. S., Bhatia, A. C., Stewart, B., Arndt, K. A. Topical 5-ALA combined with intense pulsed light in the treatment of photoaging. *Arch Dermatol*. 141: 1247-1252, **2005**.
- Driskell, R. R., Lichtenberger, B. M., Hoste, e., Kretzschmar, K., Simons, B. D., Charalombous, M., Ferron, S. R., Herault, Y., Pavlovic, G., Fergusen-Smith, a. C., Wat, F. M. Distinct fibroblast lineage determine dermal architecture in skin development as a repair. *Nature*. 504 (7479): 277-81, 2013.
- Doyle, A., AND Griffiths, J. B. Cell and tissue culture laboratory procedures in Biotechnology. John Wiley and Sons Ltd: Chichester, **1998**.
- Dusa Pharmaceuticals. *Summary of product charecteristics, Levulan*® *Kerastick*®, NDA20-965/ S-006. Wilmington, MA: Dusa Pharmaceuticals, **2009**.
- Eibenschutz, L., Marenda, S., Buccini, P., De Simone, P., Ferrari, A., Mariani, G., Silipo, V., Catricalà, C. Giant and large basal cell carcinoma treated with topical photodynamic therapy. *Eur J Dermatol*. 18 (6): 663-666, **2008**.
- El-Sharabasy, M. M. H., El-Waseef, A. M., Hafez, M. M., Salim, S. A. Porphyrin metabolism in some malignant diseases. *Br J Cancer.* 65:409-412, **1992**.

- Enk, C. D., Levi, A. Low-irradiated red LED traffic lamps as light source in PDT for actinic keratosis. *Photodermatology, photoimmunology and photomedicine*. 28(6): 332-34, **2012**.
- Epsztejin, S., Kakhlon, O., Glickstein, H., Breuer, W., Cabantchik, Z. I. Fluorescence analysis of the labile iron pool of mammalian cells. *Analytical Biochemistry.* 248: 31-40, **1997**.
- Ericson, M., Sandberg, C., Stenquist, B. Photodynamic therapy of actinic keratosis at varying fluence rates assessment of photobleaching, pain and primary clinical outcome. *Br. J. Dermatol*. 151: 1204-1212, **2004**.
- Ericson, M. B., Wennberg, A. M., and Larkö, O. Review of photodynamic therapy in actinic keratosis and basal cell carcinoma. *Therapeutics and clinical risk management*. 4(1): 1-9, **2008**.
- Erskine, P. T, Norton, E., Cooper, J. B., Lambert, R., Coker, A., Lewis, G., Spencer, P., Sarwar, M., Wood, S. P., Warren, M. J., Shoolingin-Jordan, P. M. X-ray structure of 5-aminolevulinic acid dehydratase from Escherichia coli complexed with the inhibitor levulinic acid at 2.0 A resolution. *Biochemistry*. 38 (14), 4266-76, **1999**.
- Evensen, J. F. The use of porphyrins and non-ionizing radiation for treatment of cancer. *Acta Oncol.* 81,103-110, **1995**.
- Fabris, C., Jori, G., Giuntini, F., Roncucci, G. Photosensitizing properties of a boronated phthalocyanine: studies at the molecular and cellular level. *J. Photochem. Photobiol. B*. 64(1): 1-7, **2001.**

- Festjens, N., Vanden Berghe, T., Vandenabeele, P. Necrosis, a well-orchestrated form of cell demise: signalling cascades, important mediators and concomitant immune response. *Biochim Biophys Acta*. 1757:1371-87, **2006**.

- Feuerstein, T., Schauder, A., and Malik, Z. Silencing the ALA dehydratase affects ALA- photodynamic therapy efficacy in K562 erythroleukemic cells. *Photochem. Photobiol. Sci.* 8: 1461-1466, **2009**.

- Fink-Puches, R., Hofer, A., Smolle, J., Kerl, H., Wolf, P. Primary clinical response and long term follow up of solar keratoses treated with topically applied 5-ALA and irradiation by different wave bands of light. *J Photochem Photobiol B.* 41: 145-151, **1997**.

- Fisher, A. M. R., Murphree, A. L., Gomer, C. J. Clinical and preclinical PDT. *Lasers Surg Med.* 17: 2-31, **1995**.

- Foley, P., Freeman, M., Menter, A., Siller, G., El Azhary, R. A., Gebauer, K., Lowe, N. J., Jarratt, M. T., Murrell, D. F., Rich, P., Pariser, D. M., Oseroff, A. R., Barnetson, R., Anderson, C., Kossard, S., Gibson, L. E., Tope, W. D. Photodynamic therapy with methyl aminolevulinate for primary nodular basal cell carcinoma: results of two randomised studies. *Int J Dermatol.* 48 (11): 1236-1245, **2009**.

- Foote, C. S., Peak, J. G., and Peak M. J. Effects of glycerol upon the biological actions of near ultraviolet light: spectra and concentration dependence for transforming DNA and for Escherichia Coli B/r. *Photochem. Photobiol*. 36(4): 413-16, **1982**.

- Frankenberg, N., Frankenberg, N., Erskine, P. T., Cooper, J. B., Shoolingin-Jordan, P. M., Jahn, D., Heinz, D. W. High resolution crystal structure of Mg^{2+}-dependent prophobilinogen synthase. *J. Mol. Biol.* 289 (3): 591-602, **1999**.
- Freeberg. Fitzpatrick's dermatology in general medicine. (6^{th} edition). McGraw-Hill, **2003**.
- Galderma. *Summary of product charecteristics, Metvix*. Watford: Galderma,**2008**.
- Gao, J., and Richardson, D. R. The potential of iron chelators of the pyridoxal isonicotinoyl hydrazone class as effective antiproliferative agents, IV: The mechanisms involved in inhibiting cell-cycle progression. *Blood*. 98 (3): 842-850, **2001**.
- Gaullier, J. M., Berg, K., Peng et al. Use of 5-aminolevulinic acid esters to improve photodynamic therapy on cells in culture. *Cancer Res.* 57: 1481-1486, **1997**.
- Gerber-Leszczyszyn, H., Ziolkowski, P., Marszalik, P. Photodynamic therapy of head and neck tumours and non tumour like disorders. *Otoryngol. Pol.* 58: 339-343, **2004**.
- Gederaas, O. A., Holroyd, A., Brown, S. B.,Vernon, D., Moan, J., Berg, K. 5-aminolevulinic acid methyl ester transport on amino acid carriers in a human colon adenocarcinoma cell line. *Photochem Photobiol.* 73, 721-732, **2001**. Gerritsen, M. J., Smits, T., Kleinpenning, M. M., van de Kerkhof., van Erp, P. E. Pre-treatment to enhance protoporphyrin IX accumulation in photodynamic therapy. *Dermatology.* 218: 193-202, **2009**.

- Giordani, A., Morlier, P., Aubailly, M., and Santus, R. Photoinactivation of cellular catalase by ultraviolet radiation. *Redox. Rep*. 3, 49-55, **1997**.
- Girotti, A. W. Photosensitised oxidation of membrane lipids: reaction pathways, cytotoxic effects, and cytoprotective mechanisms. *J Photochem Photobiol B*. 63 (1-3): 103-13, **2001**.
- Glickstein, H., El, R. B., Shvartsman, M., Cabantchik, Z. I. Intracellular labile iron pools as direct targets of iron chelators: a fluorescence study of chelator action in living cells. *Blood.* 106: 3242-3250, **2005**.
- Golab, J., Wilczynski, G., Zagozdon, R., Stoklosa, T., Dabrowska, A., Rybczynska, J., Wasik, M., Machaj, E., Ołda, T., Kozar, K., Kamiński, R., Giermasz, A., Czajka, A., Lasek, W., Feleszko, W., Jakóbisiak, M. Potentiation of the antitumor effects of Photofrin-based photodynamic therapy by localised treatment with G-CSF. *Br J Cancer.* 82: 1485-1491, **2000**.
- Gold, M. H., Bradshaw, V. L., Boring, M. M., Bridges, T. M., Biron, J. A. Treatment of sebaceous gland huperplasia by photodynamic therapy with 5-aminolevulinic acid and a blue light source or intense pulsed light source. *J Drugs Dermatol*. 3(6): 6-9, **2004**.
- Gomes, A. J., Lunardi, C. N., Tedesco, A. C. Characterisation of biodegradable poly (D, L-lactide-co-glycolide) nanoparticles loaded with bacteriochlorophyll-a for photodynamic therapy. *Photomed Laser Surg.* 25(5): 428-435, **2007**.
- Grapengiesser, S., Ericson, M., Gudmundsson, F., Larkö, O., Rosén, A., Wennberg, A. M. Pain caused by photodynamic therapy of skin cancer. *Clin Exp Dermatol.*27: 493-497, **2002**.

- Green, D. A., Antholine, W. E., Green, D. A., Antholine, W. E., Wong, S. J., Richardson, D. R., Chitambar, C. R. Inhibition of malignant cell growth by 311, a novel iron chelator of the pyridoxal isonicotinoyl hydrazone class: effect on the R2 subunit of ribonucleotide reductase. *Clin Cancer Res*. 7 (11): 3574-3579, **2001**.

- Greenbaum, L., Gozlan, Y., Schwartz, D., Katcoff, D. J., Malik, Z. Nuclear distribution of phorphobilinogen deaminase in glioma cells: a regulatory role in cancer transformation. *Br J Cancer.* 86: 1006-1011, **2002**.

- Grinblat, B., Pour, N., Malik, Z. Regulation of porphyrin synthesis and photodynamic therapy in heavy metal intoxication. *J. Environ. Pathol. Toxicol. Oncol.* 25: 145-158, **2006**.

- Haedersdal, M., Togsverd-Bo, K., Wulf, H., C. Evidence-based review of lasers, light sources and photodynamic therapy in the treatment of acne vulgaris. *J Eur Acad Dermatol Venereol*. 22 (3): 267-78, **2008**.

- Halldin, C. B., Paoli, J., Sandberg, C., Gonzalez, H., and Wennberg, A. M. Nerve blocks enable adequate pain relief during topical photodynamic therapy of field cancerization on the forehead and scalp. *Br J Dermatol*. 160: 795-800, **2009**.

- Halliwell, B., Gutterridge, J. M. C. Free radicals in biology and medicine. *3rd ed, Oxford University Press, Oxford, UK*. **1999**.

- Halliwell, B., Gutterdige, J. M. C. Role of free radicals and catalytic metal ions in human disease: an overview. *Methods Enzymol.*1-85,186, **1990**.

- Hampton, M. B., Orrenius, S. Dual regulation of caspase activity by hydrogen peroxide: implications for apoptosis. *FEBS Lett.* 414, 552-556, **1997**.

- Hanania, J., Malik, Z. The effect of EDTA and serum on endogenous porphyrin accumulation and photodynamic sensitization of human K562 leukemic cells. *Can Lets.* 65:127-131, **1992**.

- Hauschild, A., Stockfletch, E., Popp, G., Borrosch, F., Brüning, H., Dominicus, R., Mensing, H., Reinhold, U., Reich, K., Moor, A. C., Stocker, M., Ortland, C., Brunnert, M., Szeimies, R. M. Optimisation of photodynamic therapy with a novel self-adhesive 5-aminolevulinic acid patch: results of two randomized controlled phase III studies. *Br J Dermatol*. 160: 1066-74, **2009**.

- Hayame, J., Okamoto, H., Sugihara, A., Horio, T. Immunosuppression effects of photodynamic therapy by topical aminolevulinic acid. *J Dermatol.* 34(5): 320-7, **2007**.

- He, D., Sassa, S., Lim, H. W. Effect of UVA and blue light on porphyrin biosynthesis in epidermal cells. *Photochem Photobiol* 57:825-829, **1993**.

- Hemmi, H., Kaisho, T., Takeuchi, O., Sato, S., Sanjo, H., Hoshino, K., Horiuchi, T., Tomizawa, H., Takeda, K., Akira, S. Small anti-viral compounds activate immune cells via the TLR7 MyD88-dependent signalling pathway. *Nat Immunol*. 3 (2): 196-200, **2000**.

- Henderson, B. W., Dougherty, T. J. How does photodynamic therapy work? *Photochem Photobiol*.55: 145-157, **1992**.

- Henderson, B. W., Waldow, S. M., Potter, W. R., Dougherty, T. J. Interaction of photodynamic therapy and hyperthermia: Tumor response and cell survival studies after treatment of mice *in vivo. Cancer Res*. 45 (12 Pt 1):6071-7, **1985**.

- Heyerdahl, H., Warloe, T., Peng, Q., Svanberg, K., Moan, J., Steen, H., Svaasand, L., and Giercksky, K. Dosimetry and light distribution systems for photodynamic therapy at the Norwegian Radium Hospital. *In Photodynamic Therapy of Cancer.* Jori G, Moan J, Star W. (eds) pp.27-36. SPJE: Bellingham, **1993**.

- Hider, R. C., Porter, J. B., Singh, H. The design of therapeutically useful iron chelators, in Bergeron RJ, Brittenham GM (eds): The development of iron chelators for clinical use. *Boca Raton, FL*, *CRC,* p353, **1994**.

- Hider, R. C., Singh, S., Porter, J. B. Iron chlelating agents for clinical significance. *Proc Roy soc Edinburgh*. 9913: 137, **1992**.

- Holmes, M V., Dawe, R. S., Fergusson, J., Ibbotson, S. H. A randomized, double-blind, placebo-controlled study of the efficacy of tetracaine gel (Ametop) for pain relief during topical photodynamic therapy. *Br J Dermatol*.150: 337-340, **2004**.

- Hongeharu, W., Taylor, C. R., Chang, Y., Aghassi, D., Suthamjayari, K., Anderson, R. R. Topical ALA-PDT for the treatment of Acne vulgaris. *J Invest Dermatol* 115: 183-192, **2000**.

- Hopper, C. photodynamic therapy: a clinical reality in the treatment of cancer. *Lancet Oncol.* 1: 212-219, **2000**.

- Horn, M., Wolf, P., Wulf, H. C., Horn, M., Wolf, P., Wulf, H. C., Warloe, T., Fritsch, C., Rhodes, L. E., Kaufmann, R., De Rie, M., Legat, F. J., Stender, I. M., Solér, A. M., Wennberg, A. M., Wong, G. A., Larkö, O. Topical methyl aminolevulinate photodynamic therapy in patients with basal cell carcinoma prone to complications and poor cosmetic outcome with conventional treatment. *Br J Dermatol.* 149: 1242-49, **2003**.

- Hruskova, K., Kovarikova, P., Bendova, P., Hoskova, P., Stariat, J., Vavrova, A., Vavrova, K., Simunek, T. Synthesis and initial *in vitro* evaluations of novel antioxidant aroylhydrazone iron chelators with increased stability against plasma hydrolysis. *Chem Res Toxical*. 24 (3): 290-302, **2011**.
- Hua, Z. S., Gibson, S. L., Foster, T. H., Hilf, R. Effectiveness of ALA induced protoporphyrin as a photosensitiser for photodynamic therapy in vivo. *Cencer Res.* 55: 1723-1713, **1995**.
- Huang, Z. A review of progress in clinical photodynamic therapy. *Technol Cancer Res Treat.* 4: 283-293, **2005.**
- Huang, A. R., Ponka, P. A study of the mechanism of action of pyridoxal isonicotinoyl hydrazine at the cellular level using reticulocytes loaded with non heme 59Fe. *Biochim Biophys Acta*. 757(3): 306-15. **1983**.
- Ibbotson, S. H., Jong, C., Lesar, A., Ferguson, J. S., Padgett, M., O'Dwyer, M., Barnetson, R., Ferguson, J. Characteristics of ALA-induced PPIX fluorescence in human skin in vivo. *Photodermatol Photoimmunol Photomed.* 22: 105-110, **2006**.
- Ibboston, S. H., Valentine, R., and Hearn, R. Is the pain of topical photodynamic therapy with methyl aminolevulinate any different from that with 5-aminolevulinic acid? *Photodermatology, Photoimmunology & Photomedicine*. 28: 272-73, **2012**.
- Ickowicz, S. D., Gozlan, Y., Greenbaum, L., Babushkina, T., Katcoff, D. J., Malik, Z. Differentiation-dependent photodynamic therapy regulated by porphobilinogen deaminase in B16 melanoma. *Br. J. Cancer.* 90: 1833-1841**, 2004.**
- Ihnat, P. M., Vennerstorm, J. L., Robinson, D. H. Synthesis and solution preparation of desferroxamine amides. *J Pharm Sci*. 89 (12): 1525-36, **2000**.

- Iinuma, S., Farshi, S. S., Ortel, B., and Hasan, T. A mechanistic study of cellular photodestruction with 5-aminolevulonic acid-induced porphyrin. *Br. J. Cancer.* 70: 21-28, **1994**.
- Itkin, A., Gilchrest, B. A. Delta-aminolevulinic acid and blue light photodynamic therapy for treatment of multiple basal cell carcinomas in two patients with nevoid basal cell carcinoma syndrome. *Dermatol Surg*. 30 (7): 1054-1061, **2004**.
- James, W., Berger, T., Elston, D. Diseases of the skin. Clinical Dermatology (10th ed). Saunders. Pages 1, 11-12, **2005**.
- Jang, W. D., Nishiyama, N., Zhang, G. D.,Harada, A., Jiang, D. L., Kawauchi, S., Morimoto, Y., Kikuchi, M., Koyama, H., Aida, T., Kataoka, K.supramolecular nanocarrier of anionic dendrimer porphyrins with cationic block copolymers modified with polyethylene glycol to enhance intracellular photodynamic efficiency. *Angew Chem Int Ed Engl*. 44(3): 419-423, **2005**.
- Johnson, D. K., Murphy, T. B., Rose, N. J., Goodwin, W. H., and Pickart, L. Cytotoxic chelators and chelates 1. Inhibition of DNA synthesis in cultured rodent and human cells by aroylhydrazone and by a copper (II) complex of salicylaldehyde benzoyl hydrazone. *Inorg Chim Acta*. 67: 159-165, **1982**.
- Jori, G. Far-red-absorbing photosensitisers: their use in the photodynamic therapy of tumors. *J. Photochem. Photobiol A*. 62: 371-378, **1992**.
- Junjing, Z., Yan, Z., and Baolu, Z. Scavenging effects of Dexrazoxane on free radicals. *J. Clin. Biochem. Nutr.* 47: 238-245, **2010**.
- Juzeniene, A., Juzenas, P., Iani, V., Moan, J. Topical application of 5-aminolevulinic acid and its methylesters, hexylesters and octylester derivatives:

consideration for dosimetry in Mouse skin models. *Photochem. Photobiol*. 76: 329-334, **2002**.

- Juzeniene, A., Juzenas, P., Ma, L. W., Moan, J. Effectiveness of different Light sources for 5-ALA-PDT. *Lasers Med Sci.* 19: 139-149, **2004**.
- Kalinowski, D. S., and Richardson, D. R. The evolution of iron chelators for the treatment of iron overload disease and cancer. *Pharmacol Rev*. 57(4): 547-583, **2005**.
- Kalka, K., Merk, H., Mukhtar, H. Photodynamic therapy in dermatology. *J. Am Acad Dermatol.*42, 389-413, **2000**.
- Kanay, H. E., Gerstenblith, M. R. Ultraviolet radiation and melanoma. *Semin Cutan Med Surg*. 30 (4): 222-8, 2011.
- Karrer, S., Abel, C., Szeimies, R. M., Bäumler, W., Dellian, M., Hohenleutner, U., Goetz, A. E., Landthaler, M. Topical application of a first porphycene dye for photodynamic therapy penetration studies in human perilesional skin and basal cell carcinoma. *Arch Dermatol Res*. 289: 132-137, **1997**.
- Karrer, S., Szeimies, R. M., Hohenleutner, U., Heine, A., Landthaler, M. Unilateral localized basaliomatosis.: treatment with topical PDT after application of 5-ALA. *Dermatology.* 190: 218-222, **1995**.
- Kasche, A., Luderschmidt, S., Ring, J., Hein, R. Photodynamic therapy induces less pain in patients treated with methyl aminolevulinate compared to aminolevulinic acid. *J Drugs Dermatol.* 5: 353-356, **2006**.

- Kasper, B., Hoa, D., Egerer, G. Is there an indication for high dose chromatography in the treatment of bone and soft-tissue sarcoma? *Oncology*. 68 (2-3): 115-21, **2005**.

- Kawauchi, S., Morimoto, Y., Sato, S., Arai, T., Seguchi, K., Asanuma, H., Kikuchi, M. Differences between cytotoxicity in PDT using a pulsed laser and a continuous water laser: study of oxygen consumption and photo-bleaching. *Lasers Med Sci*.18: 179-183, **2004**.

- Kelly, J. F., Snell, M. E., Berenbraum, M. C. Photodynamic destruction of human bladder carcinoma. *Br. J. Cancer.* 31: 237-244, **1975**.

- Kennedy, J. c., Pottier, R. H., Pross, D. C. Photodynamic therapy with endogenous propoporphyrin IX. Basic principles and present clinical experience. *J Photobiol Photochem B Biol*. 6: 143-148, **1990**.

- Kessel, D., Thompson, P., Saatio, K., Nantwi, K. D. Tumor localisation and photosensitisation by sulfonated derivatives of tetraphenylporphine. *Photochem Photobiol*. 45: 787-790, **1987**.

- Kiesslich, T., Plaetzer, K., Oberdanner, C. B., Berlanada, J., Obermair, F. J., Krammer, B. Differential effects of glucose deprivation on the cellular sensitivity towards photodynamic treatment-based production of reactive oxygen species anf apoptosis-induction. *FEBS Lett*. 579: 185-190, **2005**.

- Kim, H. S., Yoo, J. Y., Cho, K. H., Kwon, O. S., Moon, S. E. Topical photodynamic therapy using intense pulsed light for treatment of actinic keratosis: Clinical and histopathologic evaluation. *Dermatol Surg*. 31 (1): 33-6, **2005**.

- Kimel, S., Svaasand, L. O., Hammer-Wilson, M., Gottfried, V., Cheng, S., Svaasaand, E., Berns, M. W. Demonstration of synergistic effects of hyperthermia and photodynamic therapy using the chick chorioallantoic membrane model. *Lasers Surg Med.*12: 432-440, **1992**.
- Kirveliene, V., Sadauskaite, A., Kadziauskas, J., Sasnauskienne, S., Juodka, B. Correlation of death modes of photosensitised cells with intracellular ATP concentration. *FEBS Lett*. 553:167-172, **2003**.
- Klein, A., Babilas, P., Karrer, S., Landthaler, M., Szeimies, R. M. Photodynamic therapy in dermatology-an update 2008. *JDDG.* 6: 839-845, **2008**.
- Kloek, J., Van Henegouven, G. M. J. B. Prodrugs of 5-aminolevulinc acid for photodynamic therapy. *Photochem. Photobiol.* 64: 994-1000, **1996**.
- Klotz, L. O., Brivida, K., Sies, H. Singlet oxygen mediates the activation of JNK by UVA radiation in human skin fibroblasts. *FEBS Lett.* 289-291, 408, **1997**.
- Kübler, A.C., Haase, T., Staff, C., Kahle, B., Rheinwald, M., Mühling, J. Photodynamic therapy of primary nonmelanomatous skin tumors of the head and neck. *Lasers Surg Med.* 25: 60-68, **1999**.
- Konan, Y. N., Gurny, R., Allemann, E. State of the art in the delivery of photosensitisers for photodynamic therapy. *J Photochem Photobiol B Biol*. 66(2): 89-106, **2002**.
- Korbelik, M., Krosl, G. Photofrin accumulation in malignant and host cell populations of various tumors. *Br. J. Cancer*.73: 506-513, **1996**.
- Kormeili, T., Yamauchi, P. S., Lowe, N. J. Topical photodynamic therapy in clinical dermatology. *Br J of dermatology*, Blackwell publishing. 150 (6), **2004**.

- Kreimeier-Birnbaum, M. Modified porphyrins, chlorins, phtalocyanines and purpurins: second generation photosensitisers for PDT. *Semin Hematol*. 26: 157-173, **1989**.
- Krieg, R. C., Messmann, H., Schlottmann, K., Endlicher, E., Seeger, S., Schölmerich, J., Knuechel, R. Intracellular localization is a cofactor for the phototoxicity of protoporphyrin IX in the gastrointestinal tract: in vitro study. *Photochem. Photobiol.* 78(4): 393-399, **2003**.
- Krishna, V., Sharma and Lester, M., Davids. Hypericin- PDT- induced rapid necrotic death in human squamous cell carcinoma cultures after multiple treatment. *Cell Biol. Int.* 36, 1261-1266, **2012**.
- Kubin, A., Wierrni, F., Burner, U., Alth, G., Grunberger, W. Hypericin- the facts about a controversial agent. *Curr. Pharm. Des*. 11: 233-252, **2005**.
- Kuijpers, D. I., Thissen, M. R., Thissen, C. A., Neumann, M. H. Similar effectiveness of methyl aminolevulinate and 5-aminolevulinate in topical photodynamic therapy of nodular basal cell carcinoma. *J Drugs Dermatol.* 5(7): 642-645, **2006**.
- Kurz, T., Gustafsson, B., Brunk, U. T. Intralysosomal iron chelation protects against oxidative stress-induced cellular damage. *FEBSJ*. 273 (13):3106-17, **2006**.
- Kurz, T. Can lipofuscin accumulation be prevented? *Rejuvenation Res*. 11 (2):441-3, **2008**.
- Langan, S. M., Collins, P. Randomized, double-blind, placebo-controlled prospective study of the efficacy of topical anaesthesia with a eutectic mixture of

lignocaine 2.5% and prilocaine 2.5% for topical 5-aminolevulinic acid-photodynamic therapy for extensive scalp actinic keratoses. *Br. J. Dermatol.*154: 146-149, **2006**.

- Lehmann, P. Methyl aminolevulinate-photodynamic therapy: a review of clinical trials in the treatment of actinic keratoses and non-melanoma skin cancer. *Bj J Dermatol.* 156: 793-801, **2007**.

- Leman, J. A., Morton, C. A. Photodynamic therapy: applications in dermatology. *Expert Opin Biol Ther*. 2(1): 45-53, **2002**.

- Levell, N. J., Igali, L., Wright, K. A., Greenberg, D. C. Basal cell carcinoma epidemiology in the UK: the elephant in the room. *Clin Exp Dermatol*, 38(4):367-9, **2013**.

- Li, Q., Gao, T., Long, H. A., Ujiie, H. Clearance of a thick invasive squamous cell carcinoma after multiple treatments with topical photodynamic therapy. *Photomed Laser Surg*. 28 (5): 703-705, **2010**.

- Licznerski, B., Shanler, S. D., Paszkiewicz, G., Whitaker, J. E., Wan, W., Oseroff, A. R. Effect of available iron on the accumulation of protoporphyrin IX, an endogenously synthesized photosensitiser produced from exogenous 5-aminolevulinic acid. *Proc Annu Meet Am Assoc Cancer Res.* 34:363, **1993**.

- Lippens, S., Hoste, E., Vandenabeele, P., Agostinis, P., Declercq, W. Cell death in the skin. *Apoptosis*. 14 (4): 549-569, **2009**.

- Lipson, R. L., Baldes, E. J., Olsen, A. M. The use of a derivative of hematoporphyrin in tumor detection. *J. natl. Cancer Inst.*1-8, 256, **1961**.

- Liu, Z.D., Hider, R. C. Design of clinically useful iron(III)-selective chelators. *Med. Res. Rev.* 22(1), 26-64, **2002**.
- Liu, H. F., Xu, S. Z., Zhang, C. R. Influence of CaNa2 EDTA on topical 5-aminolevulinic acid photodynamic therapy*. Chin. Med. J.* 117: 922-926, **2004**.
- Lloyd, J. B., Cable, H., Rice-Evans, C. Evidence that desferrioxamine cannot enter cells by passive diffusion. *Biochem Pharmacol*. 41 (9): 1361-3, **1991**.
- Lober, B. A., Lober, C. W. Actinic keratosis is squamous cell carcinoma. *South Med J.* 93: 650-655, **2000**.
- Longly, D. B., Harkin, D. P., Johston, P. G. “5-flourouracil: mechanisms of action and clinical strategies. *Nat. Rev. Cancer*. 3 (5): 330-8, **2003**.
- Lopez, R. F., Bentley, M. V., Delgado-Charro, M. B., Salomon, D., van den, B.H., Lange, N., Guy, R. H. Enhanced delivery of ALA esters by iontophoresis *in vitro*. *Photochem Photobiol.* 77: 304-308, **2003**.
- Lui, H., Anderson R. R. Photodynamic therapy in dermatology: shedding a different light on skin disease. *Arch Dermatol.* 128: 1631-1636**, 1992.**
- Ma, Y., Luo, W., Quinn, P. J., Liu, Z., Hider, R. C. Design, synthesis, physicochemical properties, and evaluation of novel iron chelators with fluorescent sensor. *J Med Chem*, 47 (25): 6349-62, **2004**.
- Madison, K. C. Barrier fuction of the skin: la raison detre of the epidermis. *J Invest Dermatol.* 121 (2): 231-241, **2003**.
- Magne, M. L., Rodriguez, C. O., Autry, S. A., Edwards, B. F., Theon, A. P., Madewell, B. R. Photodynamic therapy of facial squamous cell carcinoma in cats using a new photosensitiser. *Lasers Surg Med.* 20: 202-209, **1997**.

- Malik, Z., Ehrenberg, B., Faraggi, A. Inactivation of erythrocytic, lymphocytic and myelocytic leukemic cells by photoexcitation of endogenous porphyrins. *J Photochem Photobiol B.* 4:195-205, **1989**.
- Malik, Z., Lugaci, H. Destruction of erythroleukaemic cells by photoactivation of endogenous porphyrins. *Br J Cancer.* 56: 589-595, **1987**.
- Matei, C., Tampa, M., Poteca, T., Panea-Paunica, G., Georgescu, S. R., Ion, R. M., Giurcaneanu, C., Carol Davila. Photodynamic therapy in the treatment of basal cell carcinoma. *Journal of medicine and life*. Vol 6, Issue 1, pp.50-54, **2013**.
- McCann, J. Texas centre studies research alternative treatments. *J Natl Cancer Inst.* 89, 1485-1486, **1997**.
- McGrath, J. A., Eady, R. A., Pope, F. M. Rook's textbook of dermatology (7th ed). Blackwell publishing. P. 3.1-3.6, **2004**.
- Messmann, H., Mlkvy, P., Buonaccorsi, G., Davies, C. L., MacRobert, A. J., Bown, S. G. Enhancement of photodynamic therapy with 5-aminolevulinic acid-induced porphyrin photosensitisation in normal rat colon by threshold and light fractionation studies. *Bj J Cancer*.72: 589-594, **1995**.
- Milgrom, L., and MacRobert, S. Light years ahead. *Chem. Br.* 34, 45-50, **1998**.
- Miller, R. L., Gerster, J. F., Owens, M. L., Slade, H. B., Tomai, M. A. Imiquimod applied topically: a novel immune response modifier and a new class of drug. *Int J Immunopharmacol*. 21(1): 1-14, **1999**.
- Minton, T. J. Contemporary Moh's surgery applications. *Curr Opin Otolaryngol Head Surg*. 16 (4): 376-80, **2008**.

- Miyake, M., Ishii, M., Kawashima, K., Kodama, T., Sugano, K., Fujimoto, K., Hiraro, Y. SiRNA-mediated knockdown of the heme synthesis and degradation pathway: Modulation of treatment effect of 5-aminolevulinic acid-based photodynamic therapy in urothelial cancer cell lines. *Photochem Photobiol* 85: 1020-1027, **2009**.

- Moan, J., Berg, K. Photochemotherapy of cancer: experimental research. *Photochem.Photobiol*.55: 931-948, **1992**.

- Moan, J., Berg, K. The photodegradation of porphyrins in cells can be used to estimate the lifetime of singlet oxygen. *Photochem.Photobiol.* 53, 549-553, **1991**.

- Moan, J., Van der Akker, J. T. H. M., Juzenas, P. On the basis for tumour selectivity in the 5-aminolevulinic acid induced synthesis of propoporphyrin IX. *Journal of porphyrins and Phthalocyanines*. 5:170-76, **2001**.

- Moloney, F. J., Collins, P. Randomized, double-blind, prospective study to compare topical 5-aminolevulinic acid methylester with topical 5-aminolevulinic avid photodynamic therapy for extensive scalp actinic keratosis. *Br J Dermatol.*157: 87-91, **2007**.

- Moore, J. V., Allan, E. Pulsed ultrasound measurements of depth and regression of BCC after PDT: relationship to probability of 1-year local control. *Br J Dermatol.*149:1035-1040, **2003**.

- Moore, M. R., Goldberg, A., Yeung-Laiwah, A. A. Lead effects on the heme biosynthetic pathway. Relationship to toxicity. *Ann N Y Acad Sci*. 514: 191-203, **1987**.

- Morliere, P., Moysan, A., Santus, R., Huppe, G., Maziere, J. C., Ertret, L. UVA-induced lipid peroxidation in cultured human fibroblasts. *Biochem. Biophys. Acta*.261-268,1084, **1991**.
- Morton, C. A. Methyl aminolevulinate (Metvix) PDT-practical pearls*. J. Dermatol Treat.* 14: 23-26, **2003**.
- Morton, C. A. Topical photodynamic therapy for Bowen's Disease. *Australas J Dermatol.*46: S1, **2005**.
- Morton, C. A., Brown, S. B., Collins, S.,Ibbotson, S., Jenkinson, H., Kurwa, H., Langmack, K., McKenna, K., Moseley, H., Pearse, A. D., Stringer, M., Taylor, D. K., Wong, G., Rhodes, L. E. Guidelines for topical photodynamic therapy: report of a workshop of the British Photodermatology Group. *Br J Dermatol.*146:552-567, **2002**.
- Morton, C. A., Campbell, S., Gupta, G., Keohane, S., Lear, J., Zaki, I., Walton, S., Kerrouche, N., Thomas, G., Soto, P. right-left comparison of topical methyl aminolevulinate photodynamic therapy and cryotherapy in in subjects with actinic keratosis: a multicentre, randomized controlled study. *Br J Dermatol*. 155: 1029-1036, **2006**.
- Morton, C. A., McKena, K. E., Rhodes, L. E. Guidelines for topical photodynamic therapy: update. *Br J Dermatol.*159: 1245-1266, **2008**.
- Morton, C. A., Whitehurst, C., Moseley, H., Moore, J. V., Mackie, R. M. Development of an alternative light source to lasers for photodynamic therapy. 1. Clinical evaluation in the treatment of pre-malignant non-melanoma skin cancer. *Lasers Med Sci.*10: 165-171, **1995**.

- Mosmann, T. Rapid Colorimetric assay for cellular growth and survival application to proliferation and cyto-toxicity assays. *Journal of immunological methods*. 65: 55-63, **1983**.

- Mosterd, K., Thissen, M. R., Nelemans, P., Kelleners-Smeets, N. W., Jenssen, R. L., Broekhof, K. G., *et al*. Fractionated 5-aminolevulinic acid photodynamic therapy vs. surgical excision in the treatment of nodular basal cell carcinoma: results of randomised controlled trial. *Br J Dermatol*. 159 (4): 864-870, **2008**.

- Neckers, L. M. Regulation of transferrin receptor expression and control of cell growth. *Pathobiology* 59:11-18, **1991**.

- Neville, J. A., Welch, E., Leffell, D. J. Management of non-melanoma skin cancer in 2007. *Nat Clin Pract Oncol*. 4(8): 462-9, **2007**.

- Nowis, D., Makowski, M., Stoklosa, T., Legat, M., Issat, T., Golab Jakub. Direct damage mechanisms of photodynamic therapy. *Acta Biochim. Pol*. 52: 339-352, **2005.**

- Nyman, E. S., and Hynninen, P. H. Research advances in the use of tetrapyrrolic photosensitisers for photodynamic therapy. *J. Photochem. Photobiol. B. Biol.*1-28, 73, **2004**.

- Oberdanner, C. B., Kiesslich, T., Krammer, B., Plaetzer, K. Glucose is required to maintain high ATP levels for the energy-utilizing steps during PDT-induced apoptosis. *Photochem Photobiol*.76: 695-703, **2002**.

- Ochsner, M. Light scattering of human skin: a comparison between zinic(II)-pthalocyanine and photofrin II. *J. Photochem. Photobiol. : B. Biol*. 32: 3-9, **1996**.

- Oexle, H., Gnaiger, E., Weiss, G. Iron dependent changes in cellular energy metabolism: influence on citric acid cycle and oxidative phosphorylation. *Biochim Biophys Acta.* 1413 (3): 99-107, **1999**.

- Ohgari, Y., Miyata, Y., Chau, T. T., Kitajima, S., Adachi, Y., Taketani, S. Quinolone compounds enhance δ-aminolevulinic acid-induced accumulation of protoporphyrin IX and photosensitivity of tumour cells. *J. Biochem*. 149(2): 153-160, **2011**.

- Oleinick, N. L., Antunez, A. R., Clay, M. E., Rihter, B. D., Kennedy, M. E. New phtalocynanine photosensitisers for PDT.*Photochem Photobiol* 57: 242-247, **1993**.

- Oleinick, N. L., Morris, R. L., Belichenko, I. The role of apoptosis in response to photodynamic therapy: What, Where, Why, and How. *Photochem Photobiol Sci*. 1 (1): 1-21, **2002**.

- Olivo, M., Lau, W., Manivasager, V., Tan, P. H., Soo, K. C., Cheng, C. Macro-microscopic fluorescente of human bladder cancer using hipericina fluorescente cystoscopy and laser confocal microscopy. *Int. J. Oncol*. 23: 983-990, 2003.

- Omrod, D., Jarvis, B. Topical aminolevulinic acid HCl photodynamic therapy. *Am J. Clin. Dermatol*. 1: 133-139, **2000**.

- Orenstein, A., Kostenich, G., Roitman, L., Shechtman, Y., Kopolovic, Y., Ehrenberg, B., Malik, Z. A comparative study of tissue distribution and photodynamic therapy selectivity of chlorin e6, Photofrin II and ALA-induced PPIX in colon carcinoma model. *Br J Cancer.* 73: 937-944, **1996.**

- Orenstein, A., Kostenich, G., Tsur, H., Roitman, L., Ehrenberg, B., Malik, Z. Photodynamic therapy of human skin tumours using topical application of 5-aminolevulinic acid, DMSO and EDTA. In Brault, d., Jori, G., Moan, J., Ehrenberg, B. Photodynamic therapy of cancer II. *Proc SPIE.* 2325:100-105, **1995.**

- Orrenius, S., Zhivotovsky, B., Nicotera, P. Regulation of cell death: the calcium apoptosis link. *Nat Rov Mol Cell Biol*. 4: 552-65, **2003**.

- Ortel, B., Tanew, A., Hönigsmann, H. Lethal photosensitisation by endogenous porphyrins of PAM cells-modification by desferrioxamine. *J Photochem Photobiol B*. 17 (3): 273-8, **1993**.

- Oseroff, A. R., Shieh, S., Frawley, N. P., Cheney, R., Blumenson, L. E., Pivnick, E. K., Bellinier, D. A. Treatment of diffuse basal cell carcinomas and basaloid follicular hamartomas in nevoid basal cell carcinoma syndrome by wide area 5-aminolevulinic acid photodynamic therapy. *Arch Dermatol*. 141(1): 60-7, **2005**.

- Osiecka, B., Jurczyszyn, K., Ziolkowski, P. The application of Levulan-based photodynamic therapy with imiquimod in the treatment of recurrent basal cell carcinoma. *Med Sci Monit*. 18 (2): 15-19, **2012**.

- Pagliaro, J., Elliot, T., Bulsara, M., King, C., Vinciullo, C. Cold air analgesia in photodynamic therapy of basal cell carcinomas and Bowen's disease: an effective addition to treatment: a pilot study. *Dermatol Surg*.30: 63-69, **2004**.

- Pahl, P. M., and Horwitz, L. D. Cell permeable iron chelators as potential cancer chemotherapeutic agents. *Cancer Invest*. 23(8): 683-691, **2005**.

- Palumbo, G. Photodynamic therapy and cancer: a brief sightseeing tour. *Expert Opin. Drug Deliv.* 4(2): 131-148, **2007**.
- Paoli, J., Halldin, C., Ericson, M. B., Wennberg, A. M. Nerve blocks provide effective pain relief during topical photodynamic therapy for extensive facial actinic keratoses. *Clin Exp Dermatol*.33: 559-564, **2008**.
- Palumbo G. Photodynamic therapy and cancer: a brief sightseeing tour. *Expert Opin. Drug Deliv.* 4(2): 131-148, **2007**.
- Parihar, A., Dube, A., Gupta, P, K. Photodynamic treatment of oral squamous cell carcinoma in hamster cheek pouch model using chlorinn p6-histamine conjugate. *Photodiagnosis Photodyn Ther*, 10 (1): 79-86, **2013**.
- Peng, Q., Soler, A. M., Warloe, T., Nesland, J. M., Giercksky, K. E. Selective distribution of porphyrins in thick basal cell carcinoma after topical application of methyl 5-aminolevulinate. *J Phhotochem Photobiol B.*62: 140-45, **2001**.
- Peng, Q., Warloe, T., Berg, K., Moan, J., Kongshaug, M., Gierckcky, K. E., Nesland, J. M. 5-aminolevulinic acid-based photodynamic therapy. *Clinical research and future challenges. Cancer*. 79: 2282-2308, **1997**.
- Plaetzer, K., Kiesslich, T., Krammer, B., Hammerl, P. Characterization of the cell death modes and the associated changes in cellular energy supply in response to AlPcS4-PDT. *Photochem Photobiol Sci.* 1:172-177, **2002.**
- Plaetzer, K., Krammer, B., Berlanda, J., Berr, T., Kiesslich, T. Photophysics and photochemistry of photodynamic therapy: Fundamental aspects*. Laser. Med. Sci*. 1: 1-15, **2008**.

- Pogue, B. W., Braun, R. D., Lanzen, J. L., Erickson, C., Dewhirst, M. W. Analysis of the heterogenousity of pO_2 dynamics during photodynamic therapy with verteporfin*. Photochem. Photobiol*. 74, 700-706, **2001**.

- Pogue, B. W., and Hasan, T. A theoretical study of light fractionation and dose-rate effects in photodynamic therapy. *Radiation Res*. 147: 551-559, **1997**.

- Ponka, P., Borová J., Neuwirt, J., Fuchs, O., Necas, E. A study of intracellular iron metabolism using pyridoxal isonicotinoyl hydrazone and other synthesis chelating agents. *Biochem Biophys Acta*. 586 (2): 278-97, **1979**.

- Ponka, P., Richardson, D. R., Edward, J. T., Chubb, F. L. Iron chleators of the pyridoxal isonicotinoyl hudrazone class. Relationship of the lipophilicity of the apochelator of its ability to mobilise iron from reticulocyte *in vitro*. *Can J Physiol Pharmacol*. 72 (6): 659-66, **1994**.

- Popp, S., Waltering, S., Holtgreve-Grez, H., Jauch, A., Proby, C., Leigh, I. M., Boukamp, P. Genetic characterization of a human skin carcinoma progression model: from primary tumor to metastasis. *J Invest Dermatol*, 115 (6): 1095-1103, **2000**.

- Porter, J. B., Singh, S., Hoyes, K. P., Epemolu, O., Abysinghe, R. D., Hider, R. C. Lessons from pre-clinical and clinical studies with 1,2-diethyl-3-hydroxypyridin-4-one, CP94 and related compounds. *Adv Expt Med Biol.* 356: 361, **1994**.

- Pourzand, C., Reelfs, O., Kvam, E., and Tyrrell, R, M. IRP can determine the effectiveness of 5-aminolevulnic acid in inducing protoporphyrin IX (PPIX) in primary human skin fibroblasts. *J Invest Dermatol*. 112: 101-107, **1999b**.

- Pourzand, C., Tyrrell, R. M. Apoptosis, the role of oxidative stress and the example of solar ultraviolet radiation, *Photochem, Photobiol*. 70 (4): 380-391, **1999**.
- Prajapati, V., Barankin, B. Dermacase Actinic Keratosis. *Can Fam Physician*. 54 (5): 691-699, **2008**.
- Proby, C. M., Purdie, K. J., Sexton, C. J., Purkis, P., Navsaria, H. A., Stables, J. N., Leigh, I. M. Spontaneous keratinocyte cell lines representing early and advanced stages of malignant transformation of the epidermis. *Exp Dermatol.* 9 (2): 104-117, **2000.**
- Proksch, E., Brandner, J. M., Jensen, J. M. The skin: an indispensable barrier. *Experimental Dermatology*. 17 (12): 1063-1072, **2008**.
- Proskuryakov, S. P. A., Konoplyannikov, A. G and Gabai, V. L. Necrosis: a specific form of cell death? *Experimental cell research.* 283: 1-16, **2003**.
- Punnonen, K., Jansen, C. T., Puntala, A., Ahotoupa, M. Effects of *in vitro* UVA irradiation and PUVA treatment on membrane fatty acids and activities of antioxidant enzymes in human keratinocytes. *J. Invest. Dermatol.* 96, 255-259, **1991.**
- Pye, A., Campbell, S., Curnow, A. Enhancement of methyl-aminolevulinate photodynamic therapy by iron chelation with CP94: an in vitro investigation and clinical dose-escalating safety study for the treatment of nodular basal cell carcinoma. *J Cancer Res Clin Oncol*. 134: 841-849, **2008**.
- Pye, A., Curnow, A. A direct comparison f elta-aminolevulunic acid and methyl aminolevulinate-derived protoporphyrin IX accumulations potentiated by

desferrioxamine or the novel hydroxypyridinone iron chelator CP94 in cultured human cells. *Photochem. Photobiol*. 83: 766-773, **2007**.

- Quaedvlieg, P. J., Tirsi, E., Thissen, M.R., Krekels, G, A. Actinic Keratosis: How to differentiate the good from bad ones? *Eur J Dermatol*. 16 (4): 335-9, **2006**.
- Radka, T. Ultraviolet A split-dose therapy, a novel approach to improve theaminolevulinate-based photodynamic therapy of skin lesions. Mphil thesis. University of Bath, Department of Pharmacy and Pharmacology, **2010**.
- Rajpar, S., and Marsden, J. ABC of skin cancer. Blackwell publishing, **2008**.
- Rapini, Ronald, P., Jean, L., Joseph, L. Dermatology: 2-volume set. St. Louis: Mosby. Pp. chapter, 108, **2007**.
- Rebeiz, N., Rebeiz, C. C., Arkins, S., Kelley, K. W., Rebeiz, C. A. Photodestruction of tumor cells by induction of endogenous accumulation of protoporphyrin IX: Ehancement by 1,10-phenantroline. *Photochem Photobiol* 55:431-435, **1992**.
- Redbord, K. P., Hanke, C. W. Topical photodynamic therapy for dermatologic disorders: results and complications. *J Drugs Dermatol*. 6 (12): 1197-202, **2007**.
- Reed, J. C. Mechanisms of apoptosis. *Am J Pathol*.157: 1415-1430, **2000**.
- Reed, J. C. mechanisms of apoptosis avoidance in cancer. *Curr. Opin. Oncol.*11, 68-75, 1999.
- Reed, J. C., Jurgensmeier, J. M., Matsuyama, S. Bcl-2 Family proteins and mitochondria . *Biochim. Biophys. Acta*.127-137, 1366, **1998**.

- Reelfs, O., Eggleston, I. M., Pourzand, C. Skin protection against UVA-induced iron damage by multiantioxidants and iron chelating drugs/ prodrugs. *Curr Drug Metab.* 11 (3): 242-249, **2010**.
- Reelfs, O., Tyrrell, R, M., Pourzand, C. Ultraviolet A radiation induced immediate iron release is a key modulator of the NF-kappaB in human skin fibroblast. *J Invest Dermatol*. 122 (6): 1440-1447, **2004**.
- Renschler, M. F., Yuen, A., Panella, T. J., Wieman, T. J., Julius, C., Panjehpou, M., *et al.* Photodynamic therapy trials with lutetium texaphyrin (Lutex). *Photochem Photobiol*. 65 (S), 47 (S), **1997**.
- Richardson, D. R. Chelators to the rescue: different horses for different courses. *Chem. Res. Toxicol*. 24: 279-282, **2011**.
- Richardson, D. R. Molecular mechanisms of iron uptake by cells and the use of iron chelators for the treatment of cancer. *Curr Med Chem*. 12(23): 2711-29, **2005**.
- Richardson, D. R., and Ponka, P. The iron metabolism of the human neuroblastoma cell: lack of relationship between the efficacy of iron chelation and the inhibition of DNA synthesis. *J Lab Clin Med*. 124(5): 660-671, **1994**.
- Richardson, D. R., Tran, E. H., Ponka, P. The potential of iron chelators of pyridoxal isonicotinoyl hydrazone class as effective antiproliferative agents. *Blood*. 86 (11): 4295-4306, **1995**.
- Richardson, D. R., and Zaklina Kovacevic, Y. Tuning cell cycle regulation with an iron key. *Cell Cycle.* 6(16): 1982-1994, **2007**.

- Riley, P. A. Free radicals in biology:oxidative stress and the effects of ionising radiation. *Int. J. Radiant. Biol*. 65, 27-33, **1994**.

- Rittenhouse- Diakun, K., van Leengoed, H., Morgan, J., Hryhorenko, E., Paszkiewicz, G., Whitaker, J. E., Oseroff, A. R. The role of transferrin receptor (CD71) in photosynamic therapy of activated and malignant lympjocytes using the heme precursor α- aminolevulinic acid (ALA). *Photochem Photobiol*. 61: 523-528, **1995**.

- Robinson, D. J., Collins, P., Stringer, M. R., Vernon, D. I., Stables, G. I., Brown, S. B., Sheehan-Dare, R. A. Improved response of plaque psoriasis after multiple treatments with topical 5-ALA PDT. *Acta Dermato-Venereol*.79: 451-455, **1999**.

- Rode, H. J. Apoptosis, cytotoxicity and cell proliferation. Roche Diagnostics GmbH, 4th edition, **2008**.

- Rosenthal, I. Phtalocyanines as photodynamic photosensitisers*. Photochem Photobiol.*53: 859-870, **1991**.

- Roy, I., Ohulchanskyy, T. Y., Pudavar, H. E., Bergey, E. J., Oseroff, A. R., Morgan, J., Dougherty, T. J., Prasad, P. N. Ceramic-based nanoparticles entrapping water insoluble photosensitising anti-cancer drugs: a novel drug carrier system for photodynamic therapy. *J Am Chem Soc*. 125(26): 7860-65, **2003**.

- Rud, E., Gederaas, O., Hogst, A., Berg, K. 5-aminolevulinic acid, but not 5-aminolevlinic acid esters is transported into adenocarcinoma cells by sustemic BETA transporters. *Photochem photobiol*.71:640-647, **2000**.

- Ryter, S. W., And Trrrell, R. M. Singlet oxygen ($^1O_2$): A possible effector of eukaryotic gene expression. *Free Radic. Biol. Med*. 24, 1520-1534, **1998**.

- Sah, P. P., and Peoples, S. A. Isonicotinoyl Hydrazones an antitubercular agents and derivatives for identification of aldehydes and ketones. *J Am Pharm Assoc Am Pharm Assoc*. 43 (9): 513-24, **1954**.

- Salasche, S. J. Epidemiology of actinic keratosis and squamous cell carcinoma. *J. Am. Acad. Dermatol.*42: 4-7, **2000**.

- Sandberg, C., Stenquist, B., Rosdahl, I., Ros, A. M., Synnerstad, I., Karlsson, M., Gudmundson, F., Ericson, M. B., Larkö, O., Wennberg, A. M. Important factors for pain during photodynamic therapy for actinic keratosis. *Acta Derm Venereol*.86: 404-408, **2006**.

- Santoro, O., Bandieramonte, G., Melloni, E., Marchesini, R., Zunino, F., Lepera, P., De Palo, G. Photodynamic therapy by topical mesotetraphenylporphinessulfonate salt administration in superficial basal cell carcinomas. *Cancer Res*. 50: 4501-4503, **1990**.

- Schleyer, V., Radakovic-Fijan, S., Kerrer, S., Zwingers, T., Tanew, A., Landthaler, M., Szeimies, R. M. Disappointing results and low tolerability of photodynamic therapy with topical 5-aminolevulinic acid in psoriasis. A randomized double-blind phase I/II study. *J Eur Acad Dermatol*.20: 823-828, **2006**.

- Schmook, T., Stockfleth, E. Current treatment patterns in non-melanoma skin cancer across Europe. *J. Dermatol Treat* 149(S): 3-10, **2003**.

- Schoenfeld, N. S., Epstein, O., Lahav, M., Mamet, R., Shaklai, M., Atsmon, A. The heme biosynthetic pathway in lymphocytes of patients with malignant lymphoproliferative disorders. *Can Lets.*43:43-48, **1988**.
- Sessler, J. L., Miller, R. A. Texaphyrins. New drugs with diverse clinical applications in radiation and photodynamic therapy. *Biochem Pharmacol*. 59: 733-739, **2000**.
- Shao, J., Xue, J., Dai, Y., Liu, H., Chen, N., Jia, L., Hua, J. Inhibition of human hepatocellular carcinoma HepG2 by phthalocyanine photosensitiser: ROS production, Apoptosis, Cell cycle arrest. *European Journal of Cancer*. 48: 2086-2096, **2012**.
- Sharman, W. N., Allen, C. M., Van Lier, J. E. Photodynamic therapeutics: basic principles and clinical applications. *Drug Discov. Today*.4:507-517, **1999**.
- Singh, S., Choudhury, R., Epemolu, R. O., Hider, R. C. Metabolism and pharmacokinetics of 1-(2-hydroxyethyl) and 1-(3-hydroxypropyl)-2-ethyl-3-hydroxypyridin-4-ones. *Eur J Drug Metab Pharmacokin*. 21:33, **1996**.
- Skiveren, J., Haedersdal, M., Philipsen, P. A., Wiegell, S. R., Wulf, H. C. Morphine gel 0.3% does not relieve pain during topical photodynamic therapy: a randomized, double-blind, placebo-controlled study. *Acta Derm Venereol*.86: 409-411, **2006**.
- Smith, A. G. B., Clothier, B., Francis, J. E., Gibbs, A. H., De-Matteis, F., Hider, R. C. Protoporphyria induced by the orally active iron chelator 1,2,-diethyl-3-hydroxypyridin-4-one in C57BL/10ScSn mice. *Blood* 89: 1045-1051, **1997**.

- Soler, A. M., Warloe, T., Berner, A., Giercksky, K. E. A follow up study of recurrence and cosmesis in completely responding superficial and nodular basal cell carcinomas treated with methyl 5- aminolevulinate-based photodynamic therapy alone and with prior curettage. *Br J Dermatol*. 145 (3): 467-471, **2001**.

- Sotiriou, E., Apalla, Z., Ioannides, D. Complete resolution of a squamous cell carcinoma of the skin using intralesional PDT for SCC. *Photoderm Photoimmun Photomed*. 26: 269-71, **2010**.

- Souza, C. S., Felicio, L. B., Ferreira, J., Kurachi, C., Bentley, M. V., Tedesco, A. C. Bagnato, V. S. Long term follow up of topical 5-aminolevulinic acid photosynamic therapy diode laser single session for non-melanoma skin cancer. *Photodiagnosis Photodyn Ther*. 6 (3-4): 207-213, **2009**.

- Spikes, J. D. Photodynamic action: from paramecium to photochemotherapy. *Photochem.Photobiol.*65, 142s-147s, **1997**.

- Spikes, J. D. Phtalocynines as photosensitisers in biological systems and for PDT of tumours. *Photochem Photobiol* 43:691-699, **1986**.

- Stables, G. I., Ash, D. V. Photodynamic therapy. *Cancer Treat Rev.*21, 311-323, **1995**.

- Stebbins, W. G., and Hanke, C. W. MAL-PDT for difficult to treat nonmelanoma skin cancer. *Dermatologic Therapy*. 24: 82-93, **2011**.

- Steinbauer, J. M., Schereml, S., Babilas, P., Zeman, F., Karrer, S., Landthaler, M., Szeimies, R. M. Topical photodynamic therapy with porphyrin precursors-assessment of treatment- associated pain in a retrospective study. *Photochem Photobio Sci*. 8: 1111-16, **2009**.

- Stemberg, E.D., Dolphin, D. and Bruckner, C. porpyrin- based photosensitisers for use in photodynamic therapy. *Tetrahedron*. 54, 4151-4202, **1998**.
- Stender, I. M., Lock-Anderson, J., Wulf, H. C. Recalcitrant and foot warts successfully treated with PDT with topical 5-ALA: A pilot study. *Clin. Exp. Dermatol.* 24: 154-159, **1999**.
- Stender, I. M., Na, R., Fogh, H., Gluad, C., Wulf, H. C. Photodynamic therapy with 5-ALA or placebo for recalcitrant foot and hand warts: randomized double-blind trial. *Lancet*. 355: 963-966, **2000**.
- Stohs, S. J., Bagchi, D. Oxidative mechanisms in the toxicity of metal ions. *Free Radic. Biol. Med.* 18: 321-336; **1995.**
- Strasswinner, J., Grande, D. J. Do pulsed lasers produce and effective PDT response? *Lasers Surg Med*. 38: 22-25, **2006**.
- Stringer, M. R. Problems associated with the use of broadband illumination sources for PDT. *Phys Med Biol*.40:1733-1735, **1995**.
- Surrenti, T., De Angelis, L., Di Cecare, A., Fargnoli, M. C., Peris, K. Efficiency of photodynamic therapy with methyl aminolevulinate in the treatment of superficial and nodular basal cell carcinoma: an open pilot label trial. *Eur J Dermatol*. 17 (5): 412-415, **2007**.
- Szeimies, R. M., Abels, C., Fritsch, C., Karrer, S., Steinbach, P., Baumler, W., Goerz, G., Goetz, A. E., Landthaler, M. Wavelength dependency of photodynamic effects after sensitisation with 5-ALA *in vitro* and *in vivo*. *J Invest Dermatol* 105: 672-677, **1995**.

- Szeimies, R. M., Randy, P., Sebastian, M., Borrosch, F., Dirschka, T., Krahn-Senftleben, G., Reich, K., Pabst, G., Voss, D., Foguet, M., Gahlmann, R., Lubbert, H., Reinhold, U. Photodynamic therapy with BF-200 ALAfor the treatment of actinic keratosis: result of prospective, randomized, double blind, placebo-controlled phase III study. *Br J Dermatol*. 163: 386-94, **2010**.

- Tenopoulo, M., Doulis, P. T., Barbouti, A., Brunk, U., Galaris, D. Role of compartmentalized redox active iron in hydrogen peroxide-induced DNA damage and apoptosis. *Biochem. J.* 387: 703-710, **2005**.

- Thissen, M. R., Schroeter, C. A., Neuman, H. A. PDT with ALA for nodular BCC using a prior debulking technique. *Br J Dermatol*.142: 338-339, **2000**.

- Tierney, E., Barker, A., Abdout, J., Hanke, C. W., Moy, R. L., Kouba, D. J. Photodynamic therapy for the treatment of cutaneous neoplasia, inflammatory disorders, and photoaging. *Dermatol Surg*. 35 (5): 725-46, **2009**.

- Togsverd-Bo, K., Haak, C. S., Thaysen-Petersen, D., Wulf, H. C., Anderson, R. R., and Headesdal, M. Intensified photodynamic therapy of actinic keratoses with fractional CO_2 laser: a randomized clinical trial. *British Journal of Dermatology.* 166: 1262-69, **2012**.

- Togsverd-Bo, K., Headersdal, M., Wulf, H. C. Photodynamic therapy for tumours on the eyelid margins. *Arch Dermatol*. 149 (6): 1242-1249, **2003**.

- Togsverd-Bo, K., Lerche, C. M., Poulsen, T., Wulf, H. C., Haedersdal, M. Photodynamic therapy with topical methyl and hexyl aminolevulinate for prophylaxis and treatment of UV-induced SCC in hairless mice. *John Wiley & Sons*, 19: 166-172, **2010**.

- Trenam, C. W., Blake, D. R., Morris, C. J. Skin inflammation: Reactive oxygen species and the role of iron. *J. Invest. Dermatol.*99, 675-682, **1992**.
- Tromberg, B. J., Orenstein, A., Kimel, S., Barker, S. J., Hyatt, J., Nelson, J. S., Berns, M. W. *in vivo* tumour oxygen tension measurements for the evaluation of the efficiency of photodynamic thrapy. *Photochem. Photobiol*.52: 375-385, **1990**.
- Truchuelo, M., Fernandoz-Guarino, M., Fleta, B., Alcantara, J., Jaen, P. Effectiveness of photodynamic therapy in Bowden's disease: an observational and descriptive study in 51 lessions. *J Eur Acad Dermatol Venereol*. 26 (7): 868-74, **2012**.
- Tschen, E. H., Wong, D. S., Pariser, D. M., Dunlap, F. E., Houlihan, A., Ferdon, M. B., and the phase IV ALA-PDT Actinic Keratosis group. Photodynamic therapy using aminolevulinic acid for patients with nonhyperkeratotic actinic keratosis of the face and the scalp: Phase IV multicentre clinical trial with 12-month follow up. *Br J Dermatol*. 155: 1262-1269, **2006**.
- Tyrrell, J. S., Campbell, S. M., Curnow, A. The relationship between propophyrin IX photobleaching during real-time dermatological methy-aminolevulinate photodynamic therapy (MAL-PDT) and subsequent clinical outcome. *Lasers in Surgery and Medicine.* 42: 613-619, **2010**.
- Tyrrell, R. M. Activation of mammalian gene expression by the UV component of sunlight- from models to reality. *BioEssays*. 18: 139-148, **1996**.
- Tyrrell, R. M. In oxidative stress: Oxidants and antioxidants. Sies, H., Ed. *Academic Press, London*. pp. 57-83, **1991**.

- Tyrrell, R. M. The molecular and cellular pathology of solar UVA radiation. *Mol. Aspects Med*. (H sies, Eds) 15 (1): 1-77 Review, **1994**.
- Tyrrell, R. M., Pidoux, M. Correlation between endogenous glutathione content and sensitivity of cultured human skin cells to radiation at defined wavelengths in the solar UV range. *Photochem. Photobiol.*41, 405-412, **1988**.
- Tyrrell, R. M., and Pidoux, M. Singlet oxygen involvement in the inactivation of cultured human fibroblasts by UVA (320-400 nm) and near visible (405 nm) radiations. *Photochem. Photobiol.* 49, 407-412, **1989**.
- Uehlinger, P., Zellweger, M., Wagniere, G.,Juillerat-Jeanneret, L., van den Bergh, H., Lange, N. 5-aminolevulinic acid and its derivatives: physical chemical properties and Protoporphyrin IX formation in cultured cells. *J Photochem Photobiol B.* 54: 72-80, **2000**.A placebo-controlled, double blind, pilot study. *J Dermatolog Treat*. 20 (5): 259-65, **2009**.
- Valdés, P. A., Samkoe, K., O'Hara, J. A., Roberts, D. W., Paulsen, K. D., and Pogue, B. W. Deferoxamine iron chelation increases aminolevulinic acid induced protoporphyrin IX in Xenograft Glioma model. *Photochemistry and Photobiology*. 86: 471-475, **2010**.
- Van der Geer, S., Krekels, G. A. Treatments of actinic keratosis on the dorsum of the hands: ALA-PDT versus diclofenac 3% gel followed by ALA-PDT.
- Van Duijnhoven, F. H., Aalbers, R. I., Rovers, J. P., Terpstra, O. T., Kuppen, P. J. The immunological consequences of photodynamic treatment of cancer, a literature review. *Immunolobiology*. 207: 105-113, **2003**.

- Van Duijnhoven, F. H., Rovers, J. P., Engelmann, K., Krajina, Z., Purkiss, S. F., Zoetmulder, F. A., Vogl, T. J., Terpstra, O. T. Photodynamic therapy with 5,10,15, 20-tetrakis 9m-hydroxyphenyl) bacteriochlorin for colorectal liver matastasis is safe and feasible: results from a phase I study. *Ann Surg Oncol*.12: 808-816, **2005**.

- Van Lier, J. E., Spikes, J. D. The chemistry, Photophysics and photosensitising properties of phthalocyanines. *Ciba Found Symp*. 146: 17-26, **1989**.

- Vile, G. F., Tyrrell, R. M. UVA radiation-induced oxidative damage to lipids and proteins *in vitro* and in human skin fibroblasts is dependent on iron and singlet oxygen. *Free Radical Biol. Med.* 18, 721-730, **1995**.

- Vinciullo, C., Elliot, T., Francis, D., Gebauer, K., Spelman, L., Nguyen, R., Weightman, W., Sheridan, R., Reid, C., Czarnecki, D., Murrell, D. Photodynamic therapy with topical aminolevulinate “difficult to treat” basal cell carcinoma. *Br J Dermatol*. 152: 765-72, **2005**.

- Vitolo, M. L., Clare, B. W., Hefter, G. T., Webb, J. Chemical studies of pyridoxal isonicotinoyl hydrazine relevant to its clinical evaluation. *Birth Defects Orig Artic Ser*. 23 (5B): 71-9, **1988**.

- Wachowska, M., Muchowics, A., Firczuk, M., Cabrysiak, M., Winiarska, M., Wanczyk, M., Bojarczuk, K., and Golab, J. Aminolevulinic Acid (ALA) as a prodrug in Photodynamic Therapy of Cancer. *Molecules*. 16: 4140-4164, **2011**.

- Waldow, S. M., Dougherty, T. J. Interaction of hyperthermia and photoradiation therapy. *Radiat Res* 97: 380-385, **1984**.

- Wang, s. s., Chen, J., Keltner, L., Christophersen, J., Zheng, F., Krouse, M., Singhal, A. New technology for deep light distribution on tissue for phototherapy. *Cancer Journal*. 8 (2): 154-163, **2002**.
- Weedon, D. Weedon's skin pathology. 3rd edition. Elsevier, **2010**.
- Wennberg, A. M., Larkö, O., Lönnroth, P., Larson, G., Krogstad, A. L. Delta-aminolevulinic acid in superficial basal cell carcinomas and normal skin. A microanalysis and perfusion study. *Clin Exp Dermatol*. 25: 317-22, **2000**.
- Whitehurst, C., Byrne, K. T., Moore, J. V. Development of an alternative light source to lasers for PDT: Comparative in vitro dose response characteristics. *Lasers Med Sci*.8: 259-267, **1993**.
- Whitnall, M., Howard, J., Ponka, P., Richardson, D. R. A class of iron chelators with a wide spectrum of potent antitumor activity that overcomes resistance to chemotherapeutics. *Proc Natl Acad Sci USA.* 103 (40): 14901-14906, **2006**.
- Wiegell, S. R., Fabricius, S., Stender, I. M., Berne, B., Kroon, S., Andersen, B. L., Mørk, C., Sandberg, C., Jemec, G. B., Mogensen, M., Brocks, K. M., Philipsen, P. A., Heydenreich, J., Haedersdal, M., Wulf, H. C. A randomized multicentre study of directed daylight exposure times of 1 ½ versus 2 ½ hours in daylight mediated photodynamic therapy with methyl aminolevulinate in patients with multiple thin actinic keratoses of the face and scalp. *Br J Dermatol*. 164: 1083-90, **2011**.
- Wiegell, S. R., Headersdal, M., Philipsen, P. A., Eriksen, P., Enk, C. D., Wulf, H. C. Continuous activation of PPIX by daylight is as effective as and less painful than conventional photodynamic therapy for actinic keratosis: A randomized, controlled, single- blinded study. *Br J Dermato*l. 158: 740-746, **2008**.

- Wiegell, S., Stender, I. M., Na, R., Wulf, H. C. Pain associated with photodynamic therapy using 5-aminolevulinic acid or 5-amino-levulinic acid methylester on tape-stripped normal skin. *Arch Dermatol*.139: 1173-1177, **2003**.

- Wiegell, S., Wulf, H. C. Photodynamic therapy of acne vulgaris using 5-aminolevulinic acid versus methyl aminolevulinate. *J. Am. Acad. Dermatol*.54: 647-651, **2006**.

- Wiegell, S. R., Skiveren, P. A., Philipsen, P. A., Wulf, H. C. Pain during photodynamic therapy is associated with protoporphyrin IX fluorescence and fluence rate. *Br J Dermatol*.158:727-733, **2008**.

- Williams, A. Transdermal and topical drug delivery from theory to clinical practice. *Pharmaceutical Press*. **2003**.

- Wilson, B. C., Jeeves, W. P., Lowe, D. M., Adam, G. Light propagation in animal tissues in the wavelength range 375-825 nm. In Doiron DR, Gomer CJ, eds. Prophyrin Localization and treatment of tumours. *Liss Inc, NewYork*.115-132, **1984**.

- Wilson, B.T., Mang T. Photodynamic therapy for cutaneous malignancies. *Clin Dermatol*, 13:91-96, **1995**.

- Wlaschek, M., Wenk, J., Brenneisen, P., Brivida, K., Schwarz, A., Sies, H., Scharffetter-Kochanek, K. Singlet oxygen is an early intermediate in cytokine-dependent ultraviolet-A induction of interstitial collagenase in human dermal fibroblasts in vitro. *FEBS Lett.*239-242, 413, **1997**.

- Wolf, P., Kerl, H. Photodynamic therapy in patients with xeroderma pigmentosum. *Lancet* 337:1613-1614, **1991.**

- Woodburn, K. W., Fan, Q., Kessel, D., Wright, M., Mody, T.D., Hemmi, G.,Magda, D., Sessler, J. L., Dow, W. C., Miller, R. A., Yound, S. W. Phototherapy of cancer and atheromatous plaque with texaphyrins. *J. Clin. Laser Med Surg.* 14: 343-348, **1996**.

- Xia, Y., Huang, Y., Lin, L., Liu, X., Jiang, S., Xiong, L. A comparative study on the enhancement efficacy of specific and non-specific iron chelators for PPIX production and photosensitisation in HaCaT cells. *Med Sci*. 29 (6): 765-770, **2009**.

- Xu, W., Kozak, C. A., Desnick, R. J. Uroporphyrinogen III synthase: molecular cloning, nucleotide sequence, expression of a mouse full-length cDNA, and its localisation on mouse chromosome 7. *Genomics*. 26 (3): 556-62, **1995**.

- Yang, J., Chen, A. C. H., Wu, Q., Jiang, S., Liu, X., Xiong, L., Xia, Y. The influence of temperature on 5-aminolevulinic acid-based photodynamic reaction in keratinocytes *in vitro*. *Photodermatology, Photoimmunology & Photomedicine.* 26: 83-88, **2010**.

- Yang, J., Xia, Y., Jiang, L. Desferrioxamine shows different potential for enhancing 5-aminolevulinic acid based photodynamic therapy in several cutaneous cell lines. *Lasers Med Sci*. 25: 251-257, **2010**.

- Yasui, H. and Sakurai, H. Chemiluminescent detection and imaging of reactive oxygen species in live mouse skin exposed to UVA. *Biochem. Biophys Res. Commun*. 131-136, 269, **2000**.

- Yiakouvaki, A., Savovic, J., Al-Qenaei, A., Dowden, J., and Pourzand, C. Caged iron chelators a novel approach towards protecting skin cells against UVA-induced necrotic cell death. *J Invest Dermatol*. 126: 2287-2295, **2006**.

- Young, B. L. Synthesis of Biological Studies on “Smart” Iron Chelator Molecules. PhD thesis. University of Bath, Department of Pharmacy and Pharmacology, **2013**.
- Yu, Y., Wong, J., Lovejoy, D. R., Kalinowki, D. S., Richardson, D. R. Chelators at the cancer coalface: desferrioxamine to Triapine and beyond. *Clin Cancer Res*. 12 (23): 6876-6883. **2006**.
- Ziolkowski, P., Osiecka, B. J., Oremeck, G., Siewinski, M., Symonowicz, K., Saleh, Y., Bronowicz, A. Enhancement of photodynamic therapy by use of aminolevulinic acid/glycolic acid drug mixture. *J Exp Ther Oncol* 4: 121-129, **2004**.
- Zhao, B., and He, Y. Y. Recent advances in the prevention and treatment of skin cancer using photodynamic therapy. *Expert Rev Anticancer Ther*. 10 (11): 1797-1809, **2010**.
- Zhong, J.L., Yiakouvaki, A., Holley, P., Tyrrell, R. M., Pourzand, C. Susceptibility of skin cells to UVA-induced necrotic cell death reflects the intracellular level of labile iron. *J. Invest. Dermatol*. 123: 771-780, **2004**.
- Zuber, T, J. Punch biopsy of the skin. *American Family Physician*. 65 (6): 1155-1158, **2002**.

Web Sources:

- Cancer Research UK, skin cancer. Available from: http://www.cancerresearchuk.org/skincancer [Accessed on 1 September 2013]
- National Cancer Institute, Anatomy of skin. Available from: http://www.training.secr.cancer.gov/melanoma/anatomy [Accessed on 22 August 2013]
- The Karen Clifford Skin Cancer charity, Basal Cell Carcinoma. Available from: http://www.skcin.org/skin-cancer/types/basal-cell-carcinoma-(BCC) [Accessed 23 August 2013]
- The Mitochondria Research Society, Dr Jakubowski. Available from: http://www.microbewiki.kenyon.edu/index.php/mitochondria [Accessed 7 September 2013]
- Skin Cancer Education, melanoma. Available from: http://www.missinglink.ucsf.edu/melanoma [Accessed 5 Sep 2013]
- Skin Cancer Foundation, squamous cell carcinoma (SCC). Available from:http://www.skincancer.org/skin-cancer-info/squamous-cell-carcinoma [Accessed 10 September 2013]